Ground Water

FLOOD ROUTING THROUGH STORM DRAINS

Part I

SOLUTION OF PROBLEMS OF UNSTEADY FREE SURFACE FLOW IN STORM DRAINS

by

V. YEVJEVICH and A. H. BARNES

November 1970

HYDROLOGY PAPERS
COLORADO STATE UNIVERSITY
Fort Collins, Colorado

43

Several departments at Colorado State University have substantial research and graduate programs oriented to hydrology. These Hydrology Papers are intended to communicate in a fast way the current results of this research to the specialists interested in these activities. The papers will supply most of the background research data and results. Shorter versions will usually be published in the appropriate scientific and professional journals, or presented at national or international scientific and professional meetings and published in the proceedings of these meetings.

The investigations leading to this paper on unsteady free-surface flow in a long storm drain were supported by the U.S. Bureau of Public Roads, Federal Highway Administration during 1960-1970 and by the Public Health Service during 1962-1964. The research was conducted in the Hydrology and Water Resources Program of Civil Engineering Department at Colorado State University, Fort Collins, Colorado, U.S.A.

Dr. Arthur T. Corey, Professor, Agricultural Engineering Department

Dr. Robert E. Dils, Professor, College of Forestry and Natural Resources

Dr. Vujica Yevjevich, Professor, Civil Engineering Department

FLOOD ROUTING THROUGH STORM DRAINS

Part I

SOLUTION OF PROBLEMS OF UNSTEADY FREE SURFACE FLOW IN STORM DRAINS

by

V. Yevjevich and A. H. Barnes

HYDROLOGY PAPERS
COLORADO STATE UNIVERSITY
FORT COLLINS, COLORADO 80521

November 1970 No. 43

ACKNOWLEDGMENTS

The writers of this paper gratefully acknowledge the support and cooperation of the U. S. Bureau of Public Roads, Federal Highway Administration, in the research on flood movements through long storm drains conducted from 1960 to 1970. The writers also acknowledge the U. S. Public Health Service, National Institute of Health, for their additional support during 1962-1964.

The initiative, cooperation and support given by Mr. Carl F. Izzard to this project on flood movement through storm drains is particularly acknowledged. Mr. Izzard, presently Director, Office of Development, Federal Highway Administration, U. S. Department of Transportation, was Chief, Hydraulic Research Division, U. S. Bureau of Public Roads at the start of the project. Further acknowledgment is extended to Mr. Charles F. Scheffey, Director, Office of Research, Federal Highway Administration, for his cooperation and encouragement. Dr. Dah-Cheng Woo, Senior Hydraulic Engineer, Federal Highway Administration, has cooperated extensively with this project. His reviews and suggestions pertaining to all reports, theses and other documents produced on the project have been particularly helpful.

Mr. George Smith, Associate Professor of Civil Engineering at Colorado State University, has worked closely with the writers in the design, construction, testing, and operation of the physical research facilities during most of this project. Several graduate students, either through their thesis research or through direct work, contributed to the project. The theses and reports are listed in the bibliography of this paper under "Internal References". Dr. Shih-Tun Su, Post Doctoral Fellow, Civil Engineering Department, Colorado State University, using existing data, assisted writers in finishing this paper.

TABLE OF CONTENTS

TABLE OF CONTENTS - (Continued)

LIST OF FIGURES AND TABLES

ABSTRACT

This first part of a four-part series of hydrology papers on flood routing through storm drains presents results of experimental studies in a 3-ft diameter, 822-ft long storm conduit and theoretical studies of the unsteady free-surface flow. The derivation of the two quasi-linear hyperbolic partial differential equations of gradually varied free-surface unsteady flow based on the principles of conservations of mass and momentum are given. The numerical integrations of differential equations by the specified interval scheme of the method of characteristics, the diffusing scheme, and the Lax-Wendroff scheme are discussed; the method of characteristics is selected for the practical integration procedure whenever the complete differential equations are used. Experimental and analytical investigations of the geometric and hydraulic parameters that define the coefficients of the two differential equations are summarized. Particular attention is given to geometric characteristics of a circular conduit, to hydraulic resistance, to velocity distribution coefficients, and to junction box energy losses. The initial and boundary conditions are experimentally studied and are expressed mathematically for the numerical solutions. The analytically computed waves are then compared with the experimentally observed waves by using the same initial and boundary conditions. Qualitative and quantitative comparisons are given for depth hydrographs at different positions, for depth wave profiles at different instants in time, and for the peak-depth versus both position and time. From a practical point of view, good agreement is indicated by these comparisons. The applicabilities of simplified routing methods are also compared in general terms to the solutions obtained by solving the two partial differential equations of unsteady flow. The errors in conduit geometric parameters, in hydraulic parameters, in numerical computations, and in experimental observations are analyzed and discussed.

FLOOD ROUTING THROUGH STORM DRAINS

Part I

SOLUTION OF PROBLEMS OF UNSTEADY FREE SURFACE FLOW IN STORM DRAINS

by

V. Yevjevich* and A. H. Barnes**

Chapter 1

INTRODUCTION

1.1 Review of Methods for Routing Floods Through Storm Drains

The predominant methods used in the design of storm drains employ the steady free-surface flow approach at the selected flood peak discharge. The design flood peak of a given probability of exceedence is computed by a hydrologic procedure for a given drain section between two water inlets. The drain is designed in such a way that the design flood discharge passes through it as the free-surface flow at the largest drain flow capacity. The flood peak discharge is usually determined by the hydrologic rational method of flood estimations. Simple computations for a free-surface steady and uniform flow through a storm drain determine the basic geometric dimensions of a drain between its two inlet points. For a circular drain its diameter is the basic dimension for the given invert slope.

Because floods are mainly free-surface waves moving through storm drains, the steady-flow design approach does not take into account several factors. First, storm drains have storage capacities which attenuate the floods. Second, unsteady flows through various drain sections mutually interact; furthermore, an extensive grid of storm drains with small slopes, located in urban and combined urban-highway drainage systems, significantly affects storm flood attenuation during a local heavy storm of limited areal coverage. Third, drain conduits during storm floods have non-negligible dynamic effects in flood wave modifications as they progress along the drain. They may, under particular conditions, pass to bores (surges).

The use of approximate flood routing methods based on the simplified unsteady flow approach of storm drain design currently practiced, are the Chicago method and others. They take into account the attenuating storage effect; however, they usually neglect the dynamic effects. In other words, they mainly treat the kinematic aspects of a wave. Because some flood waves may amplify and pass to bores under given conditions, the simple flood routing methods based on the storage equation, even with some corrections, can not reproduce and take into account various aspects of dynamic effects, especially the celerities of various parts of waves as the wave evolves, movement of flood waves upstream along a long drain, and similar effects.

The advent of digital computers enhances the feasibility of using the most complete mathematical equations for the computation of unsteady free-surface flow in a storm drain. Besides, progress in urban hydrology and the improved understanding of precipitation phenomena enable a better prediction of storm flood hydrographs which enter the storm drain system. These two factors encourage applying unsteady free-surface flow equations in their most reliable mathematical forms to storm drain design.

In summary, the historical development of methods for design of storm drains may be classified in three broad classes:

A. Steady-flow approach of storm drain design, the logical consequence of the rational type formulas in predicting storm flood hydrograph peaks.

B. Simplified unsteady flow approach of storm drain design mainly based on the storage equation or its modified forms of kinematic waves, the logical consequences of unit hydrograph approach in predicting storm flood hydrographs, of limitations in accuracy of hydraulic properties of storm drains, and of available computational devices and numerical techniques in the precomputer era.

C. Unsteady free-surface flow approach of storm drain design, based on the complete equations of conservation of mass (continuity) and momentum of unsteady free-surface flow, advanced methods of predicting flood hydrographs, the use of rapid digital computers with adequate storage capacity, and the advanced numerical methods of integration of differential equations.

The potential of using improved flood routing methods through storm drains by this third approach has inspired the investigation presented in this paper.

1.2 Objectives of Investigation

This study of the hydrodynamics of unsteady free-surface flow in a storm drain has the primary objective

* Professor-in-Charge of Hydrology and Water Resources Program, Dept. of Civil Engineering, Colorado State University.
**Associate Professor of Civil Engineering, Colorado State University.

of adding the information for developing flood routing procedures adopted to a digital computer and verified by hydraulic model tests. The ultimate objective is to provide results which permit the development of working design methods applicable to various situations where drains are used for removal of storm water in the gradually varied free-surface unsteady flow.

Other objectives are the analytical study of various aspects of basic mathematical equations of unsteady free-surface flow; detailed analysis of hydraulic and geometric parameters of storm drains simulated by a long smooth circular conduit; comparison between the physical waves simulated and observed in a smooth circular conduit and the numerically integrated waves with the same initial and boundary conditions; study of particular boundary conditions and losses at singularities along a storm drain, and similar objectives.

1.3 General Initial Conditions Assumed for the Analysis

The following are the general initial conditions of a storm drain assumed for the study. The depth of water in a storm drain is shallow prior to storm inflow, as a steady low-flow regime. Storm inflow hydrographs along the drain are given either as simple hydrographs of any shape, or as composed hydrographs of successive individual storm hydrographs. Each inlet point (i) has an inflow discharge hydrograph, $Q_i(t)$, with the shape, peaks, and time of peaks of the hydrograph differing from inlet to inlet. These hydrographs depend on the catchment area of each inlet, storm characteristics, and the direction and speed of storm movement.

1.4 General Physical Constraints in This Study

To simplify basic and applied research, physical constraints of a storm drain are assumed as follows:

1. The storm drain consists of a single continuous conduit.

2. The inflows of storm water occur at discrete points of inlets located along the storm drain.

3. The inflow discharge at any inlet has a negligible momentum in the conduit direction.

4. The conduit is circular.

5. The conduit dimensions change only at manholes and conduit junction boxes, open to atmospheric pressure. The junction boxes might or might not be inlet points. No inlet occurs outside the junction boxes.

6. The conduit has both the matching crown-lines and the matching invert lines at junction boxes except in the case where a drop junction box occurs. Hydraulic characteristics of drop junction boxes should be known as boundary conditions in the form of the outflow rating curve for the outlet of upstream conduit, though this case is not analyzed in this study.

7. The head loss function of transitions at junction boxes is known in relation to the main conduit discharge, the inlet discharge if any, and a water stage. This head loss is a singular resistance at junction boxes.

8. The slope of the storm drain under field conditions is constant between junction boxes. The slope changes occur only at junction boxes. Points at which slopes change are equivalent to junction boxes without inflows. However, the slope of the long circular conduit is kept constant for a set of experiments and computations in this study.

9. The slopes may vary in both subcritical and supercritical flows, reaching three to five percent.

10. The alignment of the storm drain is straight, even though small deflection may occur at junction boxes in the field; the head loss due to deflection is included in the general singular loss of the junction boxes.

11. The flow regime is a free-surface water motion during all the movement of a storm flood through the drain.

12. The outflow at the end of the storm drain is generally free, or although some controlled end condition for wave movements without inflows are also studied. The outflow stage-discharge relation (rating curve or family of rating curves) is assumed as known.

13. The Darcy-Weisbach f-factor for steady state conditions is used to define the flow resistance.

1.5 Various Potential Applications

The free-surface unsteady water movement through pipes, tunnels, various types of storm drains and all other conduits, either of circular or any other shape, is applicable to many problems. Some of these are:

1. The problem of removing rainfall water from highway and urban areas through storm drains.

2. The problem of free-surface wave movement along water power tunnels and conduits, which involves computing the hydrograph transformation along the tunnel with free-surface flow.

3. The problem of using tunnels and conduits for storage under conditions of unsteady free-surface water flow.

4. The problem of handling the passage of flash-floods of small water courses through diversion tunnels or conduits.

5. The problem of propagating of water waves from the sea, lakes, estuaries or rivers with these waves entering the storm drains, etc.

1.6 General Approach for Investigations

The problem of unsteady free-surface flow in a storm drain in this study is investigated as follows:

1. Analysis of the hydrodynamic aspects of the problem is pursued with a minimum of basic assumptions and neglected factors.

2. Assumptions and neglected factors are discussed under conditions of removing floods through storm drains.

3. Simplifications matching the accuracy of available data, with the precision of their results, are introduced when their evaluation is possible.

Development of equations. Basic hydrodynamic equations are derived in this text, although these derivations repeat many classical studies. This is done for two reasons, to relate them to the computation of unsteady free-surface flow in a storm drain,

and to adapt these analytical expressions to specific characteristics of storm drains. Mathematical expressions that describe unsteady free-surface flow are based on a set of assumptions which means a difference between mathematically computed surface waves and physical waves is unavoidable. All methods for computing unsteady free-surface flow are only approximations, so the extent an approximation agrees with real flow is a basic question to answer for each method. There is little value in discussing merits of a method without determining its degree of approximation.

Selection of method for solving equations. Selecting a method for computing unsteady free-surface flow should depend on an economically justified degree of approximation, and on the risk and uncertainties involved. Two questions should be answered in principle, what is the degree of approximation for each method, and what degree of approximation is justified? To investigate methods for computing unsteady free-surface flow in a storm drain, two different approaches may be pursued. Applied research may be started by using a simple method giving an approximation of low accuracy. Then the method is improved by adding the previously neglected factors, so as to proceed from lower-degree approximation to a higher-degree approximation. This approach was widely used by many previous investigators. Another approach is using the most complete hydrodynamic equations as the closest mathematical approximation of the physics of the unsteady free-surface flow. Any computation of unsteady flow by these equations is assumed to be the highest-order approximation attainable at the present status of applied mathematics in fluid mechanics. Then neglecting some factors and simplifying the initial and boundary conditions, and quantities which describe these conditions, the lower-order approximations are derived. As the accuracy of computations decreases by an increase of simplification and neglect of factors, the practical optimization problem is in determining the order of approximation as the compromise between the accuracy and the economy of data procurement and computations.

Methodology used. The methodology followed in this second approach is:

1. Regardless of which mathematical expressions are used to describe unsteady free-surface flow, several assumptions are always made. They introduce the first departure between the real flow and the theoretical flow, described analytically. Effects of these assumptions are rarely discussed by investigators.

2. The two partial differential equations, usually called the De Saint-Venant equations of unsteady free-surface flow, as the continuity equation and the momentum equation, are presented in their most general form. The physics of the unsteady free-surface flow is stressed, clearly showing variables and quantities that are significant parts of equations and have effects on flow patterns.

3. These general equations are adapted for suitable computations of flood movement along a long storm drain.

4. Initial and boundary conditions are discussed whenever they affect the computation method.

5. Methods of integrating the two partial differential equations are particularly discussed in view of using the most adequate numerical computational methods and digital computers.

6. Specific hydraulic problems related to storm drains are studied in detail with the objective of testing the analytical methods of flood routing in comparison with the observed physical waves.

1.7 Various Aspects of Investigation

Physical and analytical waves. When a flood is produced in a storm drain and observed both at its beginning and its end, it will be called "the physical wave". When a initial flood wave at the storm drain entrance is assumed and the flood wave is computed at the end of this storm drain by an appropriate integration procedure, it will be called "the analytical wave". Comparing the most accurately computed analytical waves with the most accurately observed physical waves is one of the basic objectives of this study. This comparison is analyzed with regard to errors in basic data, errors inherent to methods used, and tolerable errors.

General solutions of unsteady-flow differential equations. Analytical solution in closed forms of the two partial differential equations for unsteady free-surface water flow is not possible for conduits and channels under natural conditions. As soon as simplifications which permit analytical solutions are introduced, the departures from real physical conditions may be so large that in most cases the results become invalid. Thus, methods of approximate integrations of simplified differential equations have been imposed.

One hundred years, from 1871 to 1970, of applying the two basic partial differential equations of unsteady free-surface flow for purposes of computing waves along canals, channels, and conduits have resulted in a variety of methods of solution, graphical, numerical, and analytical, with a wide range of degrees of approximation to exact solutions. Because the amount of work to be done in the past by numerical methods was very large, graphical methods of various types have dominated the field until recently. These tedious and time consuming graphical procedures have been often replaced in practice by the flood routing methods based either on the simple continuity equation, or on it and on a simplified momentum equation. A large number of these approximate methods have been developed and used [1]*, and most of them are still being used.

Recent developments. Two relatively recent developments have greatly influenced the computations of unsteady free-surface flow: (1) many new and appropriate numerical procedures came into being, mainly based on using a finite differences method of integrating the partial or characteristic differential equations, and (2) electronic computers (digital, analog, hybrid) of varying characteristics become available, which could do large computations at a relatively low cost. Innovation and constant progress within these developments have made possible the use of procedures known, but considered impractical 20 to 50 years ago. Among these procedures of integration are both the method of finite differences in solving

* The number or numbers inside the brackets designate references, and sometime their pages, given at the end of this paper.

the two partial differential equations of unsteady free-surface flow under complex conditions, and the method of finite differences applied to the characteristic differential equations as an equivalent set to the partial differential equations.

Two types of equations used by finite differences approach. Using finite differences, as the ratios of differences instead of derivatives, in the graphical or numerical methods of integrating the partial differential equations by their equivalent characteristic differential equations is usually called "the method of characteristics". The phrase "method of finite differences" will be used for both cases when the ratios of finite differences replace the partial derivatives in the partial differential equations or when the ratios of finite differences replace the derivatives of characteristic ordinary differential equations.

Junction problem. The selection of the flood routing method in the case of the junction of two or more drains is often a relevant problem. Inflow hydrographs at various inlets along adjacent storm drains may have different time lags of peak discharge occurrences, with different rising times. Water may temporarily flow in both upstream and downstream directions in a set of storm drains in an area. Junctions of storm drains create interdependence of unsteady flow in a system of storm drains. Flood routing methods, such as those based on the simple storage equation which cannot easily take these conditions into consideration, are not theoretically feasible for treating the unsteady free-surface flow in storm drains. The use of the two partial differential equations is an ideal approach for this complex and realistic flood routing case.

Selection of solution method for attaining a given accuracy of computations. Estimation of inlet hydrographs along storm drains is subject to errors. Predictions of design storms also have a limited accuracy when compared with the real storms of a given probability. There is a limit of accuracy economically justified in flood routing. This accuracy should correspond to the precision of the basic data used, particularly to the accuracy of computed inflow hydrographs along storm drains. The greater this accuracy, the more the accurate flood routing method is justified.

1.8 Justification of Investigations in This Study

Investment in storm drainage. There is a continuous increase in the total activity of urban and highway drainage for removal of storm flood waters. The investment in storm drains, both urban or highway, or combined urban-highway, in the United States is estimated at about two billion dollars per year, and these annual expenditures increase with an increase of time. Simultaneously with this progressively increasing activity and investment in storm drainage, pressure is building up to reduce cost by keeping the total risk of overflooding urban areas and highways below a given probability level. Therefore, it is reasonable to expect an increase in public and private pressure for better methods of storm drain design, particularly for the more accurate techniques of optimization between investment, maintenance, basic risk, and all uncertainties.

Basic risk and uncertainties. Basic risk is defined as the probability of a storm drain not being able to evacuate the storm floods. It is a direct result of stochastic character of floods and all other random factors in storm drain design. Uncertainties result from various errors in determining design floods of given probabilities, errors inherent in the estimation of hydraulic factors of storm drain, inaccuracies of methods used for routing floods through storm drains, and similar sources of errors. Basic risk plus all uncertainties comprise the concept of total risk as it is used in practice. While the basic risk can not be changed except by various flood control works, uncertainties may be decreased by a better prediction of design storm floods, by a better knowledge of hydraulic properties of storm drains, and by more reliable methods of routing floods through storm drains.

The justification of investigations undertaken in this study are mainly two-fold, a decrease in uncertainties in hydraulic properties of storm drains, and a development of flood routing methods for storm drains, which would enable a better optimization between cost and risk, provided these methods of flood routing through storm drains are more reliable than the presently used methods.

Combined urban-highway drainage system. Storm drainage problems studied separately for urban areas and separately for highway drainage, in urban areas with important highways crossing them, are usually not economical. The optimum solution of cost and risk is in a combined urban-highway storm drainage system. Reliable flood routing methods can contribute to better planning of these integrated storm drainage systems. As many large metropolitan areas lie in low slope terrains, the slopes of interconnected storm drains are small over large distances. An integrated storm drainage system requires flood routing methods that can solve problems of storm flood water moving through a grid of interconnected storm drains.

Pollution control and storm drainage. The pollution control of rivers, lakes, estuaries, and seas increasingly puts constraints on the quality of drainage water from urban and highway areas. The general tendency at present is to separate the storm drainage system from the sewage drainage system. This new requirement on the quality of urban and highway storm drainage water affects the various concepts in planning their surface water drainage. Reliable flood routing methods through storm drains and storage systems imposed by flood control, would undoubtedly contribute to more economical and less uncertainties-taking solutions of storm drainage systems as it concerns the water quality.

1.9 Practical Relevance of Investigations

Several aspects of these investigations are of practical relevance. It is expected that results of this study would increase the confidence of designers in using mathematical equations in the form of the two partial differential equations of unsteady free-surface flow, or their equivalent characteristics differential equations, in comparison with the present use of simplified equations, mainly either of simple storage equation or only of kinematic wave equations. Practical relevance of investigation is in showing the degrees or limits of accuracy inherent to any analytical method of solving flood routing problems. Relevance of this study is seen also in its basic direction of using exclusively the inexpensive finite differences integration method made possible by fast digital computers. As in any other systematic research approach, the by-product is the detection of various problems needing more study and better solutions by pointing out the needs and potentials for new research results of practical relevance.

1.10 Brief Historical Review of the Project

These investigations of unsteady free surface flow in a storm drain have been initiated by the original description of research project entitled "Unsteady Surface Flow in a Storm Drain", outlined by Mr. Carl F. Izzard, at that time Chief, Hydraulic Research Division, U.S. Bureau of Public Roads, and presently Director, Office of Development, Federal Highway Administration, U. S. Department of Transportation. This description is given as Appendix 1 to this paper.

The first-year investigation was limited to general and analytical studies as the basis for an advanced research program in subsequent years. As a sequence, a report also entitled "Unsteady Free Surface Flow in Storm Drain" by V. Yevjevich, Professor of Civil Engineering, Colorado State University, as a general analytical study, was submitted to the U.S. Bureau of Public Roads, Hydraulic Research Division in June 1961. This report outlined problems in detail, set-up basic mathematical techniques, discussed the initial and boundary conditions, and selected the general approach to be followed in the next phases of the research program. The above study led to the decision to build an experimental physical research facility on a hillside in the Outdoor Laboratory of the Engineering Research Center at Colorado State University, Fort Collins, Colorado, as described in Part II, Hydrology Paper No. 44, of this sequence of hydrology papers.

Since beginning, five M.S. and one Ph.D. thesis have been written from this project. Several progress reports with investigation results have been submitted to the U.S. Bureau of Public Roads.

The sequence of these four hydrology papers, including this one as the first paper, is a comprehensive description of research activities and of final results. These four papers are all entitled "Flood Routing Through Storm Drains", and the four parts are: Part I, Solution of Problems of Unsteady Free Surface Flow in Storm Drains; Part II, Physical Facilities and Experiments; Part III, Evaluation of Hydraulic and Geometric Parameters; and Part IV, Numerical Computer Methods of Solution . These four papers represent the final report and the termination of the research project.

The review of literature on unsteady free surface flow in channels has been undertaken by V. Yevjevich in 1959-60 under a U.S. Geological Survey project. That review was later published under the title "Bibliography and Discussion of Flood-Routing Methods and Unsteady Flow in Channels", as U.S. Geological Survey Water Supply Paper 1690, U.S. Government Printing Office, Washington 1964. During the ensuing period and during the project life the newest literature on unsteady free surface flow has been continuously reviewed and used in the project.. Some of these newest references are given in Appendix 2.

1.11 Organization of This Paper.

Though a sequence of four hydrology papers represents the results of this study on flood routing through storm drains, this first paper, Part I, No. 43, is conceived as presenting all material related to the study. However, the material presented in detail, in Parts II, III and IV, or hydrology papers 44, 45, and 46, is only presented in this paper in summarized form. The organization of the material is such that paper No. 43 is independent of the other three papers, except when referring additional details in the other three.

The organization of this paper is as follows. Chapter 2 presents general procedures of investigation, with the underlying approaches to the problem solution.

Chapter 3 gives detailed derivation and discussions of the two partial differential equations of gradually varied free-surface unsteady flow, and derivations and discussions of the corresponding four ordinary characteristic equations. The hypotheses underlying the development of these equations are also presented.

Chapter 4 refers to experimental facilities, which is condensed material from Hydrology Papers Nos. 44 and 45.

Chapter 5 is related to the study of finite-difference numerical integration schemes of unsteady flow equations; it basically represents a condensation of information from Hydrology Paper No. 46, and partly from No. 45.

Chapter 6 gives comparisons of the computed and observed waves. It is the major chapter of this paper treating both the qualitative and quantitative comparisons of these waves. Appendices 3, 4, and 5, containing a large number of graphs, support the discussion in this Chapter 6.

Chapter 7 discusses in a summarized form, the simplified methods of flood routing, particularly emphasizing their relations to more accurate computations by the use of complete differential equations of flood waves moving through storm drains.

Chapter 8 is a summary of the effects of individual errors, both in observing physical waves and in computing analytical waves. It also includes the effect of some simplifications in the coefficients of partial differential equations on the evolution of flood waves.

Chapter 9 gives basic conclusions, limitations in the developed methods, and recommendations for further research.

Chapter 2

GENERAL PROCEDURES OF INVESTIGATION

2.1 Specific Aims

The general procedures of the investigations described in this hydrology paper and in the three following papers, comprising a series of four papers are outlined in the subsequent text. Before the procedures are presented the specific aims of the research conducted are delineated as follows.

(1) To supply results of basic and applied research regarding flood routing methods of gradually varied free-surface unsteady flow in a storm drain using the most complete one-dimensional partial differential continuity and momentum equations. These results may enable the research sponsor or another agency to develop a set of practical design methods in the future for flooding routing through storm drains. Each design method should be a feasible procedure for given conditions of storm floods and drainage system characteristics. The design methods based on unsteady flow approach, expected to be developed in the future on the basis of information supplied by this four-part sequence of hydrology papers, should cover the range of flow conditions necessary to compute the depth, the velocity, or the discharge hydrographs at any point, and/or the wave profiles of depth, velocity or discharge along a system of storm drains at any time.

(2) To better understand flow phenomena, through basic and applied research, of gradually varied free-surface unsteady flow in conduits, especially in storm drains. This understanding may supply pertinent information for developing practical criteria that decision makers can use for storm drain design.

(3) To conduct analytical and experimental studies related to various hydrodynamic aspects of gradually varied free-surface unsteady flow in prismatic channels and conduits that could affect flood routing methods developed for storm drains using the unsteady flow approach.

(4) To produce information for improving existing design flood routing methods by using digital computers and Fortran programming, on any available digital computer manufactured in the United States.

After considering the specific aims the general procedure for doing the research on free-surface unsteady flow in storm drains was divided into three parts:

(1) Experimental hydraulic studies.
(2) Analytical studies using numerical digital computer integration procedures.
(3) Comparison of numerically integrated analytical waves with the experimentally observed corresponding waves, and the study of various aspects related to this comparison.

2.2 Experimental Phase

The experimental hydraulic studies were mainly conducted in a moveable conduit, 3 ft in diameter and 822 ft long. The conduit could be moved across a hillside, as described in summary form in Chapter 4 of this paper and in detail in Hydrology Paper No. 44.

(1) The experimental phase of the project consisted of studying, measuring and observing certain aspects of flood waves and conduit. The boundary roughness of the experimental conduit was studied under conditions of free-surface steady flow with the objective of determining whether the conduit may be considered as hydraulically smooth, and if so, how the Darcy-Weisbach friction factor is related either to the Reynolds number, or to the depth of flow. This phase of study is briefly described in Chapter 4 of this paper and in detail in Chapter 3 of Hydrology Paper No. 45. Results were then used as input data for numerical integration of flow equations by a digital computer.

(2) The relationship among the head loss, the discharges of two joining storm drains and the water levels at junction boxes of the storm drains was studied. This experimental research considered only a given junction box with two different inlet positions of the lateral drains. This phase is briefly described in Chapter 4 of this paper and in detail in Chapter 4 of Hydrology Paper No. 45. Results summarized in head loss equations were then used as input data for the numerical integration of flow equations.

(3) The relationship between the depths of free-surface flow and the discharge at the conduit outlet, as downstream boundary conditions was studied. Flow rating curves were considered in the steady flow for different conduit conditions, such as the free outflow or the controlled outflow, to be used as the downstream boundary condition for the numerical integration of the flow equations. This phase is briefly described in Chapter 5 of this paper, and in detail in Chapter 6 of Hydrology Paper No. 45.

(4) Velocity distributions in the experimental conduit flowing partly full were measured to determine as accurately as feasible the velocity distribution coefficients, α and β, for their use as input data into the numerical integration of flow equations. This phase of the study is briefly described in Chapter 4 of this paper and in detail in Chapter 5 of Hydrology Paper No. 45.

(5) Flow phenomena were observed and followed to assess the degree of development of particular problems of physical waves, such as secondary waves, third dimensional oscillations, and similar. An analytical reproduction of flow phenomena is essential for the comparison of physical waves and analytical waves numerically integrated by using a digital computer. These secondary phenomena are not usually taken into account in the one-dimensional partial differential equations of unsteady flow.

(6) The waves were studied at several slopes. For reasons of cost, only the smooth boundary conduit and one diameter were used, so the slope was a variable, while the conduit diameter and its roughness were kept as constants.

(7) Simulated floods were studied and observed in the 3 ft diameter, 822 ft long storm conduit by introducing inflow hydrographs either at the entrance of the conduit, or at both the entrance and at several

inlet points along it. The experimental procedure was to accurately record the inflow hydrographs by appropriate devices, or the discharge as a function of time. Then the movement and development of flood waves along the storm conduit and at the conduit outlet were also accurately recorded. The recorded inflow hydrographs were used as input data for the computerized numerical integration of flow equations. The recorded hydrograph at any point along the storm drain served as a basis for comparing it with the hydrograph determined for the same points by the numerical integration of flow equations.

Certain flow phenomena involving free-surface unsteady flow were not studied, such as the amplification of flood waves in channels of steep slopes, the instability of flow when the pipe is flowing nearly full, the passage from supercritical to subcritical flow through the hydraulic jump, the instability of the position of hydraulic jump in unsteady flow, and similar problems.

2.3 Numerical Integration

The reason for developing methods of integrating unsteady flow equations by numerical finite-difference schemes on a digital computer was to investigate the feasibility of using the two partial differential equations of gradually varied free-surface unsteady flow as the basic mathematical equations for routing floods through storm drains. Or rather, the hypothesis was tested that drains best can be designed by the unsteady flow approach instead of the steady flow approach. However, in this study both the dynamic and the kinematic aspects of free-surface wave movements through storm drains were taken into account, instead of just the kinematic aspects of some simplified unsteady-flow approaches, as is sometimes the case.

The influence of certain parameters in the two partial differential equations were investigated by the numerical integration of these equations for given inflow hydrographs and storm drain characteristics. The advantages of using computerized numerical integration of the two partial differential equations of free-surface unsteady flow are: (a) economy of computation; (b) rapidity of predicting or computing the evolution of flood waves along the storm drain; and (c) improved accuracy in flood wave routing, particularly if the background data are sufficient and accurate.

The computerized numerical integrations and the experimental hydraulic studies were carried out simultaneously. The results obtained by the experimental work were used in developing proper computer programs to simulate numerically physical waves as closely as practically feasible under given conditions.

Two approaches are used for the numerical integration of the two partial differential equations. The first approach uses finite-difference explicit schemes as applied to the two partial differential equations of unsteady flow, with the study of effects of increments, or finite differences of time and length on the numerical integrations. The second approach of integration applies the finite-difference numerical schemes of integration to the four characteristic ordinary differential equations, derived from the two partial differential equations. Computations from this method are compared with the observed experimental or physical waves.

Additional problems may be solved by using the results of this study. The effects of certain parameters on the flood wave propagating along a storm drain can be found which parameters define some coefficients of the two partial differential equations of gradually varied free-surface unsteady flow.

Reliable and accurate computer programs of numerical integration schemes can be developed so that some hydrodynamic problems, which are not yet solved, can be studied in the future. One of these problems is the criterion to use when a wave in a storm drain either does not change or amplifies under different wave and conduit characteristics.

Also, the computer programs presented for the numerical integration of the two partial differential equations could be used effectively by other researchers to assess the accuracy and reliability of different existing simple design flood routing methods, or to develop new simplified design flood routing methods for storm drains.

2.4 Comparison of Physical and Analytical Waves

Comparisons are essential to assess how well the numerical integration of differential equations of unsteady flow, called the analytical waves, by the most reliable numerical methods, approximate the observed or physical waves. The comparison of physical waves with the analytical waves obtained by the numerical integration of the complete equations indicates how the basic hypotheses in developing differential equations and the various errors in parameters affect the accuracy in mathematically describing and reproducing the corresponding physical waves.

The closer the analytical waves are to the physical waves, or the more reliable the numerically integrated waves are, the more valuable the two partial differential equations become for assessing the accuracy of a large number of simplified design flood routing methods, either in existence or still in a state of continuing development, under the various conditions of flood hydrographs, channel or conduit characteristics, and their boundary and initial conditions.

2.5 Relation of this Study to Other Problems of Storm Drainage

To drain highways, urban areas, and airports during storm precipitation, and to avoid their flooding for the given probability of occurrence of rainfall intensity and duration by using large storm drains, four problems should be properly solved. The inflow hydrographs into inlet points of the drainage system along the highways, or streets or airports must be accurately determined. Curb inlets must be well designated so they will not impede the free and desired conveyance of flood waters into the drainage system. The primary and secondary storm drains must be designed to avoid flooding highways, streets, and airports for all hydrographs smaller than the selected design inflow hydrographs. The water from the outlet of the main storm drain must be evacuated by either gravity flow or by pumps. The research of this study is limited, through basic and applied research, to methods of solving the problem of primary and secondary storm drains. The design inflow hydrographs, the geometry of curb inlets, and the types of outflow conditions at main storm drain outlets are assumed to be known in this study.

The gradually varied free-surface unsteady flow in storm drains is studied under two conditions. The first of these conditions is that main storm drains are often vertically positioned as close to the highway or street surface as feasible, to minimize the overburdening and to avoid the cost of reinforcing the storm drain. This means a decrease of the available water head between the flooded highway or street and the drain outlet, thus minimizing the advantage of an eventual use of drains flowing under pressure.

The second condition is that the maximum discharge for free-surface flow in conduits is approximately at the depth which is 0.9 of the conduit diameter. If the same discharge should be conveyed in a full flowing conduit, or under pressure, the slope of the energy line must exceed the bottom slope of the drain. This greater slope might not be available in most cases, even with a flooded highway, street, or airport.

Two approaches may be used to determine the dimensions of a storm drain in the unsteady flow method of flood routing through storm drains. First, the method is so simplified that the diameter or other basic cross-section dimensions can be computed directly and explicitly. Second, the dimensions of a drain are first assumed, then the design storm flood is routed through that drain. If the dimensions come out to be either smaller or larger than the best use of the assumed dimensions, say 0.9 of the diameter at the flood peak depth, new dimensions are assumed and the analysis is repeated until the right dimensions are obtained. This approach needs repeated routing, some of which require larger and some smaller dimensions than the dimensions assumed. When the two partial differential equations are used as the basis for flood routing, only this second approach seems possible and feasible. The first approach is, however, a goal that should not be neglected in future research.

Flood routing methods, generally used at present, start with any given flood hydrograph at a given point along the conduit and determine, dividing the hydrograph by a unit time Δt in many parts, the transformed hydrograph at a distance position x downstream or even upstream from this initial position. Since some design storms are often assumed as one-peak hydrographs, sometimes they may be well approximated by analytical expressions. Though the analytical integration of the two partial differential equations of unsteady flow are not the subject of this study, a potential practical, storm drain flood routing method may be developed on the basis of routing flood parameters (say the three parameters of an analytical equation for the flood hydrographs) along a long prismatic conduit, instead of routing the Δt-elements of the hydrographs. Although this method is not studied, it is briefly discussed in this paper in Chapter 7. If it is shown by future research to be practically feasible, it may be used for rapid computations in preliminary design, or it may be a way of determining initial dimensions with more accurate flood routing methods to follow. The determination of the feasibility of such a method to storm drain computations, however, is outside the scope of this study.

It is expected that future studies will likely produce a set of approximate design methods for computing unsteady flow in storm drains. Only through the comparison of either waves observed in hydraulic experiments and/or waves observed in nature can the necessary conditions and the accuracy of each new or existing design method be evaluated for its applicability. For this comparison to be valid the most accurate available numerical computation based on digital computers and the unsteady-flow approach to design of storm drains must be used.

Chapter 3

THEORETICAL CONSIDERATIONS

3.1 Derivation of the Two Partial Differential Equations for Unsteady Free-Surface Flow in Conduits

Derivation of continuity equation (law of conservation of mass). At time t the cross-section area of unsteady free-surface flow at the section x is A, 1-2 in Fig. 3.1. At the same time t and the section $x + \Delta x$ the area is $A + \frac{\partial A}{\partial x}\Delta x$, with Δx an incremental length. The mass of water between these two sections (slice 1-2-3-4-1 in Fig. 3.1) is $\rho A\Delta x + \frac{1}{2}\rho\frac{\partial A}{\partial x}(\Delta x)^2$. By neglecting the second-order differential term for $\Delta x \to dx$, the mass is $\rho A\Delta x$. Assuming that the lateral outflow or inflow is q, discharge per unit length of conduit, with q positive for inflow and negative for outflow, the change of mass with time is

$$\frac{d}{dt}(\rho A\Delta x) = \rho A\frac{d(\Delta x)}{dt} + \rho\Delta x\frac{dA}{dt} = \rho q\Delta x \qquad (3.1)$$

for an incompressible fluid with ρ as a constant water density.

In considering the velocity v, of an individual particle moving between the two cross sections for the time interval Δt, then $\Delta x = v\Delta t$. Integrating Eq. 3.1 over a cross section A, by using $\Delta x = v\Delta t$, the following integrals are obtained in passing from the particle velocity v, to the average cross section velocity V,

$$\frac{1}{VA}\iint_A v\,dA = 1, \text{ and } \frac{1}{A}\iint_A \frac{\partial v}{\partial x}\,dA = \frac{\partial V}{\partial x}\ . \qquad (3.2)$$

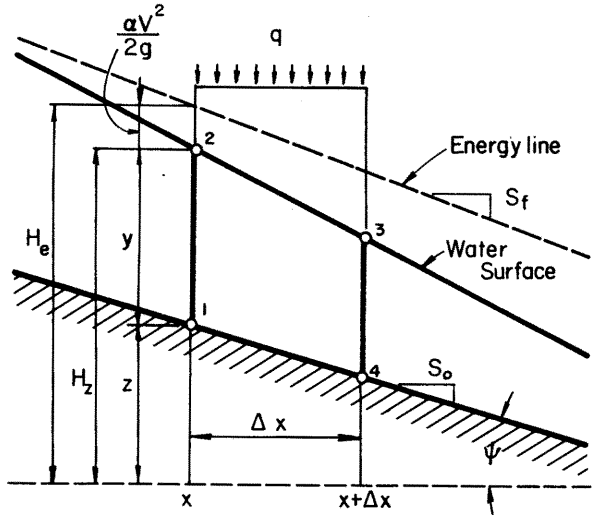

Fig. 3.1. Definition diagram for derivation of continuity and momentum equations of unsteady free-surface flow in an open channel.

The derivative $d(\Delta x)/dt$ for a moving individual particle, for Δx only a function of t, and $\Delta t \to 0$, is

$$\frac{d(\Delta x)}{dt} = \lim_{\Delta t\to 0}\frac{(v + \frac{\partial v}{\partial x}\Delta x)\Delta t - v\Delta t}{\Delta t} = \frac{\partial v}{\partial x}\Delta x. \qquad (3.3)$$

The derivative dA/dt is

$$\frac{dA}{dt} = \frac{\partial A}{\partial t} + \frac{\partial A}{\partial x}\frac{dx}{dt} = \frac{\partial A}{\partial t} + v\frac{\partial A}{\partial x}\ . \qquad (3.4)$$

For the non-prismatic channels, the derivative in x is,

$$\frac{\partial A}{\partial x} = \frac{\partial A}{\partial y}\frac{\partial y}{\partial x} + \left(\frac{\partial A}{\partial x}\right)_y\ ,$$

in which the last term is the measure of the change of cross-section area for a given y. This term can be neglected in the case of storm drains which are assumed to be prismatic conduits between any two inlet points, because a longitudinal section of drain is studied for the movement of unsteady free-surface flow.

Equation 3.1, in passing from the particle velocity to the average cross-section velocity, gives

$$A\frac{\partial V}{\partial x} + V\frac{\partial A}{\partial x} + \frac{\partial A}{\partial t} - q = 0 \qquad (3.5)$$

or

$$\frac{\partial(VA)}{\partial x} + \frac{\partial A}{\partial t} - q = 0\ , \qquad (3.6)$$

in which V is the mean velocity in a cross-section, V and A are the dependent variables, and x and t are the independent variables. Equation 3.6 is sometimes also written in the following form

$$\frac{\partial Q}{\partial x} + \frac{\partial A}{\partial t} - q = 0 \qquad (3.7)$$

with the discharge $Q = VA$, and A and Q now being dependent variables. Because $\partial A/\partial t = B\partial y/\partial t$, with B the width at the surface cross-section and y the depth of water above the bottom of the cross-section, Eq. 3.6 becomes

$$A\frac{\partial V}{\partial x} + VB\frac{\partial y}{\partial x} + B\frac{\partial y}{\partial t} - q = 0 \qquad (3.8)$$

Any of the above four equations, 3.5 through 3.8, may be used in practical applications.

Derivation of momentum (dynamic) equation. Newton's second law, the law of momentum, reads in a given direction as

$$\frac{d(mv)}{dt} = F \quad , \tag{3.9}$$

in which m is the mass, v is the velocity of an individual particle, and F is the resultant force of all forces acting on the particle. Replacing the movement of a particle by the movement of an elementary slice of water between sections x and $x + \Delta x$ of Fig. 3.1, and replacing the particle velocity v by the mean velocity V in the cross-section, the following velocity distribution coefficients must be introduced

$$\alpha = \frac{1}{AV^3} \iint_A v^3 \, dA \quad \text{,and} \quad \beta = \frac{1}{AV^2} \iint_A v^2 \, dA \; . \tag{3.10}$$

Coefficients α and β depend on velocity distributions in a cross-section A, and consequently depend on the shape, area, roughness and the mean flow velocity of a cross-section.

Equation 3.9 is applied along the direction of the conduit bottom, as shown in Fig. 3.1. All acting forces, external and internal, are projected in this direction. The tangential component, $G \sin \Psi$, of gravity force along the bottom, taking the positive sign with the direction of flow as shown by Fig. 3.2, is $\rho g A \Delta x \sin \Psi$. Friction force, F_f, with the head loss ΔH_f along the conduit bottom, is $F_f = -\rho g A S_F \Delta x$, with $\lim \Delta H_f/\Delta x = dH_f/dx = S_f$ for $\Delta x \to 0$ being the friction slope at x .

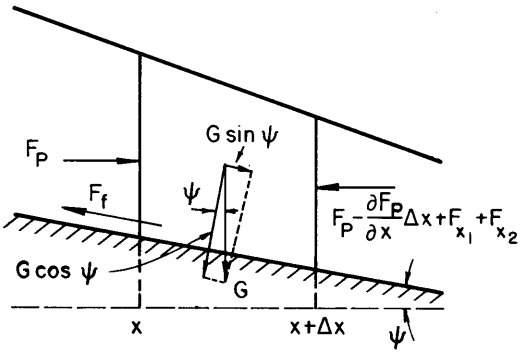

Fig. 3.2 Forces acting on the incremental volume of the channel.

Pressure forces, and other magnitudes as shown in Figs. 3.2, 3.3, and 3.4, can be expressed, assuming the hydrostatic pressure distributions along the verticals, as follows:

$$F_p = \int_0^y \rho g (y-\eta) \, B_\eta \, d\eta$$

and

$$\frac{\partial F_p}{\partial x} = \int_0^y \rho g \frac{\partial y}{\partial x} B_\eta \, d\eta + \int_0^y \rho g (y-\eta) \frac{\partial B_\eta}{\partial x} \, d\eta \quad ,$$

because y and B depend on x while η is independent of it. Since

$$\int_0^y B_\eta \, d\eta = A, \quad \text{and} \quad \Delta x \int_0^y \rho g (y-\eta) \frac{\partial B_\eta}{\partial x} \, d\eta = (F_1 + F_2) \quad ,$$

with F_1, F_2, and F_3 pressure forces defined in Fig. 3.4, then

$$\frac{\partial F_p}{\partial x} \Delta x = \rho g A \frac{\partial y}{\partial x} \Delta x - (F_1 + F_2) \quad ,$$

so that the resultant pressure force in the horizontal direction, normal to the cross-section, is

$$F_p - \left[F_p + \Delta x \, \partial F_p/\partial x + (F_1 + F_2)\right] = \Delta F_p \quad ,$$

and the pressure force in the direction of the bottom slope is given by

$$\Delta F_p = -\rho g A \frac{\partial y}{\partial x} \Delta x \cos \Psi \quad .$$

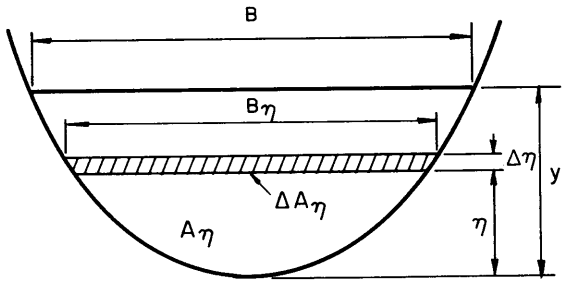

Fig. 3.3 Geometric elements of a channel with free surface flow.

The derivative of Eq. 3.9 is, without the consideration of the momentum of the total lateral inflow or outflow,

$$\frac{d(mv)}{dt} = mv \frac{\partial v}{\partial x} + m \frac{\partial v}{\partial t} + v^2 \frac{\partial m}{\partial x} + v \frac{\partial m}{\partial t} \; . \tag{3.11}$$

The mass m of an incremental area ΔA and an incremental distance Δx is $m = \rho \Delta A \Delta x = \rho v \Delta A \Delta t$. Because

$$mv \frac{\partial v}{\partial x} = \rho \Delta A \frac{1}{2} \frac{\partial (v^2)}{\partial x} \Delta x \quad ,$$

$$m \frac{\partial v}{\partial t} = \rho \Delta A \frac{\partial v}{\partial t} \Delta x \quad ,$$

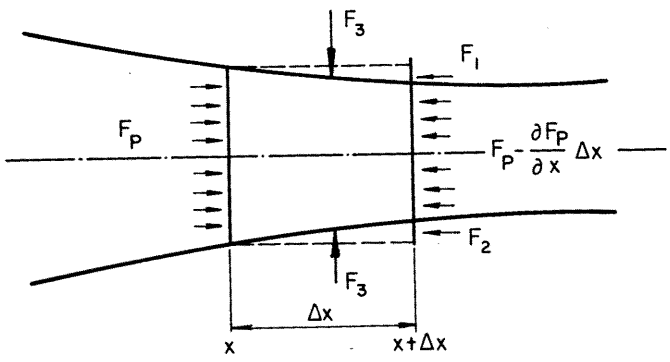

Fig. 3.4 Forces acting on an incremental slice in free-surface flow in a channel.

$\frac{\partial m}{\partial x} = \rho \Delta A \frac{\partial (\Delta x)}{\partial x} = 0$, as Δx is independent of x, and

$\frac{\partial m}{\partial t} = \rho \Delta A \frac{\partial (\Delta x)}{\partial t} = 0$, as Δx is independent of t, which gives

$$v \frac{\partial m}{\partial t} = \rho \Delta A \frac{1}{2} \frac{\partial (v^2)}{\partial x} \Delta x \quad ,$$

Eq. 3.11 now becomes

$$\frac{d(mv)}{dt} = \rho \Delta A \Delta x \left[\frac{1}{2} \frac{\partial (v^2)}{\partial x} + \frac{\partial v}{\partial t} \right] \quad . \tag{3.12}$$

Integrating Eq. 3.12 over the area A, the second term inside the brackets of Eq. 3.12 should be multiplied by β of Eq. 3.10, because the term is a function of v^2, and the first term inside the brackets of Eq. 3.12 should be multiplied by α of Eq. 3.10, because the term is a function of v^3. Therefore, Eq. 3.12 has two terms integrated over the area A in replacing ΔA by dA,

$$\iint_A \rho \frac{\partial v}{\partial t} \Delta x \, dA = \beta \rho A \Delta x \frac{\partial V}{\partial t} \quad ,$$

and

$$\frac{1}{2} \iint_A \rho \frac{\partial (v^2)}{\partial x} \Delta x dA = \frac{\alpha \rho A \Delta x}{2} \frac{\partial (V^2)}{\partial x} \quad ,$$

The momentum of the total lateral inflow or outflow, $q\Delta x$, is

$$\rho \iint_A q \Delta x v dA = \rho \iint_A q v^2 \Delta t dA = \beta \rho q \Delta x V \quad ,$$

because this term is a function of v^2, and β of Eq. 3.10 takes care of the velocity distribution across the area A. Equation 3.9 then becomes, by including the momentum of the total lateral inflow or outflow,

$$\frac{\alpha \rho A \Delta x}{2} \frac{\partial (V^2)}{\partial x} + \beta \rho A \Delta x \frac{\partial V}{\partial t} + \beta \rho q \Delta x V$$

$$= \rho g A \Delta x \sin \psi - \rho g A \Delta x S_f - \rho g A \Delta x \frac{\partial y}{\partial x} \cos \psi \quad . \tag{3.13}$$

For the approximations $\sin \psi \simeq \tan \psi = S_o$ with S_o the bottom slope, and $\cos \psi \simeq 1$ for small slopes, Eq. 3.13 changes to

$$\frac{\partial}{\partial x} \left(\frac{\alpha V^2}{2g} \right) + \frac{\beta}{g} \frac{\partial V}{\partial t} + \frac{\partial y}{\partial x} - S_o + S_f + \frac{\beta V q}{gA} = 0 \quad . \tag{3.14}$$

The slope of Fig. 3.1 is $S_o = - \partial z / \partial x$. The energy line gradiant is

$$\frac{\partial H_e}{\partial x} = \frac{\partial}{\partial x} \left(y + z + \frac{\alpha V^2}{2g} \right) \quad . \tag{3.15}$$

The general form of the momentum equation is then

$$\frac{\partial H_e}{\partial x} + \frac{\beta}{g} \frac{\partial V}{\partial t} + S_f + \frac{\beta V q}{gA} = 0 \quad . \tag{3.16}$$

Designating the terms in Eq. 3.16 by

$S_e = \frac{\partial H_e}{\partial x}$, the slope of the total energy line,

$S_a = \frac{\beta}{g} \frac{\partial V}{\partial t}$, the local acceleration slope, and

$S_q = \frac{\beta V q}{gA}$, the slope due to lateral inflow or outflow, Eq. 3.16 becomes

$$S_e + S_a + S_f + S_q = 0 \quad . \tag{3.17}$$

Multiplying Eq. 3.17 by Δx, with $\Delta H_e = S_e \Delta x$, $\Delta H_a = S_o \Delta x$, $\Delta H_f = S_f \Delta x$, and $\Delta H_q = S_q \Delta x$, then

$$\Delta H_e + \Delta H_a + \Delta H_f + \Delta H_q = 0 \quad , \tag{3.18}$$

or the sum of all slopes or of all head changes along Δx - length is zero. Equation 3.14 is sometimes given in the form

$$\alpha V \frac{\partial V}{\partial x} + \beta \frac{\partial V}{\partial t} + g \frac{\partial y}{\partial x} = g(S_o - S_f) - \frac{\beta\, Vq}{A} \quad . \quad (3.19)$$

Names and physical meanings of different terms in the two partial differential equations. The four terms in Eq. 3.5 when multiplied by $\Delta x \Delta t$ give the dimension of the volume. In the order of sequence, they have the following physical meanings: (1) wedge storage which results from the difference of depths at the beginning and the end of the elementary reach Δx by a change of area A along the conduit; (2) prism storage; (3) storage of rate-of-rise of level resulting from the rate-of-change of area A with time, and (4) storage, positive or negative, resulting from the lateral inflow or outflow.

The six terms in Eq. 3.14, in their order of sequence have the following physical meanings: (1) rate-of-change of velocity head, also called the dynamic head, the velocity-head term, the energy grade-line inclination, and the instantaneous energy gradient, which is the slope created by the change of velocity head along the conduit; (2) acceleration term as the ratio of accelerations, or the ratio of the change of velocity with time and the acceleration of gravity, also called the acceleration-head term, the velocity-hydrograph inclination, or the localized acceleration gradient; (3) rate-of-change of depth, or the depth-taper or the depth-change term, which is the slope created by the change of depth along the conduit; (4) bottom slope; (5) friction slope, and (6) part of the gradient on the energy line created by the lateral outflow or inflow. Equation 3.14 is differently expressed in various publications: dimensionless as in Eq. 3.14, or with dimensions of head, acceleration, momentum, energy, or in some other dimensions.

Selection of dependent variables. The two partial differential equations of unsteady free-surface flow are simplest in the case when the dependent variables are the mean velocity V and the depth y, with length x and time t being independent variables. In order to get a discharge hydrograph at a place x of the drain, the depth hydrograph $y(t)$, and velocity hydrograph $V(t)$ are first obtained. Then the area hydrograph $A(t)$ is determined from the depth hydrograph. The discharge hydrograph is then $Q(t) = V(t)\, A(t)$.

If the discharge hydrographs at different places should be the final result of flow routing through a storm drain, it might be convenient in some cases to use discharge Q and depth y as dependent variables, instead of velocity V and depth y. The computational procedure time using a digital computer (programming and computation time) might be somewhat longer in using Q and y than in using V and y as dependent variables.

Condition for the combined use of the two partial differential equations. The continuity equation involves the cross-section area, while the momentum equation is based on the rate-of-change of energy line, or of water surface position, plus the dynamic head. For irregular conduits with changing bottom slope and irregular cross section shape and area, the joint use of these two partial differential equations begins to create the first complexity in the mathematical analysis. The rate-of-change of cross-section characteristics, as related to the bottom position, and the rate-of-change of bottom slope with distance, when expressed in analytical form, generally enable the joint use of the two equations. Some assumptions and simplifications for cross-section, and for bottom position, are necessary to facilitate combined analytical treatment of Eqs. 3.5 and 3.14.

To use jointly Eqs. 3.5 and 3.14, the general area function in the form $A(y,x,t)$ should be available, where the variable t designates the change of the contour position with time for a movable cross-section boundary. Assuming that the conduit contours are fixed, and in some movable alluvial beds this assumption is only approximately satisfied, the area function becomes $A(y,x)$. There are two general cases to deal with when the relation of area to depth is considered for the geometry of the conduit:

(1) The conduit is prismatic, so that $A(y)$, or the area for a given y is independent of x. The simplest equation is $A = By$, a rectangular prismatic channel or conduit, with constant width B , which is usually used for the theoretical analysis of unsteady free surface flow in channels. A fit to natural channels of a power function, $A = py^s$, is often feasible with p and s constants. The area of the circular drains of a given diameter D is an arccosine function of the depth, and for a given y the area is independent of x.

(2) The geometric description of the conduit or the channel in a non-prismatic case is given by a function $A(y,x)$. The power function $A = py^s$ is applicable for some channels, with p and s being functions of x. The converging and diverging circular conduits belong to this category of conduits. This dependence of area to y and x coordinates should not be mixed with the change of area along the length of conduit in unsteady flow.

The joint use of Eq. 3.5 and 3.14 cannot be accomplished unless the relation of A and y is defined along the conduit. A storm drain is assumed to be prismatic conduit between the two successive manholes or junction boxes, so that $A(y)$ is valid for that reach, or the area is independent of x for a given y. In this case

$$\frac{\partial A}{\partial t} = \frac{\partial A}{\partial y} \frac{\partial y}{\partial t} = B \frac{\partial y}{\partial t} \quad (3.20)$$

and

$$\frac{\partial A}{\partial x} = \frac{\partial A}{\partial y} \frac{\partial y}{\partial x} = B \frac{\partial y}{\partial x} \quad , \quad (3.21)$$

with

$$B(y) = \partial A / \partial y \quad . \quad (3.22)$$

Introducing the expressions of Eqs. 3.20 and 3.21 into Eq. 3.5, it becomes

$$\frac{A}{VB} \frac{\partial V}{\partial x} + \frac{\partial y}{\partial x} + \frac{1}{V} \frac{\partial y}{\partial t} - \frac{q}{VB} = 0 \quad , \quad (3.23)$$

so that now both Eqs. 3.23 and 3.14, which describe the gradually varied free-surface unsteady flow, are given in dimensionless form.

It must be assumed also that the function of q is known in advance, which in a general form is given as $q(y,x,t)$. The variable t is necessary if there are any changes in time (slowly opening gates, or valves, and slow breaches of levees, in the case of channels or conduits). The term with q can be neglected for storm drains in general, except when they have long lateral spillway outflows, or also some continuous lateral inflows along the drain.

3.2 Discussion of Basic Assumptions Used in Derivation of the Two Partial Differential Equations

Assumptions in the derivation of differential equations. The general approach in deriving Eqs. 3.23 and 3.14 starts with the gradually varied unsteady free-surface water movement. This implies that the partial derivatives, $\partial V/\partial x$, $\partial V/\partial t$, $\partial y/\partial x$, and $\partial y/\partial t$ represent relatively small changes, in order that this basic assumption of gradually varied flow can be justified. It can be stated that the ambiguities arise mainly from the subjective interpretations by various investigators of the term "gradually varied." As far as the writers know, none of a myriad of investigations of unsteady free-surface flow since De Saint-Vernant's time, in this last hundred years, has attempted to quantify the term "gradually varied unsteady flow".

Nevertheless, the basic assumptions underlying the development and the application of Eqs. 3.23 and 3.14 are:

(1) Vertical acceleration can be neglected in comparison with the horizontal acceleration, or the vertical acceleration normal to the conduit in comparison with the acceleration along the conduit is very small, because of the gradual change of depth and discharge with time and distance. The steeper a wave, the less justified becomes this assumption. It is not applicable in the case of water surges, in the form of bores and sudden wave depressions.

(2) Unsteady flow as gradually varied has the hydrostatic pressure distribution along a vertical.

(3) Flow patterns in vertical planes parallel to the longitudinal axis of the channel are the same. This assumption in the case of curvilinear channels means that the vertical surfaces parallel to the longitudinal axis have the same flow pattern. The influence of the channel sides and their curvatures on flow patterns can be neglected. This assumption is equivalent to stating that the flow is two-dimensional, with third dimension effects negligible.

(4) Velocity distribution along a vertical in unsteady flow is the same as the velocity distribution in steady flow for the same water depth. It means that the velocity distribution coefficients α and β in Eq. 3.14 are constants for given values of discharge, depth, and velocity, or the unsteady flow does not influence these coefficients. Since this assumption depends on the rate-of-change of velocities with time and distance, it is justified only in the case of a gradually varied flow.

(5) Friction resistance in unsteady flow is the same as the friction resistance in steady flow. This assumption is justified only if the rate-of-change of velocities with respect to time and distance is small.

(6) Conduit slope is so small that $\cos \psi$ can be replaced by unity and $\sin \psi$ by $\tan \psi$.

Effects of these assumptions. There are no data in the literature that show the numerical individual effects of the above assumptions on the computed waves along the flow channel. Evidence is lacking for the justification of these six assumptions in terms of the specific characteristics of a wave, of a channel, and of a lateral inflow or outflow. Only global comparisons between the observed waves and the computed waves by using Eqs. 3.23 and 3.14, and usually with $\alpha = \beta = 1$, are available in literature, mainly in the most rudimentary form. The total influence of all of the above factors is relatively small in the case of very gradually varied unsteady flows. It is, therefore, justified to neglect the effect of six assumptions for this particular case.

It is expected that the assumption of a negligible vertical acceleration produces departures between the mathematical waves and the physical waves, which increases with an increase of rate-of-change of hydrograph. A relation $D = f(dQ/dt)$, with D the departure and dQ/dt the time rate-of-change of discharge hydrograph, would give a general picture of how the first assumption influences the computed wave movement. The second assumption is implicitly included in the effect of the first assumption, and its effect will also increase with an increase of rate-of-change of discharge hydrograph.

Mathematical methods available for the computation of unsteady free-surface flow are more accurate either for a very gradually varied flow, in the case where the two De Saint-Venant partial differential equations are used, or for a steep surge in the case where the available equations for traveling bores and steep depressions are used, than is the case for a steep wave which is between these two extremes.

The effects of the third assumption are negligible in straight line conduits, provided that the inlet conditions and lateral inflows do not create the persistent lateral oscillations of the body of water in conduit during the flood wave passage.

The effects of differences for velocity distribution coefficients and flow resistance factors between the unsteady and steady flow patterns are difficult to assess without accurate experiments and basic studies. The steeper a wave is, the more influence the constantly changing boundary layer in unsteady flow has on the flow resistances and velocity distributions. These differences must increase with an increase of the rate-of-change of the discharge hydrograph.

The effects of the sixth assumption are very small for storm drains with moderate slopes, say up to 5%.

The effects of the preceding assumptions are not simple to investigate in detail, even for a research conduit sufficiently long and with a large diameter. Although some discussions are given in other papers about effects of individual assumptions, the comparison between physical recorded waves in the research conduit and computed analytical waves by digital computer produces a general picture of the effects caused by all six assumptions. But even in computer analysis, various other errors mask an accurate detection of the resulting effects.

3.3 Derivation of Characteristic Equations

Definition of characteristics. The two partial differential equations for gradually varied unsteady free-surface flow in conduits, with the two dependent variables (V,y) and the two independent variables (x,t), have the general form

$$A_1 \frac{\partial V}{\partial x} + B_1 \frac{\partial V}{\partial t} + C_1 \frac{\partial y}{\partial x} + D_1 \frac{\partial y}{\partial t} + E_1 = 0 \ , \tag{3.24}$$

and

$$A_2 \frac{\partial V}{\partial x} + B_2 \frac{\partial V}{\partial t} + C_2 \frac{\partial y}{\partial x} + D_2 \frac{\partial y}{\partial t} + E_2 = 0 \ , \tag{3.25}$$

with the coefficients A, B, ..., and E being functions of V,y,x, and t besides being functions of conduit system properties.

Equations 3.24 and 3.25 are linear in relation to partial derivates, but the coefficients are also functions of dependent variables. Therefore, Eqs. 3.24 and 3.25 are called quasi-linear partial differential equations. For other data on the characteristic curves see reference [1]. The derivation in this study closely follows the derivation of characteristic curves derived by Courant and Friedrichs [2].

Equations 3.23 and 3.14, in order to be comparable with Eq. 3.24 and 3.25, must have the forms

$$\frac{A}{VB} \frac{\partial V}{\partial x} + \frac{\partial y}{\partial x} + \frac{1}{V} \frac{\partial y}{\partial t} - \frac{q}{VB} = 0 \tag{3.26}$$

and

$$\frac{\alpha V}{g} \frac{\partial V}{\partial x} + \frac{\beta}{g} \frac{\partial V}{\partial t} + \frac{\partial y}{\partial x} + S_f - S_o + \frac{\beta V q}{gA} = 0. \tag{3.27}$$

In this case

$$A_1 = \frac{A}{VB} \ , \ B_1 = 0, \ C_1 = 1, \ D_1 = \frac{1}{V}, \ E_1 = - \frac{q}{VB}$$

$$A_2 = \frac{\alpha V}{g} \ , \ B_2 = \frac{\beta}{g} \ , \ C_2 = 1, \ D_2 = 0, \ \text{and}$$

$$E_2 = S_f - S_o + \frac{\beta V q}{gA} \ .$$

Since E_1 and E_2 are not zero, Eq. 3.26 and 3.27 are nonhomogeneous nor are they reducible. Furthermore, the roles of dependent and independent variables are not interchangeable. In other words, the hodograph transformation of the (x,t)-plane into the (V,y)-plane is not applicable. The solution of Eqs. 3.26 and 3.27 gives the two functions V(x,t) and y(x,t).

Because the waves are gradually varied free-surface movements, it can be assumed that Eqs. 3.24 and 3.25 or Eqs. 3.26 and 3.27, as well as all coefficients in these equations, are continuous and possess as many continuous derivatives as may be required. It is also assumed that the condition

$$\frac{A_1}{A_2} = \frac{B_1}{B_2} = \frac{C_1}{C_2} = \frac{D_1}{D_2} \tag{3.28}$$

is not satisfied. This last assumption is true because from Eqs. 3.24 through 3.27, the inequality for Eq. 3.28 is

$$\frac{Ag}{\alpha V^2 B} \neq 0 \neq 1 \neq \infty \ . \tag{3.29}$$

A linear addition of Eqs. 3.24 and 3.25, with λ_1 and λ_2 the linear multipliers, respectively, gives

$$(\lambda_1 A_1 + \lambda_2 A_2) \frac{\partial V}{\partial x} + (\lambda_1 B_1 + \lambda_2 B_2) \frac{\partial V}{\partial t} + (\lambda_1 C_1 + \lambda_2 C_2) \frac{\partial y}{\partial x} +$$

$$+ (\lambda_1 D_1 + \lambda_2 D_2) \frac{\partial y}{\partial t} + (\lambda_1 E_1 + \lambda_2 E_2) = 0 \ . \tag{3.30}$$

For the (x,t)-plane, assume a curve is given as t(x). Then dt/dx is the tangent or the direction of this curve with V(x,t) and y(x,t) the solutions of Eqs. 3.24 and 3.25, or Eqs. 3.26 and 3.27. For this case, the total differentials are

$$dV = \frac{\partial V}{\partial x} dx + \frac{\partial V}{\partial t} dt \tag{3.31}$$

and

$$dy = \frac{\partial y}{\partial x} dx + \frac{\partial y}{\partial t} dt \ . \tag{3.32}$$

If λ_1 and λ_2 are selected to satisfy the condition

$$\frac{dt}{dx} = \frac{\lambda_1 A_1 + \lambda_2 A_2}{\lambda_1 B_1 + \lambda_2 B_2} = \frac{\lambda_1 C_1 + \lambda_2 C_2}{\lambda_1 D_1 + \lambda_2 D_2} \ , \tag{3.33}$$

Eq. 3.30 can be written as

$$(\lambda_1 A_1 + \lambda_2 A_2) dV + (\lambda_1 C_1 + \lambda_2 C_2) dy$$

$$+ (\lambda_1 E_1 + \lambda_2 E_2) dx = 0 \ . \tag{3.34}$$

The derivatives of V and y in Eq. 3.30 are combined in Eq. 3.34 so that the derivatives are in the same direction, dt/dx. This direction is called the characteristic direction and the corresponding curves in the (x,t)-plane are called the characteristic curves.

Equation 3.33 gives the ratio λ_1/λ_2 as

$$- \frac{\lambda_1}{\lambda_2} = \frac{A_2 dt - B_2 dx}{A_1 dx - B_1 dx} = \frac{C_2 dt - D_2 dx}{C_1 dt - D_1 dx} \ , \tag{3.35}$$

which can also be expressed as

$$a(dt)^2 - 2b \, dx \, dt + c(dx)^2 = 0 \tag{3.36}$$

with $a = A_1 C_2 - A_2 C_1$, $2b = A_1 D_2 - A_2 D_1$ and

$$c = B_1 D_2 - B_2 D_1 \ .$$

Equation 3.36 has two distinct roots for hyperbolic partial differential equations giving $b^2 - ac > 0$, excluding the case when all three coefficients (a,b, and c) vanish. Also $a \neq 0$ is satisfied in Eqs. 3.26 and 3.27 because $a = A_1C_2 - A_2C_1 = A/VB - \alpha V/g$, except for $V = \sqrt{gA/\alpha B}$, or for $V = C$, or when the water velocity is equal to the celerity of a small disturbance in quiescent water with hydraulic depth, D, equal to A/B.

Designating the slope of the characteristic curves by

$$\xi = \frac{dt}{dx} \quad , \tag{3.37}$$

Eq. 3.36 becomes

$$a\xi^2 - 2b\xi + c = 0 \quad , \tag{3.38}$$

which has two different real solutions, ξ_+ and ξ_-, (when $\xi_+ \neq \xi_-$), or

$$\xi_+ = \left(\frac{dt}{dx}\right)_+ \quad , \text{ and } \quad \xi_- = \left(\frac{dt}{dx}\right)_- \quad . \tag{3.39}$$

Because a, b, and c are functions of V, y, x, and t, so are the slopes of the characteristic curves or $(dt/dx)_+ = \xi_+(V,y,x,t)$ and $(dt/dx)_- = \xi_-(V,y,x,t)$. The two parts of Eq. 3.39 are two separate ordinary differential equations of the first order. They define two one-parameter families of characteristic curves, usually called just "characteristics", such as C_+ and C_- curves in the (x,t)-plane belonging to the solutions V (x,t) and y(x,t). These two families represent a curvilinear coordinate net and are shown in Fig. 3.5.

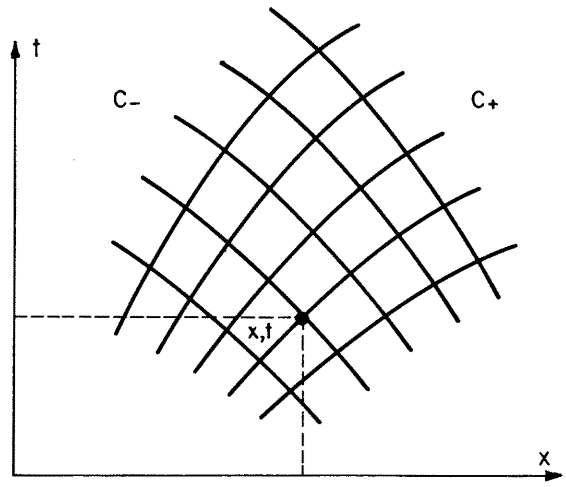

Fig. 3.5. Net of characteristic curves C_+ and C_- in (x,t)-plane.

Derivation of four characteristic ordinary differential equations. The four equations, 3.26, 3.27, 3.31, and 3.32, with four unknowns, $\partial V/\partial x$, $\partial V/\partial t$, $\partial y/\partial x$, and $\partial y/\partial t$, can be written into a single matrix equation:

$$\begin{bmatrix} A_1 & B_1 & C_1 & D_1 \\ A_2 & B_2 & C_2 & D_2 \\ dx & dt & 0 & 0 \\ 0 & 0 & dx & dt \end{bmatrix} \begin{bmatrix} \frac{\partial V}{\partial x} \\ \frac{\partial V}{\partial t} \\ \frac{\partial y}{\partial x} \\ \frac{\partial y}{\partial t} \end{bmatrix} = \begin{bmatrix} -E_1 \\ -E_2 \\ dV \\ dy \end{bmatrix} \quad . \tag{3.40}$$

Solving Eq. 3.40, the four derivatives are determined to be

$$\frac{\partial V}{\partial x} = \frac{\Delta_1}{\Delta} \, , \; \frac{\partial V}{\partial t} = \frac{\Delta_2}{\Delta} \, , \; \frac{\partial y}{\partial x} = \frac{\Delta_3}{\Delta} \, , \text{ and } \frac{\partial y}{\partial t} = \frac{\Delta_4}{\Delta} \, , \tag{3.41}$$

with

$$\Delta = \begin{bmatrix} A_1 & B_1 & C_1 & D_1 \\ A_2 & B_2 & C_2 & D_2 \\ dx & dt & 0 & 0 \\ 0 & 0 & dx & dt \end{bmatrix} \quad , \tag{3.42}$$

and Δ_1, Δ_2, Δ_3, and Δ_4 are obtained by replacing in Eq. 3.42 the first, second, third, and fourth column, respectively, by the column on the right side of Eq. 3.40.

A unique solution for the derivatives of Eq. 3.41 exists only if the determinant $\Delta \neq 0$. When the directions ξ_+ and ξ_- are such that the determinant Δ is zero there is no unique solution along these directions. It is initially assumed that the first derivatives of V and y in x and t have finite values in the (x,t)-plane. If the determinant Δ vanishes along directions ξ_+ and ξ_- then determinants Δ_1, Δ_2, Δ_3 and Δ_4 must also vanish; therefore, $\partial V/\partial x = 0/0$, $\partial V/\partial t = 0/0$, $\partial y/\partial x = 0/0$ and $\partial y/\partial t = 0/0$. Expanding Eq. 3.42 with $\Delta = 0$ it becomes $a(dt)^2 - 2b\,dx\,dt + c(dx)^2 = 0$, or Eq. 3.38 if Eq. 3.33 is satisfied. If this latter condition is not satisfied, then $2b = A_1D_2 - A_2D_1 + B_1C_2 - B_2C_1$. Equation 3.38 then gives

$$\left(\frac{dt}{dx}\right)_+ = \xi_+ = \frac{b + \sqrt{b^2 - ac}}{a} \tag{3.43}$$

and

$$\left(\frac{dt}{dx}\right)_- = \xi_- = \frac{b - \sqrt{b^2 - ac}}{a} \quad . \tag{3.44}$$

If Eqs. 3.43 and 3.44 are two real solutions, Eqs. 3.24 and 3.25 are a system of hyperbolic equations; for two complex solutions they are elliptic and for one real solution they are parabolic.

As previously mentioned, if the determinant Δ vanishes, and because the determinants Δ_1, Δ_2, Δ_3, and Δ_4 must vanish when Δ vanishes, the case of $\Delta_4 = 0$ with the determinant expanded gives, for example,

$$[(A_1C_2-A_2C_1)\frac{dt}{dx} - (B_1C_2-B_2C_1)]\frac{dy}{dx} + (A_1B_2-A_2B_1)\frac{dV}{dx} +$$

$$+ (A_1E_2-A_2E_1)\frac{dt}{dx} - (B_1E_2-B_2E_1) = 0 \quad . \qquad (3.45)$$

Substituting either $(dt/dx)_+ = \xi_+$ or $(dt/dx)_- = \xi_-$ of Eqs. 3.43 and 3.44, respectively, into Eq. 3.45, two ordinary differential equations in V and y along the characteristic curves ξ_+ and ξ_- are obtained.

Simultaneously solving these two ordinary differential equations, with the two unknowns V and y give the functions $V(x,t)$ and $y(x,t)$. No new relations are obtained when the determinants Δ_1, Δ_2, and Δ_3 are made equal to zero. Using the coefficients of Eqs. 3.24 and 3.25 as given by Eqs. 3.26 and 3.27, and putting $2b = A_1D_2-A_2D_1 + B_1C_2 - B_2C_1$ in Eqs. 3.43 and 3.44, the characteristic directions or slopes of these two latter equations become

$$\left(\frac{dt}{dx}\right)_+ = \frac{2\beta}{V(\alpha+\beta) + \sqrt{(\alpha-\beta)^2V^2 + \frac{4A\beta g}{B}}} = \xi_+ \qquad (3.46)$$

and

$$\left(\frac{dt}{dx}\right)_- = \frac{2\beta}{V(\alpha+\beta) - \sqrt{(\alpha-\beta)^2V^2 + \frac{4A\beta g}{B}}} = \xi_- \quad . \qquad (3.47)$$

The two ordinary differential equations for V and y along the characteristics curves ξ_+ and ξ_- are obtained from Eq. 3.47 by replacing dt/dx with ξ_+ and ξ_-, respectively, and introducing the coefficients from Eqs. 3.26 and 3.27. The equation becomes

$$\left[\left(\frac{A}{VB} - \frac{\alpha V}{g}\right)\xi_+ + \frac{\beta}{g}\right]\frac{dy}{dx} + \left(\frac{A\beta}{VBg}\right)\frac{dV}{dx} + \frac{A}{VB}(S_o-S_f +$$

$$+ \frac{\beta Vq}{A})\xi_+ - \frac{\beta q}{gVB} = 0 \quad , \text{ and} \qquad (3.48)$$

$$\left[\left(\frac{A}{VB} - \frac{\alpha V}{g}\right)\xi_- + \frac{\beta}{g}\right]\frac{dy}{dx} + \left(\frac{A\beta}{VBg}\right)\frac{dV}{dx} + \frac{A}{VB}(S_o-S_f +$$

$$+ \frac{\beta Vq}{gA})\xi_- - \frac{\beta q}{gVB} = 0 \quad . \qquad (3.49)$$

Equations 3.46 through 3.49 are called the four characteristic ordinary differential equations and are the equivalent set to the two partial differential equations, 3.26 and 3.27.

Assuming that $\alpha = \beta = 1$, and $q = 0$ (no distributed lateral inflow or outflow per unit length), then Eqs. 3.46 through 3.49 become

$$\left(\frac{dt}{dx}\right)_+ = \xi_+ = \frac{1}{V + \sqrt{gA/B}} \quad , \qquad (3.50)$$

$$\left(\frac{dt}{dx}\right)_- = \xi_- = \frac{1}{V - \sqrt{gA/B}} \quad , \qquad (3.51)$$

$$\left[\left(\frac{A}{VB} - \frac{V}{g}\right)\xi_+ + \frac{1}{g}\right]\frac{dy}{dx} + \frac{A}{gVB}\frac{dV}{dx} + \frac{A}{VB}(S_o-S_f)\xi_+ = 0, \qquad (3.52)$$

and

$$\left[\left(\frac{A}{VB} - \frac{V}{g}\right)\xi_- + \frac{1}{g}\right]\frac{dy}{dx} + \frac{A}{gVB}\frac{dV}{dx} + \frac{A}{VB}(S_o-S_f)\xi_- = 0. \qquad (3.53)$$

The term $\sqrt{gA/B} = C$ in Eqs. 3.50 through 3.53 is the celerity of a small disturbance in quiescent water with a cross section area A and width B.

Equation 3.26 and 3.27 are hyperbolic. Therefore, they are quasi-linear hyperbolic partial differential equations of gradually varied free-surface unsteady flow with two dependent and two independent variables.

These two sets of four equations, 3.46 through 3.49 and particularly 3.50 through 3.53, will be used predominantly in the numerical integration by the method of characteristics shown in Chapter 3, Part IV, Hydrology Paper No. 46.

General properties. The coefficients of Eqs. 3.26 and 3.27 contain, beside the variables V and y, quantities A, B, q, α, β, S_f and S_o, and a constant, g. The Darcy-Weisbach formula for resistance losses is $S_f = (f/4R)(V^2/2g)$, with f the Darcy-Weisbach friction factor, and R the hydraulic radius. The coefficient f, in general, is a function of the Reynolds number, but for pipes of a given roughness f is a constant. In this case A, B, R, f, α, β, and q are generally functions of y and x only. The quantities A, B, R, f, α, β, q, and S_o do not contain derivatives of y and V, but are functions of V, y, x and t.

The main feature of this treatment of characteristic curves is the replacement of the original system of the two partial differential equations, 3.26 and 3.27, by the characteristic system of the four ordinary differential equations, Eqs. 3.46 through 3.49 in the general case, and Eqs. 3.50 through 3.53 in the particular case. Every solution of the original system satisfies this characteristic system. The converse is also true; every solution of the characteristic system in Eqs. 3.46 through 3.49 satisfies the original system in Eqs. 3.26 and 3.27, provided that the determinant, Δ, of Eq. 3.42 does not vanish.

If the differential equations 3.26 and 3.27 are linear, then ξ_+ and ξ_- are known functions of x and t, so that Eqs. 3.46 and 3.47 are not coupled with Eqs. 3.48 and 3.49. In this case Eqs.

3.46 and 3.47 determine two families of characteristic curves, C_+ and C_-, which are independent of the solution. A linearization of Eqs. 3.26 and 3.27 introduces such a departure from real flow phenomena that this case will not be pursued further.

If $E_1 = E_2 = 0$, and if $A_1,\ldots,D_2$ depend on V and y only, which would be a gross approximation of real flow conditions, the situation is similar in that the differential equations are reducible, the slopes ξ_+ and ξ_- are known functions of V and y and Eqs. 3.48 and 3.49 are independent of x and t. The same case occurs when E_1 and E_2 do not vanish but depend on V and y only. This last case is applicable to Eqs. 3.26 and 3.27 under the condition that the conduit is prismatic and the bottom slope, S_o, is constant, because all coefficients $A_1,\ldots,E_2$ may be considered as dependent only on V and y. The characteristic curves in the (V,y)-plane, designated as Γ_+ and Γ_- are the images of the characteristic curves C_+ and C_- in the (x,t)-plane, and are independent of the special solution of $V(x,t)$ and $y(x,t)$. However, these assumptions made to convert Eqs. 3.26 and 3.27 into reducible equations are already an approximation of real free-surface unsteady flow.

Because the objective of this study is to determine the effects of different assumptions or the effects of neglected factors, any restriction in the basic general differential equations would mean a departure from the study's basic approach.

The boundary conditions are of a major importance in any integration using hyperbolic differential equations. A curve, with all values of V and y in the (x,t)-plane must be known. In the most general case, and for a free-surface unsteady flow in conduits, either a velocity hydrograph, $V(t)$, or a discharge hydrograph, $Q(t)$, is known for a given x-value. In the first case, the boundary conditions are given along a constant distance line in the (x,t)-plane for which all values of $Q(t)$ are known. The initial conditions are given along a constant time line in the (x,t)-plane with the corresponding values of V and y known. As soon as the initial line is known, a solution of $V(x,t)$, $y(x,t)$ of Eqs. 3.26 and 3.27 must be found which approximates the initial line and which takes on the prescribed values of V and y.

Using the characteristic form (Eqs. 3.46 through 3.49, or Eqs. 3.50 through 3.53) of the partial differential equations, 3.26 and 3.27, the integration problem can be treated as the corresponding problem for the ordinary differential equations.

The integration process shows that the values V and y at the point $P(x,t)$ depend on the initial values along the line $t = 0$ between the points (o,x_1) and (o,x_2) as indicated in Fig. 3.6. In other words, the values V and y at point $P(x,t)$ depend only on the values V and y in the segment x_1 to x_2 or on the values V and y between the characteristic curve C_- through x_2 and the characteristic curve C_+ through x_1. The interval x_1 to x_2 and the two characteristic curves, C_+ and C_-, passing through point $P(x,t)$ in Fig. 3.6, determine the domain of dependence. The values V and y at $P(x,t)$ are affected by the values V and y inside the domain of dependence and are not affected by the values outside.

On the other hand, if a point $R(x,o)$ is selected in the initial line of Fig. 3.6, with the initial values V and y, the characteristic curves C_+ and C_- through point R determine the range of influence. Only the values V and y at the points (x, t) inside the range of influence depend on the initial values of V and y of point R; the outside points do not.

If the values of the first and higher partial derivatives of V and y are continuous along the initial line, they are also continuous in all the points in the (x,t)-plane. If, however, there are some places of discontinuity, either at the initial line $(\partial V/\partial x,\ \partial V/\partial t,\ \partial y/\partial x,\ \partial y/\partial t)$ or higher, the partial derivatives are not continuous. This means that if some disturbances exist, or the discontinuities are introduced at some points in the (x,t)-plane, then the discontinuities in derivatives occur only along characteristics passing through the discontinuity points on the initial line. Another way of expressing it is that the discontinuities in the first or higher partial derivatives of V and y propagate along the characteristic lines in the (x,t)-plane. These discontinuities propagate along one or both of the two characteristics through the point of the source of discontinuity, and they can never disappear. The discontinuities refer to the derivatives of V and y, but not to the discontinuities in V and y themselves, which propagate as surges (bores or depressions).

The characteristic form (Eqs. 3.46 through 3.49, or Eqs. 3.50 through 3.53) of differential equations 3.26 and 3.27 are especially useful for numerical solutions. If the differential equations are replaced by equations of finite differences the numerical solutions can be done easily, especially if a digital computer is used.

The characteristic curves, particularly in their simplified form, are useful in analyzing the properties of the solutions and studying the initial and boundary conditions.

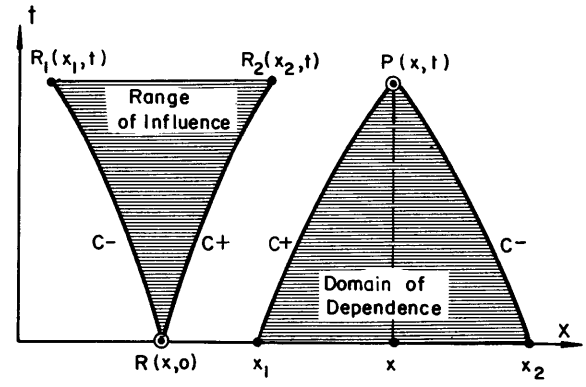

Fig. 3.6. Domain of dependence and range of influence of characteristic curves in the (x,t)-plane.

Chapter 4

PHYSICAL WAVES, EXPERIMENTAL WORK AND RESULTS

A detailed description of the experimental facilities used for this study is given in Hydrology Paper No. 44. Therefore, only a brief summary is given here.

4.1 Experimental Facilities

Circular conduit system. A pipeline 822 ft long with a 3 ft outside diameter was used as the experimental conduit. The entire 822 ft of pipe was supported on inclined rails about 20 ft apart, which permitted the pipe to be moved along the inclined plane to any slope between 0 and approximately 4 percent. Flow was introduced into the circular storm conduit by means of an inlet structure that could be adjusted to develop the desired subcritical or supercritical flow conditions at the entrance to the storm conduit and which included a baffle system for developing a uniform entrance condition with minimum downstream surface waves. This type of intake structure was developed from a special reduced model study on a much smaller scale.

Three square junction boxes for lateral inflows were installed along the storm conduit, thus dividing the conduit into four straight sections each about 200 ft long. Flow from a 12-in lateral pipe entered into each junction box at a 90-degree angle, simulating the actual junctions of storm drains. Experiments were conducted on the 822 ft conduit without the junction boxes and with the junction boxes. The outflow of free-surface flowing water was either as a free fall or as a controlled outfall.

Water supply to the 3-ft diameter storm conduit was by gravity through a 26-in underground pipeline from the nearby Horsetooth Reservoir and was conveyed into College Lake after it passed through a special collecting and energy dissipating structure. Figure 4.1 gives the general layout of this experimental facility in the outdoor laboratory of the Engineering Research Center at Colorado State University. Figures 4.2 and 4.3 show the facility from the upstream and downstream sides.

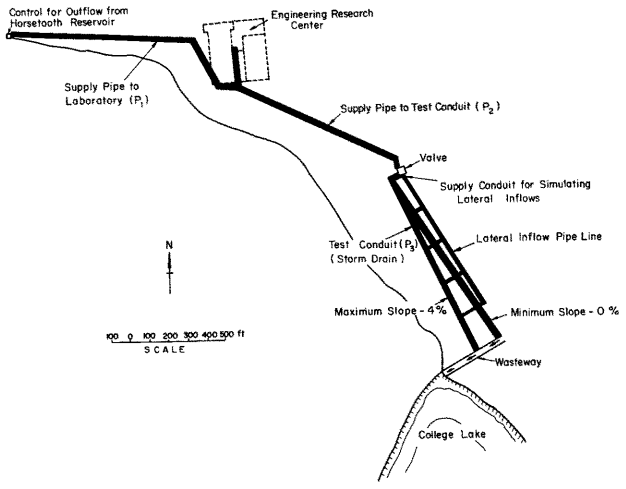

Fig. 4.1. General scheme of the experimental conduit with water supply and removal.

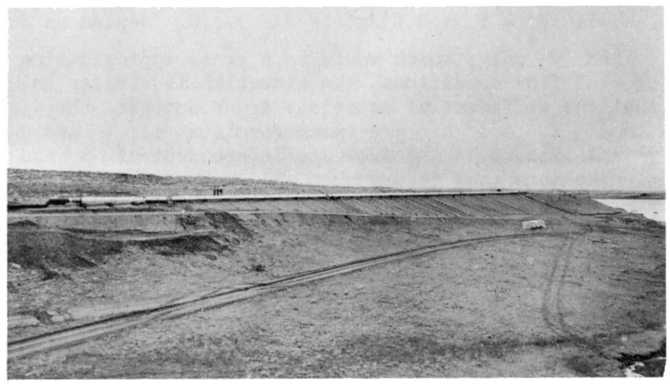

Fig. 4.2. A view from upstream of the circular storm conduit on the hillside of the outdoor laboratory at Colorado State University Engineering Research Center.

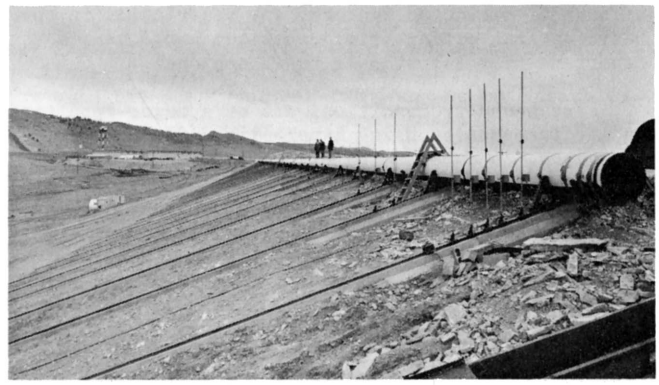

Fig. 4.3. A view from downstream of circular storm conduit and the inclined rails.

Instrumentation. Three sizes of sharp-edged circular orifice plates, based on the different orifice-to-pipe diameter ratios, were designed, calibrated, and used to measure the main inflow rate into the storm conduit. The three sizes were needed to accurately measure small, medium and large discharges through the conduit. The ratios of the diameter of orifice (d) to the diameter of pipe (D) were 0.35, 0.50, and 0.70, with area ratios of approximately 1/8, 1/4 and 1/2, respectively. The calibration equations, $Q = C_d m A \sqrt{2gH}$ obtained for the three orifice meters under steady flow conditions are: for $m = d/D = 0.35$, $Q_1 = 2.102 \sqrt{H}$, with $C_d = 0.606$; for $m = d/D = 0.50$, $Q_2 = 4.439 \sqrt{H}$, with $C_d = 0.627$, and for $m = d/D = 0.70$, $Q_3 = 9.783 \sqrt{H}$ with $C_d = 0.705$. In t ese equations C_d is the discharge coefficient, H is the differential head across the orifice in feet, A is the cross section area of the conduit in square feet, and Q is the discharge in cubic feet per second. Results indicate that each of the three discharge coefficients, C_d is constant for the Reynolds number within the range 2×10^5 to

2×10^6. Considerations were also given to the problem of orifice calibration equations under unsteady flow conditions, but no significant deviation was found. (For more details see Hydrology Paper No. 44, Chapter 3, Pages 19-20).

Small propeller current meters with electric counters, manufactured by Ott, were selected to measure the flow velocity distributions in the storm conduit. The current meters were first carefully recalibrated by making several runs by a tow car at a constant speed over a given distance, and then by operating the tow cars at different speed covering their operational range. Good agreement was obtained between the recalibration values and those furnished by the manufacturer. (For more details see Hydrology Paper No. 44, Chapter 3, Pages 20-26).

Pressure transducers were used to measure water levels and pressure differences in various measurements. The calibration of pressure transducers was considered from these standpoints: (a) that the output voltage be zero for zero pressure input; (b) that the output voltage be a linear function of the impressed pressure differential; (c) that the output voltage did not change with time and if it does, it must be systematically checked, and (d) that the proportionality constant between the input and output be known before the observed data is interpreted. These conditions were checked for all transducers used, and with sufficient care in installation and adequate warm-up time, all transducers met the necessary conditions. (For further details see Hydrology Paper No. 44, Chapter 3, pages 26-27).

Data recording system. The outdoor circular storm conduit is located about 1,500-ft from the Colorado State University Engineering Research buildings. Data taken from the storm conduit were transformed into electric voltage signals by the pressure transducers and were then transmitted by individual shielded cables to an indoor analog-to-digital converter. The digitized information was punched onto cards or paper tape, for later computer analysis. Figure 4.4 shows the general scheme of the data recording system. (For more details see Hydrology Paper No. 44, Chapter 4, pages 28-29).

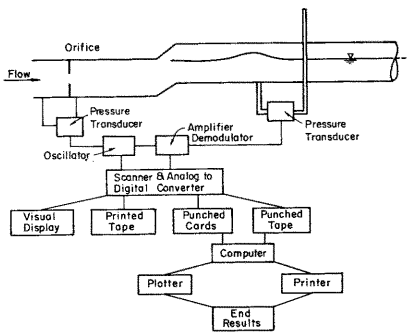

Fig. 4.4. Scheme of the general data recording system.

4.2 Results of Steady Flow Measurements

Hydraulic resistance. An experimental approach to the determination of conduit boundary roughness was investigated. The Darcy-Weisbach friction factor (f) and the corresponding Reynolds number (R_e) were computed from measured depths and discharges. Figure 4.5 represents the results in a range of depths from 0.56 to 2.6 feet, or depth-to-diameter ratios of 0.19 to 0.89. The discharges varied from 2.25 to 72.0 cfs. The corresponding Reynolds number range is from approximately 3×10^4 to 1×10^6. The Prantl-von Karman equation

$$\frac{1}{\sqrt{f}} = a \log_{10} (R_e \sqrt{f}) + b, \qquad (4.1)$$

with $a = 2.0$ and $b = 0.4$ for smooth boundary flow is also plotted in Fig. 4.5. The two points in Fig. 4.4 that extremely vary over the other points and the curve of the Prandtl-von Karman equation are assumed as mistakes either in observation or in the processing of data. For data shown in Fig. 4.5, the values of the constants a and b in Eq. 4.1 are 2.075 and 0.1434, respectively, or the boundary of the conduit used in this experimental study is hydraulically smooth.

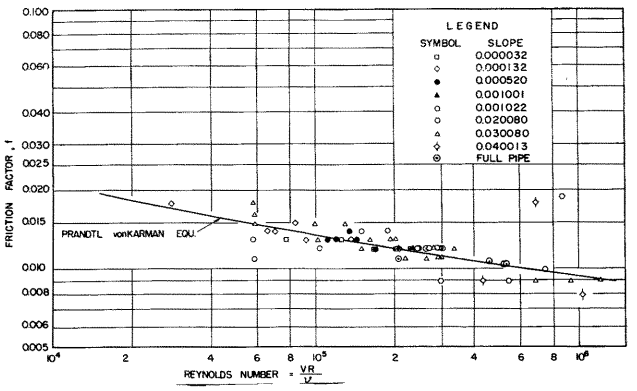

Fig. 4.5. Relationship of the Darcy-Weisbach friction factor f to Reynolds number R_e.

The evaluation of f from Eq. 4.1 for a given R_e requires an iterative procedure. To simplify computations (within practical limits of Reynolds numbers for specific conditions) it is convenient to use a simplified form of the f to R_e relation. A practical form of the expression for this relation is

$$f = c(R_e)^d \quad , \qquad (4.2)$$

in which c and d are constants; they were evaluated from data in Fig. 4.5 and found to be 0.10939 and -0.17944, respectively.

Although Fig. 4.5 shows a decrease of f with an increase of R_e it can be shown that for a limited range of R_e the changing Darcy-Weisbach friction factor f may be replaced by an average value or a representative constant. An average Darcy-Weisbach friction factor of 0.012 is considered representative of the experimental conduit for the range of R_e obtained in this study. (For details of this derivation see Hydrology Paper No. 44, Chapter 5, pages 30-31, and Hydrology Paper No. 45, Chapter 3, pages 10-15).

Junction box losses. The evaluation of energy losses accompanying lateral inflow into a main conduit with free-surface flow was accomplished through two separate experimental facilities. A plastic pipe

with a 6-in diameter was used to economically develop the basic evaluations of junction box losses. The results were then verified by the tests in the 3-ft diameter conduit. Agreement between the two systems was good, based on the Froude similitude relation.

The junction box used in the large model study was square above the half-full level of the storm conduit. Two positions of the inlet were tested, the upper and lower. The crown of the upper inlet was the same elevation as the crown of the storm conduit at its point of entry into the junction box. The invert of the lower inlet was made coincident with the invert of the storm conduit at their junction point, which was the centerline of the junction box. The arrangement of the model junction box is shown in Fig. 4.6.

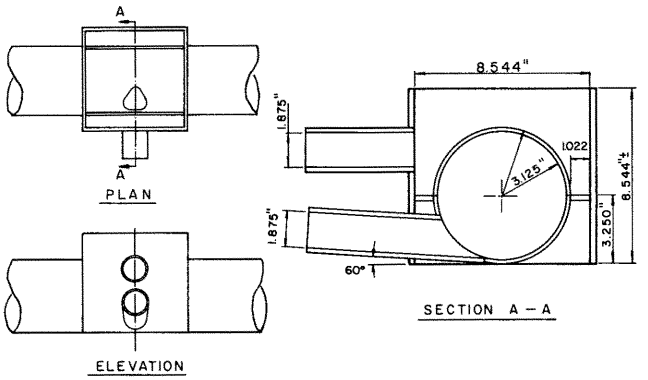

Fig. 4.6. The junction box used in the model study.

The power at any given cross section of the conduit is found by multiplying the energy at its section by the weight rate of flow past the section. The power equation can be written then as

$$P = \gamma Q E \tag{4.3}$$

or

$$P = \gamma Q\left(z + y + \frac{V^2}{2g}\right) , \tag{4.4}$$

in which P is the power in foot-pounds per second, Q is the discharge in cubic feet per second, γ is the specific weight of water in pounds per cubic feet, z is the elevation of the channel bottom above the zero datum, y is depth of flow, and V is the mean velocity.

It was assumed that the power loss ratio, P_r, could be expressed as a function of the relative discharge, Q_r, of the lateral to the main conduit flow when using the upper inlet. The functional relation between the power loss ratio and the discharge ratio was found to be

$$(P_r - 0.77)(Q_r + 0.55) = -0.482 \tag{4.5}$$

for the upper inlet.

Power losses for the lower inlet were analyzed in terms of the ratio of lateral inflow discharge to the main conduit discharge, Q_r, and the ratio of the upstream depth to the conduit diameter, D_r. The power loss ratio from this procedure is

$$P_r = \frac{-2.78 + 1.71\ D_r}{Q_r + 3.122 - 0.167\ D_r} + 0.77, \tag{4.6}$$

for the lower inlet. (For additional details of the study of junction box head losses see Hydrology Paper No. 44, Chapter 2, Pages 6-13, and Hydrology Paper No. 45, Chapter 4, Pages 16-20).

Cross-sectional velocity distributions. To determine experimentally the velocity distribution coefficients, α and β, measurements of the distribution of conduit cross-sectional velocities were conducted. Time-average point velocities were measured by the Ott current meters. A special procedure was developed for measuring velocities and for computing the velocity distribution coefficients, as described in Hydrology Paper No. 45, Chapter 5.

It was expected that the velocity distribution coefficients would differ with changes in those parameters that determine the velocity profiles. The parameters that primarily affect the velocity profile are the geometry of the cross section, the properties of the fluid, the condition of the boundary surface (roughness), and the mean velocity. All of these variables are encompassed in the Reynolds number (VR/ν) and the Darcy-Weisbach friction factor (f).

Because the Darcy-Weisbach friction factor is related to the Reynolds number, one would expect to be able to predict α and β coefficients to the friction factor f. Since the range of the Darcy-Weisbach friction factor is small for the series of data in this study, and because the Reynolds number fluctuates within a limited range, the spread of computed α and β coefficients is apparently due to other causes.

Figure 4.7 displays the relation of α and β with the Reynolds number. These results indicate an increase of the velocity distribution coefficients with a decrease of Reynolds number. The apparent scatter of points around a smooth curve may be assumed to be a result of observational and computational errors.

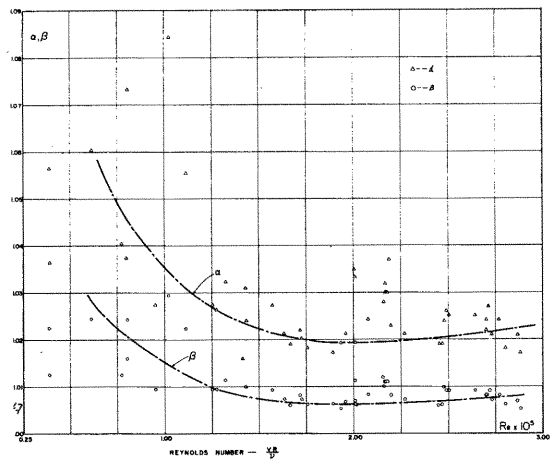

Fig. 4.7. Velocity distribution coefficients as related to the Reynolds number.

The effect of depth on the velocity distribution coefficients is presented in Fig. 4.8. This figure

indicates slightly increasing values of both β and α as depth decreases. This is expected because deviation from the mean velocity becomes greater and the friction factor becomes effectively larger as the depth decreases. At a depth of half the conduit diameter the β - coefficient has a value of approximately 1.01 and the α - coefficient has a value of approximately 1.03. At greater depths, β reduces to approximately 1.007 and α to approximately 1.022. For depths less than half the conduit diameter, both coefficients tend to increase. Data were not available for depths less than one-fourth of a diameter.

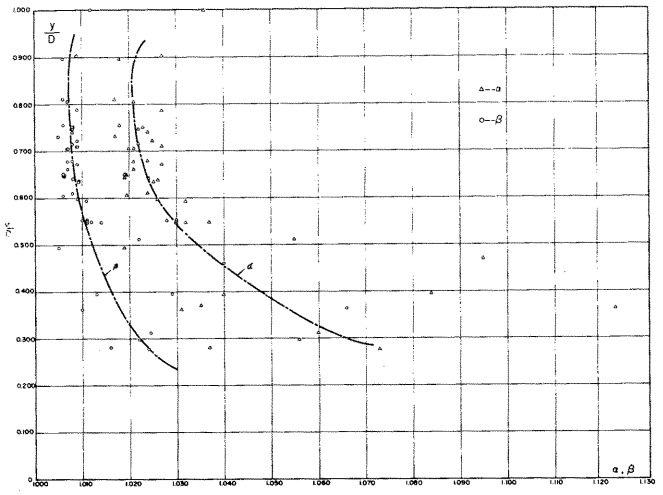

Fig. 4.8. Velocity distribution coefficients as related to the depth of flow in a circular cross section.

The results of this study are applicable to hydraulically smooth circular cross sections flowing partially full and having Reynolds numbers in the range 0.4×10^5 to 3.00×10^5. For smaller Reynolds numbers the observed velocity distribution coefficients are greater but display a greater dispersion about a smooth curve. For larger Reynolds numbers the values tend toward invariance with lesser dispersion. The relation between α and β has been demonstrated both theoretically and experimentally and can be expressed: $(\alpha-1)/(\beta-1) = 2.3$ to 3.0. The value of 3.0 is representative of the experimental results. A representative value of α for the experimental conditions is 1.03 and a representative value of β for the experimental conditions is 1.01. (For additional details of the study of velocity distribution coefficients see Hydrology Paper No. 45, Chapter 5, pages 21-29).

Controlled and free outfall. The mathematical simulation of the downstream boundary condition for the controlled outflow required the calibration of a terminal (end) restriction. Any geometric configuration was acceptable if it satisfied certain criteria:

1. The discharge as a function of depth could be expressed simply, such as $Q = my^n$ in which m and n are constants experimentally determined and y is the depth of flow upstream of the restrictions.
2. The restriction was not so great as to cause the pipe to flow full under the maximum anticipated hydrograph discharge.
3. The approach-velocity distribution was symmetrical and did not differ appreciably from the undisturbed flow.

These criteria were satisfied by a constriction consisting of five 7-inch vertical wooden slats held in position by two 1/2-inch wide vertical aluminum H-sections. The clear opening was five inches between supports. The discharge could thus be controlled by varying the vertical position or by removing one or more slats.

Calibration of various combinations of openings was made by measuring the corresponding discharge and the water surface elevation approximately 20 ft upstream of the control. For the range of discharges anticipated in the unsteady flow runs, it was concluded that the best combination of openings was with the three center slats removed.

For this condition the relation between discharge and depth was determined to be

$$Q = 4.84\ y^{1.35} \quad . \qquad (4.7)$$

This relation applies for depths between approximately one-third and eight-tenths of full diameter, and at 20 feet upstream from the conduit end. This gate configuration and flow relation was used for all subsequent evaluations of boundary conditions in which backwater profiles were the initial condition. No attempt was made to modify this steady state relation for unsteady flows.

For a free outfall the location of the theoretically computed critical depth occurs some distance upstream from the end of the conduit. The purpose of experimental measurements was to determine the location of the critical depth. This position then served as the location of the downstream boundary. Water-surface profiles were measured for a range of discharges from 2.10 to 16.62 cfs. The channel slope ranged from 0.000032 to 0.001022 foot per foot.

Figure 4.9 presents the water-surface profiles and the locations of the computed critical depth within the range of observed end depths; the mean ratio of end-depth to critical-depth was 0.750. This ratio tended to be smaller than the mean for the lower depths.

The location of the computed critical depth from the channel end varied from less than 3.5 times the critical depth to almost 5.5 times the critical depth. A location of 4.5 times the critical depth was considered typical and was used in subsequent computations. (For details of free or controlled outflow boundary conditions see Hydrology Paper No. 44, Chapter 5, pages 30-32, and Hydrology Paper No. 45, Chapter 6, pages 30-32).

Flow regimes. The steady non-uniform flow in subcritical and supercritical regimes were established experimentally in the storm conduit. The steady non-uniform flows (backwater curves) at the hydrograph base discharge were used as initial conditions in computing the unsteady flow equations. (For details on how the initial non-uniform steady conditions were computed see Hydrology Paper No. 45, Chapter 7, pages 33-36).

The discharge and slope corresponding to the desired depth of flow in subcritical or supercritical

regimes were estimated from observations. The downstream control gate was adjusted to produce the desired type of backwater or drawdown curve. Because of the time required for steady state conditions to develop, it was not practical to adjust the downstream control until a constant depth developed throughout the length of the pipe. Thus, several conditions of non-uniform flow were established both above and below normal depth. Hook gage readings at the various piezometer locations were made at approximately 15-minute intervals until such time as the readings indicated stabilization.

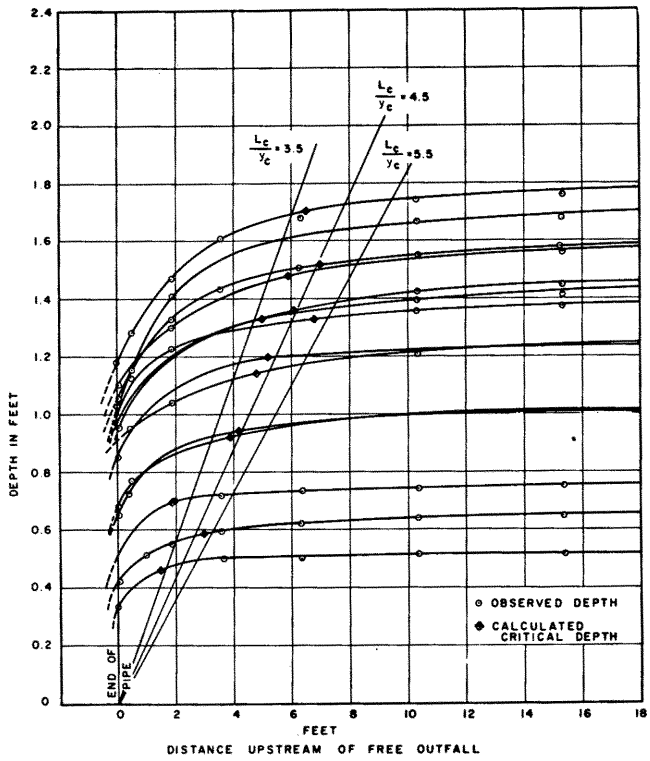

Fig. 4.9. Location of the critical depth of a circular cross section free outfall.

Water surface elevations were determined by means of hook gage readings taken in gage wells located at 16 positions along the pipe. These wells were connected to the invert of the pipe through a flexible hose. The piezometer openings were 1/16 in in diameter. At each position there were a sufficient number of openings to insure a reasonable response time for each well.

The invert slope of the pipe was carefully determined by a precise self-leveling level with an optical micrometer which permitted measurements of the invert to the nearest 1/1000 of an inch. Readings were taken every 20 ft and a least-square determination of the mean slope was computed. If the maximum deviations at any point exceeded approximately 3/100 of a foot, from the mean line, adjustments to the pipe invert were made.

4.3 Physical Waves

Inflow hydrographs. Inflow hydrographs were developed by a motor operated 26-in diameter ball-valve at the upstream inlet of the main storm conduit and the 12-in diameter gate-valves on the lateral inflow pipelines. The initial and maximum discharges were established for a given experiment, and the valve operated at constant speed within this range. The lateral inflow discharges varied as the openings of the main valve. The discharge hydrographs were measured and recorded by pressure transducers connected across the orifices which were installed a short distance downstream of the valves. Figures 4.10 and 4.11 show the experimentally observed inflow discharge hydrographs of the main storm conduit and the lateral flow, respectively.

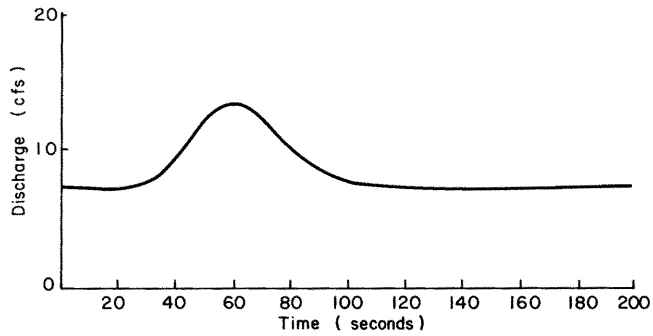

Fig. 4.10. A recorded inflow discharge hydrograph to the main conduit.

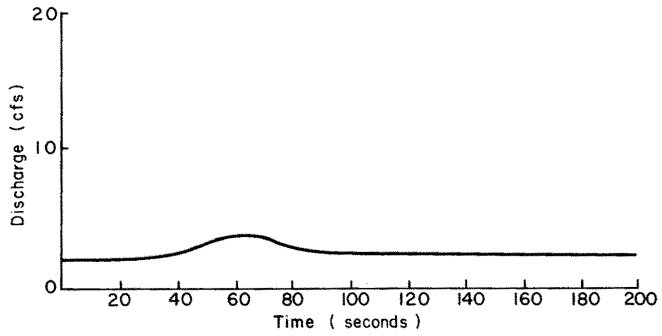

Fig. 4.11. A recorded inflow discharge hydrograph from a lateral conduit.

Wave propagation. After the generation of inflow hydrographs, the subsequent wave depths were measured at several stations downstream as the flood-wave propagated along the conduit. Waves were measured at distances of 50.00 ft, 410.00 ft, and 771.70 ft from the entrance during experiments conducted the summer of 1965 and at distances of 50.00 ft, 251.24 ft, 387.70 ft, 462.56 ft, 669.83 ft, and 771.70 ft during experiments conducted the summer of 1966. Flood wave depths were measured by pressure transducers connected between the conduit invert and a set of manometers.

The measured quantities were plotted as (1) depth versus time relations, (2) depth versus distance relations, and (3) wave peak depth versus distance and time relations. These experimentally measured physical waves were used to compare and check the analytically computed mathematical waves. Complete results of measured inflow hydrographs and physical waves are presented in Appendices 3, 4, and 5. Analysis of the comparison between physical waves and computed waves is given in Chapter 6 of this paper.

Chapter 5

COMPUTATION OF WAVES BY ANALYTICAL METHODS

This chapter describes briefly a few finite-difference schemes used for the numerical solution of the two quasi-linear hyperbolic partial differential equations of gradually varied free-surface unsteady flow. A description of the subject is presented in more detail in Hydrology Paper No. 46.

5.1 Basic Equations

The two basic partial differential equations of gradually varied free-surface unsteady flow are derived in Chapter 3, and given as Eqs. 3.23 and 3.19. To reiterate, the continuity equation in dimensionless form is

$$\frac{A}{VB}\frac{\partial V}{\partial x} + \frac{\partial y}{\partial x} + \frac{1}{V}\frac{\partial y}{\partial t} = \frac{q}{VB} , \qquad (5.1)$$

and the momentum equation in dimensionless form is

$$\frac{\alpha V}{g}\frac{\partial V}{\partial x} + \frac{\beta}{g}\frac{\partial V}{\partial t} + \frac{\partial y}{\partial x} = (S_o - S_f) - \frac{Vq}{Ag} , \qquad (5.2)$$

in which

- A = the cross section area,
- B = the mean cross section velocity as a dependent variable,
- y = the water depth in the conduit as a dependent variable,
- x = the length along the conduit as an independent variable,
- t = the time as an independent variable,
- B = the free surface width,
- α = the energy velocity distribution coefficient,
- β = the momentum velocity distribution coefficient,
- g = the gravitational acceleration,
- S_o = the slope of the channel invert,
- S_f = the energy gradient, and
- q = the distributed lateral inflow (or outflow) as discharge per unit length of the conduit.

The energy gradient, measuring the energy head loss along the conduit, is expressed by the Darcy-Weisbach equation in the form

$$S_f = \frac{fV^2}{8gR} , \qquad (5.3)$$

in which f is the Darcy-Weisbach friction factor, R is the hydraulic radius of a partially full conduit, with $R = A/P$, and P is the wetted perimeter.

The friction factor is expressed in this study for the hydraulically smooth boundary as a function of Reynolds number, $R_e = VR/\nu$, with ν the kinematic viscosity of the water.

Equations 5.1 and 5.2 generally give the closest approximations of the actual flood movement through channels and conduits for the one-dimensional unsteady flow, if the basic conditions for applying the two equations are approximately satisfied. The most important condition is that of gradual variability of the flood hydrograph; this condition is nearly always fulfilled for storm floods entering into and moving along storm drains.

5.2 Methods of Solution

Because of the mathematical difficulties of obtaining the analytical solution in a closed form to Eqs. 5.1 and 5.2, numerical finite-difference methods of integration must be employed. For solving Eqs. 5.1 and 5.2, finite-difference approximations are made as follows. Since there are two independent variables (x,t) and two dependent variables (V,y), the designation of the time-distance locations of the variables is based on the subscripts and superscripts of the variables. The subscript refers to the distance (space) location, and the superscript refers to the time location, as shown in Fig. 5.1.

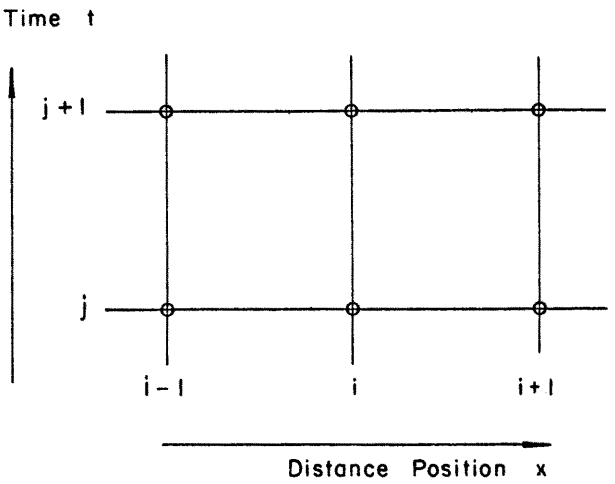

Fig. 5.1. Definition graph for the finite-difference scheme.

Thus, the depth at distance location i and at time j is y_i^j, and the four partial derivatives of Eqs. 5.1 and 5.2 may be approximated by

$$\frac{\partial V}{\partial x} \approx \frac{V_{i+1}^j - V_i^j}{x_{i+1}^j - x_i^j} , \qquad (5.4)$$

$$\frac{\partial V}{\partial t} \approx \frac{V_i^{j+1} - V_i^j}{t_i^{j+1} - t_i^j} , \qquad (5.5)$$

$$\frac{\partial y}{\partial x} \approx \frac{y_{i+1}^j - y_i^j}{x_{i+1}^j - x_i^j} , \qquad (5.6)$$

and

$$\frac{\partial y}{\partial t} \approx \frac{y_i^{j+1} - y_i^j}{t_i^{j+1} - t_i^j} . \qquad (5.7)$$

The unknown quantities in these expressions are generally the values at the incremental time locations j+1. Thus V_i^{j+1} and y_i^{j+1} are the unknown values for the time j+1, and the distance i. With the two equations of unsteady flow, these two unknowns may be solved for simultaneously. This is an explicit scheme procedure in that the conditions at a later time, j+1, are determined directly from the conditions at the preceding time, j.

Two approaches of the explicit schemes, the diffusing scheme and the Lax-Wendroff scheme as applied to the two partial differential equations, were used and as discussed in this study. A third approach used in this study, is the specified intervals scheme as applied to the four ordinary characteristic differential equations, as equivalent to the two partial differential equations. This latter approach will be called the specified intervals scheme of the method of characteristics.

Diffusing scheme. The diffusing scheme evolves from an approximation regarding the partial derivatives with respect to time. It is assumed the dependent variables are known for all positions at time j. These dependent variables will be designated as U in this development, and may refer either to V or y dependent variables of the two partial differential equations. The objective is to represent the partial derivatives as functions of the unknown dependent variable U at distance location i and time location j+1. The partial derivative of U in t is approximated by

$$\left(\frac{\partial U}{\partial t}\right)_i \approx \left(\frac{\Delta U}{\Delta t}\right)_i \quad , \tag{5.8}$$

in which

$$\Delta U_i = U_i^{j+1} - U_i^j \quad . \tag{5.9}$$

Expressing U_i^j as an average,

$$U_i^j \approx \frac{U_{i+1}^j + U_{i-1}^j}{2} \quad , \tag{5.10}$$

then

$$\Delta U_i = U_i^{j+1} - \frac{U_{i+1}^j + U_{i-1}^j}{2} \quad , \tag{5.11}$$

and finally the ratio of finite differences of this partial derivative is

$$\left(\frac{\Delta U}{\Delta t}\right)_i = \frac{U_i^{j+1} - \frac{U_{i+1}^j + U_{i-1}^j}{2}}{\Delta t}$$

$$= \frac{2U_i^{j+1} - U_{i+1}^j - U_{i-1}^j}{2\Delta t} \quad . \tag{5.12}$$

Similarly, the partial derivative with respect to the distance x is approximated by

$$\left(\frac{\partial U}{\partial x}\right)_i \approx \left(\frac{\Delta U}{\Delta x}\right)_i \quad , \tag{5.13}$$

in which

$$\left(\frac{\Delta U}{\Delta x}\right)_i = \frac{1}{2}\left[\frac{U_{i+1}^j - U_i^j}{\Delta x} + \frac{U_i^j - U_{i-1}^j}{\Delta x}\right] \quad , \tag{5.14}$$

so that

$$\left(\frac{\Delta U}{\Delta x}\right)_i = \frac{1}{2\Delta x}\left(U_{i+1}^j - U_{i-1}^j\right) \quad . \tag{5.15}$$

It is to be noted that Eq. 5.12 is an approximation for $\partial U/\partial t$ at the position i, j+1/2; and Eq. 5.15 is an approximation for the position i, j.

Lax-Wendroff scheme. To eliminate some of the deficiencies of the diffusing scheme, the Lax-Wendroff finite-difference scheme was investigated. The summary of the scheme is as follows. It is assumed that all functions are continuous and contain as many continuous derivatives as required. It is also assumed that products of first-order partial derivatives and any derivative of S_f in x and t are negligible quantities.

The expressions $\frac{\partial A}{\partial t} = B\frac{\partial y}{\partial t}$ and $\frac{\partial A}{\partial x} = B\frac{\partial y}{\partial x}$

relate A, B, and y. Therefore, the equation of continuity reduces to

$$\frac{\partial y}{\partial t} = -\frac{A}{B}\frac{\partial V}{\partial x} - V\frac{\partial y}{\partial x} \quad . \tag{5.16}$$

The intended application of the Taylor series, requires the use of second-order partial derivatives. Thus,

$$\frac{\partial^2 y}{\partial t^2} = -\frac{A}{B}\frac{\partial^2 V}{\partial x \partial t} - V\frac{\partial^2 y}{\partial x \partial t} \quad , \tag{5.17}$$

and

$$\frac{\partial^2 y}{\partial x \partial t} = -\frac{A}{B}\frac{\partial^2 V}{\partial x^2} - V\frac{\partial^2 y}{\partial x^2} \quad . \tag{5.18}$$

The momentum equation, 5.2, rewritten here in the form

$$\frac{\partial V}{\partial t} = -\frac{\alpha}{\beta}V\frac{\partial V}{\partial x} - \frac{g}{\beta}\frac{\partial y}{\partial x} - \frac{g}{\beta}(S_f - S_o) \tag{5.19}$$

gives

$$\frac{\partial^2 V}{\partial x \partial t} = -\frac{\alpha}{\beta}V\frac{\partial^2 V}{\partial x^2} - \frac{g}{\beta}\frac{\partial^2 y}{\partial x^2} \quad . \tag{5.20}$$

Hence, Eq. 5.17 becomes

$$\frac{\partial^2 y}{\partial t^2} = \left(\frac{\alpha}{\beta} + 1\right)\frac{AV}{B}\frac{\partial^2 V}{\partial x^2} + \left(\frac{g}{\beta}\frac{A}{B} + V^2\right)\frac{\partial^2 y}{\partial x^2} \quad . \tag{5.21}$$

Equation 5.19 then gives

$$\frac{\partial^2 V}{\partial t^2} = -\frac{\alpha}{\beta} V \frac{\partial^2 V}{\partial x \partial t} - \frac{g}{\beta} \frac{\partial^2 y}{\partial x \partial t} \quad . \tag{5.22}$$

Substituting Eqs. 5.18 and 5.20 into Eq. 5.22 yields

$$\frac{\partial^2 V}{\partial t^2} = \left[\left(\frac{\alpha}{\beta}\right)^2 V^2 + \frac{g}{\beta}\frac{A}{B}\right] \frac{\partial^2 V}{\partial x^2} + \left(\frac{\alpha}{\beta} + 1\right) \frac{g}{\beta} V \frac{\partial^2 y}{\partial x^2} \quad . \tag{5.23}$$

Again designating U as the symbol for any dependent variable V or y, the first and second partial derivatives with respect to x are approximated by

$$\frac{\partial U}{\partial x} = \frac{U^j_{i+1} - U^j_{i-1}}{2\Delta x} \tag{5.24}$$

and

$$\frac{\partial^2 U}{\partial x^2} = \frac{U^j_{i+1} - 2U^j_i + U^j_{i-1}}{(\Delta x)^2} \quad . \tag{5.25}$$

Similar equations are obtained with respect to t. Thus, recurrence relations for finding approximate solutions to V and y in Eqs. 5.21 and 5.23 are

$$y^{j+1}_i = y^j_i - \frac{\Delta t}{2\Delta x}\left[\left(\frac{A}{B}\right)^j_i (V^j_{i+1} - V^j_{i-1}) + (V^j_i\, y^j_{i+1} - y^j_{i-1})\right]$$

$$+ \frac{1}{2}\left(\frac{\Delta t}{\Delta x}\right)^2 \left\{\left(\frac{\alpha}{\beta} + 1\right)\left(\frac{A}{B}\right)^j_i (V^j_i V^j_{i+1} - 2V^j_i + V^j_{i-1})\right.$$

$$\left. + \left[\frac{g}{\beta}\left(\frac{A}{B}\right)^j_i + (V^j_i)^2\right](y^j_{i+1} - 2y^j_i + y^j_{i-1})\right\} \tag{5.26}$$

and

$$V^{j+1}_i = V^j_i - \frac{\Delta t}{2\beta\Delta x}\left[\alpha V^j_i (V^j_{i+1} - V^j_{i-1}) + g(y^j_{i+1} - y^j_{i-1}) + 2g\Delta x (S_f - S_o)\right]$$

$$+ \frac{1}{2}\left(\frac{\Delta t}{\Delta x}\right)^2 \left\{\left[\left(\frac{\alpha}{\beta}\right)^2 (V^j_i)^2 + \frac{g}{\beta}\left(\frac{A}{B}\right)^j_i\right](V^j_{i+1} - 2V^j_i + V^j_{i-1})\right.$$

$$\left. + \left(\frac{\alpha}{\beta} + 1\right)\frac{g}{\beta} V^j_i (y^j_{i+1} - 2y^j_i + y^j_{i-1})\right\} \quad . \tag{5.27}$$

The previous equations are based on the neglect of both the products of the first-order partial derivatives and the derivatives of S_f. For those cases in which these products of the first-order partial derivatives and the derivatives of S_f cannot be disregarded, difference equations analogous to Eqs. 5.26 and 5.27 may be derived.

Specified intervals scheme of the method of characteristics. The two partial differential equations of gradually varied free-surface unsteady flow, Eqs. 5.1 and 5.2, when transformed give the four ordinary characteristics differential equations. Their development is shown in Chapter 3. The equations with $\alpha = \beta = 1$, and $q = 0$ (Eqs. 3.50 to 3.53), are the initial equations. To reiterate, they are

$$\xi_+ = \left(\frac{dt}{dx}\right)_+ = \frac{1}{V + \sqrt{gA/B}} \quad , \tag{5.28}$$

$$\xi_- = \left(\frac{dt}{dx}\right)_- = \frac{1}{V - \sqrt{gA/B}} \quad , \tag{5.29}$$

$$\left\{\left(\frac{A}{VB} - \frac{V}{g}\right)\xi_+ + \frac{1}{g}\right\}\frac{dy}{dx} + \frac{A}{gVB}\frac{dV}{dx} + \frac{A}{VB}(S_o - S_f)\xi_+ = 0, \tag{5.30}$$

and

$$\left\{\left(\frac{A}{VB} - \frac{V}{g}\right)\xi_- + \frac{1}{g}\right\}\frac{dy}{dx} + \frac{A}{gVB}\frac{dV}{dx} + \frac{A}{VB}(S_o - S_f)\xi_- = 0, \tag{5.31}$$

with the symbols the same as those defined for Eqs. 5.1 and 5.2. These four dependent equations form the basis for numerical solutions in the method of characteristics, in this case by the specified intervals numerical integration scheme.

There are several procedures that may be used and these procedures may be broadly divided into two categories, the grid system and the specified intervals system. In the second category, which is used in this study, the dependent variables V and y are known functions of the independent variables x and t either as initial conditions at $t = 0$ or as the results of previous time computations. For example, it is assumed that V and y are known along distance x at time t. Figure 5.2 represents the rectangular grid in the (x,t)-plane with intervals Δx and Δt in the x and t coordinates, respectively. In this case, V and y at points M_j, A_j, B_j,...,N_j are known. The values of V and y at the time position $j+1$, and particularly at points M_{j+1}, A_{j+1}, B_{j+1},...,N_{j+1}, can be computed from equations 5.28 through 5.31 and from the boundary conditions. The process can be continued as far as desired or meaningful. This method was selected for in this study because x and t at points M_{j+1}, A_{j+1}, B_{j+1},...,N_{j+1} are exactly known, so only the values of V and y at these points must be determined.

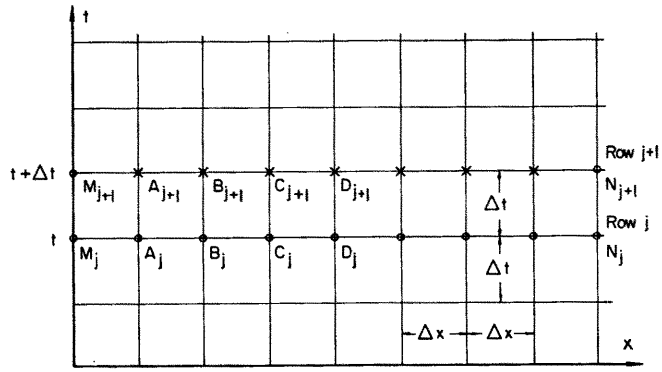

Fig. 5.2. Network of specified intervals for the solution of characteristic equations.

In this method, V and y at point P on the (x,t)-plane of Fig. 5.3 are to be computed from the initial conditions or from previous values of V and y at points A, B, and C using two assumptions:

(a) Δt is sufficiently small so that the parts of the characteristics between P and R and between P and S are considered straight lines, and points R and S fall within the interval AB, and

(b) the slope of the straight line PR at point P is equal to the positive characteristic direction at the position C, (ξ_+), and the slope of the straight line PS at point P is equal to the negative characteristic direction at the position C, (ξ_-).

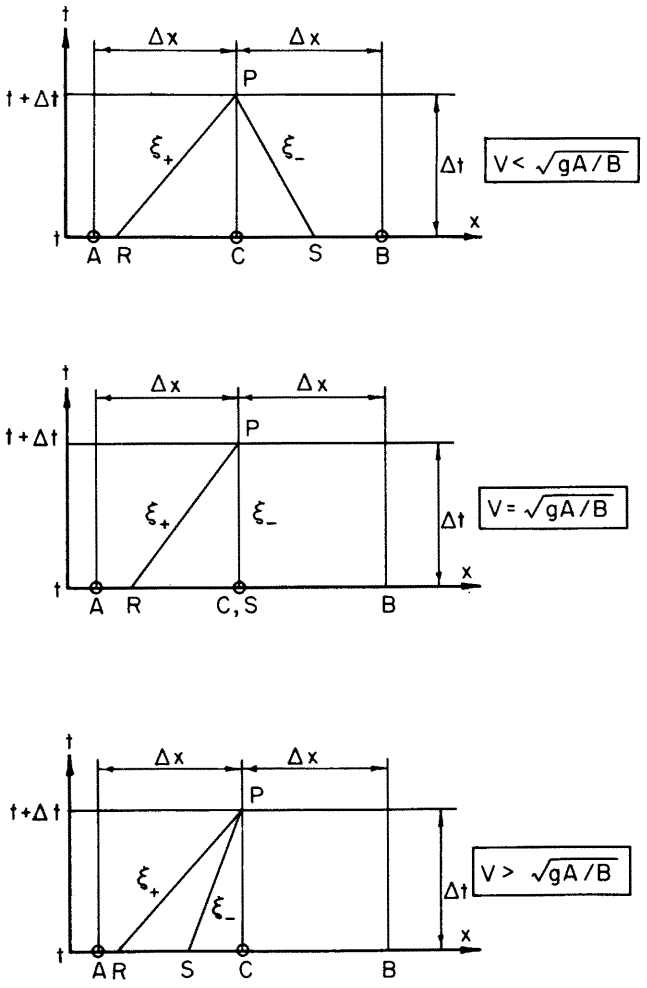

Fig. 5.3. Rectangular grid for the solution by the system of specified intervals, Δt and Δx: subcritical flow (upper graph), critical flow (center graph), and supercritical flow (lower graph).

5.3 Initial and Boundary Conditions

Solution of the two partial differential equations Eqs. 5.1 and 5.2, requires an initial condition and two independent boundary conditions.

Initial conditions. The necessary initial conditions for unsteady free-surface flow are that all velocities and depths of water along the channel must be known at a given time. In this study, it was assumed that the discharge was constant throughout the reach at the initial time. Thus, the problem can be treated as steady non-uniform flow. Velocities and depths along the channel were then determined by computations of conventional backwater or drawdown surface profiles, depending on the downstream control conditions. This procedure used the standard step method.

Boundary conditions. One of the two boundary conditions is the discharge-time relation existing at the inlet cross section of the channel under study. This relation can be either expressed in a mathematical form, or given as discrete points of discharge at selected intervals of time.

The other boundary condition imposed on the problem is that of a discharge-versus-depth relation at the downstream end, characterized either by a control structure or by the critical depth at a free outfall. This is the boundary condition that must exist for subcritical flow of the base discharge.

If the base discharge is in the supercritical range or on a supercritical slope the boundary condition must be expressed at the inlet end. This function may take the form of a discharge-versus-depth relation. This condition, in combination with the condition of a discharge-versus-time relation is somewhat difficult to visualize physically; however, it is a necessary condition because the characteristic directions both have a positive slope and thus there is no influence of the downstream conditions on the upstream conditions.

The following discussion presents a detailed analysis of these boundary conditions. Arbitrary inflow hydrographs were investigated to test and verify the computer program and also to provide results for evaluating the significance of variations in the hydraulic parameters.

The boundary condition at the upstream inlet is given by an inflow hydrograph, Q(t), with no limitation on the shape of the hydrograph. A hypothetical hydrograph, with a Pearson Type III distribution and four parameters, was selected for evaluating the effect of variations in the parameter, shown by Fig. 5.4. Thus, the inflow Q at time t designated by Q(t) may be described by

$$Q(t) = Q_b + Q_o e^{-(t-t_p)/(t_g-t_p)} (t/t_p)^{t/(t_g-t_p)}, \quad (5.32)$$

in which Q_b is the constant base flow, Q_o is the difference between the base flow and the peak flow, t_p is the time from the beginning of storm runoff to peak discharge, and t_g is the time from the beginning of the storm runoff to the center of mass of storm runoff, G. One hydrograph with arbitrary values of Q_b, Q_o, t_p, and t_g was used in this portion of the study. The shape along with these arbitrary values of parameters are shown in Fig. 5.4.

The boundary conditions at the downstream outlet are generally given by a stage-discharge relation. In this portion of the study a free outfall at the end of the conduit was assumed. For the free outfall a critical flow at the downstream end exists, with

$$\frac{V}{\sqrt{g\frac{A}{B}}} = 1 , \quad (5.33)$$

in which A is the cross section area and B is the top width of the downstream boundary.

It was also assumed that critical depth occurs at a distance of 4.5 times the critical depth from the

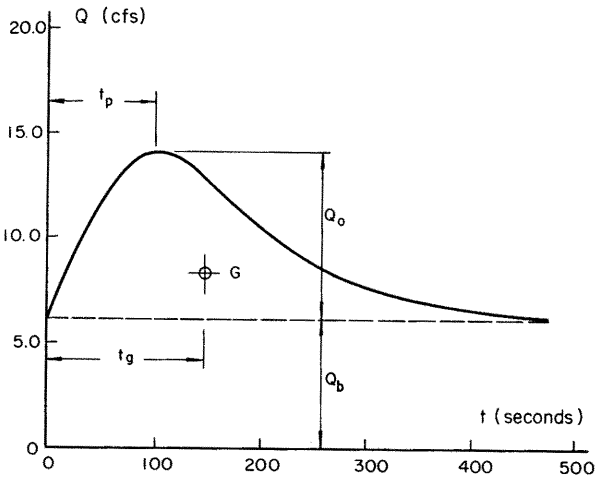

Fig. 5.4. Hypothetical inflow hydrograph of a Pearson Type III function, Eq. 5.32, with the selected parameters: Q_b = 6.21 cfs, Q_o = 8.00 cfs, t_p = 100.00 sec., and t_q = 150.0 sec.

end. This assumption was also applied to the unsteady case, with critical depth computed from the base discharge, Q_b. Therefore, the total distance x_L from the inlet to the downstream boundary is determined by

$$x_L = x_F - 4.5\ y_c \quad , \tag{5.34}$$

in which x_F is the total length of the conduit and y_c is the critical depth for discharge Q_b.

For the case wherein the downstream end of the channel is restricted, it is necessary to know the relationship between the discharge and the corresponding depth. This relationship can generally be expressed as:

$$Q = my^n \tag{5.35}$$

in which "m" and "m" are constants. These constants may be estimated from previous experience or computed from measured discharges and depths. In this study, these constants were experimentally determined for specific outlet geometry.

5.4 Comparison of Three Finite-Difference Schemes of Numerical Integration

Criteria for comparison of schemes. Comparison of the three finite-difference schemes, diffusing, Lax-Wendroff, and the specified intervals scheme of the method of characteristics, for numerical integration and computer solution and the eventual selection of the most desirable for particular application depend on simplicity, stability, accuracy, flexibility, and the resulting computer time.

The simplicity of a particular scheme is related to both the algebraic description of its numerical algorithm and the computer programming involved. Simplified algebra, however, does not necessarily infer simplicity in the computer algorithm. The stability of a solution infers that the process will coverge to a real solution. This criterion is satisfied in the case of solving the De Saint-Venant equations if the mesh size $\Delta t/\Delta x$ ratio is less than dt/dx, for any part of the (x,t)-plane used in the integration solutions. The accuracy of a method in this study infers that the algorithm will reproduce the initial conditions for the steady state boundary conditions. As a corollary, the algorithm should be able to compute the steady state conditions from any arbitrary initial conditions. If the algorithm satisfies this criterion, it may be inferred there will be good agreement between the computed and the observed quantities. The flexibility of a computer algorithm depends on the range of conditions the algorithm will accommodate. For the unsteady flow solutions, it is desirable that the algorithm provide for all conditions of depth, velocity, and discharge within expected physical ranges. Generally, this must include both the subcritical and the supercritical conditions. Since numerical procedures at some stage require interpolations, a computer decision is required to determine the appropriate interpolation.

Properties of diffusing scheme. The diffusing scheme is the simplest of the three to develop and is represented in algebraic form. The stability of this scheme is assured provided the ratio of $\Delta t/\Delta x$ does not exceed the absolute maximum value of dt/dx at any point in the (x,t)-plane.

The accuracy of the scheme, however, suffers during eventual periods of supercritical flow. This is because the characteristics intersect at a relatively great distance from the solution point. Accuracy is further limited because the dependent variables are assumed to vary linearly within the interval of $2\Delta x$. Thus, if the actual value of a dependent variable at a given x-position is more than the interpolated value, the computed value at the later time will be less than the true value. This produces a dampening effect in time at a fixed location. The greater the curvature of the free surface the more pronounced is this effect.

To reduce this effect the physical size of Δx may be reduced, but this increases the computer time by the square of the number n of distance intervals, Δx. Subsequent comparisons indicate the diffusing scheme requires more computer time than the other two schemes.

Properties of Lax-Wendroff scheme. The Lax-Wendroff scheme is an improvement over the diffusing scheme in that it accommodates the curvature in the variation of dependent variables. This, however, involves a more complicated numerical algorithm.

The Lax-Wendroff scheme also results in a more accurate solution in comparison with the diffusing scheme for the same Δx and Δt intervals, without a significant increase in computer time. An indication of this accuracy is demonstrated in Fig. 5.5. The Lax-Wendroff method consistently produces the same depth over a very long period of time, whereas, the diffusing scheme produces a consistent change.

With regard to its flexibility in accommodating a wide range of flow conditions, the Lax-Wendroff scheme possesses the same inherent limitations as the diffusing scheme. Thus, by the Lax-Wendroff scheme the further the intersection of the two characteristic curves from the solution point, the less accurate the solution.

Properties of specified intervals scheme of the method of characteristics. Inherent complications in the specified intervals scheme of the method of characteristics are justified by its superior accuracy. Using this scheme, the points of solutions are at the intersections of characteristic curves, rather than at any point within the domain of dependence.

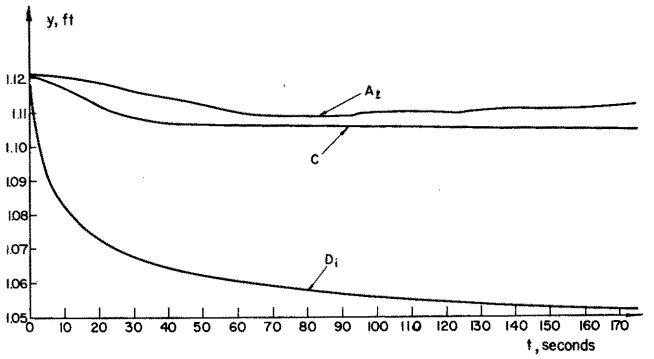

Fig. 5.5. Comparison of diffusing scheme (D_i), Lax-Wendroff scheme (A_ℓ), and the specified intervals scheme of method of characteristics (C) in reproducing the steady initial conditions along the conduit, at the distance x = 796.7 ft.

The linear interpolation of this scheme requires determination of the interpolation interval in order to accommodate flow conditions in both subcritical and supercritical regime. The accuracy of this scheme is demonstrated in Fig. 5.5; it is good when compared to the diffusing and Lax-Wendroff schemes. It is apparent that this finite-difference scheme of the method of characteristics produces a rapidly convergent and stable value, which is comparable to the same property of the Lax-Wendroff scheme.

The non-linear interpolation in the specified intervals scheme of the method of characteristics for dependent variables along distances for a given time is an improvement over the linear interpolation. However, linear interpolation is used in producing results (C) of Fig. 5.5 for this method of characteristics.

Based on the previous comparisons and on the results shown in Fig. 5.5, it was decided to use the specified intervals scheme of the method of characteristics on subsequent computations of analytical waves.

Chapter 6

COMPARISON OF RESULTS OF COMPUTED AND OBSERVED WAVES IN SUBCRITICAL FLOW

6.1 Methods of Comparison

The computed depths and the observed depths of flood hydrographs moving along a storm drain for the same physical conditions of the conduit and the same wave may be compared in numerous ways. A visual inspection of the plotted data as the first comparison presented in Appendices 3, 4, and 5, provides a qualitative comparison. Quantitative comparisons may be made in various ways depending on the comparison quantities that are considered important. The basic quantities compared in this study are the depth of flow as a function of time at fixed locations, and the depth of flow as a function of distance at fixed instants of time. The computed waves have the same initial and boundary conditions as the observed waves. The computed waves are obtained by numerical integration of the analytical equations of the specified intervals scheme of the method of characteristics, described briefly in Chapter 5 of this paper and in detail in Hydrology Paper No. 46. The observed waves are those physically produced in the 822-ft long conduit. Comparisons in this chapter refer only to the waves in the subcritical flow regime.

The comparison of computed and observed waves in supercritical flow should not be different from the subcritical flow, provided the two boundary conditions at the inlet of the conduit for the supercritical flow are properly defined. Therefore, any difference between comparisons in supercritical and subcritical flow would be only a measure of how the assumed depth-to-discharge relation at the inlet for the supercritical flow reflects the real physical relation.

The wave property experimentally observed in this study is the depth as a function of time at selected locations along the conduit. A qualitative comparison of the computed depth versus time and the observed depth versus time, for a representative case, is presented in Fig. 6.1. In visual inspection the conclusion regarding the degree of agreement is a subjective decision. A quantitative comparison depends on the consideration of not only the difference in the depths at a given instant of time but also the difference in time for a given depth. A test of agreement could then be a statistic expressing the difference in depth at an instant, or a difference in time for a constant depth, or a combination of depth and time differences.

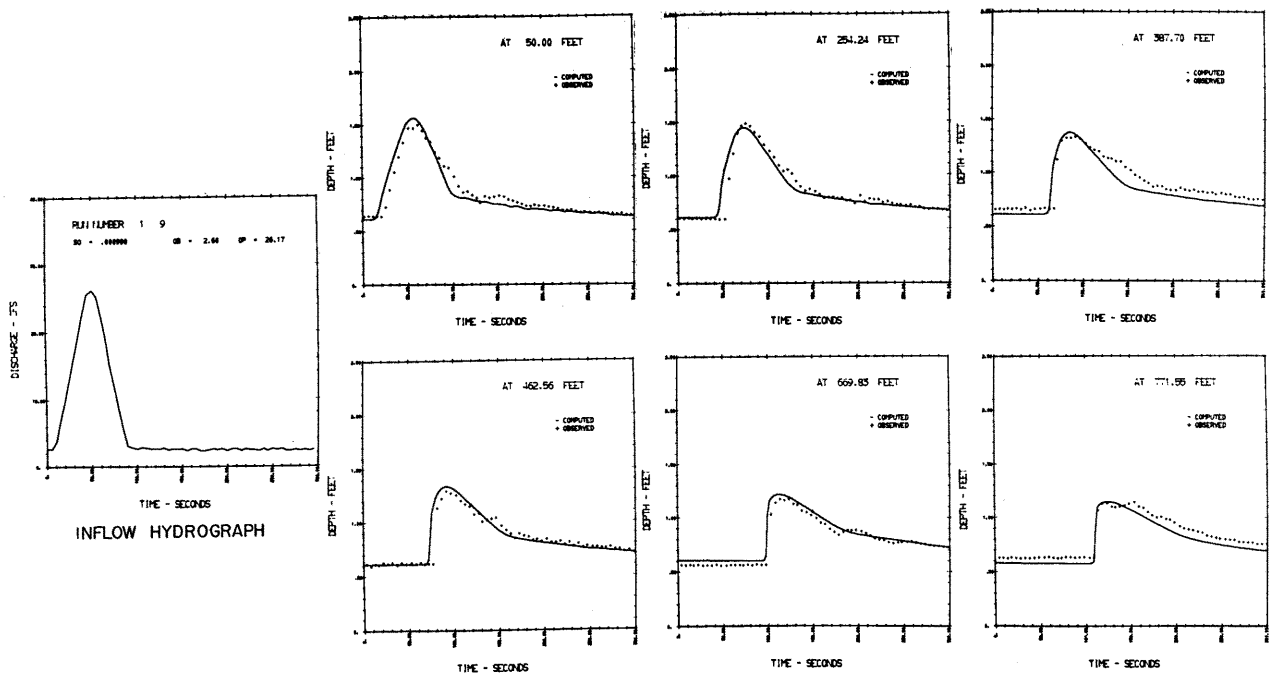

Fig. 6.1. Type of comparison of computed and observed waves for a qualitative comparison by visual inspection with depth versus time for given positions.

Another comparison was made between the computed and observed wave depths along the conduit at successive instants of time. The observed values are obtained from basic data on flood hydrographs at different positions of the conduit. Figure 6.2 presents the typical experimental values, and the corresponding computed curves. These values and curves represent instantaneous water surface profiles; differences between the depths at each position may be used as a comparison. The difference between locations of the same depth for computed and observed waves also can be used as a comparison. However, this comparison does not appear to be reasonable in the majority of the cases presented in Appendix 3 because of additional errors involved in the interpolation of wave profiles along the conduit.

A third comparison is made between the maximum or peak depths of computed and observed waves by considering them as a function of both time and distance. The maximum depth of a wave for a given conduit and for given boundary conditions is perhaps the most meaningful comparison for the design engineer, because this depth eventually determines the conduit dimension for a given design hydrograph. A typical comparison of the computed and observed maximum depth as functions of distance and time is presented in Fig. 6.3. Appendix 4 presents these comparisons for some experimental conditions for the experimental data obtained at the Colorado State University Engineering Research Center.

This chapter refers only to the general comparison of computed and observed flood waves. Both the computed and observed waves are subject to errors. The general comparison then integrates the effects of all sources of errors. Chapter 8 of this paper presents a systematic discussion of errors, and effects of some of the simplifications in the coefficients of the two partial differential equations of gradually varied free-surface unsteady flow.

6.2 Methods of Qualitative Comparison

The observed experimental data on physical waves, subsequently called the observed data, and the numerically computed data by integrating the analytical equations, subsequently called the computed data, are compared in three ways.

First, waves in the form of depth hydrographs, encountered at different points along the conduit, are compared. Plots showing the computed and observed depths of waves at given locations, as a function of time, are shown as the first graph of each run in Appendix 3. The graphs in Appendix 3 consist of wave plots at each position that depth measurements were taken, as well as a plot showing the inflow hydrograph as discharge versus time. The solid curves are the computed depths and the plus sign, +, indicates an observed depth (discrete points delineate the observed depth hydrographs).

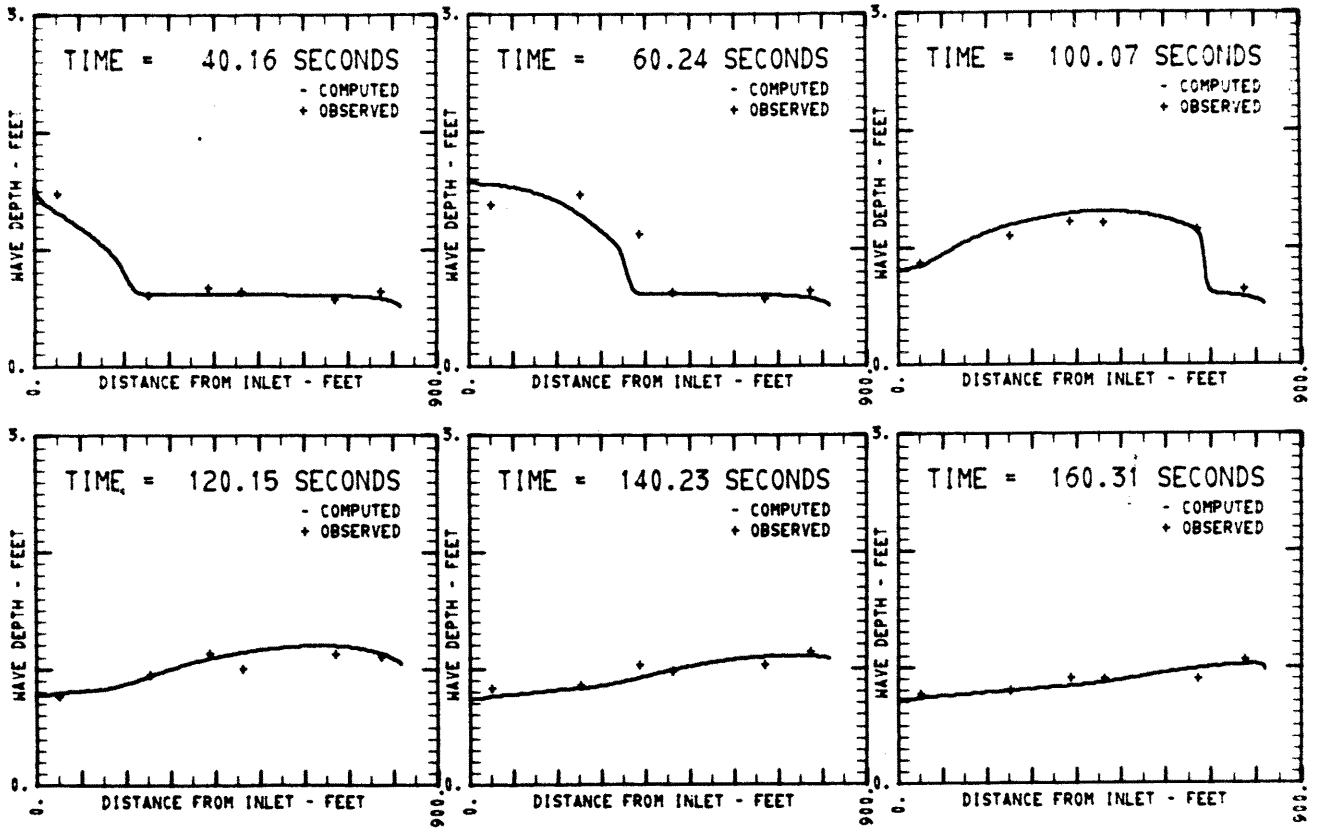

Fig. 6.2. Type of comparison of computed and observed waves for qualitative comparison by visual inspection, of depth versus distance for given times.

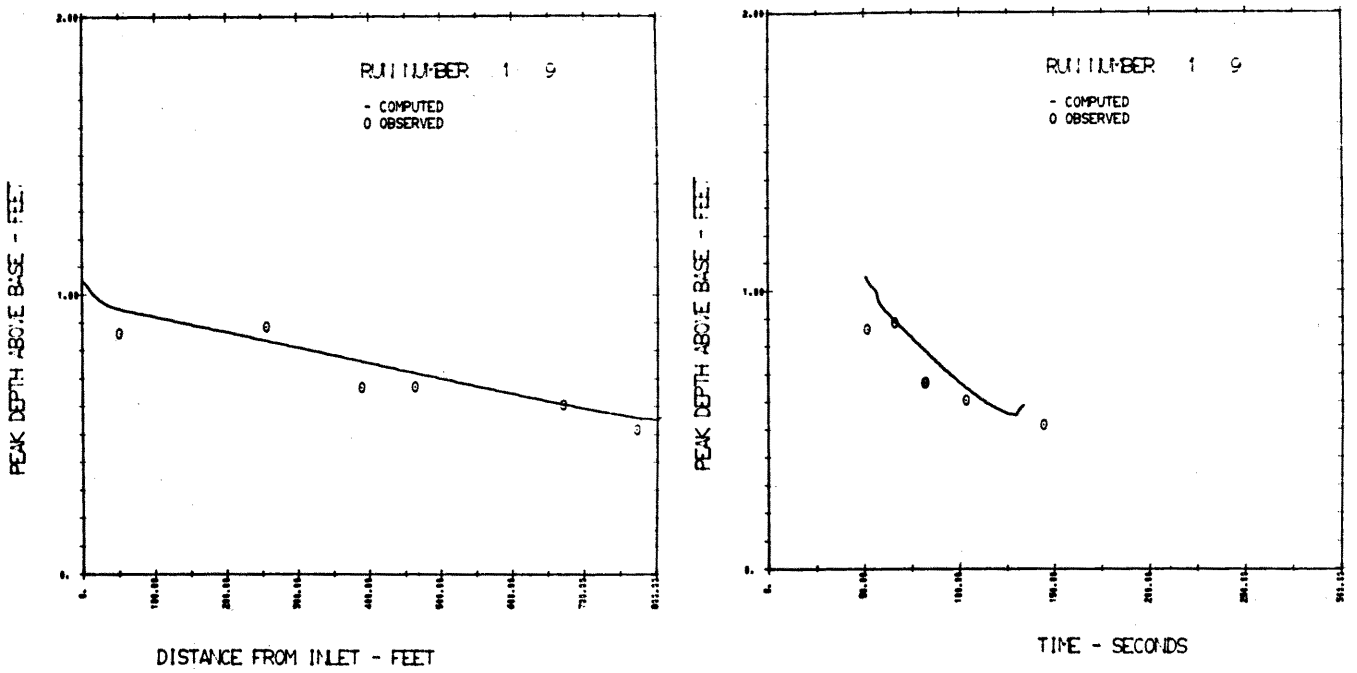

Fig. 6.3. Type of comparison of computed and observed wave peak depths as functions of distance or time, for a qualitative comparison by visual inspection.

Appendix 3 gives the results only of those runs of computed and observed waves that were conducted at the two conduit slopes, the nominal slope of 0.05 percent (0.0005) which actually varied after adjustment from S_o = 0.00048 (0.048 percent) to S_o = 0.000550 (0.055 percent), and the nominal slope of 0.1 percent (0.0010), which became S_o = 0.000990 (0.0990 percent), after practical adjustment. For economy of reproduction, results of other slopes are not presented in this Appendix because it is considered that a small nominal slope (0.05 percent), and the double of this small nominal slope (0.1 percent) are sufficient to indicate the results of comparison for the subcritical regime.

Second, qualitative comparisons are made for the computed and observed waves at an instant of time. The depth is plotted versus distance, which is also shown in Appendix 3. In this case, either three or six different times were chosen to represent the waves at different positions along the conduit. Again, the solid curves represent computed values while observed points are indicated by ⊙ . However, depths versus distance are plotted from a horizontal line, rather than from the slope S_o. Therefore, some depths appear to have negative slopes, which results from the manner in which the depths are plotted. The negative slopes of the waves, plotted as function of distance for a given time, should not exceed the bottom slope.

Appendix 3 gives the same results of depth versus distance for given instants of time of computed and observed waves, for the same runs and the same slopes as those given in the comparison of depths versus time of the computed and observed waves at given positions. Introductory remarks at the beginning of Appendix 3 explain these runs, and there presentation. The results of Appendix 3 refer to three particular sets of runs: (1) when the main conduit is used only with an inflow hydrograph at its entrance; (2) when the inflow is at the main conduit entrance and at one of the three lateral inlets; and (3) when the inflow is at the main conduit entrance and at each of the three lateral inlets.

Third, the plotted comparison of computed and observed waves in the form of peak depths (with the peak depth defined as the maximum depth minus the base flow depth), versus both the distance and time, is presented in Appendix 4. The peak depths are computed from the maximum depths attained by subtracting the constant base flow depth. The time in the plots of peak depths-versus-time indicate the times at which the maximum depths have occurred. Base depths were subtracted from the maximum depths to obtain peak depths for two reasons: first, to remove the shift systematic errors resulting from inaccurate measurements of the base depth, and second, to allow for an expanded depth scale in the comparisons. The computed peak depths are solid lines, and points indicate the observed peak depths.

Similarly as in the case of the plotted wave depth versus the distance for a given time, the peak depth is also plotted versus distance in the horizontal line rather than from the line of the slope, S_o. Because the attenuation rate of peak depth is greater than the slope, S_o, the plots in Appendix 4 do not show negative slopes.

This appendix does give the results of peak depth versus distance and peak depth versus time of computed and observed waves for the same runs and the same slopes as those given in Appendix 3. Introductory remarks at the beginning of Appendix 4 also explain the runs, and their presentation. These runs refer to the same three cases: (1) inflow at the main conduit entrance only; (2) inflow at the main conduit entrance and at one of the three lateral inlets; and (3) inflow at the main conduit entrance and at each of the three lateral inlets.

In these three approaches of comparing computed and observed waves, the method of comparison showing wave-depth as a function of time provides the best comparison, because the amount of observed data is much greater in this case. Besides, the measurements of depth are taken continuously in time at different positions along the conduit. The method of comparison by the depth versus the distance shows the shape of the entire wave at different times as it traverses the conduit.

Even though the depths are plotted from the horizontal line and not from the slope, S_o, this second method of comparison shows how the wave becomes steeper, changes shape, and attenuates with time. However, in this case, there are only as many observed points as there were observational positions. The comparisons of peak-depth versus distance and time are illustrations of the rates of attenuation of various waves. Here again, there are only as many observed points for comparison as there were observation positions.

The comparison of wave forms as a function of time and as a function of distance are dependent upon their respective origins. The computed wave forms are based on the time origin defined by the start of the inflow hydrograph at the beginning of the conduit reach or at $x = 0$.

The observed wave forms were the consequence of an inflow hydrograph as recorded at the measuring orifice. The orifice was upstream of the assumed beginning of the channel, and in a full conduit flow. This was necessary because of the baffles and transitions from the closed conduit flow to the conduit free-surface flow. However, this approaching length introduced the effect of a time shift in the boundary condition of inflow hydrograph, roughly equal to this conduit section length divided by the mean velocity. This condition also tended to modify the hydrograph shape due to the change in storage in the free-surface portion of this transition section. No direct quantitive evaluation of these effects was attempted. The comparisons that are made attempt to reduce the difference in the time origin by shifting the computed depth-time wave so that the peak depths of the computed and observed peaks coincide.

6.3. Results of Qualitative Comparisons

A review of various graphs in Appendices 3 and 4 reveal some patterns that warrant a brief discussion, though the discussion is based on visual inspection.

Many depth hydrographs (depth versus time) at given conduit positions show significant shifts both vertically (shift in positions of base flow depth) and horizontally (shift in time of the peak) in the case of both the inflow at the main conduit entrance only, and the inflows at the main conduit entrance and at one or at all three lateral inlets.

Two main reasons can be cited for these differences for the subcritical flow regime and the inflow hydrograph only at the main conduit entrance. First, the constant vertical depth difference between computed and observed hydrographs results from an error in the measurement of the base flow depth. It was also possible that the transducer output was not zero for the base flow depth. This resulted in a constant shift of all observed depths, but this is easy to eliminate, provided the observed base flow depth is shifted to coincide with the computed base flow depth.

Second, the constant time shift between the computed and observed depth hydrographs may be the result of an error in determining the time between the wave passing the flow measuring orifice meter and the $x = 0$ position of the conduit. Besides, coordinating the observed time at $x = 0$ and the computational time at the same position may result in a systematic time shift. This constant shift can also be corrected for the sake of comparison.

Both the depth and time constants shifts of various runs, with the inflow at the main conduit entrance only, were not corrected in presenting the data in Appendices 3 and 4 in order to obtain various qualitative and quantitative comparisons. They represent experimental, systematic errors, and are kept as such in comparison. However, these systematic errors or shifts are mainly in the observed waves as observational errors.

For the systematic shifts at depth hydrographs in case the inflows are both at the main conduit entrance and at one lateral inlet only, or at all three lateral inlets, an additional shift results from the error in estimating the heat losses at the junction boxes. Because the differences of head loss at junction boxes between the computed and observed waves accumulate in the case of three lateral inlets, and because they are superposed to the systematic shifts of the base flow depth and the time, the systematic error-difference should be either larger at the upstream part of the conduit and smaller at the downstream part, or the opposite, depending on whether the systematic errors in the estimates of head losses are of the same or opposite sign as the base flow depth and time shifts.

Similarly, for the shifts in depth hydrographs at given positions, the shifts both in depth and time are identifiable for the wave profiles as the depth versus distance representation for various times. Appendix 3 clearly demonstrates these various shifts. However, it is not easy to determine which of the two shifts predominates and should be taken into account. The difficulty of determining the shifts is compounded by the way of plotting depths versus distance, since they are plotted from the horizontal line rather than from the corresponding slope line (S_o).

Similar systematic shifts are shown for the comparison of peak depths versus distance or peak depths versus time between the computed and observed waves (Appendix 4), as it was shown for the two previous qualitative comparison by visual inspection. However, these shifts for peak depths seem to be relatively smaller, on the average, than for the total depth hydrographs or total wave profiles along the conduit. This should be expected since the constant shift in the base flow depth and in time should have the least relative effect on the maximum depths, and therefore on the peak depths.

The hypothesis that the systematic transverse oscillations of the wave in the free-surface conduit flow, or that standing wave phenomenon has occurred along the conduit, thus producing the systematic depth shifts, must be assigned a smaller probability than the unaccounted shifts in the voltage of pressure transducers. No significant transverse oscillations were observed, however.

Visual inspection of graphs presented in Appendices 3 and 4 leads to the following general conclusions:

(1) Taking into account the systematic depth and time shifts in observed waves, the agreement between the computed waves, which are obtained by using the specified intervals scheme of the method of characteristics, and the observed free-surface waves, which are recorded in the 822 ft long conduit, is reasonably good. This good agreement is surprising due to various sources of systematic and random errors in both the computed and the observed waves.

(2) The attenuation of flood peaks along the conduit or in time, which is the most practical design aspect of the comparison of computed and observed waves, also shows a very good agreement provided the systematic shifts are taken into account or corrected.

(3) Because of effects of systematic errors in the experiments, it is likely that these errors, on the average, are either of the same order of magnitude or of the larger magnitude, than the difference between the analytical waves (waves accurately integrated from the two partial differential equations) and the physical waves (true waves in the conduit without systematic and random errors). Therefore, the above comparisons can not detect the differences between the analytical waves and the physical waves, which result from basic assumptions in the derivation of the continuity and momentum partial differential equations of gradually varied free-surface unsteady flow.

(4) In general, the waves computed by the integration procedure in this study, using the most complete partial differential equations, should be considered sufficiently accurate for all practical purposes of storm drain design.

6.4 Quantitative Comparison of Results by Depth-Versus-Time Relations

The computed and observed depth-versus-time waves at a given point were compared in five different ways The definition of terms is graphically presented in Fig. 6.4. These terms are:

(1) The depth hydrograph area (the total area under the wave hydrograph minus the area of the base flow hydrograph);

(2) The first moment of the depth-hydrograph area about the time of the maximum depth;

(3) From the first moment, the time from the wave peak to the centroid of the depth hydrograph area is computed with t_c defined as this characteristic time of the depth hydrograph,

(4) From the second moment the standard deviation of the depth hydrograph area about the time of the maximum depth is computed by

$$\sigma_p = \left[\frac{\int t^2\, y\, dt}{\int y\, dt}\right]^{\frac{1}{2}} \qquad (6.1)$$

with A the area of depth hydrograph; and

(5) A dimensionless parameter defined as the ratio

$$R = \frac{\sigma_p}{t_c} \qquad (6.2)$$

The areas of depth hydrographs provide a bulk comparison without regard to the distribution of the depth hydrographs. The first moment about the peak is a measure of symmetry; t_c is an indication of

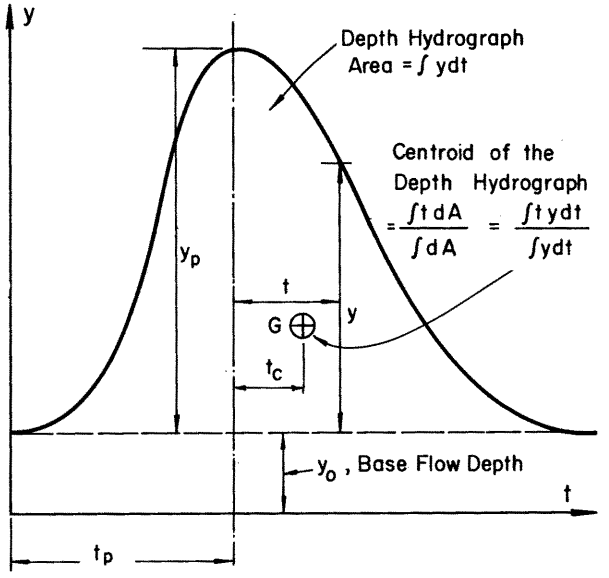

Fig. 6.4. Definitions of basic magnitudes of the wave-depth hydrograph.

Table 6.1. Quantitative comparison by five parameters of computed and observed waves at given three conduit positions, with no corrections for shifts in observed waves.

RUN NO.	POSITION (FT)	TOTAL AREA OF WAVE FORM ABOVE BASE (FT-SEC) OBSERVED	TOTAL AREA OF WAVE FORM ABOVE BASE (FT-SEC) COMPUTED	FIRST MOMENT OF AREA ABOUT PEAK (FT-SEC2) OBSERVED	FIRST MOMENT OF AREA ABOUT PEAK (FT-SEC2) COMPUTED	TIME FROM PEAK TO CENTROID OF WAVE FORM (SEC) OBSERVED	TIME FROM PEAK TO CENTROID OF WAVE FORM (SEC) COMPUTED	STANDARD DEVIATION OF WAVE FORM ABOUT PEAK (SEC) OBSERVED	STANDARD DEVIATION OF WAVE FORM ABOUT PEAK (SEC) COMPUTED	RATIO OBSERVED	RATIO COMPUTED
B2AR51	90.00	2.69	2.31	19.07	24.51	7.38	10.54	21.40	38.81	2.910	2.849
B2AR51	410.00	1.76	1.39	15.92	14.39	7.99	10.37	7.39	21.66	.937	2.189
B2AR51	771.70	-.12	.84	-.57	5.96	29.62	9.19	27.52	19.86	.929	1.659
B2AR52	90.00	26.47	24.56	481.62	491.45	15.13	18.53	37.84	49.00	2.440	2.648
B2AR52	410.00	21.41	18.76	949.25	910.91	26.46	27.66	46.86	46.81	1.910	1.664
B2AR52	771.70	18.96	15.94	672.11	499.75	56.21	31.36	75.91	44.19	1.265	1.439
B2AR53	90.00	39.52	36.17	894.48	736.52	22.75	20.96	46.05	51.22	2.159	2.515
B2AR53	410.00	31.65	28.78	782.93	816.76	24.73	28.38	45.21	47.45	1.827	1.672
B2AR53	771.70	28.15	24.42	900.99	743.22	36.16	30.44	47.76	44.76	1.397	1.478
B3AR51	90.00	1.66	3.42	4.43	67.36	2.68	19.66	8.05	34.25	5.383	1.742
B3AR51	410.00	1.44	1.84	4.24	19.79	2.95	10.74	6.45	18.64	2.183	1.679
B3AR51	771.70	-.36	.11	-.36	-.44	1.00	-3.94	1.00	4.16	1.000	-1.054
B3AR52	90.00	15.64	15.96	98.99	94.64	5.58	2.26	19.68	28.74	9.498	9.179
B3AR52	410.00	15.96	15.91	297.01	144.14	21.54	10.05	32.16	21.96	1.567	2.038
B3AR52	771.70	15.62	14.81	249.78	362.71	18.94	21.66	28.23	31.78	1.565	1.471
B3AR53	90.00	33.23	36.48	564.88	756.71	17.60	20.76	41.76	52.78	2.372	2.543
B3AR53	410.00	28.47	31.24	673.18	815.86	23.66	26.12	41.57	46.87	1.798	1.948
B3AR53	771.70	25.71	29.27	786.23	615.97	27.47	21.77	39.23	39.61	1.428	1.826
C2AR52	90.00	49.96	35.16	1424.96	691.57	28.53	19.67	53.69	49.72	1.887	2.520
C2AR52	410.00	35.23	28.33	1248.43	839.67	35.21	29.58	54.21	49.33	1.426	1.672
C2AR52	771.70	35.18	24.91	970.37	646.81	27.62	34.96	44.38	47.91	1.595	1.587
C2AR53	90.00	67.83	46.61	1540.81	488.54	22.78	10.48	48.65	39.87	2.136	3.884
C2AR53	410.00	54.19	38.99	1935.75	826.66	35.79	21.27	52.19	39.18	1.458	1.841
C2AR53	771.70	56.74	38.98	784.45	1047.96	13.46	29.12	38.71	43.62	2.904	1.477
C3AR51	90.00	8.77	16.17	86.96	111.38	9.91	16.95	24.86	31.33	2.960	2.863
C3AR51	410.00	7.16	7.64	111.52	166.80	15.44	13.96	29.01	26.96	1.672	1.899
C3AR51	771.70	4.89	6.91	48.86	119.47	19.12	18.38	17.98	26.43	1.887	1.441
C3AR52	90.00	23.44	20.39	394.42	441.29	16.66	16.72	38.41	41.89	2.369	2.916
C3AR52	410.00	19.98	21.16	285.49	479.94	17.98	22.78	34.26	39.88	1.664	1.758
C3AR52	771.70	18.36	19.61	469.35	988.72	22.37	28.86	32.73	39.67	1.465	1.375
C3AR53	90.00	35.67	39.61	497.81	365.19	13.96	9.22	33.95	35.54	2.433	3.856
C3AR53	410.00	29.83	32.99	549.96	647.67	16.95	18.66	32.21	34.88	1.981	1.869
C3AR53	771.70	32.56	31.83	966.72	819.64	18.32	25.89	32.56	37.63	1.777	1.693
B2AR61	90.00	28.87	42.96	-829.79	1367.17	-39.97	31.83	71.48	61.48	-1.987	1.952
B2AR61	410.00	25.97	38.86	964.92	1679.86	19.44	46.81	17.61	69.11	.996	1.476
B2AR61	771.70	52.90	28.15	1787.99	1218.99	91.79	46.34	64.44	62.17	1.244	1.342
B2AR61	90.00	42.73	36.87	1542.78	825.84	31.42	23.96	57.43	52.82	1.820	2.243
B2AR61	410.00	27.49	29.14	1699.97	1890.91	30.86	37.76	56.95	58.93	1.454	1.563
B2AR61	771.70	26.47	23.90	988.39	981.79	19.91	41.62	36.86	56.11	2.666	1.548
B2AR69	90.00	80.18	77.91	2226.49	1914.39	24.99	19.44	51.98	54.61	2.864	2.684
B2AR69	410.00	64.88	69.88	2256.88	1950.86	34.96	29.88	52.99	52.43	1.944	1.775
B2AR69	771.70	66.98	57.45	812.61	2628.98	8.14	55.26	36.79	91.78	4.912	1.460
B3AR61	90.00	19.33	17.95	223.46	216.99	14.98	11.79	32.47	32.38	2.228	2.745
B3AR61	410.00	11.52	14.18	198.77	223.89	16.94	15.89	27.72	29.44	1.674	1.952
B3AR61	771.70	16.63	11.87	168.51	248.43	15.96	28.76	23.14	29.34	1.487	1.415
B3AR62	90.00	59.91	58.22	1367.19	1220.95	24.29	21.87	51.53	51.58	2.125	2.448
B3AR62	410.00	42.62	51.89	1916.33	1582.56	36.19	34.88	57.16	53.45	1.564	1.782
B3AR62	771.70	41.19	48.18	1146.19	1418.88	28.39	31.46	41.77	48.89	1.645	1.954
B3AR69	90.00	67.87	74.65	1112.79	1178.32	16.48	15.88	44.79	46.86	2.752	2.908
B3AR69	410.00	62.21	69.98	1322.73	1489.76	25.34	25.49	46.87	47.28	1.898	2.815
B3AR69	771.70	64.99	58.98	981.47	748.48	18.87	12.87	32.81	37.96	3.674	3.826

Table 6.2. Quantitative comparison by five parameters of computed and observed waves at given six conduit positions, with no corrections for shifts in observed waves.

RUN NO.	POSITION (FT)	TOTAL AREA OF WAVE FORM ABOVE BASE (FT-SEC) OBSERVED	TOTAL AREA OF WAVE FORM ABOVE BASE (FT-SEC) COMPUTED	FIRST MOMENT OF AREA ABOUT PEAK (FT-SEC2) OBSERVED	FIRST MOMENT OF AREA ABOUT PEAK (FT-SEC2) COMPUTED	TIME FROM PEAK TO CENTROID OF WAVE FORM (SEC) OBSERVED	TIME FROM PEAK TO CENTROID OF WAVE FORM (SEC) COMPUTED	STANDARD DEVIATION OF WAVE FORM ABOUT PEAK (SEC) OBSERVED	STANDARD DEVIATION OF WAVE FORM ABOUT PEAK (SEC) COMPUTED	RATIO OBSERVED	RATIO COMPUTED
1 3	50.00	35.66	36.11	755.83	486.84	21.14	13.46	43.18	40.61	2.043	3.017
1 3	254.24	36.64	31.72	1028.15	911.24	28.06	16.12	48.22	37.37	1.719	2.319
1 3	387.78	32.82	29.87	816.19	599.81	24.87	20.08	37.37	39.12	1.503	1.949
1 3	462.56	31.26	28.75	1018.89	599.19	32.59	20.84	47.14	38.21	1.447	1.835
1 3	669.83	16.25	26.73	454.55	675.76	28.01	25.28	41.20	40.48	1.471	1.681
1 3	771.55	30.49	27.34	744.93	715.95	24.43	26.19	38.05	38.95	1.557	1.487
1 4	50.00	54.91	53.76	1521.06	912.23	24.06	16.97	49.56	48.21	2.060	2.841
1 4	254.24	49.45	50.02	1435.65	1128.95	29.05	22.57	54.64	50.61	1.882	2.243
1 4	387.78	50.25	46.59	1543.22	1148.74	30.73	24.65	52.39	49.43	1.705	2.026
1 4	462.56	42.89	44.21	1525.75	1048.65	36.91	23.54	53.38	47.49	1.724	2.018
1 4	669.83	31.97	42.83	680.66	1324.60	21.29	30.93	36.72	51.54	1.725	1.666
1 4	771.55	44.61	42.23	1211.31	1176.13	27.15	27.85	43.43	45.19	1.599	1.629
1 8	50.00	49.88	55.51	1405.25	1094.49	28.17	19.72	53.40	50.04	1.896	2.538
1 8	254.24	47.22	49.78	1286.31	1372.78	27.24	27.58	51.15	51.09	1.878	1.855
1 8	387.78	42.00	45.18	1434.11	1411.58	34.14	31.36	54.43	52.31	1.594	1.671
1 8	462.56	35.77	42.88	1128.29	1393.76	31.54	32.51	53.46	52.73	1.695	1.622
1 8	669.83	30.94	36.84	910.59	1322.84	29.45	35.91	44.47	55.01	1.511	1.476
1 8	771.55	33.00	36.35	1694.36	1316.13	51.21	36.21	61.83	51.35	1.207	1.418
1 9	50.00	62.75	64.91	1721.31	1546.13	27.44	23.82	54.93	55.82	2.002	2.344
1 9	254.24	60.55	57.17	2095.59	1679.85	34.61	29.38	57.56	54.56	1.665	1.857
1 9	387.78	53.29	53.34	1819.19	1756.77	34.13	32.93	56.07	55.88	1.643	1.697
1 9	462.56	45.58	50.05	1795.42	1724.80	39.52	34.46	58.38	55.53	1.477	1.611
1 9	669.83	41.02	43.78	1464.22	1594.45	35.78	36.42	51.84	54.72	1.452	1.532
1 9	771.55	42.18	44.07	387.84	1626.38	9.28	36.91	36.83	52.79	4.006	1.431
19919	50.00	62.48	71.12	1287.43	668.78	20.63	9.48	48.19	41.21	2.336	4.383
19919	254.24	60.77	62.24	1953.95	1826.97	32.28	16.58	45.89	48.46	2.060	2.452
19919	387.78	52.28	54.86	1381.87	932.83	26.47	16.99	45.77	37.75	1.729	2.222
19919	462.56	46.78	52.88	1288.36	976.14	27.37	18.49	45.99	37.57	1.680	2.032
19919	669.83	37.54	39.57	654.55	496.95	16.98	12.54	35.85	31.93	2.121	2.546
19919	771.55	30.65	37.37	-134.65	529.30	-3.54	14.16	31.82	33.89	-8.993	2.336
1 10	50.00	94.47	89.68	3724.92	3233.31	39.43	36.06	76.55	75.73	1.941	2.188
1 10	254.24	106.81	83.52	5068.98	3764.48	47.81	45.07	81.95	78.75	1.714	1.747
1 10	387.78	88.82	79.12	4828.86	3865.82	54.86	48.84	84.43	81.52	1.539	1.669
1 10	462.56	82.36	76.16	4687.93	3712.39	56.92	48.75	87.84	79.72	1.529	1.695
1 10	669.83	72.61	68.67	4458.72	3571.25	61.41	51.99	86.88	79.15	1.402	1.522
1 10	771.55	62.79	65.16	1873.92	3188.68	29.84	47.71	63.14	72.88	2.116	1.526
1 11	50.00	19.11	21.17	164.67	224.85	8.62	10.58	24.84	30.15	2.789	2.848
1 11	254.24	15.74	18.63	67.49	225.91	4.91	12.12	8.95	27.46	1.824	2.265
1 11	387.78	16.12	16.77	244.15	219.56	15.15	12.49	25.43	25.16	1.547	2.014
1 11	462.56	12.89	16.00	287.78	225.58	16.12	13.97	23.34	25.58	1.448	1.825
1 11	669.83	11.16	13.61	211.85	218.82	18.91	16.88	29.41	24.44	1.555	1.528
1 11	771.55	12.98	13.30	184.68	220.35	11.99	16.81	19.48	25.63	1.618	1.525
1 12	50.00	41.35	44.32	984.88	729.81	21.06	16.47	47.32	47.77	2.164	2.901
1 12	254.24	36.33	39.77	932.88	798.38	25.66	19.87	49.15	45.88	1.916	2.309
1 12	387.78	36.92	37.98	1178.35	868.37	31.91	23.83	54.22	46.13	1.699	2.005
1 12	462.56	38.29	36.64	848.73	914.88	27.92	24.97	46.48	47.18	1.665	1.889
1 12	669.83	36.16	38.22	1016.18	1099.18	33.69	31.21	54.38	51.37	1.613	1.646
1 12	771.55	34.43	38.29	1141.21	947.32	33.18	26.86	48.49	43.38	1.469	1.613

RUN NO.	POSITION (FT)	TOTAL AREA OF WAVE FORM ABOVE BASE (FT-SEC) OBSERVED	TOTAL AREA OF WAVE FORM ABOVE BASE (FT-SEC) COMPUTED	FIRST MOMENT OF AREA ABOUT PEAK (FT-SEC2) OBSERVED	FIRST MOMENT OF AREA ABOUT PEAK (FT-SEC2) COMPUTED	TIME FROM PEAK TO CENTROID OF WAVE FORM (SEC) OBSERVED	TIME FROM PEAK TO CENTROID OF WAVE FORM (SEC) COMPUTED	STANDARD DEVIATION OF WAVE FORM ABOUT PEAK (SEC) OBSERVED	STANDARD DEVIATION OF WAVE FORM ABOUT PEAK (SEC) COMPUTED	RATIO OBSERVED	RATIO COMPUTED
1 13	50.00	89.05	80.72	799.71	1105.54	8.98	13.70	45.02	46.96	5.019	3.429
1 13	254.24	78.28	73.58	1330.87	1238.15	17.01	16.85	46.94	45.19	2.760	2.683
1 13	387.78	77.96	69.97	985.06	1302.76	12.61	18.62	43.44	45.77	3.445	2.458
1 13	462.56	64.17	66.68	-169.12	1277.95	-2.64	19.16	39.12	44.49	-14.846	2.321
1 13	669.83	61.08	65.85	1190.30	1498.84	19.51	23.48	42.52	46.13	2.179	1.965
1 13	771.55	64.82	65.94	1429.16	1454.61	22.05	22.44	48.79	42.59	1.850	1.898
19913	50.00	77.19	72.34	940.27	877.58	12.18	12.13	44.27	44.06	3.634	3.632
19913	254.24	66.94	67.84	941.46	1236.88	14.06	18.46	45.97	45.73	3.127	2.479
19913	387.78	71.72	62.68	1196.65	1173.11	16.68	18.74	44.01	43.55	2.638	2.324
19913	462.56	56.85	60.37	1337.21	1196.77	23.53	19.82	46.12	43.66	1.960	2.202
19913	669.83	58.68	58.99	1319.13	1364.93	26.85	23.14	46.16	45.31	1.773	1.958
19913	771.55	55.11	57.48	1199.61	1229.68	21.77	21.39	39.49	40.52	1.814	1.894
0 1	50.00	80.48	86.44	-4.59	-377.58	-.05	-4.37	60.45	60.86	-1163.345	-13.935
0 1	254.24	86.83	80.46	385.95	32.72	4.46	.41	63.48	66.67	14.237	149.185
0 1	387.78	81.84	75.91	52.56	269.22	.66	3.55	58.28	60.39	88.747	17.529
0 1	462.56	67.35	74.48	636.02	374.88	9.44	5.03	58.53	60.08	6.177	11.937
0 1	669.83	58.94	78.89	-945.88	519.55	-16.81	7.41	60.92	57.27	-3.605	7.726
0 1	771.55	66.34	68.29	-338.51	271.41	-4.98	3.97	50.73	51.72	-10.185	13.014
9 1	50.00	22.83	24.48	475.83	651.78	20.81	25.98	48.17	53.29	1.930	2.058
9 1	254.24	21.13	21.39	689.21	680.66	32.62	31.83	51.47	54.89	1.578	1.725
9 1	387.78	18.16	19.12	602.38	652.58	33.17	34.13	49.78	53.94	1.498	1.580
9 1	462.56	16.32	17.79	580.64	618.98	35.57	34.22	52.65	52.38	1.480	1.551
9 1	669.83	11.79	15.78	417.89	587.58	34.93	37.43	45.35	52.79	1.314	1.410
9 1	771.55	13.84	14.62	332.62	499.43	24.03	34.16	37.19	46.27	1.548	1.355
9 2	50.00	78.25	78.82	2536.24	2718.66	33.26	38.39	73.43	77.55	2.208	2.028
9 2	254.24	65.13	63.78	3298.81	2902.81	50.64	45.51	81.89	79.69	1.631	1.751
9 2	387.78	59.76	68.51	2537.55	2974.98	42.46	49.17	72.08	80.99	1.698	1.647
9 2	462.56	52.57	59.67	2895.84	2981.38	53.94	50.47	80.29	80.95	1.488	1.604
9 2	669.83	47.12	52.52	2457.78	2522.21	52.16	48.02	76.98	73.54	1.476	1.531
9 2	771.55	45.12	47.91	1756.41	1858.44	38.93	38.62	63.39	63.51	1.628	1.644
9 3	50.00	12.71	12.16	146.74	46.72	11.54	3.84	29.44	21.94	2.551	5.718
9 3	254.24	9.68	10.66	4.78	86.58	.50	8.12	11.76	21.19	23.621	2.648
9 3	387.78	9.91	9.78	93.42	98.78	9.42	9.56	14.51	20.11	1.540	2.149
9 3	462.56	8.86	9.88	144.78	95.52	16.33	10.38	24.05	19.84	1.473	1.849
9 3	669.83	7.16	7.61	68.66	88.84	9.59	11.57	19.76	18.31	2.060	1.582
9 3	771.98	6.76	7.82	98.89	108.79	13.32	14.47	18.16	21.64	1.363	1.496
9 4	98.88	51.57	49.79	987.58	548.25	17.68	11.81	43.99	42.67	2.500	3.875
9 4	254.24	47.63	48.46	872.47	664.24	18.32	14.39	43.11	41.71	2.354	2.898
9 4	387.78	44.86	41.92	738.16	687.23	16.39	16.48	41.18	48.83	2.508	2.491
9 4	462.56	38.47	48.83	422.99	857.98	11.88	18.43	38.46	48.88	3.497	2.439
9 4	669.83	52.61	59.67	39.99	796.62	1.23	20.88	34.98	41.88	28.524	2.881
9 4	771.98	33.01	38.18	888.69	976.37	16.92	18.11	34.94	35.67	2.868	2.961

symmetry. A negative t_c indicates that a majority of the depth hydrograph lies under the ascending limb, a positive t_c indcates a similar condition under the descending limb. All but two of the computed t_c values were positive, as shown in Tables 6.1 and 6.2. The standard deviation of the depth hydrograph about the peak, σ_p, is a measure of the dispersion of the wave-form about the peak, and the closeness of the computed σ_p to the observed σ_p indicates how well the computed depth hydrograph matches the observed depth hydrograph. Similarly, the ratio R measures the closeness of the computed and observed hydrographs.

These same five comparisons were also made with the observed peak depths shifted in time, so that the observed time, t_c, from the wave peak to the wave centroid was the same as for the computed value of t_c. This was done because the first and second moment comparisons are dependent upon the position of observed peak, and because the fluctuations of observed depth were such that most waves had several points that could have been specified as the wave peaks. Thus, the time to centroid of the observed and computed waves were made coincident.

In general, the time shifts necessary to equate the t_c values for computed and observed depth hydrographs were less than 5 seconds. The comparison of five parameters for the corrected times of peaks of observed waves are given in Tables 6.3 and 6.4. The shifts listed in Tables 6.3 and 6.4 are positive for a shift toward the time origin and negative for a shift away from the time origin.

Computed and observed values for all five parameters are plotted for no shift in Fig. 6.5 and for shifted peaks in Fig. 6.6. It should be noted that the points in these figures are not independent. That is, there are either three or six related points for each run which all make up a related group within the points of these figures.

The depth hydrograph areas are not affected by the shifts in peaks and so both of these comparisons are approximately the same. The only differences result from the condition that points were not plotted in Fig. 6.6 for any of the parameters if any one of them was negative. Thus, whenever a shift in a peak eliminated the negative value in the parameters of comparison, that comparison will appear in the plots of Fig. 6.6 but not in the plots of Fig. 6.5.

Comparisons of the hydrograph areas are consistent, that is, nearly all the values fall within the ±20 percent error-curves, as shown by Figs. 6.5 and 6.6. The unshifted first moments, however, show considerable scatter, with nearly 50 points falling outside the ±30 percent error curves. The effect of shifting the observed peaks results in reducing this number of outside points to only four, most points moved within the ±20 percent error-curves. The plots of the computed and observed times from peaks to centroids of wave hydrographs show almost a random scatter for no shifted observed peak times, and no error for the shifted times, by definition. The comparisons show the standard deviations of wave hydrographs about peaks to be, for most data, within the ±20 percent error-envelopes for the unshifted points, and within ±10 percent error-envelopes for the shifted observed peaks. Similarly, comparisons of the ratios of Eq. 6.2 are scattered but they are generally within ±30 percent error-curves for the unshifted peaks, and within ±20 percent error-curves for the shifted peaks.

The comparisons in Tables 6.1 through 6.4 and in Figs. 6.5 and 6.6 refer only to cases that treat the inflow of water only at the main conduit entrance as presented in Appendices 3 and 4. They do not refer to any inflow through the three lateral inlets.

Results on the runs that do involve inflows through lateral inlets are not summarized in the form of quantitative comparisons of the five parameters of comparisons, because of difficulties of applying the parameters as defined in Fig. 6.4.

6.5 Quantitative Comparison of Results by Depth-Versus-Distance Relations

The computed and observed waves as seen at an instant of time were compared by measuring the deviations between the corresponding points of computed curves and the points of observed waves at the positions of observation. These differences are listed in Tables 6.5 through 6.8. They give the depth deviation either at three or at each of six positions, x = 50.00, 254.24, 387.70, 462.56, 669.89, and 771.55 ft; absolute average deviation of the six points for each instant in time; and the ratio of the average difference of six differences to the conduit diameter. The mean of this ratio of the average difference versus the diameter for all runs and all times is 0.0256. The standard deviation of all differences is 0.0954 ft. Thus, if the distribution of these deviations is assumed to be normal, this last figure indicates that 67 percent of the computed points will fall within 0.0954 ft of the observed points. Again, the comparisons refer to runs for inflows only through the main conduit entrance.

6.6 General Comparison of Results by Wave-Peak-Depth Versus Distance and Time.

In Appendix 4, the computed and observed wave-peak depths are shown plotted versus both distance and time. For a quantitative comparison, the five parameters as defined by Fig. 6.4 are not applicable. Therefore, it was decided to make general visual comparisons of computed and observed data, not only for the observed data in this study but also with other data, on the rate of attenuation of flood peaks along free-surface flowing circular conduits. For this purpose, data on the attenuation of flood waves in partly full pipes, obtained experimentally at the Hydraulics Research Station, Wallingford, Berkshire, England, were used [4,5].

Graphs in Appendix 4, as stated above, are comparisons of computed and observed data on peak depth attenuations with distance and time as obtained in this study. The summary of experimental data obtained at Colorado State University, used for this comparison, are given in Table 6.9. Similarly, the summary of experimental data obtained at Wallingford, and used for this comparison, are given in Table 6.10. The graphs in Appendix 5 give the observed attenuations of peak depths versus distance or time of the Wallingford data and the computed attenuations by using the specified intervals scheme of the method of characteristics. These computations were made by using the inflow hydrographs of the Wallingford Report No. Int. 31, Fig. 2 of reference [4], for the conduit conditions used in the Wallingford study (3 inch diameter and a 300 ft long). The comparison of computed waves and observed waves at Wallingford was possible only for the peak depth attenuations, because this was the only dynamic wave data available in the report.

Table 6.3. Quantitative comparison by five parameters of computed and observed waves at given three conduit positions, with corrections of observed peak depths shifted in time.

RUN NO.	SHIFT (SEC)	TOTAL AREA OF WAVE FORM ABOVE BASE (FT-SEC)		FIRST MOMENT OF AREA ABOUT PEAK (FT-SEC2)		TIME FROM PEAK TO CENTROID OF WAVE FORM (SEC)		STANDARD DEVIATION OF WAVE FORM ABOUT PEAK (SEC)		RATIO	
		OBSERVED	COMPUTED	OBSERVED	COMPUTED	OBSERVED	COMPUTED	OBSERVED	COMPUTED	OBSERVED	COMPUTED
B2ARS1	3.15	2.69	2.31	28.36	24.30	10.53	10.54	22.75	20.01	2.160	2.849
B2ARS1	2.47	1.76	1.39	18.28	14.39	10.36	10.37	9.99	21.66	.964	2.089
B2ARS1	-20.42	-.02	.64	-.18	5.90	9.20	9.19	5.91	15.06	.643	1.639
B2A0S2	3.40	26.47	24.36	490.58	451.45	18.53	18.53	38.55	49.08	2.080	2.648
B2A0S2	1.25	21.41	18.76	592.08	518.91	27.65	27.66	40.90	46.01	1.479	1.664
B2A0S2	-4.84	18.56	15.94	582.18	499.75	31.36	31.36	42.08	44.19	1.342	1.439
B2A0S3	-2.38	39.32	36.17	800.87	736.52	20.37	20.36	45.74	51.22	2.245	2.515
B2A0S3	3.64	31.65	28.78	898.12	816.75	28.37	28.38	47.29	47.45	1.667	1.672
B2A0S3	-4.72	28.13	24.42	856.31	743.22	30.44	30.44	44.34	44.75	1.457	1.470
B3A0S1	16.98	1.65	3.42	32.52	67.30	19.66	19.66	21.39	34.25	1.088	1.742
B3A0S1	7.78	1.44	1.84	15.42	19.79	10.74	10.74	12.17	18.04	1.134	1.679
B3A0S1	-4.94	-.36	.11	1.45	-.44	-3.94	-3.94	3.94	4.16	-1.000	-1.054
B3A0S2	-1.32	15.64	15.95	35.39	36.04	2.26	2.26	19.48	20.74	8.612	9.179
B3A0S2	-10.50	13.96	13.31	151.19	144.14	10.83	10.83	26.38	21.98	2.436	2.030
B3A0S2	3.56	13.62	14.01	294.18	302.71	21.60	21.60	30.63	31.78	1.418	1.471
B3A0S3	3.15	33.23	36.45	689.61	756.71	20.75	20.76	43.18	52.78	2.080	2.545
B3A0S3	2.47	28.47	31.24	743.41	815.80	26.11	26.12	43.02	50.87	1.648	1.948
B3A0S3	-5.78	25.71	28.27	559.75	615.37	21.77	21.77	35.47	39.61	1.629	1.820
C2A0S2	-8.85	49.95	35.16	982.71	691.57	19.67	19.67	49.71	49.72	2.527	2.528
C2A0S2	-5.71	35.23	28.33	1039.19	855.67	29.50	29.50	46.38	49.33	1.572	1.672
C2A0S2	6.73	35.10	24.51	1212.62	846.81	34.55	34.55	48.88	47.91	1.415	1.387
C2A0S3	-12.29	67.83	46.61	711.15	498.54	10.48	10.48	44.24	39.87	4.220	3.804
C2A0S3	-14.51	54.09	38.59	1150.63	820.66	21.27	21.27	43.54	39.15	2.047	1.841
C2A0S3	13.66	50.74	35.98	1477.61	1047.96	29.12	29.12	45.91	43.02	1.577	1.477
C3A0S1	1.03	8.77	10.17	95.97	111.30	10.94	10.95	25.29	31.33	2.311	2.863
C3A0S1	-1.46	7.16	7.64	100.10	106.88	13.99	13.98	24.97	26.56	1.785	1.899
C3A0S1	8.23	4.83	6.51	88.55	119.47	18.35	18.35	22.93	26.43	1.250	1.440
C3A0S2	.85	23.44	26.39	391.68	441.23	16.71	16.72	38.42	41.89	2.299	2.506
C3A0S2	4.88	15.88	21.06	361.75	479.98	22.78	22.78	33.34	39.88	1.464	1.750
C3A0S2	6.48	18.38	19.61	527.90	565.72	28.85	28.85	37.46	39.67	1.298	1.375
C3A0S3	-4.73	35.67	39.61	328.92	365.09	9.22	9.22	32.29	35.54	3.502	3.856
C3A0S3	1.69	29.83	32.59	556.18	607.67	18.64	18.65	33.13	34.85	1.777	1.869
C3A0S3	7.57	32.56	31.63	843.06	819.04	25.89	25.89	37.34	37.63	1.442	1.453
D2ARS1	71.39	28.87	42.95	664.22	1367.17	31.82	31.83	75.25	61.48	2.364	1.932
D2ARS1	27.37	25.97	35.88	1215.69	1675.86	46.81	46.81	38.77	69.11	.828	1.476
D2ARS1	-5.45	32.98	26.13	1520.82	1218.98	46.34	46.34	60.14	62.17	1.298	1.342
D2A0S1	-7.87	42.73	35.87	1086.42	825.84	25.55	25.55	53.53	52.82	2.273	2.243
D2A0S1	-.85	27.49	29.14	1056.49	1098.51	37.71	37.70	55.46	58.95	1.471	1.563
D2A0S1	27.81	26.47	23.59	1181.35	981.73	41.61	41.62	53.81	56.11	1.293	1.348
D2A0S3	-9.88	89.18	77.91	1731.94	1514.38	19.44	19.44	49.13	50.61	2.527	2.684
D2A0S3	-9.43	64.98	68.88	1986.36	1995.86	29.53	29.53	49.18	52.43	1.664	1.775
D2A0S3	27.12	62.98	87.43	2219.86	2829.88	35.26	36.26	50.26	51.78	1.425	1.468
D3A0S1	-2.78	15.33	17.55	180.83	206.99	11.80	11.79	31.32	32.38	2.656	2.745
D3A0S1	-.66	11.52	14.08	183.19	225.85	15.90	15.89	27.35	29.44	1.719	1.852
D3A0S1	5.20	10.63	11.87	220.78	246.43	20.76	20.76	26.91	29.34	1.296	1.415
D3A0S2	-3.17	53.91	58.22	1136.27	1226.95	21.08	21.07	50.12	51.58	2.378	2.448
D3A0S2	-6.09	42.82	50.09	1260.54	1502.56	30.00	30.00	53.53	53.45	1.784	1.782
D3A0S2	6.06	41.19	45.18	1295.77	1418.65	31.46	31.46	45.71	48.89	1.453	1.554
D3A0S3	-.71	67.87	74.63	1864.49	1178.32	15.68	15.68	44.54	46.86	2.840	2.988
D3A0S3	-1.98	52.21	63.58	1223.38	1489.76	23.43	23.43	45.56	47.20	1.944	2.015
D3A0S3	1.99	54.99	58.98	691.83	748.48	12.57	12.57	33.21	37.96	2.643	3.028

Table 6.4. Quantitative comparison by five parameters of computed and observed waves at given six conduit positions, with corrections of observed peak depths shifted in time.

RUN NO.		SHIFT (SEC)	TOTAL AREA OF WAVE FORM ABOVE BASE (FT-SEC)		FIRST MOMENT OF AREA ABOUT PEAK (FT-SEC2)		TIME FROM PEAK TO CENTROID OF WAVE FORM (SEC)		STANDARD DEVIATION OF WAVE FORM ABOUT PEAK (SEC)		RATIO	
			OBSERVED	COMPUTED	OBSERVED	COMPUTED	OBSERVED	COMPUTED	OBSERVED	COMPUTED	OBSERVED	COMPUTED
1	3	-7.60	35.66	36.11	488.12	486.84	13.46	13.46	39.99	43.61	2.970	3.017
1	3	-11.94	36.64	31.72	598.74	511.24	16.12	16.12	42.48	37.37	2.638	2.319
1	3	-4.78	32.82	29.87	699.88	599.81	20.88	20.88	34.37	39.12	1.712	1.949
1	3	-11.75	31.26	28.75	651.62	599.19	20.84	20.84	39.94	38.21	1.916	1.855
1	3	-2.73	16.23	26.75	418.27	675.76	25.20	25.20	39.39	48.48	1.558	1.601
1	3	1.75	30.49	27.34	790.95	715.95	26.19	26.19	39.28	38.95	1.497	1.487
1	4	-7.89	54.91	53.76	951.89	912.23	16.97	16.97	46.54	48.21	2.742	2.841
1	4	-6.46	49.45	50.02	1116.19	1128.95	22.57	22.57	51.58	50.61	2.282	2.243
1	4	-6.87	50.23	46.59	1230.44	1148.74	24.66	24.65	49.88	49.43	1.991	2.035
1	4	-7.37	42.89	44.21	1089.69	1048.05	25.54	25.54	49.39	47.49	2.098	2.018
1	4	9.65	31.97	42.03	900.62	1324.60	30.92	30.93	45.03	51.54	1.391	1.666
1	4	.69	44.61	42.23	1242.28	1176.13	27.85	27.85	45.86	45.19	1.575	1.629
1	8	-8.45	49.88	55.51	983.66	1094.49	19.72	19.72	49.47	50.94	2.509	2.938
1	8	.33	47.22	49.78	1302.11	1372.78	27.57	27.58	51.33	51.09	1.862	1.853
1	8	-2.84	42.88	45.18	1314.76	1411.58	31.38	31.38	52.69	52.31	1.683	1.671
1	8	.96	35.77	42.88	1162.55	1393.76	32.58	32.51	54.03	52.73	1.662	1.622
1	8	6.47	38.94	36.84	1118.98	1322.84	35.91	35.91	48.99	53.01	1.364	1.476
1	8	-15.88	33.88	36.35	1198.88	1316.13	36.21	36.21	50.12	51.35	1.384	1.418
1	9	-3.62	62.73	64.91	1494.38	1546.13	23.82	23.82	55.21	55.82	2.234	2.344
1	9	-5.23	60.55	57.17	1779.12	1679.85	29.38	29.38	54.58	54.56	1.858	1.857
1	9	-1.28	53.29	53.34	1755.38	1756.77	32.94	32.93	55.35	55.88	1.680	1.697
1	9	-5.86	49.38	50.15	1563.76	1724.60	34.46	34.46	55.18	55.53	1.598	1.611
1	9	.72	41.82	45.78	1493.66	1594.43	36.42	36.42	52.34	54.72	1.437	1.502
1	9	27.71	42.18	44.87	1956.47	1626.38	36.96	36.91	51.32	52.79	1.391	1.451
19919		-11.23	62.48	71.12	586.81	668.78	9.48	9.48	44.56	41.21	4.738	4.383
19919		-8.78	69.77	62.24	1812.98	1626.97	16.58	16.58	45.38	40.46	2.629	2.452
19919		-9.48	52.28	54.86	887.21	952.05	16.99	16.99	41.42	37.75	2.414	2.222
19919		-8.88	46.78	52.88	868.14	976.14	18.49	18.49	41.35	37.57	2.235	2.032
19919		-4.36	37.54	39.87	471.62	496.35	12.95	12.94	34.01	31.95	2.711	2.546
19919		17.78	30.89	37.37	930.82	929.58	14.16	14.16	34.66	33.89	2.447	2.336
1	10	-5.37	94.47	89.68	3486.31	3295.91	36.86	36.86	74.87	75.73	2.076	2.180
1	10	-2.74	106.81	83.52	4778.58	3764.48	45.87	45.87	80.38	78.75	1.783	1.747
1	10	-6.82	80.82	79.12	4299.83	3865.82	48.84	48.84	80.65	81.52	1.651	1.669
1	10	-8.17	82.36	76.16	4815.13	3712.39	48.78	48.75	81.83	79.72	1.681	1.635
1	10	-9.42	72.68	68.67	3774.72	3576.25	51.99	51.99	79.65	79.15	1.532	1.522
1	10	17.86	62.79	66.16	2998.74	3188.68	47.71	47.71	73.38	72.88	1.536	1.526
1	11	1.96	19.11	21.17	282.18	224.85	18.58	18.58	24.81	30.15	2.345	2.848
1	11	7.21	15.74	18.63	166.57	225.91	12.12	12.12	6.52	27.46	.538	2.269
1	11	-2.66	16.12	16.77	201.42	289.56	12.58	12.49	21.81	25.16	1.745	2.014
1	11	-2.14	12.89	16.88	188.15	225.58	15.98	15.97	21.92	25.51	1.568	1.825
1	11	-2.85	11.16	13.61	179.48	218.82	16.88	16.88	27.67	24.44	1.728	1.524
1	11	4.82	12.98	13.98	216.76	228.35	16.81	16.81	22.69	25.63	1.358	1.525
1	12	-8.39	41.38	44.32	681.03	729.88	16.47	16.47	45.88	47.77	2.737	2.981
1	12	-8.78	36.33	39.77	722.12	798.38	19.87	19.87	46.39	45.88	2.334	2.389
1	12	-8.88	36.92	37.98	858.94	868.37	23.83	23.83	49.52	46.15	2.158	2.003
1	12	-2.96	30.29	36.64	786.42	914.88	24.98	24.97	44.77	47.18	1.793	1.889
1	12	-2.48	38.16	36.22	941.38	1199.15	31.21	31.21	52.85	51.37	1.693	1.646
1	12	-6.38	34.43	38.29	824.46	947.32	26.88	28.86	44.43	43.38	1.656	1.613

RUN NO.		SHIFT (SEC)	TOTAL AREA OF WAVE FORM ABOVE BASE (FT-SEC)		FIRST MOMENT OF AREA ABOUT PEAK (FT-SEC2)		TIME FROM PEAK TO CENTROID OF WAVE FORM (SEC)		STANDARD DEVIATION OF WAVE FORM ABOUT PEAK (SEC)		RATIO	
			OBSERVED	COMPUTED	OBSERVED	COMPUTED	OBSERVED	COMPUTED	OBSERVED	COMPUTED	OBSERVED	COMPUTED
1	15	4.71	89.85	88.72	1219.24	1105.54	13.69	13.78	46.19	46.96	3.375	3.429
1	15	-.16	78.28	73.58	1317.58	1258.15	16.85	16.85	46.89	45.19	2.783	2.683
1	15	6.81	77.96	69.97	1451.22	1382.76	18.61	18.62	45.54	45.77	2.447	2.458
1	15	21.88	64.17	66.68	1229.68	1277.95	19.16	19.16	45.48	44.49	2.269	2.321
1	15	9.97	61.88	65.85	1432.29	1498.84	25.48	25.48	44.48	46.13	1.894	1.965
1	15	.39	64.82	65.94	1454.15	1454.61	22.43	22.44	41.88	42.59	1.828	1.898
19915		-.85	77.19	72.34	936.59	877.58	12.13	12.13	44.26	44.86	3.648	3.652
19915		4.38	66.94	67.84	1254.62	1256.88	18.44	18.45	45.56	45.73	2.471	2.479
19915		2.85	71.72	62.68	1345.78	1175.11	18.74	18.74	44.85	43.55	2.392	2.324
19915		-9.78	56.85	60.37	1126.89	1196.77	19.85	19.82	44.35	43.66	2.256	2.232
19915		-2.89	58.68	58.99	1172.85	1364.93	23.14	23.14	44.59	45.31	1.927	1.958
19915		-.37	55.11	57.48	1179.28	1229.68	21.48	21.39	39.29	40.52	1.836	1.894
8	1	-4.31	88.48	86.44	-385.78	-377.58	-4.36	-4.37	60.61	60.86	-13.891	-13.935
8	1	-4.85	86.85	88.46	35.32	32.72	.41	.41	63.32	60.67	154.215	149.185
8	1	2.89	88.84	79.91	283.62	269.22	3.54	3.55	58.38	60.39	16.475	17.029
8	1	-4.41	67.95	74.48	339.29	374.88	5.84	5.83	57.78	60.88	11.469	11.957
8	1	23.42	58.94	78.89	436.72	519.53	7.41	7.41	59.25	67.27	7.996	7.726
8	1	8.95	66.34	68.29	263.35	271.41	3.97	3.97	58.64	51.72	12.758	13.314
9	1	5.89	22.85	24.48	591.16	651.78	25.89	25.98	45.12	55.29	1.662	2.358
9	1	-.79	21.15	21.39	672.56	680.66	31.83	31.83	54.98	54.89	1.602	1.725
9	1	.95	18.16	19.12	619.67	652.58	34.12	34.13	58.34	53.94	1.475	1.582
9	1	-1.35	16.32	17.79	558.62	608.98	34.22	34.22	51.75	52.38	1.512	1.531
9	1	2.89	11.79	15.78	441.21	587.58	37.42	37.43	47.68	52.79	1.272	1.413
9	1	18.12	13.84	14.62	472.75	499.43	34.15	34.16	44.48	46.27	1.308	1.355
9	2	5.13	70.25	70.82	2696.68	2718.66	38.39	38.39	75.89	77.55	1.977	2.028
9	2	-5.12	65.13	63.78	2964.32	2982.88	45.51	45.51	77.99	79.69	1.714	1.751
9	2	6.78	59.76	60.51	2938.83	2974.98	49.16	49.17	76.22	80.99	1.550	1.647
9	2	-3.46	52.57	59.67	2655.71	2981.38	50.48	50.47	70.88	80.95	1.545	1.604
9	2	-4.14	47.12	52.52	2262.69	2522.28	48.02	48.02	74.24	73.54	1.546	1.531
9	2	-.38	45.12	47.91	1742.75	1858.44	38.63	38.62	65.28	65.51	1.636	1.644
9	3	-7.78	12.71	12.16	48.98	46.72	3.85	3.84	27.36	21.94	7.113	5.713
9	3	7.62	9.68	10.66	77.97	86.58	8.12	8.12	8.52	21.19	1.049	2.608
9	3	-.86	9.91	9.78	92.81	90.78	9.36	9.36	14.47	20.11	1.546	2.149
9	3	-6.13	8.86	9.88	91.27	99.52	10.30	10.30	20.44	19.04	1.984	1.849
9	3	1.98	7.16	7.61	82.82	88.14	11.57	11.57	20.88	18.31	1.797	1.582
9	3	1.19	6.76	7.52	97.86	108.79	14.47	14.47	19.81	21.64	1.314	1.495
9	4	-6.88	51.57	49.79	568.88	548.25	11.02	11.01	41.79	42.67	3.794	3.875
9	4	-5.92	47.69	48.46	685.72	694.24	14.48	14.59	41.68	41.71	2.889	2.898
9	4	.88	44.96	41.92	738.34	687.23	16.39	16.48	41.11	40.83	2.508	2.491
9	4	5.44	38.47	40.89	632.18	687.98	16.45	16.45	40.38	40.88	2.455	2.459
9	4	18.88	32.61	38.87	484.78	798.62	28.88	28.88	48.32	41.88	2.888	2.881
9	4	-1.81	38.81	38.18	498.91	578.37	18.11	18.11	34.18	38.67	2.256	2.361

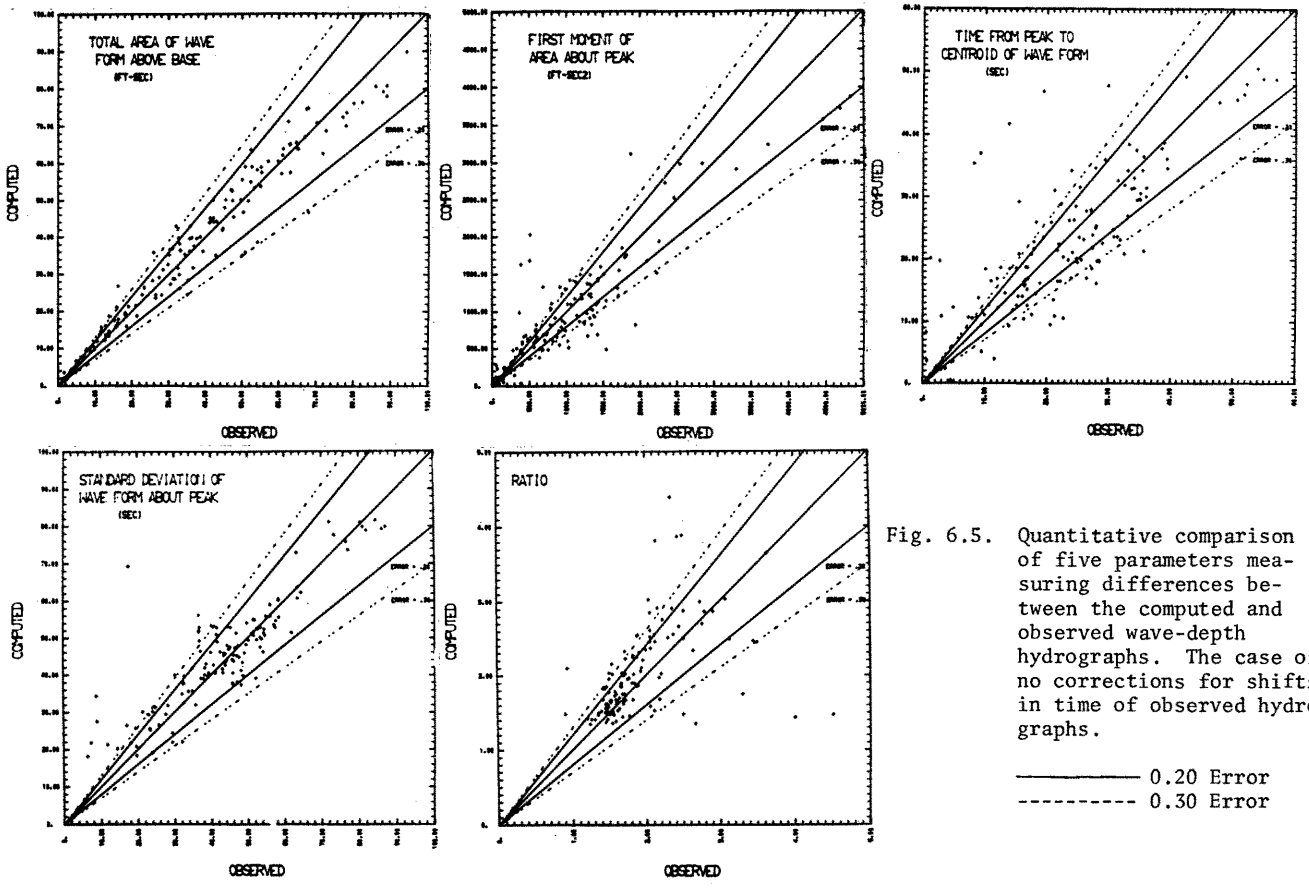

Fig. 6.5. Quantitative comparison of five parameters measuring differences between the computed and observed wave-depth hydrographs. The case of no corrections for shifts in time of observed hydrographs.

———— 0.20 Error
---------- 0.30 Error

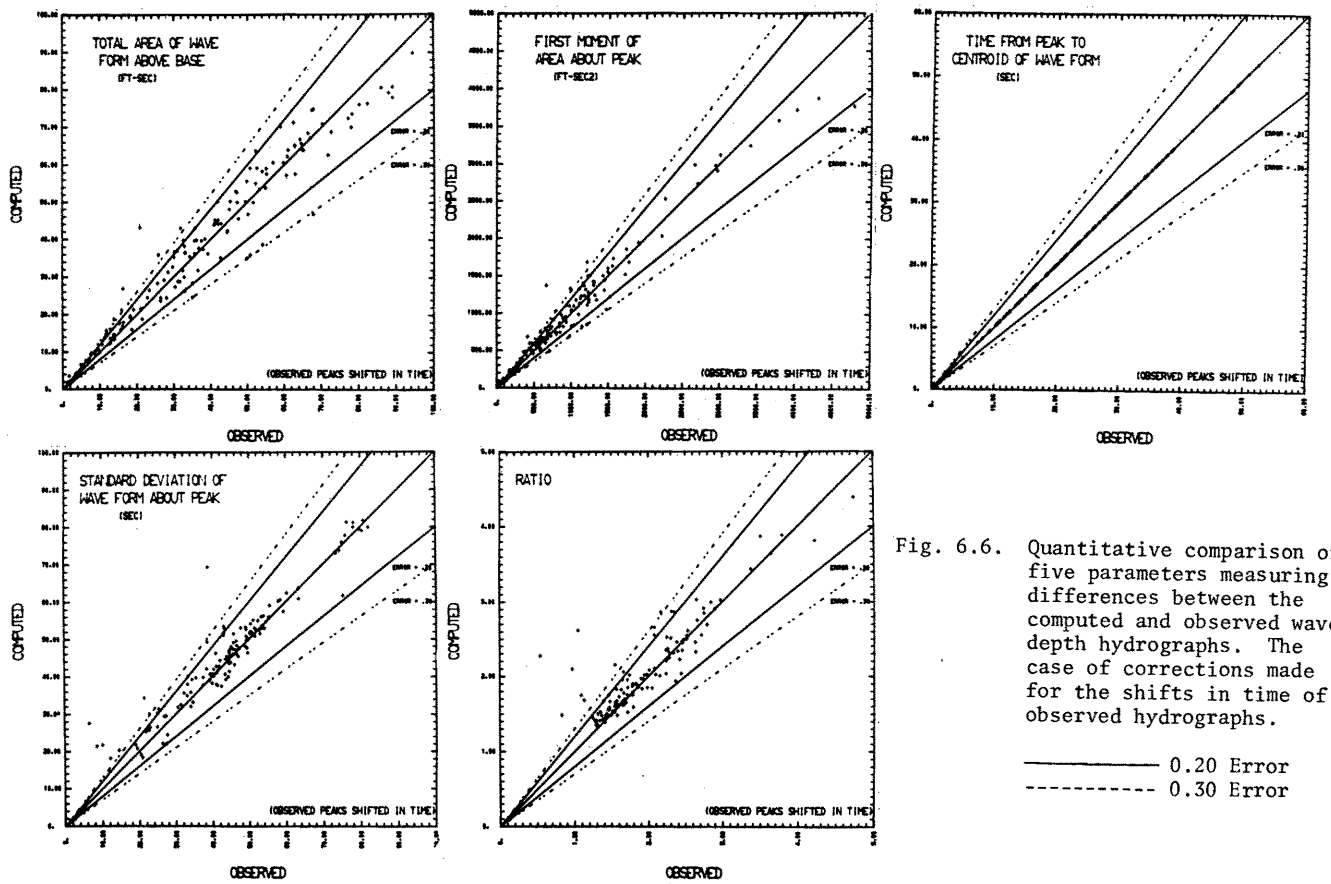

Fig. 6.6. Quantitative comparison of five parameters measuring differences between the computed and observed wave-depth hydrographs. The case of corrections made for the shifts in time of observed hydrographs.

———— 0.20 Error
---------- 0.30 Error

Table 6.5. Qualitative comparison of computed and observed depth-versus-distance wave profiles.

RUN	TIME	- DIFFERENCES IN FEET BETWEEN OBSERVED AND COMPUTED POINTS - POSITIONS 1	2	3	4	5	6	AVERAGE	AVERAGE/DIA RATIO
B2ARS1	30.13	-.1006	-.0459	-.0688				.0718	.02452
B2ARS1	60.26	-.0866	-.0463	-.0631				.0653	.02233
B2ARS1	90.40	-.0802	-.0467	-.0514				.0594	.02031
B2ARS1	120.13	-.0856	-.0408	-.0417				.0560	.01915
B2ARS1	150.26	-.0872	-.0404	-.0581				.0619	.02116
B2ARS1	180.40	-.0864	-.0569	-.0482				.0638	.02182
B2A0S2	30.12	.0865	-.0772	-.0589				.0742	.02535
B2A0S2	60.25	-.1212	-.0676	-.0464				.0784	.02678
B2A0S2	90.01	-.0858	-.0809	-.0564				.0743	.02540
B2A0S2	120.14	-.0654	-.0396	.2052				.1034	.03534
B2A0S2	150.26	-.0614	-.0561	-.0579				.0518	.01770
B2A0S2	180.05	-.0728	-.0327	-.0244				.0433	.01480
B2A0S2	210.15	-.0768	-.0579	-.0285				.0540	.01846
B2A0S2	240.28	-.0758	-.0437	-.0341				.0512	.01748
B2A0S2	270.04	-.0696	-.0508	-.0377				.0524	.01792
B2A0S3	30.27	.0249	-.0589	-.0588				.0475	.01624
B2A0S3	60.20	-.1064	-.0598	-.0480				.0714	.02441
B2A0S3	90.13	-.1050	-.0933	-.0513				.0832	.02844
B2A0S3	120.05	-.0714	-.0554	.2612				.1293	.04420
B2A0S3	150.33	-.0956	-.0181	-.0539				.0559	.01909
B2A0S3	180.26	-.0959	-.0251	-.0200				.0470	.01606
B2A0S3	210.18	-.1041	-.0410	-.0151				.0534	.01824
B2A0S3	240.11	-.1030	-.0315	-.0571				.0571	.01953
B2A0S3	270.04	-.0944	-.0413	-.0330				.0562	.01922
B3A0S1	30.15	.0197	.0205	.0097				.0166	.00568
B3A0S1	60.30	.0221	.0420	.0248				.0296	.01012
B3A0S1	90.08	.0211	.0200	.0225				.0212	.00724
B3A0S2	30.31	.0100	.0199	.0168				.0156	.00531
B3A0S2	60.26	-.0207	.1045	.0185				.0746	.02548
B3A0S2	90.22	.0172	.0072	.0200				.0148	.00506
B3A0S2	120.18	.0098	.0277	.0230				.0199	.00680
B3A0S2	150.13	.0134	.0382	.0201				.0239	.00816
B3A0S2	180.09	.0115	.0265	.0239				.0206	.00705
B3A0S2	210.05	.0127	.0326	.0269				.0240	.00822
B3A0S2	240.00	.0132	.0304	.0294				.0243	.00832
B3A0S3	30.35	.0357	.0170	.0122				.0210	.00716
B3A0S3	60.32	-.0258	.0646	.0208				.0368	.01257
B3A0S3	90.32	.0410	-.0067	.0173				.0217	.00741
B3A0S3	120.31	.0328	.0075	.0070				.0158	.00539
B3A0S3	150.30	.0257	.0273	.0009				.0180	.00614
B3A0S3	180.29	.0135	.0202	.0159				.0166	.00566
B3A0S3	210.20	.0220	.0186	.0268				.0227	.00776
B3A0S3	240.28	.0254	.0257	.0247				.0253	.00863
B3A0S3	270.27	.0287	.0231	.0270				.0263	.00897

RUN	TIME	- DIFFERENCES IN FEET BETWEEN OBSERVED AND COMPUTED POINTS - POSITIONS 1	2	3	4	5	6	AVERAGE	AVERAGE/DIA RATIO
C2A0S2	30.21	.0606	-.2269	-.2050				.1642	.05610
C2A0S2	60.08	-.2474	.2633	-.2015				.2374	.08113
C2A0S2	90.29	-.1789	-.2694	-.1982				.2155	.07365
C2A0S2	120.16	-.1654	-.1127	-.1588				.1456	.04977
C2A0S2	150.03	-.2214	-.1632	-.1303				.1716	.05866
C2A0S2	180.24	-.2294	-.1613	-.1046				.1651	.05641
C2A0S2	210.11	-.2419	-.1726	-.1117				.1754	.05995
C2A0S2	240.32	-.2522	-.1603	-.1367				.1831	.06257
C2A0S2	270.19	-.2596	-.1799	-.1439				.1945	.06645
C2A0S3	30.11	.0965	-.1961	-.1703				.1542	.05271
C2A0S3	60.22	-.2985	.1142	-.1656				.1928	.06588
C2A0S3	90.00	-.2229	-.2400	-.1657				.2089	.07137
C2A0S3	120.11	-.2314	-.0841	-.1704				.1620	.05536
C2A0S3	150.22	-.2767	-.1163	-.0985				.1638	.05599
C2A0S3	180.01	-.2973	-.1709	-.0786				.1823	.06230
C2A0S3	210.12	-.3240	-.1888	-.0996				.2041	.06976
C2A0S3	240.23	-.3442	-.1933	-.1478				.2285	.07807
C2A0S3	270.01	-.3496	-.2309	-.1665				.2490	.08509
C3A0S1	30.09	-.0083	.0476	.0634				.0398	.01359
C3A0S1	60.17	.0795	.0667	.0753				.0738	.02523
C3A0S1	90.26	.0844	.0512	.0650				.0669	.02285
C3A0S1	120.34	.0821	.0703	.0376				.0634	.02165
C3A0S1	150.08	.0718	.0779	.0781				.0759	.02595
C3A0S1	180.16	.0749	.0487	.0625				.0594	.02030
C3A0S2	30.20	.0121	.0744	.0562				.0475	.01625
C3A0S2	60.07	.0878	-.0085	.0594				.0519	.01775
C3A0S2	90.27	.0856	.0099	.0584				.0513	.01753
C3A0S2	120.14	.0906	.0198	.0815				.0639	.02185
C3A0S2	150.01	.0861	.0369	.0673				.0634	.02168
C3A0S2	180.22	.0822	.0330	.0687				.0613	.02095
C3A0S2	210.09	.0751	.0342	.0709				.0594	.02030
C3A0S2	240.29	.0852	.0472	.0725				.0683	.02333
C3A0S3	30.05	-.0116	.0567	.0070				.0251	.00858
C3A0S3	60.18	-.0327	.0442	.0238				.0336	.01148
C3A0S3	90.15	.0070	-.0329	.0257				.0219	.00748
C3A0S3	120.20	.0286	.0186	.0190				.0220	.00753
C3A0S3	150.25	.0039	.0141	.0157				.0112	.00384
C3A0S3	180.29	-.0016	.0050	.0081				.0049	.00167
C3A0S3	210.02	.0005	.0010	.0147				.0054	.00186
C3A0S3	240.07	.0007	-.0005	.0175				.0089	.00304
D2ARS1	30.08	-.1716	-.2073	-.1852				.1881	.06427
D2ARS1	60.17	-.0503	-.4679	-.1859				.2347	.08021
D2ARS1	90.25	-.1087	-.1634	-.1863				.1928	.05222
D2ARS1	120.33	-.1856	-.0652	-.1797				.1435	.04904
D2ARS1	150.08	-.1682	-.0642	-.0763				.1029	.03517
D2ARS1	180.16	-.0254	-.0941	-.0409				.0535	.01827
D2ARS1	210.24	.0013	-.1074	-.0289				.0459	.01567
D2ARS1	240.33	.0194	-.1142	-.0516				.0617	.02110
D2ARS1	270.07	.0299	-.0233	-.0682				.0405	.01382

Table 6.6. Qualitative comparison of computed and observed depth-versus-distance wave profiles.

RUN	TIME	- DIFFERENCES IN FEET BETWEEN OBSERVED AND COMPUTED POINTS - POSITIONS 1	2	3	4	5	6	AVERAGE	AVERAGE/DIA RATIO
D2A0S1	30.23	-.1160	-.1819	-.1729				.1572	.05372
D2A0S1	60.12	-.0189	-.2348	-.1771				.1436	.04906
D2A0S1	90.01	-.0563	-.1801	-.1785				.1382	.04724
D2A0S1	120.24	-.0885	-.1778	-.1909				.1524	.05208
D2A0S1	150.13	-.0667	-.0958	-.1005				.0875	.02983
D2A0S1	180.02	-.0812	-.1040	-.0903				.0918	.03138
D2A0S1	210.25	-.0891	-.1058	-.0646				.0865	.02957
D2A0S1	240.14	-.0997	-.1157	-.0770				.0975	.03331
D2A0S1	270.03	-.1072	-.1160	-.0785				.1008	.03444
D2A0S3	30.26	-.1381	-.1278	-.1146				.1268	.04334
D2A0S3	60.21	-.1018	-.4500	-.1250				.2249	.07686
D2A0S3	90.17	-.0831	-.2101	-.1217				.1116	.03815
D2A0S3	120.12	-.0986	-.1871	-.1635				.1497	.05117
D2A0S3	150.07	-.0739	-.0000	-.0285				.0368	.01257
D2A0S3	180.02	-.1067	-.1111	-.0329				.0836	.02855
D2A0S3	210.28	-.1405	-.0889	.0142				.0811	.02772
D2A0S3	240.23	-.1550	-.1061	-.0422				.1011	.03455
D2A0S3	270.19	-.1710	-.1137	-.0494				.1114	.03807
D3A0S1	30.26	-.0196	.0655	.0304				.0385	.01316
D3A0S1	60.19	-.0142	.0471	.0373				.0329	.01124
D3A0S1	90.12	.0399	-.0063	.3066				.1176	.04018
D3A0S1	120.05	.0555	.0517	-.0272				.0448	.01531
D3A0S1	150.31	.0393	.0664	.0290				.0449	.01534
D3A0S1	180.24	.0365	.0593	.0305				.0421	.01438
D3A0S2	30.11	-.0455	.0625	.0382				.0488	.01667
D3A0S2	60.22	-.0652	-.0143	.0512				.0436	.01489
D3A0S2	90.02	.0706	-.1254	-.0200				.0720	.02461
D3A0S2	120.13	.0356	.0306	.0234				.0299	.01021
D3A0S2	150.25	.0492	.0468	.0138				.0366	.01251
D3A0S2	180.05	.0309	.0715	.0362				.0462	.01579
D3A0S2	210.16	.0296	.0607	.0627				.0537	.01834
D3A0S2	240.27	.0324	.0756	.0642				.0567	.01938
D3A0S2	270.07	.0203	.0626	.0652				.0521	.01779
D3A0S3	30.18	-.0349	.0366	.0360				.0358	.01224
D3A0S3	60.21	-.0327	.0560	.0578				.0488	.01668
D3A0S3	90.01	-.0260	-.1286	-.0369				.0638	.02181
D3A0S3	120.12	-.0210	-.0240	.0186				.0212	.00726
D3A0S3	150.22	-.0164	.0058	-.0260				.0161	.00549
D3A0S3	180.02	.0013	-.0230	.0256				.0169	.00577
D3A0S3	210.15	-.0023	-.0058	.0084				.0027	.00093
D3A0S3	240.25	-.0106	-.0036	.0028				.0056	.00192
D3A0S3	270.04	-.0100	-.0220	.0111				.0146	.00500

RUN		TIME	- DIFFERENCES IN FEET BETWEEN OBSERVED AND COMPUTED POINTS - POSITIONS 1	2	3	4	5	6	AVERAGE	AVERAGE/DIA RATIO
1	3	20.15	.0491	-.0204	.0626	-.0277	-.0484	-.1631	.0619	.02114
1	3	40.29	-.0127	.0554	.0929	-.0182	-.0714	-.1777	.0714	.02439
1	3	60.12	-.0284	-.0903	.1375	.0425	-.0574	-.1497	.0843	.02881
1	3	80.27	-.0270	-.1669	-.0553	-.1580	.1734	-.1573	.1230	.04204
1	3	100.10	-.0268	-.1108	.0450	-.0576	-.1561	-.1287	.0875	.02990
1	3	120.24	.0152	-.0637	.0547	-.0522	-.2067	-.1755	.0943	.03222
1	3	140.07	-.0209	-.0391	.0363	-.0102	-.0382	-.1821	.0545	.01861
1	3	160.22	-.0107	-.0361	-.0080	-.0225	-.0647	-.1492	.0485	.01657
1	3	180.04	-.0225	-.0494	-.0637	-.0878	-.0550	-.1715	.0749	.02561
1	3	200.19	-.0336	-.1138	-.0545	-.1467	-.0740	-.1810	.1005	.03434
1	3	220.02	-.0409	-.1109	-.0494	-.1282	-.0809	-.1947	.1008	.03446
1	3	240.17	-.0247	-.0933	-.0294	-.1264	-.0745	-.1840	.0887	.03032
1	4	20.27	.0172	-.0391	.0000	-.0775	-.1057	-.2005	.0733	.02505
1	4	40.24	.0392	.0052	-.0152	-.0040	-.0024	-.2355	.0769	.02628
1	4	60.20	-.1036	.0789	.1280	-.0481	-.1136	-.2226	.1158	.03957
1	4	80.16	-.0665	-.1200	-.0307	-.0920	-.1095	-.2115	.1050	.03590
1	4	100.12	-.0411	-.0529	.0366	-.2135	-.1848	-.0921	.1035	.03538
1	4	120.08	-.0117	.0049	.0496	-.1061	-.2668	-.1732	.1020	.03487
1	4	140.05	-.0260	.0061	.0202	-.0416	-.2600	-.2084	.0937	.03202
1	4	160.01	-.0060	-.0119	.0022	-.0468	-.0695	-.1685	.0508	.01735
1	4	180.28	-.0113	.0172	.0098	-.0127	-.0917	-.1732	.0527	.01800
1	4	200.24	-.0268	.0026	.0220	-.0390	-.0939	-.1848	.0615	.02102
1	4	220.21	-.0522	-.0672	.0259	-.0243	-.0909	-.1579	.0561	.01916
1	4	240.17	-.0293	-.0039	.0088	-.0324	-.0473	-.1865	.0513	.01754
1	4	260.13	-.0298	-.0011	-.0091	-.0578	-.1156	-.1865	.0665	.02273
1	4	280.09	-.0272	-.0068	-.0059	-.0397	-.0587	-.1928	.0552	.01886
1	8	20.38	.1583	.0373	.0494	.1235	.0752	.0824	.0877	.02997
1	8	40.27	.0517	.0865	.0737	.1215	.0313	.0848	.0749	.02559
1	8	60.24	-.2494	.1219	.0816	.1223	.0032	.0804	.1798	.06145
1	8	80.21	-.0236	-.0869	-.0956	.0413	.0328	.0874	.0611	.02089
1	8	100.18	.0540	-.0973	-.1035	-.0780	.4233	.1236	.1419	.04850
1	8	120.15	-.0313	.0086	-.0022	-.0688	-.0578	.0138	.0304	.01040
1	8	140.12	.0252	.0162	.0607	.0294	-.0882	.0455	.0442	.01511
1	8	160.09	.0278	.0250	.0208	.0771	-.0656	.0276	.0408	.01395
1	8	180.06	.0228	.0157	.0309	.0771	.0079	.0445	.0331	.01130
1	8	200.03	.0308	.0760	.0201	.0867	.0195	.0450	.0469	.01602
1	8	220.01	.0199	.0867	.0412	.0925	.0020	.0518	.0440	.01504
1	8	240.30	-.0067	.0294	.0378	.0892	.0067	.0575	.0378	.01293
1	8	260.27	-.0066	.0245	.0281	.0964	.0098	.0582	.0372	.01271
1	8	280.26	.0092	.0179	.0308	.0504	.0146	.0507	.0330	.01126

Table 6.7. Qualitative comparison of computed and observed depth-versus-distance wave profiles

RUN	TIME	- DIFFERENCES IN FEET BETWEEN OBSERVED AND COMPUTED POINTS - POSITIONS 1	2	3	4	5	6	AVERAGE	AVERAGE/DIA RATIO
1 9	20.08	.0920	-.0132	.0415	.0087	-.0472	.0413	.0407	.01389
1 9	40.16	.1079	-.0212	.0449	.0073	-.0485	.0490	.0464	.01587
1 9	60.24	-.1802	.1538	.5864	.0015	-.0440	.0437	.1349	.04610
1 9	80.32	-.1113	-.0549	-.0331	.0236	-.0396	.0500	.0521	.01780
1 9	100.07	.0278	-.0711	-.0705	-.1281	.0088	.1838	.0817	.02791
1 9	120.15	-.0320	.0065	.0308	-.1211	-.0813	-.0441	.0526	.01799
1 9	140.23	.0625	.0206	.1081	.0034	-.0944	.0236	.0521	.01780
1 9	160.31	.0317	-.0077	.0676	-.0030	-.1116	.0133	.0391	.01338
1 9	180.07	.0318	-.0136	.0390	-.0011	-.0165	.0448	.0245	.00857
1 9	200.15	.0151	.0172	.0606	-.0011	-.0019	.0432	.0232	.00792
1 9	220.23	.0095	.0216	.0589	.0060	-.0378	.0533	.0312	.01065
1 9	240.31	.0016	.0031	.0665	.0080	-.0227	.0397	.0236	.00806
1 9	260.06	-.0077	-.0084	.0497	.0141	-.0172	.0374	.0224	.00767
1 9	280.14	.0042	-.0090	.0446	-.0016	-.0123	.0438	.0193	.00658
19909	20.25	.2790	.2092	.2890	.2307	.1974	.2662	.2452	.08381
19909	40.19	.1587	.2071	.2984	.2296	.1957	.2687	.2250	.07690
19909	60.13	.0552	.2825	.2866	.2290	.1959	.2665	.2193	.07494
19909	80.07	-.1671	.1603	.2940	.0073	.1967	.2657	.3152	.10771
19909	100.01	-.0321	-.0376	.0376	.1017	.7066	.2684	.1973	.06744
19909	120.26	.0421	-.0274	.0143	-.0457	.1552	.0530	.1896	.06480
19909	140.20	.0692	.0358	.1224	.0204	.0145	.1257	.0643	.02198
19909	160.14	.0798	.0372	.1488	.0188	-.0245	.1251	.0724	.02473
19909	180.08	.0593	.0439	.1307	.0768	-.0447	.1150	.0784	.02680
19909	200.02	.0684	.0307	.1317	.0562	.0949	.1154	.0829	.02832
19909	220.27	.0492	.0744	.1384	.0697	.0413	.1025	.0793	.02708
19909	240.21	.0458	.0598	.1371	.0582	.0352	.0846	.0701	.02396
19909	260.15	.0418	.0558	.1378	.0582	.0509	.0924	.0727	.02484
19909	280.09	.0432	.0406	.1272	.0469	.0407	.0931	.0653	.02231
1 10	20.16	.1979	-.0115	.0577	.0237	-.0355	.0644	.0651	.02225
1 10	40.08	.1755	.0629	.0716	.0319	-.0266	.0677	.0727	.02483
1 10	60.16	.0585	.4191	.2653	.0343	-.0286	.0647	.1417	.04844
1 10	80.08	-.1885	.1575	.1671	.2777	-.0217	.0694	.1437	.04909
1 10	100.16	-.0859	-.0420	-.0358	.0008	.6743	.0701	.1514	.05172
1 10	120.01	-.0169	.0341	-.0438	-.1172	-.0048	.3288	.0409	.01398
1 10	140.17	.0357	.0097	.0911	-.0387	-.0886	-.0305	.0490	.01676
1 10	160.01	.0229	-.0047	.0843	-.0167	-.1276	-.0205	.0461	.01576
1 10	180.17	.0148	-.0060	.0566	.0260	-.0240	.0089	.0226	.00772
1 10	200.01	.0035	.0345	.0593	.0295	.0093	.0190	.0258	.00883
1 10	220.17	-.0110	.0192	.0569	.0306	-.0221	.0252	.0275	.00940
1 10	240.01	-.0089	.0165	.0632	.0285	-.0247	.0259	.0279	.00955
1 10	260.17	-.0199	.0004	.0518	.0297	-.0198	.0371	.0265	.00904
1 10	280.01	-.0224	-.0088	.0308	.0208	-.0283	.0377	.0247	.00843
1 10	300.17	-.0222	-.0143	.0427	-.0029	-.0192	.0428	.0240	.00821
1 10	320.01	-.0244	-.0297	.0382	.0075	-.0203	.0403	.0267	.00914
1 10	340.18	-.0259	-.0314	.0137	.0035	-.0299	.0376	.0237	.00809
1 10	360.02	-.0234	-.0370	.0201	-.0144	-.0394	.0346	.0283	.00967
1 10	380.18	-.0307	-.0422	.0188	-.0244	-.0406	.0316	.0314	.01073

RUN	TIME	- DIFFERENCES IN FEET BETWEEN OBSERVED AND COMPUTED POINTS - POSITIONS 1	2	3	4	5	6	AVERAGE	AVERAGE/DIA RATIO
1 11	20.11	.1394	-.0221	.0715	-.0022	-.0418	.0286	.0509	.01740
1 11	40.21	-.0633	.1631	.0493	.0016	-.0465	.0278	.0586	.02002
1 11	60.32	-.0593	-.1490	.1739	.2207	-.0532	.0266	.1138	.03888
1 11	80.18	.0292	-.0770	-.0379	-.1330	.1346	.0332	.0741	.02534
1 11	100.20	.0063	-.0279	.0621	-.0145	-.1646	.0356	.0518	.01771
1 11	120.31	.0424	-.0350	.0656	.0016	-.1607	.0093	.0524	.01791
1 11	140.09	.0346	-.0188	.0517	.0195	-.0538	.0101	.0314	.01074
1 11	160.19	.0164	-.0225	.0498	.0217	-.0300	.0370	.0295	.01010
1 11	180.30	.0224	-.0080	.0663	.0152	-.0434	.0357	.0318	.01088
1 12	20.18	.0726	-.0396	.1008	-.0179	-.0568	.0507	.0564	.01927
1 12	40.04	.0458	.0759	.0983	-.0114	-.0587	.0110	.0495	.01692
1 12	60.22	-.1568	-.0220	.2195	.1289	-.0498	.0927	.1102	.03767
1 12	80.08	-.1015	-.2305	-.0126	-.1204	.0192	.0390	.0872	.02980
1 12	100.25	-.0188	-.0795	.0350	-.2401	-.1327	.0728	.0963	.03292
1 12	120.11	.0241	-.0488	.1034	-.0815	-.2270	-.0163	.0822	.02808
1 12	140.29	-.0052	-.0471	.0836	-.0207	-.1588	-.0366	.0587	.02005
1 12	160.15	-.0103	-.0640	.0640	-.0362	-.0428	.0070	.0374	.01277
1 12	180.01	.0031	-.0147	.0763	-.0230	-.0648	.0049	.0311	.01064
1 12	200.19	-.0184	-.0355	.0797	-.0444	-.0717	.0414	.0485	.01658
1 12	220.05	-.0361	-.0553	.0892	-.0428	-.0669	.0378	.0547	.01868
1 12	240.23	-.0175	-.0585	.0691	-.0397	-.0643	.0290	.0465	.01584
1 12	260.09	-.0248	-.0565	.0767	-.0568	-.0699	.0225	.0512	.01750
1 12	280.27	-.0164	-.0534	.0609	-.0353	-.0758	.0206	.0437	.01494
1 13	20.16	.1165	-.0366	.0571	-.0347	-.0348	.0634	.0572	.01953
1 13	40.01	.1412	.1064	.0656	-.0361	-.0365	.0316	.0696	.02378
1 13	60.17	.1178	.1131	.2614	.1099	-.0716	.0033	.1128	.03856
1 13	80.03	.1193	.0236	.1994	.0228	.1467	.0526	.0941	.03215
1 13	100.19	-.0392	-.0564	.2304	-.0694	.0577	.2245	.1129	.03859
1 13	120.04	.0251	-.0855	.1314	-.0447	-.0311	.1519	.0783	.02675
1 13	140.20	.0934	-.0252	.1050	-.1210	-.1514	.0538	.0915	.03126
1 13	160.06	.0837	.0530	.1025	-.0248	-.0261	-.0198	.0518	.01770
1 13	180.22	.0373	.0465	.1146	.0159	.0040	.0089	.0378	.01293
1 13	200.07	.0370	.0453	.1126	.0257	-.0178	.0208	.0432	.01476
1 13	220.23	.0235	.0143	.1135	-.0384	.0100	.0528	.0421	.01438
1 13	240.09	.0377	.0365	.1274	-.0037	-.0106	.0553	.0452	.01545
1 13	260.25	.0385	.0076	.1049	-.0031	-.0096	.0596	.0373	.01273
1 13	280.10	.0303	.0177	.0963	-.0200	.0000	.0598	.0373	.01276
19913	20.12	.0213	-.0311	.0523	-.0113	-.0322	.0418	.0317	.01082
19913	40.23	.0568	-.0378	.0615	-.0123	-.0334	.0516	.0422	.01444
19913	60.04	.0985	.0156	.1774	-.0069	-.0333	.0529	.0641	.02191
19913	80.16	.1314	.0228	.1241	-.0060	-.0333	.0512	.0616	.02106
19913	100.28	-.0095	-.0752	.2268	-.0521	-.0380	.1594	.0935	.03196
19913	120.09	-.0163	-.1075	.1150	-.0694	-.0909	.0663	.0776	.02650
19913	140.20	.0751	-.0539	.1186	-.1131	-.1793	.0319	.0940	.03211
19913	160.02	.0534	.0020	.0642	-.0344	-.0469	.0029	.0340	.01161
19913	180.13	.0525	.0568	.0960	-.0149	-.0361	.0146	.0420	.01434
19913	200.25	.0223	.0145	.0814	.0214	-.0596	.0299	.0382	.01305
19913	220.06	.0028	.0058	.1129	.0203	-.0107	.0413	.0335	.01145
19913	240.18	-.0016	-.0059	.0778	.0019	-.0033	.0522	.0236	.00805
19913	260.29	.0227	-.0126	.0781	-.0101	-.0069	.0544	.0316	.01081
19913	280.10	.0097	-.0060	.0627	-.0130	-.0145	.0548	.0268	.00916

Table 6.8. Qualitative comparison of computed and observed depth-versus-distance wave profiles.

- DIFFERENCES IN FEET BETWEEN OBSERVED AND COMPUTED POINTS -

RUN		TIME	POSITIONS 1	2	3	4	5	6	AVERAGE	AVERAGE/DIA RATIO
8	1	20.05	.0122	-.0462	.0407	-.0250	-.0628	.0500	.0395	.01549
8	1	40.11	.0716	-.0494	.0351	-.0192	-.0626	.0494	.0479	.01637
8	1	60.16	-.0096	.0628	.0442	-.0306	-.0627	.0569	.0445	.01519
8	1	80.22	.0102	-.0185	.1024	.0672	-.0657	.0554	.0529	.01809
8	1	100.27	.0291	-.0350	.0296	-.0955	.1174	.0532	.0599	.02048
8	1	120.32	.0454	-.0369	.0835	-.1141	-.1306	.1163	.0878	.03001
8	1	140.04	-.0684	.0030	.1195	-.0297	-.1455	.0528	.0698	.02386
8	1	160.10	-.0429	-.0150	.0639	-.0422	-.1621	.0441	.0617	.02108
8	1	180.15	.0342	-.0235	.0584	-.0597	-.2009	.0497	.0710	.02428
8	1	200.21	.0377	.0044	.0363	-.0397	-.1674	.0284	.0523	.01787
8	1	220.26	.0298	.0386	.0639	-.0034	-.0746	.0189	.0382	.01305
8	1	240.31	.0169	.0450	.0736	-.0056	-.0642	.0325	.0396	.01355
8	1	260.03	.0078	.0330	.0797	.0084	-.0373	.0595	.0376	.01285
8	1	280.09	.0037	.0272	.0785	.0037	-.0273	.0638	.0340	.01163
8	1	300.14	.0083	.0180	.0676	.0000	-.0282	.0768	.0332	.01133
8	1	320.20	.0160	.0177	.0586	-.0124	-.0285	.0798	.0355	.01214
8	1	340.25	.0179	.0185	.0547	-.0113	-.0348	.0705	.0333	.01137
8	1	360.30	.0172	.0025	.0543	-.0097	-.0415	.0710	.0327	.01116
8	1	380.02	.0121	-.0017	.0543	-.0080	-.0396	.0692	.0308	.01054
9	1	20.09	.0226	-.0402	.0165	.0514	-.0406	.0119	.0319	.01089
9	1	40.19	.0701	-.0459	.0211	.0527	-.0359	.0141	.0400	.01366
9	1	60.28	-.0507	.1808	.0180	.0517	-.0389	.0162	.0594	.02029
9	1	80.03	-.0066	-.0953	.1781	.0542	-.0347	.0166	.0643	.02196
9	1	100.12	.0066	-.0512	-.0308	-.0017	-.0323	.0205	.0239	.00815
9	1	120.22	.0511	-.0165	.0224	.0324	.0073	.0177	.0246	.00840
9	1	140.31	.0398	-.0262	.0365	.0382	-.1059	.0057	.0420	.01436
9	1	160.05	.0894	-.0355	.0210	.0579	-.0688	.0039	.0528	.01120
9	1	180.15	.0216	-.0015	.0190	.0603	-.0172	.0008	.0201	.00586
9	1	200.24	.0165	-.0101	.0199	.0604	-.0221	.0212	.0250	.00855
9	1	220.34	.0111	-.0180	.0346	.0556	-.0313	.0240	.0291	.00995
9	1	240.08	.0139	-.0273	.0336	.0655	-.0303	.0274	.0330	.01128
9	1	260.17	.0156	-.0340	.0266	.0585	-.0211	.0298	.0309	.01056
9	1	280.27	.0221	-.0297	.0225	.0593	-.0192	.0315	.0307	.01049
9	2	20.14	.0134	-.0497	.0220	-.0181	-.0409	-.0152	.0266	.00908
9	2	40.28	.1320	-.0439	.0210	-.0178	-.0372	-.0105	.0437	.01494
9	2	60.08	.0952	.1786	.0196	-.0184	-.0385	-.0111	.0602	.02058
9	2	80.21	-.0253	.0357	.3910	-.0130	-.0414	-.0066	.0856	.02926
9	2	100.02	-.1093	-.1297	.0312	.0240	-.0339	-.0085	.0561	.01918
9	2	120.15	-.0760	-.0582	-.0362	-.1291	.2928	-.0046	.0995	.03399
9	2	140.29	.0543	-.0598	.0281	-.0897	-.1254	-.0155	.0621	.02124
9	2	160.09	.0178	-.0183	.0280	-.0684	-.1752	-.0519	.0599	.02048
9	2	180.25	.0511	-.0458	.0248	-.0172	-.0686	-.0759	.0472	.01614
9	2	200.03	.0070	.0237	.0204	-.0024	-.0216	-.0407	.0193	.00660
9	2	220.17	-.0008	.0212	.0464	-.0025	-.0400	-.0263	.0229	.00782
9	2	240.31	.0059	-.0035	.0568	.0233	-.0518	-.0115	.0255	.00870
9	2	260.11	.0204	-.0119	.0501	.0129	-.0212	-.0071	.0206	.00704
9	2	280.25	.0143	-.0126	.0374	.0093	-.0061	.0056	.0142	.00485
9	2	300.05	.0125	-.0190	.0254	-.0006	-.0087	.0190	.0140	.00478
9	2	320.19	.0196	-.0185	.0284	-.0066	-.0146	.0187	.0177	.00605
9	2	340.32	.0225	-.0295	.0301	.0014	-.0124	.0144	.0174	.00593
9	2	360.13	.0202	-.0203	.0264	.0043	-.0161	.0188	.0162	.00555
9	2	380.26	.0188	-.0228	.0368	.0073	-.0272	.0042	.0193	.00658

- DIFFERENCES IN FEET BETWEEN OBSERVED AND COMPUTED POINTS -

RUN		TIME	POSITIONS 1	2	3	4	5	6	AVERAGE	AVERAGE/DIA RATIO
9	3	20.16	-.0002	-.0481	.0185	-.0277	-.0652	-.0419	.0336	.01148
9	3	40.32	.0119	-.0483	.0259	-.0243	-.0616	-.0398	.0353	.01206
9	3	60.13	-.0017	-.0146	.0256	-.0230	-.0575	-.0380	.0267	.00913
9	3	80.29	.0045	-.0301	.0169	-.0375	-.0609	-.0372	.0312	.01066
9	3	100.10	.0230	-.0302	.0380	-.0430	-.0479	-.0345	.0361	.01234
9	3	120.25	.0176	-.0371	.0486	-.0203	-.1163	-.0427	.0471	.01610
9	3	140.07	.0068	-.0436	.0298	-.0196	-.0609	-.0391	.0333	.01139
9	3	160.22	.0118	-.0255	.0366	-.0142	-.0346	-.0444	.0279	.00952
9	3	180.05	.0033	-.0205	.0348	-.0168	-.0601	-.0288	.0274	.00936
9	4	20.19	.0053	-.0469	.0174	-.0118	-.0467	.0157	.0240	.00819
9	4	40.05	.0424	-.0405	.0190	-.0126	-.0507	.0189	.0307	.01048
9	4	60.23	.0485	.0441	.0231	.0014	-.0434	.0247	.0309	.01054
9	4	80.09	-.0029	.0230	.0770	-.0333	-.0463	.0261	.0348	.01188
9	4	100.28	-.0341	-.0364	.0425	-.0166	-.0425	.0267	.0331	.01132
9	4	120.14	.0201	-.0352	.0192	-.0627	-.0655	.0609	.0439	.01502
9	4	140.32	.0531	-.0362	.0348	-.0534	-.1681	-.0076	.0589	.02011
9	4	160.18	.0327	-.0319	.0299	-.0208	-.0776	-.0387	.0386	.01319
9	4	180.04	.0188	.0159	.0364	-.0003	-.0374	-.0081	.0193	.00661
9	4	200.23	.0077	.0099	.0486	.0063	-.0464	-.0094	.0201	.00685
9	4	220.08	.0039	.0060	.0594	.0198	-.0422	.0081	.0233	.00795
9	4	240.27	.0185	-.0118	.0489	.0042	-.0165	.0304	.0203	.00694
9	4	260.13	.0156	-.0102	.0326	.0012	-.0136	.0362	.0182	.00623
9	4	280.32	.0124	-.0116	.0244	-.0055	-.0143	.0364	.0174	.00596

THE MEAN OF THE AVERAGE DIFFERENCE/DIAMETER RATIOS = .02347
THE STANDARD DEVIATION OF THE AVERAGE DIFFERENCE/DIAMETER RATIOS = .01885
THE STANDARD DEVIATION OF ALL DIFFERENCES = .09841

Table 6.9. Summary of data on CSU Experimental Waves.

RUN	SLOPE	PROPORTIONAL BASE DEPTH H/DIA	BASE FLOW DISCHARGE (CFS)	PEAK FLOW DISCHARGE (CFS)	PEAK/ BASE	WAVE DURATION (SEC)	WAVE VOLUME (CU-FT)
B2ARS1	.0001100	.21666	1.600	3.870	2.41875	27.000	31.215
B2A0S2	.0001100	.21666	1.540	15.020	8.45455	67.000	382.415
B2A0S3	.0001100	.20846	1.470	15.290	10.40136	78.000	579.665
B5A0S1	.0001100	.37660	4.100	6.948	1.66029	24.000	41.715
B5A0S2	.0001100	.35131	3.490	15.010	4.30086	59.000	373.435
B5A0S3	.0001100	.34993	4.350	17.930	4.12184	85.000	787.330
C2A0S2	.0005500	.16198	2.500	20.330	7.07984	77.000	621.690
C2A0S3	.0005500	.16484	2.410	26.250	10.89212	95.000	986.745
C5A0S1	.0005530	.36040	5.070	14.380	2.83629	42.000	199.295
C5A0S2	.0005500	.36190	4.910	21.920	4.46436	61.000	532.945
C5A0S3	.0005500	.35260	4.990	28.270	5.66533	80.000	924.520
D2ARS1	.0010300	.14729	2.990	19.230	6.43144	60.000	595.650
D2A0S1	.0010300	.15412	2.500	18.550	7.42000	78.000	538.000
D2A0S3	.0010300	.17292	2.990	32.870	10.99331	97.000	1549.060
D5A0S1	.0010300	.37216	7.610	21.450	2.81866	57.000	385.065
D5A0S2	.0010300	.34892	6.940	33.510	4.82853	90.000	1235.195
D5A0S3	.0010300	.33901	6.330	39.370	6.21959	104.000	1772.535
1 5	.0009900	.34482	6.992	28.871	4.01474	74.478	808.529
1 4	.0009900	.34311	7.592	32.582	4.29165	90.000	1198.544
1 8	.0009900	.20812	1.913	24.396	12.75290	85.478	890.639
1 9	.0009900	.21666	2.682	26.174	10.05925	89.000	1035.399
19989	.0009900	.21290	.984	38.484	39.72119	95.000	1585.264
1 10	.0009900	.20120	2.004	28.326	13.59221	110.000	1340.131
1 11	.0009900	.34994	6.053	22.912	3.34329	60.000	486.610
1 12	.0009900	.34652	6.031	31.685	4.40767	80.500	995.741
1 13	.0009900	.35849	7.200	36.835	5.01300	120.000	1938.881
19913	.0009900	.36464	7.466	36.936	4.94717	110.000	1766.589
8 1	.0009900	.36917	8.439	28.779	3.62037	180.000	1660.597
9 1	.0004800	.24981	2.472	13.577	5.49213	97.000	345.446
9 2	.0004800	.28162	2.836	21.338	8.01970	94.000	998.381
9 3	.0004800	.30336	3.135	18.214	5.92204	93.000	277.884
9 4	.0004800	.30005	3.292	22.340	4.22307	107.000	1090.925

Table 6.10. Summary of data on Wallingford experimental waves.

RUN	SLOPE	PROPORTIONAL BASE DEPTH H/DIA	BASE FLOW DISCHARGE (CFS)	PEAK FLOW DISCHARGE (CFS)	PEAK/ BASE	WAVE DURATION (SEC)	WAVE VOLUME (CU-FT)
57	.0040	.4700	.04150	.0839	2.0217	67.650	1.565
58	.0040	.4700	.04150	.0846	2.0386	36.665	.862
60	.0040	.4700	.04150	.0655	1.5735	67.650	.878
61	.0040	.4700	.04150	.0655	1.5735	36.665	.476
62	.0040	.4700	.04150	.0655	1.5735	18.337	.238
83	.0020	.4700	.02740	.0882	3.2190	18.337	.638
84	.0020	.4700	.02740	.0875	3.1934	9.196	.321
85	.0020	.4700	.02740	.0754	2.7518	67.650	1.771
86	.0020	.4700	.02740	.0717	2.6168	36.665	.886
87	.0020	.4700	.02740	.0709	2.5876	18.337	.456
88	.0020	.4700	.02740	.0712	2.5985	9.196	.219
89	.0020	.4700	.02740	.0554	1.9489	67.650	.959
90	.0020	.4700	.02740	.0551	1.9380	36.665	.515
91	.0020	.4700	.02740	.0525	1.9161	18.337	.251
92	.0020	.4700	.02740	.0524	1.9124	9.196	.125
94	.0020	.2320	.00695	.0687	9.8849	67.650	2.277
98	.0020	.2320	.00695	.0551	7.9137	67.650	1.771
99	.0020	.2320	.00695	.0515	7.3813	36.665	.886
102	.0020	.2320	.00695	.0330	4.7482	67.650	.961
103	.0020	.2320	.00695	.0327	4.7050	36.665	.515
114	.0010	.4700	.01890	.0521	2.7566	67.650	1.225
115	.0010	.4700	.01890	.0552	2.8148	36.665	.686
116	.0010	.4700	.01890	.0550	2.8042	18.337	.341
117	.0010	.4700	.01890	.0531	2.8195	9.196	.171
118	.0010	.4700	.01890	.0469	2.4815	67.650	1.233
119	.0010	.4700	.01890	.0465	2.4603	36.665	.552
120	.0010	.4700	.01890	.0475	2.5132	18.337	.286
121	.0010	.4700	.01890	.0469	2.4815	9.196	.140
122	.0010	.4700	.01890	.0345	1.8148	67.650	.568
123	.0010	.4700	.01890	.0347	1.8360	36.665	.316
124	.0010	.4700	.01890	.0345	1.8254	9.196	.070
125	.0010	.2320	.00470	.0388	8.2553	44.265	.941
126	.0010	.2320	.00470	.0379	8.0638	67.650	1.225
127	.0010	.2320	.00470	.0390	8.2979	36.665	.686
128	.0010	.2320	.00470	.0388	8.2553	18.337	.341
130	.0010	.2320	.00470	.0327	6.9574	67.650	1.233
131	.0010	.2320	.00470	.0323	6.8723	36.665	.552
132	.0010	.2320	.00470	.0333	7.0851	18.337	.286
134	.0010	.2320	.00470	.0201	4.2766	67.650	.560
135	.0010	.2320	.00470	.0205	4.3617	36.665	.316
136	.0010	.2320	.00470	.0207	4.4043	18.337	.160

The peak depth versus distance and time relations of the computed and observed waves were compared by determining differences between the computed and observed points. These differences are averaged over six points in the CSU data and over five points in the Wallingford data; ratios of these average differences to the conduit diameter are also computed. The differences, average differences, and ratios of the average difference to the conduit diameter are presented in Table 6.11 for the CSU data. The table on the left shows the results of peak depth versus distance relations, and the table on the right shows the results of the peak depth versus time relations. The corresponding results for the Wallingford data are given in Table 6.12.

For the CSU data, the means of the ratio of average differences to conduit diameter for peak depths versus distance and time are 0.0177 and 0.0213, respectively. For the Wallingford data, the corresponding figures are 0.0216 and 0.0223. Similarly, the standard deviation of all differences divided by the diameter for the CSU data is 0.0253 for peak depth versus distance and 0.0316 for peak depth versus time. The corresponding figures for the Wallingford data are 0.0209 and 0.0251. The consistency of these figures show a definite reliability in computational schemes presented in this study to predict the rates of attenuation of flood peaks with distance and time.

Differences in the comparisons of the computed and observed peaks of the Wallingford data, as shown in Table 6.12 and by graphs in Appendix 5, may be explained in part by the reliability of the data from the Wallingford report. The experimental procedure at Wallingford employed a calibrated butterfly valve to obtain the inflow discharge hydrograph. Only depth recordings were reported to have been made during the tests. Test runs were made with four slopes, with four base flows, and with three or four peak discharges. The Wallingford data of the maximum depth versus distance show a rapid drop at the end of the computed curves (Appendix 5), while similar CSU data (Appendix 4) show a rise at the end point. These differences can be explained by the different ways in which the peak depths were computed. For the CSU data the base depths were subtracted from the maximum depths, and the base depths were taken from the initial condition of the M2 backwater curves, with a sharp drop at the conduit end.

The Wallingford data have only one maximum depth value for each position and particular time. These maximum depths were limited only to five points from x = 0 to x = 290 ft, because the total length of pipe was only 300 ft. The large pipe friction factors (f = 0.027 to 0.045) and the large length to diameter ratio (x/D = 1200) of the small Wallingford conduit system with a diameter of 0.264 ft, produced flow depths that, except at the outlet, were essentially normal depths throughout the conduit. Since the maximum peak depths were not measured at the outlet, and since the base flow depths were virtually a constant value, the subtraction of the base flow depths were virtually a constant value, the subtraction of the base flow depths for Wallingford data has no effect on the attenuation curves, except to somewhat lower ordinates.

In the CSU conduit system, a maximum peak depth and the corresponding time were recorded for all distance positions from x = 0 to x = a point at the free overfall. The method of determining the peak depth values is as follows. First, the variables

Table 6.11. Comparison of data for wave-peak versus distance and time for CSU experimental data.

- DIFFERENCES IN FEET BETWEEN OBSERVED AND COMPUTED POINTS -

RUN	POSITIONS 1	2	3	4	5	6	AVERAGE	AVERAGE/DIA RATIO
B2ARS1	.0265	.0705	.0581				.0543	.01056
B2A0S2	.0217	-.0179	-.0360				.0135	.00461
B2A0S3	.0139	-.0522	.0190				.0203	.00960
B3A0S1	.0101	.0290	-.0447				.0279	.00954
B3A0S2	-.0239	-.0178	.0216				.0231	.00686
B3A0S3	-.0154	-.0276	-.0371				.0161	.00548
C2A0S2	.0996	-.0034	.0678				.0573	.01947
C2A0S3	.0340	.0140	.0650				.0377	.01287
C3A0S1	-.0452	-.0327	.0435				.0405	.01383
C3A0S2	-.0849	-.1039	.0229				.0734	.02494
C3A0S3	-.0398	-.0792	.0364				.0518	.01771
D2ARS1	.0352	-.0219	-.0014				.0195	.00666
D2A0S1	.0214	-.0541	.0317				.0357	.01222
D2A0S3	.0467	-.0800	.0122				.0463	.01582
D3A0S1	-.0455	-.0745	-.0180				.0462	.01579
D3A0S2	-.0732	-.1638	.0151				.0853	.02897
D3A0S3	-.0827	-.1342	.0198				.0786	.02680
1 3	-.0186	-.0289	.0272	-.0782	-.0422	-.1547	.0570	.01947
1 4	.0301	.0457	-.0121	-.0602	-.0442	-.1373	.0546	.01866
1 8	-.1025	-.0068	-.1766	-.0726	-.0154	-.1498	.1006	.03438
1 9	-.0874	.0498	-.0937	-.0496	-.0012	-.0439	.0543	.01854
19989	-.2945	-.0614	-.1906	-.1265	-.0556	-.1261	.1425	.04869
1 10	-.0048	.2162	-.0037	.0468	.0724	-.0659	.0682	.02330
1 11	-.0507	-.0654	-.0159	-.0600	-.0243	-.0175	.0386	.01320
1 12	-.0944	-.0543	-.0129	-.1189	-.0485	-.0332	.0590	.02017
1 13	.1906	.0585	.2602	-.0334	.0145	.1040	.1090	.03725
19913	.1577	.0664	.1708	-.0537	-.0324	.0207	.0836	.02858
0 1	.0591	.0395	.0576	-.0156	-.0630	-.0005	.0360	.01231
9 1	-.0253	-.0053	-.0138	.0311	-.0362	-.0008	.0107	.00641
9 2	-.0290	-.0205	-.0259	-.0041	-.0845	-.0271	.0486	.01859
9 3	-.0145	-.0036	-.0055	-.0011	-.0095	-.0415	.0336	.01147
9 4	.0180	.0440	-.0088	-.0244	-.0427	-.0390	.0271	.00926

THE MEAN OF THE AVERAGE DIFFERENCE/DIAMETER RATIOS = .01760
THE STANDARD DEVIATION OF THE AVERAGE DIFFERENCE/DIAMETER RATIOS = .00981
THE STANDARD DEVIATION OF ALL DIFFERENCES = .07390

- DIFFERENCES IN FEET BETWEEN OBSERVED AND COMPUTED POINTS -

RUN	POSITIONS 1	2	3	4	5	6	AVERAGE	AVERAGE/DIA RATIO
B2ARS1	.0287	.0748	.0547				.0501	.01711
B2A0S2	-.0072	-.0349	-.0242				.0221	.00756
B2A0S3	-.0539	-.0379	.0011				.0309	.01058
B3A0S1	.0377	.0287	-.0674				.0346	.01182
B3A0S2	-.0343	-.0431	.0199				.0324	.01109
B3A0S3	-.0379	-.0391	-.0186				.0318	.01088
C2A0S2	.0476	-.0549	.0762				.0596	.02036
C2A0S3	-.1590	-.0644	.0315				.0850	.02904
C3A0S1	-.0602	-.0406	.0451				.0486	.01662
C3A0S2	-.0818	-.1062	.0261				.0714	.02438
C3A0S3	-.0542	-.0754	.0256				.0518	.01769
D2ARS1	.0326	-.0238	.0022				.0185	.00633
D2A0S1	.0250	-.0519					.0374	.01280
D2A0S3	-.0381	-.0960					.0520	.01778
D3A0S1	-.0956	-.1071	-.0453				.0827	.02825
D3A0S2	-.0757	-.1010	.0103				.0913	.03119
D3A0S3	-.4255	-.2650	.0141				.2342	.08002
1 3	-.0047	-.0140	.0330	-.0651	-.0629		.0355	.01214
1 4	.0167	.0443	-.0148	-.0492	-.0213	-.1724	.0531	.01814
1 8	-.1628	.0414	-.1397	-.0181	-.0358	-.1998	.0945	.03228
1 9	-.0644	.0602	-.0561	-.0490	.0049		.0469	.01603
19909	-.2491	-.0418	-.1977	-.1541	-.0848		.1455	.04973
1 10	.0564	.2546	.0266	.0593	.0481		.0870	.03001
1 11	-.0274	-.0512	-.0078	-.0562	-.0149		.0315	.01076
1 12	-.0790	-.0588	.0019	-.0989	-.0253	-.0313	.0459	.01568
1 13	.2595	.0838	.3176	.0669	.0488	.1034	.1465	.05008
19913	.2051	.1147	.2140	-.0380	-.0279	.0201	.1033	.03531
0 1	.0516	.0560	.0812	-.0065	0.		.0488	.01668
9 1	.0037	.0048	.0071	.0513	-.0307	-.0139	.0186	.00634
9 2	.0479	-.0121	.0093	-.0705	-.0602	-.0471	.0438	.01496
9 3	-.0016	.0115	.0064	-.0465	-.0560	-.0493	.0285	.00975
9 4	.0146	.0061	.0251	.0139	0.		.0273	.00933

THE MEAN OF THE AVERAGE DIFFERENCE/DIAMETER RATIOS = .02127
THE STANDARD DEVIATION OF THE AVERAGE DIFFERENCE/DIAMETER RATIOS = .01529
THE STANDARD DEVIATION OF ALL DIFFERENCES = .09256

Table 6.12. Comparison of data for wave-peak versus distance and time for Wallingford experimental data.

• DIFFERENCES IN FEET BETWEEN OBSERVED AND COMPUTED POINTS •

RUN	POSITIONS 1	2	3	4	5	AVERAGE	AVERAGE/DIA RATIO
87	.0135	.0100	.0111	.0070	.0050	.0096	.03651
88	.0159	.0050	.0092	.0003	-.0003	.0063	.02379
60	.0064	.0036	.0035	.0023	.0006	.0033	.01247
61	.0149	.0106	.0090	.0063	.0041	.0106	.04009
62	.0165	.0124	.0102	.0022	.0011	.0085	.03211
83	.0051	.0120	.0191	.0015	.0000	.0077	.02921
84	.0060	.0197	.0144	.0070		.0122	.04606
85	.0052	.0074	-.0027	.0004	-.0010	.0035	.01321
86	.0077	.0050	.0037	.0059	-.0050	.0054	.02063
87	.0121	.0129	.0209	-.0017		.0119	.04505
88	.0119	.0107	.0079			.0102	.03853
89	.0060	.0049	.0058	.0008	.0042	.0059	.02245
90	-.0021	.0054	.0012	.0007	.0011	.0021	.00788
91	-.0044	-.0042	.0004			.0030	.01128
92	.0028	.0033	.0020			.0030	.01121
94	.0065	-.0004	-.0034	-.0013	-.0026	.0028	.01061
98	.0229	.0073	.0066	.0001	-.0024	.0079	.02978
99	.0115	.0140	.0065	.0039	.0050	.0082	.03101
102	.0026	.0015	-.0005	-.0007	-.0037	.0018	.00682
103	.0037	.0103	.0030	.0045	.0002	.0043	.01648
114	.0122	.0002	.0061	.0084		.0067	.02550
115	.0095	.0102	.0100	.0106		.0101	.03817
116	.0088	.0030	.0048			.0056	.02104
117	.0154	.0059	.0036			.0083	.03138
118	.0086	-.0004	.0059	.0070		.0055	.02075
119	.0082	-.0014	.0023			.0040	.01510
120	.0108	.0040	.0142			.0097	.03661
121	.0095	.0082	.0087			.0088	.02581
122	.0042	.0013	.0041	.0002		.0045	.01686
123	.0069	.0100	.0091			.0087	.03284
124	.0058	.0003				.0031	.01172
125	.0031	.0044	-.0008	-.0001		.0021	.00800
126	.0055	.0020	.0065	.0001	.0011	.0030	.01152
127	.0089	.0048	.0073	.0029	-.0025	.0053	.02001
128	-.0079	.0085	-.0019	-.0017		.0050	.01904
130	.0022	.0047	.0044	.0018		.0033	.01257
131	.0085	.0023	-.0018	-.0051		.0044	.01676
132	.0029	.0083	-.0023	-.0007		.0036	.01349
134	.0036	-.0009	-.0029			.0025	.00929
135	.0023	.0016	.0021	-.0002		.0015	.00587
136	.0045	.0025	.0008			.0026	.00984

THE MEAN OF THE AVERAGE DIFFERENCE/DIAMETER RATIOS • .02164
THE STANDARD DEVIATION OF THE AVERAGE DIFFERENCE/DIAMETER RATIOS • .01124
THE STANDARD DEVIATION OF ALL DIFFERENCES • .00582

• DIFFERENCES IN FEET BETWEEN OBSERVED AND COMPUTED POINTS •

RUN	POSITIONS 1	2	3	4	5	AVERAGE	AVERAGE/DIA RATIO
87	.0123	.0092	.0110	.0102	.0105	.0106	.04089
88	.0177	.0094	.0134	.0034		.0110	.04153
60	.0052	.0029	.0041	.0033	.0023	.0036	.01347
61	.0135	.0101	.0106	.0071	.0045	.0109	.04147
62	.0104	.0146	.0111	.0025	.0015	.0096	.03644
83	.0108	.0176	.0173	.0011	.0011	.0094	.03570
84	.0168	.0239	.0125	.0079		.0153	.05724
85	-.0067	-.0018	-.0066	.0011	.0001	.0033	.01233
86	-.0009	.0053	.0051	.0075	-.0054	.0048	.01852
87	.0083	.0161	.0203	-.0036		.0121	.04573
88	.0105	.0131	.0072			.0129	.04897
89	.0030	.0044	.0075	.0103	.0055	.0061	.02324
90	-.0076	.0050	.0019	.0009	.0012	.0033	.01251
91	-.0044	-.0029	.0025			.0032	.01224
92	.0050	.0052	.0048			.0050	.01888
94	-.0150	-.0001	.0031	.0049	.0067	.0059	.02252
98	.0118	.0088	.0090	.0030	.0007	.0049	.01862
99	-.0005	.0138	.0071	.0060	.0084	.0072	.02712
102	-.0067	-.0045	-.0010	-.0003	-.0031	.0031	.01164
103	.0003	.0094	.0022	.0058	.0001	.0035	.01340
114	.0075	-.0058	.0035	.0057	-.0027	.0051	.01918
115	.0025	.0139	.0078	.0089	.0060	.0078	.02948
116	.0091	.0085	.0095	.0053		.0066	.02502
117	.0167	.0097	.0050	.0042		.0089	.03370
118	.0038	-.0042	.0024	.0039	-.0031	.0035	.01322
119	-.0003	-.0017	-.0004			.0008	.00309
120	.0097	.0069	.0125	.0099		.0097	.03690
121	.0046	.0111	.0097			.0085	.03202
122	-.0011	-.0022	.0010	.0062		.0026	.00995
123	.0019	.0096	.0074	.0031		.0055	.02080
124	.0042	.0015				.0028	.01076
125	-.0106	-.0001	-.0039	-.0020		.0042	.01581
126	-.0030	-.0035	.0053	-.0013	.0012	.0029	.01089
127	-.0015	.0027	.0055	.0011	-.0030	.0028	.01046
128	-.0078	.0046	-.0032	-.0016		.0043	.01621
130	-.0072	-.0013	.0079	.0011		.0031	.01188
131	.0001	-.0010	-.0032	-.0064		.0027	.01017
132	.0097	.0118	-.0042	-.0001		.0064	.02437
134	-.0030	-.0064	-.0025			.0040	.01533
135	-.0027	-.0003	.0025	.0001	-.0007	.0013	.00476
136	-.0034	-.0010	.0036			.0017	.00633

THE MEAN OF THE AVERAGE DIFFERENCE/DIAMETER RATIOS • .02227
THE STANDARD DEVIATION OF THE AVERAGE DIFFERENCE/DIAMETER RATIOS • .01318
THE STANDARD DEVIATION OF ALL DIFFERENCES • .00665

defined as the maxima were set equal to zero for all points in space. Then for each Δt, and each position, the new depth values were compared with the corresponding previous maxima, and the new maxima were set equal to the new depths whenever they were greater than the previous maxima. The time of peak depth was then recorded. Since the computed peak depths at the outlet often show a slight increase over previous values, the outfall sharp drop of the base depth was able to influence the peak depth versus distance relations. Because the base depths are subtracted at the outlet, they may be grossly in error, and they may be very small relative to the base depths subtracted upstream. The effect is that at the end of the attenuation curves a small sharp rise at their downstream ends is shown.

The difference in the computing methods of the peak depth also shows why the CSU comparisons of peak depth versus time tend to rise and even curl back at the ends, while the corresponding Wallingford data do not. In the Wallingford data, peak depths were recorded at different times, so that each time has but one peak value. In the CSU data, however, peak depths were recorded for each distance position; and the times that the peaks were reached was recorded as secondary information. Thus, two peak depths may be recorded as occurring at the same instant in time at two different positions.

The comparison plots shown in Appendices 4 and 5 are nearly all consistent and require no additional explanation. However, in the CSU data of Appendix 4, there are several experimental runs that should be viewed with caution because of limitations or errors in data. The inflow hydrograph of Run No. B2ARS1 had a Q_p/Q_b ratio of only 2.42 and the depth transducers at $x = 410.00$ ft and $x = 771.70$ ft were virtually unable to distinguish the wave from the base flow. Also, during Run No. B3A0S1, the recording system was prematurely shutoff so that no wave was recorded at $x = 771.70$ ft. Other irregular data are found in Run No. D2ARS1. It appears that a secondary wave was generated after the main experimental wave. This would not effect the peak comparisons but other comparisons for this run must be disregarded.

The inflow hydrograph of Run No. D3A0S3 has a point on the descending limb where the discharge jumps from 30 cfs to 39 cfs and then returns to 28 cfs, after which it continues to drop uniformly. Because of its erratic nature, it would first appear that this recording was a result of a malfunction in the orifice transducer. Closer examination, however, reveals that this unusual peak is observed at all three recording stations along the conduit. Therefore, it must be concluded that this wave actually occurred in this manner.

In summary, the comparison of CSU computed and observed data, and the comparison of Wallingford observed data and the corresponding CSU computed data on flood peak depth attenuations with distance and time in partly full circular conduits show similar agreements. Even though the experimental shifts and errors significantly affect these comparisons, for all practical purposes the numerically integration solutions of the partial differential equations approximate the flood peak attenuations of observed waves extremely well.

Chapter 7

SIMPLIFIED METHODS OF FLOOD ROUTING

7.1 General Definitions and Descriptions of Simplified Methods

After writing the momentum equation, Eq. 5.2., in its particular form, then the steady uniform, the steady nonuniform, and the unsteady flow conditions can be defined as [7, p. 287]

$$S_f = S_o - \frac{\partial y}{\partial x} - \frac{V\partial V}{g\partial x} - \frac{1\partial V}{g\partial t} ,$$

Steady uniform flow

steady nonuniform flow

unsteady flow

in which $S_f = fV^2/8gR$. Unsteady flow conditions are usually called the kinematic flow whenever a balance between gravitational and friction forces is achieved. This means that the derivatives in Eq. 5.2., or the derivatives in the above equation, are negligible when compared to the effect of gravity (measured by S_o) and the effect of friction (measured by S_f).

Therefore, Eq. 5.2 can be reduced to the simple form

$$S_f = S_o \quad , \tag{7.1}$$

with S_f the friction slope (or the slope of the energy line) and S_o the bottom slope. Therefore, the continuity equation, Eq. 5.1, is the primary equation governing unsteady flow, provided Eq. 7.1 is satisfied, with S_f given by Eq. 5.3.

The simplified flood routing methods generally called the "storage-routing methods" are those based only on the storage differential equation, or on the continuity or mass-conservation differential equation, Eq. 5.1, using the principle that for any reach of a channel the difference between the inflow and the outflow is equal to the stored or depleted water in a given time interval.

When the space is defined that contains the inflow, outflow, and water storage change (a fixed reach of the channel), Eq. 5.1 can be expressed as

$$P - Q = \frac{dW}{dt} = A\frac{dy}{dt}, \tag{7.2}$$

in which P is the inflow discharge, Q is the outflow discharge, and W is the stored volume of water, with $dW = Ady$, where A is the area of channel water surface, and y is the average depth or elevation of that area. The inflow is given as $P = f(t)$, and the storage is generally given as $W = f(y)$, or $W = f(y_1, y_2,..)$ with $y_1, y_2,...,$ consecutive depths. So, if $Q = f(y)$, then, by elimination, the function $W = f(Q)$ can be determined. In this case, Eq. 7.2 has only two variables, Q and t, in the form of a differential equation, whose integration gives $Q = f(t)$.

Equation 7.2 generally serves for the computation of relations among five functions in any small channel reach: (1) inflow hydrograph, $P = f_1(t)$; (2) outflow hydrograph, $Q = f_2(t)$; (3) stage hydrograph, $y = f_3(t)$; (4) outflow rating curve, $Q = f_4(y)$, and (5) storage function, $W = f_5(y)$, with the five variables, Q, P, y, W, and t. When three of the five functions with boundary conditions are given or the three variables can be excluded, Eq. 7.2 facilitates the computation of the relation between the two remaining variables.

The basic conditions for applying Eq. 7.2 to flood routing are: (1) the storage of a channel reach responds in less time to any unsteady inflow or outflow, than the time unit generally used for integrating Eq. 7.2 by finite differences; (2) the wave is long, so that the change of the discharge is gradual; (3) the accuracy of the basic data and the required accuracy of the results do not justify any method that takes into consideration dynamic effects in unsteady flow, and (4) the velocity and its changes along the channel reach are relatively small, so that the dynamic effect is negligible in comparison with the storage effect during wave movements.

Equation 7.2 has been applied to flood routing studies in channels, with some adaptations for the more complex discharge-storage or stage-storage relations in a channel reach. Many integration methods have been developed.

The analytical integration method was used successfully by some authors with schematic inflow hydrographs and simple linear approximate relations of storage and outflow discharge. The formulas were obtained for computing the decrease of flash-flood peaks and relatively small water-surface fluctuations. The difficulties in fitting tractable mathematical expressions to natural inflow hydrographs, and the difficulties of analytical integration when these expressions become complex, limit this integration method to specific problems.

The numerical integration of Eq. 7.2 written in finite-difference form is

$$(P - Q)\,\Delta t = A\,\Delta y = \Delta W \quad , \tag{7.3}$$

in which P, Q, and A are mean values during the time interval Δt, and the corresponding level difference Δy. Using P_1 and P_2, Q_1 and Q_2, and A_1 and A_2, the values at the beginning and the end of Δt, with a linear change during a sufficiently small Δt, then becomes

$$\left[\frac{P_1 + P_2}{2} - \frac{Q_1 + Q_2}{2}\right]\Delta t = \frac{A_1 + A_2}{2}\,\Delta y = \Delta W \tag{7.4}$$

For known P_1, P_2, Q_1, A_1, and Δt, and for known relations of W to Q, or A to y, and Q to y, it is possible by trial and error to determine the value Q_2. Expressing Eq. 7.4 in different ways, especially by using storage factors, $(W + Q\Delta t/2)$ and $(W - Q\Delta t/2)$, as functions of Q, a trial and error method may be replaced by direct numerical integration.

Individual differences between investigators in arranging Eqs. 7.3 and 7.4 for step by step computations may account for differences of the tabular numerical procedures. Procedures vary according to which basic difference factor (Δt, Δy, ΔW, or ΔQ) is known at the beginning of the equation and which factor must be determined. The accuracy of a method depends on the accuracy of selecting the basic difference factors (Δx and Δt), apart from the accuracy involved in the use of only one differential equation.

Equations 7.2 through 7.4 may be arranged in several combinations to facilitate graphical integration of a simple differential equation. There are numerous graphical procedures, with different shortcuts, for computing an outflow hydrograph or solving other problems.

Two general approaches in graphical integration are: (1) a mass-curve procedure, that represents the given hydrograph in form of its summation or mass curve, and obtains the routed hydrograph in the form of its mass curve; and (2) a procedure that uses the inflow or outflow directly for integration. Flash floods are not suitable for routing by the mass-curve procedure, because of non-negligible dynamic effects. Also, there are many semi-graphical methods in the literature [1], which combine a numerical tabular procedure with partial graphical integration. The graphical methods are generally restricted to simple problems, because for complex problems with several routing computations, the time involved becomes economically prohibitive.

Some simplified flood routing relations, often called coefficient methods, comprise a group of procedures that approximate the complex relations existing between the volume of water stored in a channel reach and the hydraulic magnitudes (inflow and outflow discharge, stages, slope, or others). The relations, consisting of coefficients, give weight in a specific way to each variable involved, the simplest being the weight coefficients for inflow and outflow discharge and for the time of travel of a wave moving along a reach. The coefficients are empirical as determined from flood wave movements that have actually occurred, or from waves analytically determined by an accurate integration procedure of complete differential equations. The empirical coefficients account, in part, for the effect of changing inflow and outflow on the water stored in a reach.

This group of procedures can be considered as an attempt to bridge two methods, the method of the two partial differential equations and the method of storage differential equation; this group uses empirical coefficients to take care of the dynamic conditions in a reach. The principal disadvantage of the coefficient methods is their dependence on empirical coefficients which require a large body of data to provide reliable estimates.

Although flood routing methods based on the simple storage differential equation have been used ever since the routings of inflow hydrographs and flood prediction along channels were began, there are only a few studies which compare the flood routing methods based on a solution of the two partial differential equations to those based on the storage differential equation only. Only a few studies compare accuracy, cost, advantages and disadvantages of various methods, devices, or speedups under different conditions of waves, channel and lateral inflows or outflows.

7.2 Flood Routing Based on Simplified Partial Differential Equations

Another group of flood routing methods represents transitions between those methods that use only the storage (continuity) equation. Some terms in the two partial differential equations, mostly in the momentum equation, are omitted, or some additional assumptions are made (constant bottom slope, linear change of channel characteristics between two cross sections used, separate routings of storage component and translation component of a flood wave, and others). Examples of these transitional cases are the omission of the acceleration term, $\partial V/\partial t$, the omission of the velocity head term, $V\partial V/\partial x$, or the omission of both the acceleration and velocity terms; division of the total discharge in two parts, as discharge of steady flow plus a changing discharge caused by the unsteady flow, with some simplifications in the momentum equation, and similar simplifications. See some references related to these simplification in [1].

The basic characteristic of most of these transition methods is the use of wave celerity, so both the wave translation and the channel storage are taken into account.

Again, there is a lack of comparative studies this time between the transition methods and other methods. For certain conditions, it could be demonstrated that the transition methods would give more accurate results than methods based on the storage differential equation, at little increase in computer cost. Under some conditions, however, the transition method may give less accurate results at substantial savings in work time, compared with methods based on the two partial differential equations. There has been more effort in the past to invent or derive new methods of integrating the different types of equations in flood routing than to analyze the particular limitations and advantages of each method and to compare all of them in general.

7.3 Basic Properties of Simplified Methods

The simplified methods such as the Muskingum method, time-lag method, and similar methods based primarily on the continuity equation have certain main characteristics:

(1) For given types of flood waves and given channel characteristics these methods need information a priori on flood waves, which is used to evaluate the coefficients or various other parameters of these simplified methods.

This information on flood waves may come from one or more of the following three sources:

(a) data on observed flood waves and observed properties of free-surface flowing water conveyance structures in nature;
(b) data on observed flood waves and on properties of the experimental channels or conduits;

(c) data on conveyance structures, and data on the flood waves obtained by reliable numerical integration methods using the complete continuity and momentum partial differential equations of one-dimensional gradually varied free-surface unsteady flow. This information is based on the hypothesis that the difference between analytical waves and corresponding physical waves is much smaller than the difference between these analytical waves and the waves computed by the simplified flood routing methods.

(2) Simplified methods in general assume a reduced cost of computation compared with the more accurate methods available, to compensate for decreased accuracy in predicting flood waves.

(3) Limited accuracy of the simplified methods is justified by the corresponding limited accuracy of all data used in flood routing, particularly of data on channel, boundary, and initial conditions.

Two basic properties of simplified flood routing methods that warrant discussion are the prior information required for the evaluation of various flood waves along a given channel and conduit, and the economy of computations as a counter-balance to a decreased or imposed level of accuracy.

A discussion of properties of simplified methods can not be separated from an analysis of the objectives the simplified methods serve. Basically these methods are used either for purposes of design in determining the sizes of open channels and free-surface flowing conduits, or for prediction of flood hydrographs resulting from a given storm at known points of an existing storm drainage system. Most of the methods have been developed mainly to predict flood movements along known channels. But, in general, this objective should be considered secondary in comparison to the first objective of storm drainage design. The usefulness of any prediction can only depend on the lag between the time of the prediction after the storm occurred and the time of occurrence of flood waves at given positions. The shorter this lag the less economically attractive is the prediction. The prediction of flood waves at given positions seems to be less important than design in cases of urban, highway or airport storm drainage systems. In other words, once a drainage system has been designed by peak flow, it really is not very important that the extent of the damage can be predicted. The exception may eventually be in those cases for which the pumps evacuate the storm water, or the operation and safety of the system depend on flood movement through storm drains.

The simplified methods of flood routing through storm drains may be useful for predicting purposes, provided these methods are based on observations of flood waves in nature, observations of waves in experimental conduits or accurately computed data on waves for various expected flood hydrographs. However, for the design of new storm drains, particularly under conditions of an interconnected system of drains, the simplified methods that require a prior information on flood waves are less attractive than the explicit and accurate methods of flood routing for given initial and boundary conditions, and assumed dimensions of storm drains. Since this study is oriented toward producing information that can be used for new designs of storm drains, based on the unsteady flow approach, a discussion of simplified methods is not overly relevant. However, since the initial dimensions for a newly designed storm drain must be first assumed, the simplified methods might produce the information needed for these assumptions. Then, the more accurate procedure developed in this study can be used for the final computations. With this in mind, three simplified methods are discussed in this chapter; the potential of each method to give a reliable first estimate of storm-drain dimensions is reviewed. The three methods are the Muskingum, time-lag, and non-dimensional methods.

Before these methods are reviewed, however, a discussion of computer economy is presented. Generally, the cost of computer time is about the same for both an accurate and a simplified method of flood routing. Usually, economy of computation in the electronic computer age does not prohibit accuracy.

For example, assume the computer time is t_i for a given unit flood routing operation, with given Δx and Δt increments, by the specified interval scheme of the method of characteristics, as proposed by this study for future computations of floods moving through storm drains. Further assume the corresponding unit operation with the same increments is t_j for a particular simplified method. Also assume that $t_j < t_i$; otherwise, the simplified method is meaningless in regard to more expensive and less accurate results than by the method of characteristics. Though the algebraic operation of the given simplified method may be cheaper in computer time, the same or similar accuracy of the simplified method in comparison with the accuracy of the method of characteristics, may often require a smaller Δx and correspondingly a smaller Δt. Let the total length of the conduit be L, and let the corresponding total integration time be T. For given Δx and Δt, the number of unit operations is

$$n = \frac{L}{\Delta x} \cdot \frac{T}{\Delta t} \quad . \tag{7.5}$$

If $\Delta x_j < \Delta x_i$ and $\Delta t_j < \Delta t_i$, then for n_j and n_i the corresponding numbers of unit operations multiplied by the unit computer time give

$$t_i n_i = \frac{LTt_i}{\Delta x_i \Delta t_i} \lessgtr \frac{LTt_j}{\Delta x_j \Delta t_j} = t_j n_j \quad . \tag{7.6}$$

Because Δx_i and Δt_i can be taken as the largest values by preserving a given degree of accuracy, $t_i/\Delta x_i\, \Delta t_i$ may be smaller, or much smaller than $t_j/\Delta x_j\, \Delta t_j$, even though $t_j < t_i$. In other words, the computer time for a unit of operation of given Δx and Δt is not the only measure of economy. Methods must be compared on the basis of given accuracy, because if a relaxation is given for the accuracy of a simplified method, its application to the method of characteristics results in a larger Δx-value and correspondingly in a larger Δt-value, and a decrease in n_i-value.

Even if $t_i n_i > t_j n_j$, it still does not prove the economy of a simplified method. For development of this method, observed or computed data are necessary. In this latter case, assume that k-total flood routing runs are necessary to derive and check the coefficients of simplified method. In this case, by using the method of characteristics the necessary computer time is $k\, t_i\, n_i$. Assume that the simplified method will be used for N cases, similar to floods and conduits for which the coefficients are derived and checked. Then the equality of cost gives

$$k\, t_i n_i + N t_j n_j = N t_i n_i \quad , \text{ or}$$

$$(1 - \frac{k}{N}) t_i n_i = t_j n_j \quad , \tag{7.7}$$

The larger k needed, and the smaller N will be, the less attractive becomes the simplified method, even though $t_j n_j < t_i n_i$ for $k/N = 0$. This general analysis shows that the economy of computations is a more complex problem that just comparing t_j with t_i.

7.4 Muskingum Simplified Method.

The summary of the Muskingum method is taken from reference 9 [pp. 605-607], but different symbols are used for inflow (P instead of I) outflow (Q instead of O), and storage (W instead of S). The storage, W, in a channel reach for unsteady flow depends primarily on the inflow (P) and outflow (Q) discharges and on the geometric and hydraulic characteristics of the channel and its control features. It can be assumed that the upstream and downstream end sections of a reach have the same mean discharge and storage relations with respect to the depth of flow (y). Thus, the equations may be written that

$$P = a y_u^n \;,\quad Q = a y_d^n \;,\quad W_u = b y_u^m \;, \text{ and } W_d = b y_d^m \tag{7.8}$$

in which the subscript u refers to the upstream and d to the downstream end of the reach, a and n express the constants of the depth-discharge relation at the two sections, b and m express the constants of the mean depth-storage relation of the reach, and W_u and W_d are the storages referred to the corresponding depths at the upstream and downstream ends, respectively. Eliminating y in these equations, then

$$W_u = b \left(\frac{P}{a}\right)^{m/n} \;, \text{ and } W_d = b \left(\frac{Q}{a}\right)^{m/n} \tag{7.9}$$

Designating by X a dimensionless factor that defines the relative weights given to inflow and outflow in the determination of the storage volume within the reach, then the storage of the reach at any given time is expressed by

$$W = X W_u + (1-X) W_d \quad . \tag{7.10}$$

Substituting Eqs. 7.9 in Eq. 7.10 and simplifying

$$W = K[X P^r + (1-X) Q^r] \quad , \tag{7.11}$$

in which $K = b/a^{m/n}$ and $r = m/n$. In case $r = 1$ (or the linear relation of storage and discharge), Eq. 7.11 becomes

$$W = K[XP + (1-X)Q] \quad , \tag{7.12}$$

which is the basis of the Muskingum method.

Further substituting Eq. 7.12 into Eq. 7.2 gives

$$KX \frac{dP}{dt} + K(1-X) \frac{dQ}{dt} = P - Q \; . \tag{7.13}$$

Using the approximate relations of finite differences,

$$\frac{dP}{dt} \simeq \frac{P_2 - P_1}{\Delta t} \;,\quad \frac{dQ}{dt} \simeq \frac{Q_2 - Q_1}{\Delta t} \;,\quad P \simeq \frac{P_1 + P_2}{2} \;, \text{ and } Q \simeq \frac{Q_1 + Q_2}{2}$$

in Eq. 7.13 gives

$$Q_2 = C_1 P_1 + C_2 P_2 + C_3 Q_1 \quad , \tag{7.14}$$

with

$$C_1 = \frac{KX + 0.5\Delta t}{K(1-X) + 0.5\Delta t} \;,\quad C_2 = \frac{-KX + 0.5\Delta t}{K(1-X) + 0.5\Delta t} \;, \text{ and}$$

$$C_3 = \frac{K(1-X) - 0.5\Delta t}{K(1-X) + 0.5\Delta t} \quad . \tag{7.15}$$

Equation 7.14 is the final form of the Muskingum method.

In Eq. 7.12 the term KQ represents the water volume of the prismatic storage in the reach which corresponds to the outflow discharge, and KX(P-Q) represents the additional storage (wedge storage) which is positive or negative depending on whether P>Q or P<Q. In this case, K has the dimension of time, while X is a dimensionless parameter. If fact, the reach length Δx is included in the coefficient K, which can be then defined as $K = \Delta x/C$, with C representing celerity of the wave along the reach.

The application of this simplified method requires the estimation of two quantities. First, K is both a time constant, which depends on the incremental length selected, and the channel characteristics that affect resistance to flow and hence the time of wave travel. Thus, K is the incorporation of several physical facotrs of the system. Second, the value of X must be estimated. Since this relates to the difference in inflow and outflow it is a measure of the shape of the discharge hydrograph passing through the reach. The two coefficients, X and K then account for the necessary conditions of channel shape, slope, and roughness, and the hydrograph to be routed. However, these parameters cannot be determined without information a prior. Information on waves and on the channel is necessary to estimate the weight X for the P and Q in Eq. 7.10, and it is needed to estimate a, b, m, and n of Eqs. 7.8 in order to compute K. Inaccuracies in these estimates are usually the main sources of errors in the Muskingum

method. Only through observed waves, or through computed waves based on a more accurate procedure of computation, may K and X be determined with any exactness.

Because flood hydrographs may have different shapes, which affect the weight X, the application of the Muskingum method to the design of storm routing systems is limited. Both the thesis by Suvich [see Internal References, 11], and the paper by Harris [8] arrived at this limitation for the Muskingum method as applied to the design of storm drains. Also, it is not even evident that the computer time necessary for a given level of accuracy is less than that required by the specified intervals scheme of the method of characteristics.

7.5 Time-Lag Routing Simplified Method

In his paper [8], Harris discusses the possibility of a simplified routing method that would provide the comparable results to observed discharge hydrographs. By using the method of characteristics as a standard, after the CSU data verified the method of characteristics, he found that the "progressive average lag routing method" meets the required good agreement between discharge hydrographs for particular circular conduits. According to Harris, this method also requires considerably less computer time.

For a given hydrograph at the upstream end of the reach, as given in Fig. 7.1 (left graph), the point R of Fig. 7.1 (right graph) on the routed hydrograph at the downstream end of the reach is obtained by

$$q_r = \frac{1}{n} \sum_{j=i-n}^{i} q_j \quad , \tag{7.16}$$

in which the point q_i and q_{i-1} are separated by the time increment Δt, q_r is lagged by time t_ℓ and n is the number of ordinates of upstream hydrograph averaged to determine an ordinate of the downstream hydrograph. This is a moving-average scheme in smoothing the upstream hydrograph, and it is translated by the time lag, t_ℓ, to obtain the downstream hydrograph.

The three parameters to be selected and used in this simplified method are: Δt, the time increment of the hydrograph; n, the number of points on the hydrograph to be averaged and t_ℓ the time lag. These routing coefficients for a given conduit were determined by computing the routed waves by the method of characteristics for three inflow hydrographs.

The procedure by Harris was to adjust the coefficients so that the first output hydrograph was reproduced accurately by the time-lag method.

These coefficients were then used to compute the other two hydrographs by the simplified time-lag method, and then compare with the hydrographs computed by the method of characteristics. Harris states that minor adjustments were required to make all three hydrographs fit well.

The results for a series of tests on different conduit diameters includes the size, length, and shape of each conduit. It is concluded then that the "progressive average-lag method", or "moving-average time-lag method", does provide answers which are the same as calculated by the method of characteristics.

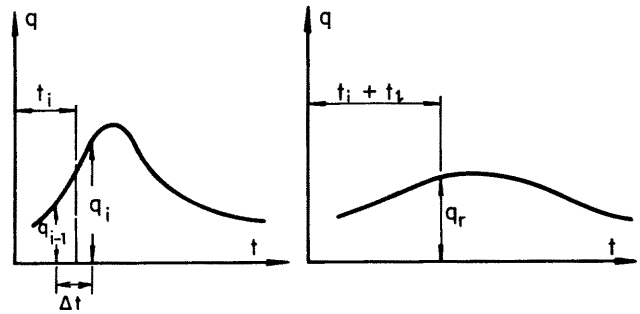

Fig. 7.1. The hydrograph of the upstream reach end, left graph, and the computed hydrograph of the downstream reach end, right graph, by the time-lag simplified flood routing method.

In summary, the simplified method proposed by Harris, and based on prior work by Dooge and the U.S. Army Corps of Engineers [8], depends on expressing the discharges of the hydrograph at a later time (further downstream) as a centered average of n number of equally time spaced discharge values of the earlier hydrograph. The time between the two hydrographs is a coefficient of the conduit properties and the reach length. The time-lag term includes the effect of the channel shape, slope, and roughness. The number n of discharge values to be averaged is the other routing coefficients for a given Δt. This number n of discharge quantities takes into account the change in the inflow hydrograph shape. Thus, the procedure appears to take into account the physical conditions determining the downstream hydrograph.

There is no procedure a priori for evaluating the routing coefficients. For a given channel, they are determined by observing physical waves and the channel, or by computing waves based on an accurate method of computation, such as those by Harris using the accurage integration scheme by the method of characteristics.

The time-lag routing method, like the Muskingum method or its variations, assumes, in general, constant values of coefficients for all stages of a hydrograph. This condition is not physically possible for shapes such as the circular section of a partly full flowing conduit. However, for modest ranges of base flow, and the inflow hydrographs of limited range, the coefficients may exhibit reasonable constancy.

The simplified methods, like the moving-average time-lag method, may offer an approximate flood routing of inflow hydrographs through storm drains for purposes of design. However, they do not permit a direct evaluation of corresponding depths. Neither do they give the maximum depth determined either as a function of position along the conduit or in time. Since the maximum depth does not occur at the same time as the maximum discharge, it is not to be expected that the routed discharge hydrograph would be an indicator of maximum depth.

7.6 Non-dimensionality Approach

Parameters of non-dimensionality. A convenient procedure for estimating discharge and depth hydrographs is by a non-dimensional generalization of functions of time and distance, boundary and initial

conditions, and other factors. This approach requires the identification of pertinent physical properties of the system, the quantitative measures of the phenomenon studied, and the appropriate dimensionless relations between them.

For unsteady flow in open channels the given or assumed parameters are basically those describing the channel geometry. The boundary conditions are described by the characteristics of the inflow hydrograph and the depth-discharge relations at either the upstream or the downstream cross sections. For subcritical flow, the second boundary condition is at the downstream end, and for supercritical flow, the second boundary condition is at the upstream end. A third group of variables describes the initial conditions.

Within each of these three basic groups are numerous variables, some of which are of primary importance and some of which may have only negligible effects on the quantity to be predicted. The three basic groups of variables are:

A. Channel Geometry.

1. Cross section shape

   a. Circular shape, diameter, D ,

   b. Trapezoidal shape, base width and side slope, B_o, z ,

   c. Parabolic shape, rate of change of width with depth, k ,

2. Channel bed slope, S_o ,

3. Channel boundary roughness

   a. Darcy-Weisbach friction factor, f ,

   b. Velocity distribution coefficients, α and β .

B. Boundary Conditions.

1. Inflow hydrograph

   a. Base flow, Q_b ,

   b. Peak flow, $Q_o + Q_b$, with Q_o the maximum discharge in excess of the base flow,

   c. Time from beginning of hydrograph to time of maximum flow, t_p ,

   d. Volume of hydrograph, W ,

   e. Time to center of mass of wave, t_g ,

   f. Time duration of hydrograph, t_b ,

2. Downstream depth versus discharge relation, $y(Q)$, or

3. Upstream depth versus base discharge relation, $y(Q)$.

C. Initial Conditions.

1. Steady uniform flow with a constant depth, y_o , or

2. Steady nonuniform flow with

   a. Subcritical slope or

      (1) Backwater or M1 curve, $y(x)$, or
      (2) Drawdown or M2 curve, $y(x)$.

   b. Supercritical slope

      (1) S1 curve, $y(x)$, or
      (2) S2 curve, $y(x)$.

Thus, there are numerous variables to be related into a reduced number of significant dimensionless parameters describing the conditions of the phenomena.

The functions to be related to the above basic variables are:

A. Wave Profiles as a function of

1. Distance, $y(x)$,

2. Time, $y(t)$.

B. Maximum Depth as a function of

1. Distance, $y_p(x)$,

2. Time, $y_p(t)$.

C. Discharge Hydrograph at any location, $Q(t,x)$.

The significance and usefulness of these quantities depend on the reason for the analysis. For example, for the design of a storm drainage system, one important consideration is the determination of the peak depth as a function of distance. From this information the location of a change in channel size can be determined. For the problems of an existing storm drainage system related to time, the desirable information would relate the discharge to the time. The recording of existing conditions and then the prediction of a later event would permit direct control and reductions of peak flows.

The complications of the problem of non-dimensionality may be realized if one considers the number of independent dimensionless parameters that describe the unsteady flow process. According to the Buckingham Pi theorems, the number of independent dimensionless parameters necessary to describe a physical process is equal to the number of variables minus the number of dimensional categories (such as length, force, time). For the description of unsteady flow, considering all variables listed above, there would be approximately 20 variables and 2 dimensional quantities (length and time). The number of dimensionless parameters would then be approximately 18, depending on the physical conditions to be represented. The systematic correlation of these parameters requires holding all but one or two of them constant at a time and then observing or computing their effect on the quantity to be predicted.

An exploratory attempt was made to demonstrate a non-dimensional approach to the description of unsteady flow. A series of flood waves were computed by the method of characteristics for the subcritical and supercritical base flow conditions. The hypothetical inflow hydrograph was defined by a Pearson Type III distribution:

$$Q(t) = Q_b + Q_o e^{-(t-t_p)/(t_g-t_p)} (t/t_p)^{t_p/(t_g-t_p)}.$$

The shape was defined by the base flow Q_b, the maximum discharge in excess of the base flow, Q_o, the time to the maximum discharge, t_p, the time to the centroid of the inflow hydrograph, t_g, and e, the base of the Naperian logarithms. These parameters were varied over a limited range to identify their effect on the resultant maximum depths of flow.

Subcritical flow. The conditions used for the subcritical flow computer runs are listed in Table 7.1. The dependent variable computed for each of these conditions was the maximum depth of flow as a function of position along the conduit. Figure 7.2 presents a typical attenuation curve for the maximum depth for subcritical flow. For that position of the curve, relatively unaffected by the free outfall end condition, the depth may be represented by the relation $D = a + ix$, in which i is the attenuation rate.

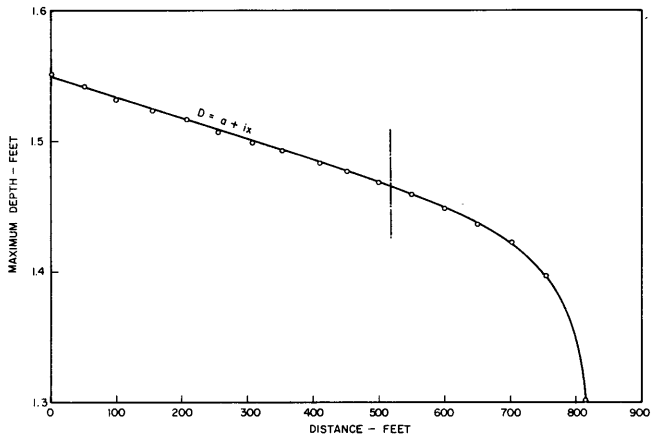

Fig. 7.2. Maximum depth versus distance for Run No. 200 of Table 7.1.

In the subcritical flow, Q_b and Q_o played a more important role in the rate of attenuation of wave than t_p and t_g. It was found that the attenuation rate varied as $(1/Q_b+Q_o)^{0.34}$, as seen in Table 7.2. The effect of the relative values of Q_b and Q_o is shown in Table 7.3; $(Q_b/Q_o)^{0.3}$ was found to be the appropriate dimensionless parameter. The effect of the relative values of t_p and t_g was negligible, but the rate of attenuation varied as $t_g^{0.1}$, as shown in Table 7.4. Table 7.5 shows the effect of the diameter; the effect of the diameter was defined by $D^{0.8}$.

Table 7.2. Effect of absolute values of Q_b and Q_o in subcritical flow for t_p = 50 sec., t_g = 100 sec.

Run	Q_b cfs	Q_o cfs	t_p sec.	t_g sec.	$(\frac{1}{Q_b+Q_o})^{0.34}$	i	$i(\frac{1}{Q_b+Q_o})^{0.34}$
200	10	10	50	100	0.360	-162.65×10^{-6}	-58.6×10^{-6}
201	5	5	50	100	0.457	-122.65×10^{-6}	-56.1×10^{-6}
202	7.5	7.5	50	100	0.398	-141.55×10^{-6}	-56.4×10^{-6}
203	9	9	50	100	0.374	-153.76×10^{-6}	-57.5×10^{-6}

Table 7.3. Effect of relative values of Q_b and Q_o in subcritical flow for t_p = 50 sec., and t_g = 100 sec.

Run	Q_b cfs	Q_o cfs	t_p sec.	t_g sec.	$(\frac{Q_b}{Q_o})^{.3}$	i	$i(\frac{Q_b}{Q_o})^{.3}$
204	17	10	50	100	1.173	-168.9×10^{-6}	-198×10^{-6}
205	10	17	50	100	.856	-253.4×10^{-6}	-216.5×10^{-6}
206	12	15	50	100	.935	-221.4×10^{-6}	-207×10^{-6}
207	15	12	50	100	1.069	-186.5×10^{-6}	-199.1×10^{-6}

Table 7.4. Effect of absolute value of t_g in subcritical flow for Q_b = 10 cfs, and Q_o = 10 cfs

Run	Q_b cfs	Q_o cfs	t_p sec.	t_g sec.	$(t_g)^{0.1}$	i	$i(t_g)^{0.1}$
208	10	10	50	100	1.66	-275.9×10^{-6}	-457×10^{-6}
212	10	10	40	80	1.62	-283.7×10^{-6}	-459×10^{-6}
213	10	10	30	60	1.57	-292.1×10^{-6}	-459×10^{-6}
214	10	10	60	120	1.69	-268.7×10^{-6}	-455×10^{-6}

Table 7.5. Effect of diameter in subcritical flow for Q_b = 10 cfs, Q_o = 10 cfs, t_p = 50 sec., and t_g = 100 sec.

Run	Q_b cfs	Q_o cfs	t_p sec.	t_g sec.	D ft	$D^{0.8}$	i	$i(D)^{0.8}$
208	10	10	50	100	3	2.41	-275.9×10^{-6}	-665×10^{-6}
215	10	10	50	100	5	3.62	-176.3×10^{-6}	-636×10^{-6}
216	10	10	50	100	7	4.75	-150.2×10^{-6}	-715×10^{-6}

Four dimensionless parameters were found to define the rate of attenuation of the wave peak in the subcritical flow:

$\pi_1 = i$, the rate of attenuation;

$\pi_2 = \left(\frac{Q_b}{Q_o}\right)^{0.3}$, the parameter defining the relative value of base flow to the superimposed peak flow;

$\pi_3 = \left(\frac{1}{Q_b+Q_o}\right)^{0.34}(t_g)^{0.1}(D)^{0.8}(g)^{0.22}$, the parameter representing the absolute values of Q_b, Q_o, t_g/D, and the gravitational acceleration, and

$\pi_4 = \frac{S_o}{f^{2.88}}$, the parameter measuring the effects of the channel slope and friction factor. Combining π_1, π_2 and π_3 into one-dimensionless parameter gives

$$\pi_5 = \pi_1 \pi_2 \pi_3 = i \left(\frac{Q_b}{Q_o}\right)^{0.3} \left(\frac{1}{Q_b + Q_o}\right)^{0.34} (t_g)^{0.1} (D)^{0.8} (g)^{.22} \quad .$$

A plot of π_5 versus π_4 is shown in Fig. 7.3

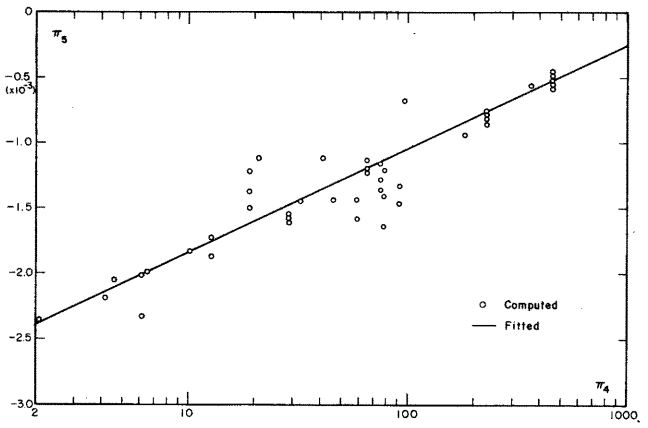

Fig. 7.3. Attenuation of wave peak for a theoretical hydrograph in subcritical flow.

Supercritical flow. The condition for transition from subcritical to supercritical flow may be estimated from the Darcy-Weisbach energy loss equation and the expression for critical flow.

$$\frac{S_o}{f} = \frac{Q^2}{8gRA^2} \quad \text{- Darcy-Weisbach}$$

$$1 = \frac{Q^2 B}{gA^3} \quad \text{- Critical flow.}$$

The ratio of these two equations results in:

$$\frac{S_o}{f} = \frac{P}{8B} \quad .$$

For a circular conduit flowing one-half full, the wetted perimeter $P = \pi D/2$ and the surface width $B = D$. Thus

$$\frac{S_o}{f} \simeq 0.2 \quad .$$

It is to be noted that S_o/f required for the change of flow from supercritical to subcritical flow is approximately one-tenth of S_o/f needed for change of flow from an attenuating to an amplifying wave. The waves in subcritical flow always attenuate, while the waves in the supercritical regime can either attenuate or amplify.

To determine how the profile of an attenuating wave in supercritical flow responds to parameters of slope, friction factor, and diameter, four consecutive runs were made in which the inflow hydrograph was the same for all four runs. The conditions of these runs are given in Table 7.6. Figure 7.4 shows the profile of Run 97. The profile is initially convex, it then becomes concave. Figure 7.5 shows the profile of Run 98 which depicts the effect of an increase in slope; the profile is a straight line. Figure 7.6 shows the profile of Run 99; the effect of a decrease in friction factor is the same as an increase in slope, and the profile is again a straight line. Figure 7.7 is the profile of an attenuating wave, Run 100, routed in a conduit with a diameter of 7.0 ft, as compared with a diameter of 3.0 ft in the previous three runs. The profile still has the initial convex segment with the following concave segment, but the concavity and convexity are not very pronounced. Another type of wave profile encountered in the course of computer runs is when the depth of the base flow is near one-half full. The profile of Run 45 is shown in Fig. 7.8 and it has a pronounced concavity.

Table 7.6. Conditions of Runs 97, 98, 99, and 100

Run	Q_b cfs	Q_o cfs	t_p sec	t_g sec	S_o	f	D ft
97	30	10	50	100	0.01	0.02	3.0
98	30	10	50	100	0.03	0.02	3.0
99	30	10	50	100	0.01	0.005	3.0
100	30	10	50	100	0.01	0.02	7.00

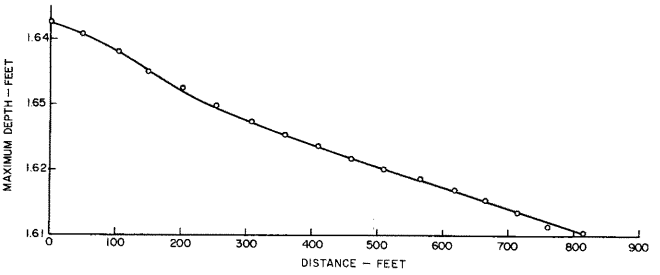

Fig. 7.4. Maximum depth vs. distance for Run No. 97 of Table 7.6.

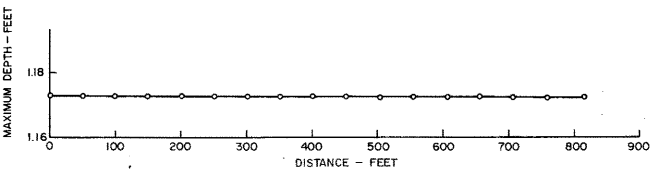

Fig. 7.5. Maximum depth vs. distance for Run No. 98 of Table 7.6.

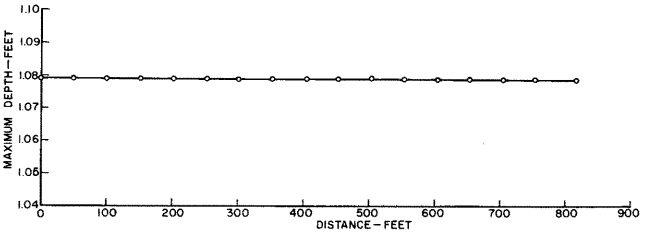

Fig. 7.6. Maximum depth vs. distance for Run No. 99 of Table 7.6.

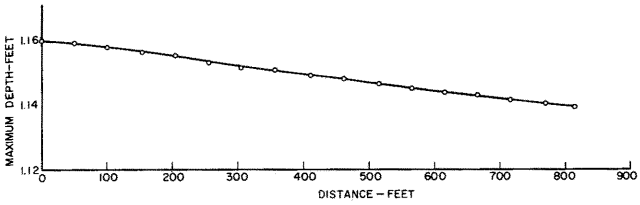

Fig. 7.7. Maximum depth vs. distance for Run No. 100 of Table 7.6.

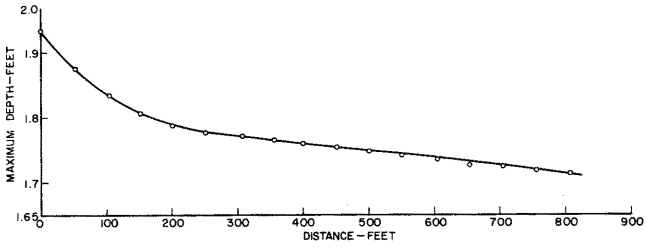

Fig. 7.8. Maximum depth vs. distance for Run No. 45 of Table 7.7.

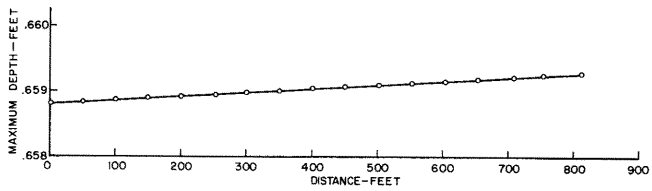

Fig. 7.9. Maximum depth vs. distance for Run No. 18 of Table 7.7.

The condition for the amplification of a wave in the supercritical regime was assumed to be $S_o/f > 2$ (or Froude number $F > 2$). The amplitude of waves grows but only slightly, as observed by comparing Figs. 7.8 and 7.9. In Fig. 7.8 the general slope of the curve is 116.2×10^{-6}, where as the general slope of the curve in Fig. 7.9 is 0.614×10^{-6}. If the above condition for amplification is satisfied, then the profile of the wave amplification is nearly a straight line in this case. Figure 7.9 shows a typical amplification of maximum wave depth.

The attenuation characteristics of a Pearson Type III function inflow hydrograph in the supercritical regime were analyzed by computational methods. The parameters of the hydrograph control the volume and steepness of the wave. The effects of given parameters of the physical system, conduit diameter D, its slope S_o, and the friction factor f, on the attenuation rate of flood waves were investigated. The attenuation rate of the maximum depth was defined for the supercritical flow by

$$y_p = ae^{ix} , \qquad (7.17)$$

in which i is the parameter of the exponential attenuation rate. The parameter i in Eq. 7.17 was determined for each attenuating wave.

The conditions of each run are given in Table 7.7. Parameters defining the attenuation rate are representative of the hypothetical conditions. The use of attenuation rates beyond the computed range, however, may not be reliable.

The attenuation rate was correlated with the characteristics of the inflow hydrograph and the circular conduit. To determine the general parameters in question, computer runs were carried out which simulated actual conditions. The effect of each of the seven variables was evaluated by changing one of the variables while keeping the rest constant. It was found that the attenuation rate varied as $[(t_g-t_p)/t_g]^{0.25}$, as seen in Table 7.8. The effect of the absolute value of t_g is shown in Table 7.9, the attenuation rate varied as $(t_g)^{0.75}$. Tables 7.10, 7.11, and 7.12 show that $[1/(Q_b+Q_o)]^{0.47}$, $(Q_b/Q_o)^{0.5}$, and $D^{0.8}$ may be appropriate parameters.

Table 7.8. Effect of the relative value of t_p and t_g in supercritical flow for $Q_b = 25$ cfs, and $Q_o = 10$ cfs.

Run	Q_b cfs	Q_o cfs	t_p sec	t_g sec	$\left(\frac{t_g-t_p}{t_g}\right)^{.25}$	i	$i\left(\frac{t_g-t_p}{t_g}\right)^{.25}$
53	25	10	50	100	0.841	-116×10^{-6}	-97.8×10^{-6}
55	25	10	70	80	0.595	-170×10^{-6}	-99.5×10^{-6}
66	25	10	60	90	0.760	-129×10^{-6}	-98.0×10^{-6}
67	25	10	40	110	0.893	-111×10^{-6}	-99.0×10^{-6}

Table 7.9. Effect of the absolute value of t_g in supercritical flow for $Q_b = 25$ cfs, and $Q_o = 10$ cfs

Run	Q_b cfs	Q_o cfs	t_p sec	t_g sec	$(t_g)^{0.75}$	i	$i(t_g)^{0.75}$
53	25	10	50	100	31.6	-116×10^{-6}	-3665×10^{-6}
54	25	10	25	50	18.8	-174×10^{-6}	-3270×10^{-6}
63	25	10	75	150	42.8	-828×10^{-6}	-3542×10^{-6}
64	25	10	100	200	53.0	-608×10^{-6}	-3225×10^{-6}

Therefore, the attenuation characteristics of the waves in the supercritical regime of flow can be defined in terms of five dimensionless parameters:

$\pi_1 = i$, the rate of attenuation;

Table 7.10. Effect of the absolute values of Q_b and Q_o in supercritical flow for $t_p = 50$ sec. and $t_g = 100$ sec.

Run	Q_b cfs	Q_o cfs	t_p sec	t_g sec	$\left(\frac{1}{Q_b+Q_o}\right)^{0.47}$	i	$i\left(\frac{1}{Q_b+Q_o}\right)^{0.47}$
57	20	8	50	100	$\frac{1}{4.8}$	-88.3×10^{-6}	-18.4×10^{-6}
58	15	6	50	100	$\frac{1}{4.18}$	-66.2×10^{-6}	-15.8×10^{-6}
59	10	4	50	100	$\frac{1}{3.46}$	-47.1×10^{-6}	-13.6×10^{-6}

Table 7.1. Conditions of different runs in the subcritical regime

Run	Q_b cfs	Q_o cfs	t_p seconds	t_g seconds	S_o	f	D ft
200	10	10	50	100	.001	.01	3
201	5	5	50	100	.001	.01	3
202	7.5	7.5	50	100	.001	.01	3
203	9	9	50	100	.001	.01	3
204	17	10	50	100	.001	.01	3
205	10	17	50	100	.001	.01	3
206	12	15	50	100	.001	.01	3
207	15	12	50	100	.001	.01	3
208	10	10	50	100	.0005	.01	3
209	10	10	70	80	.0005	.01	3
210	10	10	40	110	.0005	.01	3
211	10	10	60	90	.0005	.01	3
212	10	10	40	80	.0005	.01	3
213	10	10	30	60	.0005	.01	3
214	10	10	60	120	.0005	.01	3
215	10	10	50	100	.0005	.01	5
216	10	10	50	100	.0005	.01	7
217	10	10	50	100	.0001	.01	4
218	10	10	50	100	.0001	.02	4
219	10	10	50	100	.0001	.03	4
220	10	10	40	90	.00005	.01	4
221	9	8	50	90	.00005	.01	4
222	9	8	70	80	.00005	.01	4
223	10	10	60	70	.00002	.005	4
224	9	8	50	80	.00002	.005	4
225	8	7	40	80	.00002	.005	4
226	10	9	50	100	.00001	.006	5
227	10	9	50	100	.00003	.006	5
228	10	9	50	100	.00004	.006	5
229	10	9	50	70	.00006	.007	3.5
230	15	10	40	80	.00007	.007	3.7
231	8	9	40	80	.00001	.006	5
232	2	4	30	50	.00001	.006	5
234	14	9	40	70	.00003	.006	5
235	5	4	30	80	.00003	.006	5
236	17	10	50	100	.00004	.006	5
237	5	7	40	80	.00004	.006	5
238	5	5	150	100	.00006	.007	3.5
239	7	4	40	70	.00006	.007	3.5
240	10	8	50	100	.0002	.02	4
241	9	11	60	90	.0002	.02	4
242	12	10	60	80	.0002	.01	4
243	13	8	50	100	.0003	.03	4
244	10	10	50	100	.0003	.03	4
250	10	10	40	80	.0004	.01	3
251	10	10	50	90	.0008	.01	3
252	4	3	50	80	.00001	.01	6
254	15	25	80	100	.001	.02	4
255	15	10	50	100	.0015	.02	4.5
256	10	9	60	100	.0005	.02	3
257	8	6	50	30	.00005	.02	7.5
258	15	10	60	120	.00001	.02	7
259	5	5	60	90	.001	.03	4
260	12	10	40	80	.0005	.03	4
261	10	10	50	100	.0002	.03	4
262	5	4	50	90	.00005	.03	4.5
263	15	12	60	90	.002	.03	3

Table 7.7. Conditions of different runs in the supercritical regime

Run	Q_b cfs	Q_o cfs	t_p sec	t_g sec	S_o	f	D ft
6	10	8	100	150	.006	.01	2.9262
7	15	12	100	150	.006	.01	2.9262
8	10	8	100	150	.007	.01	2.9262
10	10	8	100	150	.010	.01	2.9262
11	20	16	100	150	.015	.01	2.9262
12	20	16	100	150	.050	.01	2.9262
13	20	16	100	150	.030	.01	2.9262
14	20	16	100	150	.070	.01	2.9262
15	10	8	100	150	.025	.01	2.9262
16	20	16	100	150	.008	.01	2.9262
17	15	12	100	150	.015	.01	2.9262
18	10	8	50	100	.025	.01	2.9262
19	10	8	150	200	.025	.01	2.9262
20	20	16	50	100	.010	.01	2.9262
21	20	16	50	100	.008	.01	2.9262
22	20	16	25	50	.02	.01	2.9262
23	25	20	25	50	.01	.01	2.9262
24	15	12	25	50	.01	.01	2.9262
25	20	16	25	50	.05	.01	2.9262
26	20	16	10	20	.05	.01	2.9262
29	20	15	100	150	.02	.01	2.9262
30	20	15	75	100	.02	.01	2.9262
31	20	15	25	50	.02	.01	2.9262
32	20	15	10	20	.02	.01	2.9262
33	20	15	20	20	.02	.01	2.9262
34	20	16	100	150	.07	.01	2.9262
35	20	14	25	50	.06	.01	2.9262
36	20	14	35	40	.06	.01	2.9262
37	20	14	30	40	.06	.01	2.9262
38	20	14	60	80	.06	.01	2.9262
39	20	10	50	100	.005	.01	2.9262
40	10	20	50	100	.005	.01	2.9262
41	5	25	50	100	.005	.01	2.9262
42	10	10	50	100	.005	.01	2.9262
43	10	5	50	100	.005	.01	2.9262
44	20	10	50	75	.005	.01	2.9262
45	20	18	50	100	.003	.01	2.9262
47	20	10	75	100	.006	.02	2.9262
48	30	10	50	90	.01	.02	2.9262
53	25	10	50	100	.005	.02	2.9262
54	25	10	25	50	.005	.02	2.9262
55	25	10	70	80	.005	.02	2.9262
56	15	20	50	100	.005	.02	2.9262
57	20	8	50	100	.005	.02	2.9262
58	15	6	50	100	.005	.02	2.9262
59	10	4	50	100	.005	.02	2.9262
60	20	15	50	100	.005	.02	2.9262
61	10	25	50	100	.005	.02	2.9262
62	5	30	50	100	.005	.02	2.9262
63	25	10	75	150	.005	.02	2.9262
64	25	10	100	200	.005	.02	2.9262
65	25	10	10	20	.005	.02	2.9262
66	25	10	60	90	.005	.02	2.9262
67	25	10	40	110	.005	.02	2.9262
69	40	20	50	100	.01	.04	5.00
70	40	20	50	100	.01	.04	8.00
71	40	20	50	100	.01	.04	10.0
73	25	10	75	150	.04	.02	2.9262
74	25	10	75	150	.08	.04	2.9262
75	25	10	75	150	.0028	.01	2.9262
76	25	10	75	150	.0025	.01	2.9262
77	40	30	100	200	.003	.005	7.00
78	20	15	100	200	.003	.005	7.00
79	50	20	100	200	.003	.005	7.00
80	60	30	100	200	.003	.005	7.00

Table 7.11. Effect of absolute and relative values of Q_b and Q_o in supercritical flow for t_p = 50 sec, and t_g = 100 sec.

Run	Q_b cfs	Q_o cfs	t_p sec	t_g sec	$\left(\frac{Q_b}{Q_o}\right)^{.5}\left(\frac{1}{Q_b+Q_o}\right)^{.47}$	i	$i\left(\frac{Q_b}{Q_o}\right)^{0.5}\left(\frac{1}{Q_b+Q_o}\right)^{.47}$
39	20	10	50	100	0.285	-48.5×10^{-6}	-13.8×10^{-6}
41	5	25	50	100	0.0903	-145×10^{-6}	-13.1×10^{-6}
42	10	10	50	100	.245	-51.3×10^{-6}	-12.5×10^{-6}
43	10	5	50	100	.396	-28.5×10^{-6}	-11.3×10^{-6}

Table 7.12. Effect of diameter in supercritical flow for Q_b = 40 cfs, Q_o = 20 cfs, t_p = 50 sec, and t_g = 100 sec.

Run	Q_b cfs	Q_o cfs	t_p sec	t_g sec	D ft	$(D)^{0.8}$	i	$i(D)^{0.8}$
69	40	20	50	100	5.0	3.62	-71.5×10^{-6}	-260×10^{-6}
70	40	20	50	100	8.0	5.27	-47.1×10^{-6}	-248×10^{-6}
71	40	20	50	100	10.0	6.31	-41.4×10^{-6}	-260×10^{-6}

$\pi_2 = \left(\frac{Q_b}{Q_o}\right)^{0.5}$, the parameter defining the effects of the relative value of base flow to peak superimposed flow;

$\pi_3 = \left(\frac{t_g - t_p}{t_g}\right)^{0.25}$, the parameter defining the effects of t_p and t_g;

$\pi_4 = \left(\frac{1}{Q_b+Q_o}\right)^{0.47}(t_g)^{0.75}(D)^{0.8}(g)^{0.61}$, where g is gravitational acceleration, and π_4 correlates the absolute value to t_g, Q_b, and Q_o; and $\pi_5 = S_o/f^{0.5}$, the parameter correlating the effects of channel slope and friction factor.

A new parameter was obtained by combining π_1, π_2, π_3, and π_4 into $\pi_7 = \pi_1\pi_2\pi_3\pi_4$, or

$$\pi_7 = i\left(\frac{Q_b}{Q_o}\right)^{0.5}\left(\frac{t_g-t_p}{t_g}\right)^{0.25}\left(\frac{1}{Q_b+Q_o}\right)^{0.47}(t_g)^{0.75}(D)^{0.8}(g)^{0.61}$$

The plot of π_7 versus π_5 is given in Fig. 7.10.

In conclusion, it is possible to approximate the attenuation rate of a flood wave peak in the supercritical flow in a plot of:

$$i\left(\frac{1}{Q_b+Q_o}\right)^{0.47}\left(\frac{Q_b}{Q_o}\right)^{0.5}(t_g)^{0.75}\left(\frac{t_g-t_p}{t_g}\right)^{0.25}(D)^{0.8}(g)^{0.61}$$

versus $\frac{S_o}{f^{0.5}}$, and in the subcritical regime of

$$i\left(\frac{Q_b}{Q_o}\right)^{0.3}\left(\frac{1}{Q_b+Q_o}\right)^{0.34}(t_g)^{0.1}(D)^{0.8}(g)^{0.22}$$ versus $\frac{S_o}{f^{2.88}}$.

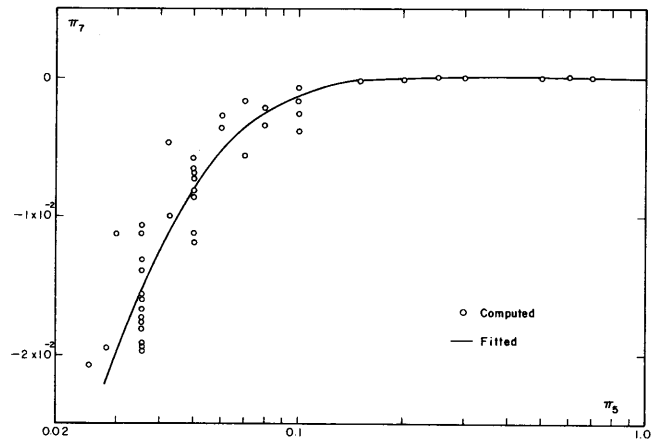

Fig. 7.10. Attenuation of wave peak for theoretical hydrograph in supercritical flow.

This analysis is only an attempt to show that the non-dimensionalization of variables in gradually varied free-surface unsteady flow has some promise in the future research. The accurate integration of hypothetical waves and conduit conditions by the method of characteristics may yield computer "experimental data", for further investigating the non-dimensional approach of flood peak attenuation.

It is not recommended that the rate of highly amplifying flood waves be studied by this approach, because the transition of the gradually varied waves to rapidly varied waves may have just the same criterion as the criterion when a wave starts to amplify. In other words, the gradually varied unsteady flow equations may be used for studying the conditions when waves start to amplify but not for studying the rate of amplification. The non-dimensionality of changes in unsteady flow regimes requires that the conduits be prismatic and very long. The local energy losses have to be incorporated into the general conduit losses.

Chapter 8

ANALYSIS OF ERRORS IN THE SOLUTION OF PROBLEMS

8.1 Errors in Geometric Parameters

The steel conduit used for free-surface unsteady flow experiments was 3 ft in diameter, 1/2-inch thick rolled-plate with a longitudinal welded joint. The 20-ft sections were butt-welded together and were supported on steel rails at approximately 20-ft spacing, not necessarily at the conduit joints. As a result of the manufacturing process, handling, field welding, and the method of support, the conduit is not perfectly circular and does not possess a straight line invert profile. The errors caused by physical departures from the mathematical geometric forms in the conduit cross section and longitudinal invert slope are defined as the errors in geometric parameters.

Errors in parameters as a function of errors in depth. The error in each of the dependent parameters can be expressed in terms of the relative error in the depth as follows:

(1) Wetted perimeter $P = D\theta/2$ has the relative error $dP/P = d\theta/\theta$, with $\theta = 2\cos^{-1}(1-2y/D)$, the central angle of water surface, in which y is the water depth at the invert of a partly full circular conduit, and D is the conduit diameter. The relative error is then

$$\frac{d\theta}{\theta} = \frac{1}{(\frac{D}{y}-1)^{\frac{1}{2}}\cos^{-1}(1-\frac{2y}{D})}(\frac{dy}{D}) \quad . \tag{8.1}$$

(2) Surface width $B = D \sin(\theta/2)$ has the relative error

$$\frac{dB}{B} = \frac{1}{(\frac{D}{y}-1)^{\frac{1}{2}}\tan\frac{\theta}{2}}(\frac{dy}{y}) \quad . \tag{8.2}$$

(3) Area $A = D^2(\theta-\sin\theta)/8$ has the relative error

$$\frac{dA}{A} = \frac{1-\cos\theta}{1-\frac{\sin\theta}{\theta}}(\frac{d\theta}{\theta}) \quad . \tag{8.3}$$

(4) Hydraulic depth $y_* = A/B$ has the relative error

$$\frac{dy_*}{y_*} = \frac{dA}{A} - \frac{dB}{B} \quad . \tag{8.4}$$

(5) Hydraulic radius $R = A/P$ has the relative error

$$\frac{dR}{R} = \frac{dA}{A} - \frac{dP}{P} \quad . \tag{8.5}$$

(6) Section factor $Z = AR^{\frac{1}{2}}$ has the relative error

$$\frac{dZ}{Z} = \frac{dA}{A} + \frac{dR}{2R} \quad . \tag{8.6}$$

These relative errors (Eqs. 8.1 through 8.6) as functions of depth are plotted as ratios of the relative-depth error in Fig. 8.1. The relative errors in all parameters except for the wetted perimeter and hydraulic depth decrease as depth increases for a given relative depth error, dy/y. The significance of these curves is demonstrated in the calculation of friction factors and Reynolds numbers.

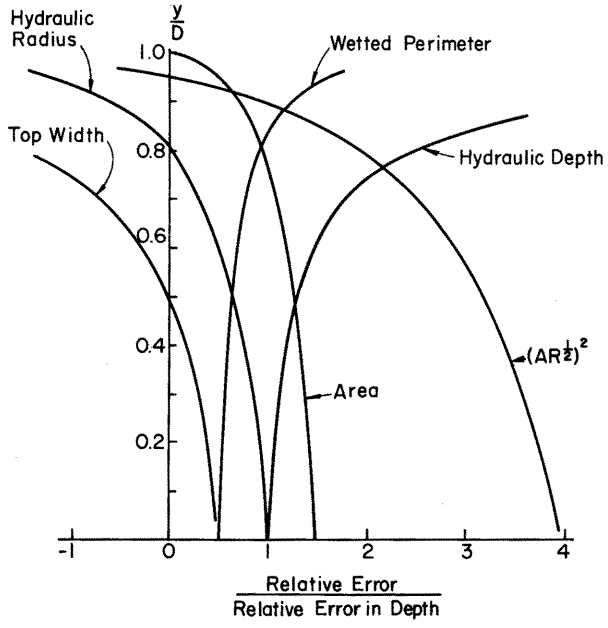

Fig. 8.1. Relative errors in parameters of circular cross section versus relative error in depth.

Errors in parameters as a function of ellipticity. Since no physical conduit has a truly geometric circular shape, it is necessary to determine the effects of deviations from circularity. An elliptical shape is assumed. Parameters describing the departure from a circular cross section are then the eccentricity and the direction of the principal axes. The eccentricity is defined as $e = \sqrt{1-(b/a)^2}$, in which a and b are the major and minor ellipse semi-diameter, respectively. The direction of the principal axes is the angle α that the minor axis makes with the vertical as shown in Fig. 8.2.

To compare circular segments with elliptical segments the percent of difference between the two was computed for depths from the bottom up to the center of the ellipse. Eccentricity was varied in increments of 0.05 up to 0.30 and α ranged from 0

to $\pi/2$ in increments of $\pi/10$. The area of the complete ellipse was made equal to the area of the complete circle. Depth was relative to the center of the ellipse. The results of these calculations are shown in Fig. 8.3.

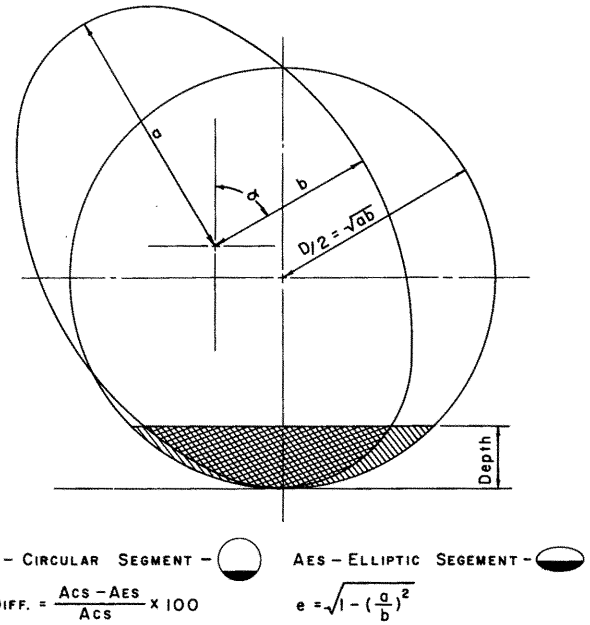

Fig. 8.2. Definition sketch for the relation of circular and elliptical cross sections.

These calculations indicate

(1) that the relative error in area increases with increased eccentricity;

(2) that the relative error in area decreases with increasing depth, and

(3) that the relative error in area is maximum at the vertical and horizontal positions of the principal axes and is minimum at an angular position of 45° with the horizontal.

Measurements to the nearest 0.001 inch were made of the inside diameter of the pipe at 60° intervals at cross sections spaced 40 feet apart before the inside of the conduit was painted and at intervals of 20 feet after the inside was painted. An ellipse was fitted to the three measured diameters at each cross section and its orientation determined. The results of these calculations are presented in Table 8.1. The differences between the means of each of the parameters for the two surveys are not significant on the 5 percent level. This indicates that the painting of the conduit had no effect on the internal geometry, and that doubling the number of stations did not significantly improve knowledge about the inside geometry of the conduit.

Accepting an average area of 968.41 square inches (6.725 square ft) the mean diameter of the conduit is 2.9262 feet. This figure was used for the conduit diameter in all calculations.

Because of the interrelated effects of depth, eccentricity, and α it appears that an error in the computation of the flow area by assuming a circular cross section instead of an approximated ellipse may range from zero to 3 percent with 1 percent representative.

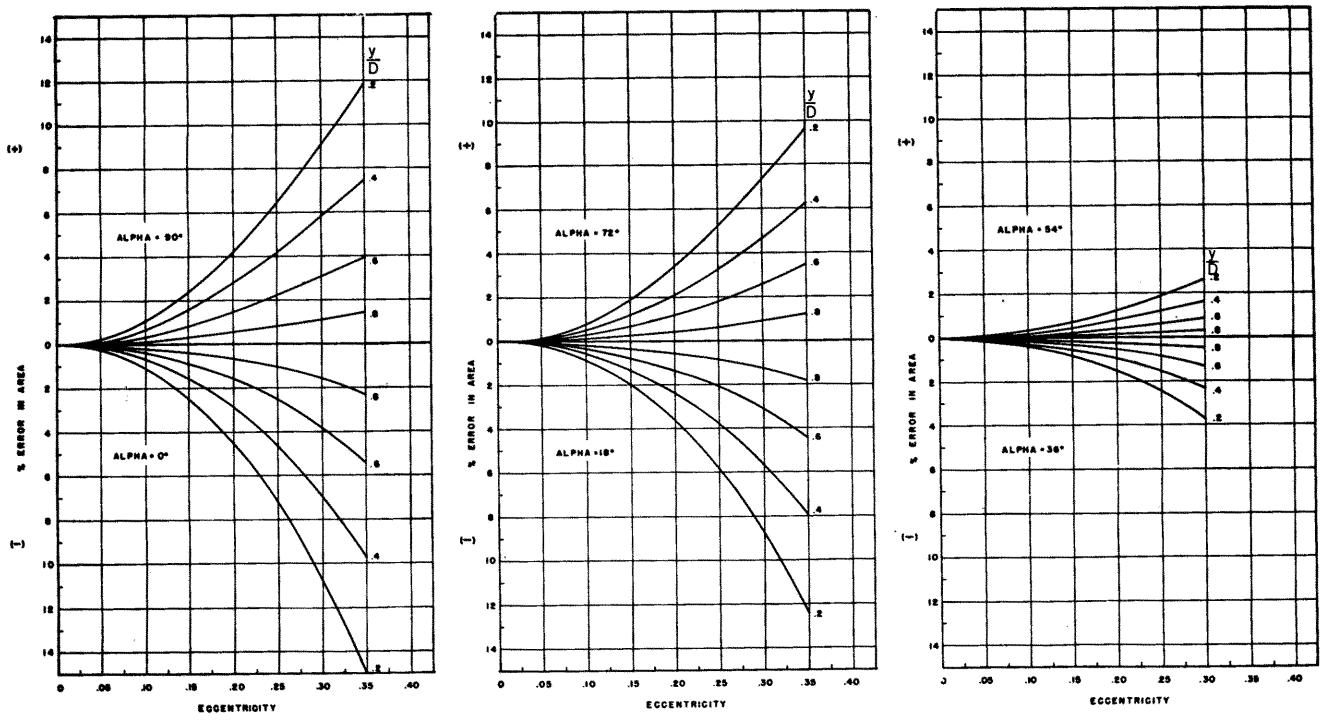

Fig. 8.3. Percent difference in area versus eccentricity and depth.

Table 8.1. Geometry of the experimental conduit.

	Number of Stations	Maximum	Mean	Minimum	Standard Deviation
Major Axis (in.)	21	17.869	17.617	17.538	0.175
	41	17.913*	17.604	17.554	0.047
Minor Axis (in.)	21	17.626	17.516	17.435	0.0375
	41	17.680	17.510	17.430	0.031
Eccentricity	21	0.176	0.1021	0.046	0.0310
	41	0.175	0.0993	0.051	0.0244
Alpha α (degrees)	21	165.58	84.84	13.71	46.5
	41	160.37	82.94	7.78	49.43
Area (sq. in)	21	989.5	969.47	965.3	3.84
	41	994.9*	968.4	964.1*	3.94
Wetted Perimeter (in)	21	111.51	110.373	110.13	0.2769
	41	111.82*	110.314	110.07*	0.2167
Hydraulic Radius (in)	21	8.87	8.7785	8.76	0.0183
	41	8.89	8.7742	8.75*	0.0181

*occurred at same section;
The first row of figures refers to the unpainted interior of the conduit, while the second refers to the painted interior.

Errors because of vertical displacements of a circular cross section. The deviations of a given conduit from a mathematically straight alignment may be:

(1) the surface irregularities which contribute directly to viscous shear and consequent hydraulic roughness;

(2) unintentional misalignments of the conduit which occur gradually when it is extremely long;

(3) intentional changes in conduit direction to alter the direction of flow.

The effects of surface irregularities and intentional conduit realignments on surface profiles, in general, are easily computed. However, the gradual conduit misalignments are usually ignored or assumed to have a negligible effect on the surface profile. Based on energy conversions relating to such changes in cross section area, the foregoing assumptions may be justified, since energy transfers are small by definition, and may well be masked by the uncertainty of the mean turbulent energy loss as well as by the time variable. Depths computed from any commonly used formula represent only the time-distance mean values. Equations 8.7 and 8.8 given by Henderson [6] are used in this study to estimate the effect of vertical conduit misalignments on the water surface elevations by considering a sinusoidal channel-bottom profile. (Details of the derivations of Eq. 8.7 and 8.8 are given in Hydrology Paper No. 45). The amplitude of the depth wave can be evaluated from

$$\varepsilon = -\frac{2\pi z_a \sin\phi}{3 S_o L} \tag{8.7}$$

in which ε is the ratio of amplitude to the uniform depth y_o, and ϕ is the phase angle for the depth wave. The value of ϕ is

$$\phi = \tan^{-1}\left[\frac{-3 S_o L}{2\pi y_o (1 - F_o^2)}\right], \tag{8.8}$$

with z_a and L the amplitude and wave-length of the sinsoidally varying bottom, respectively, S_o is the bottom slope, and F_o is the Froude number in uniform flow.

Equations 8.7 and 8.8 were solved for various combinations of channel slope, wave length of channel irregularity, amplitude of channel irregularity, and normal depth. The Darcy-Weisbach friction factor was taken as a constant 0.012. Table 8.2 presents the results of these calculations. As expected, for a Froude number greater than one the depth wave is nearly in phase with the bottom wave. The slight difference is due to flow resistance. For a Froude number less than one the depth wave is out of phase with the bottom wave by essentially π. Again, the slight difference is caused by flow resistance.

The amplitude of the depth wave is unchanged for various lengths of the bottom wave, provided that other parameters are also unchanged. The amplitude of the depth wave compared to the length of the bottom wave ranges from approximately one for low Froude numbers to approximately three for Froude numbers close to one.

Because of unavoidable irregularities in successive sections of the conduit and the method used to join sections, it was impossible to completely eliminate all deviations from the mean slope. Table 8.3 presents the results of mean slope determinations and the corresponding maximum and root-mean-square deviations from the slope of the least-square fit. These results show that the invert profile of the conduit had an undulating bottom with approximately 0.01 foot of amplitude and 20 to 40 feet of wave length.

8.2 Errors in Hydraulic Parameters

Errors in friction factor. To estimate the effect of observational errors on computed friction factors, certain assumptions are required. For the following analysis the assumptions about the numerical values of parameters and errors are: the internal diameter of the conduit (D) is 3 ft, the depth (y) is 1.5 ft with an error of ±0.005 ft, the bottom slope S_o is 0.001 with an error of ±.00001, and the discharge (Q) is 30 cfs with an error of ±0.3 cfs. These values will be used in the expression for the friction factor

$$f = \frac{8 g S_o RA^2}{Q^2} \quad . \tag{8.9}$$

By differentiating Eq. 8.9, the error equation for the assumed independent errors in the four quantities, y, $S_f = S_o$, RA^2, and Q is

$$\varepsilon^2(f) = \left[\frac{\partial f}{\partial S_f}\,\varepsilon(S_f)\right]^2 + \left[\frac{\partial f}{\partial (RA^2)}\,\varepsilon(RA^2)\right]^2 + \left[\frac{\partial f}{\partial Q}\,\varepsilon(Q)\right]^2 \quad , \tag{8.10}$$

Table 8.2. Theoretical effect of bottom irregularity on water surface profiles.

Slope	Froude No.	z_a-ft	L-ft	ϕ-Rad	εy_o-ft	Slope	Froude No.	z_a-ft	L-ft	ϕ-Rad	εy_o-ft
.0100	2.582	.01	20	6.266	.002			.03	20	3.170	.090
			40	6.249	.002				40	3.198	.090
			60	6.232	.002				60	3.227	.090
			80	6.216	.002				80	3.255	.090
		.02	20	6.266	.004			.04	20	3.170	.120
			40	6.249	.004				40	3.198	.120
			60	6.232	.004				60	3.227	.120
			80	6.216	.004				80	3.255	.120
		.03	20	6.266	.005	.0001	.258	.01	20	3.142	.011
			40	6.249	.005				40	3.143	.011
			60	6.232	.005				60	3.144	.011
			80	6.216	.005				80	3.145	.011
		.04	20	6.266	.007			.02	20	3.142	.021
			40	6.249	.007				40	3.143	.021
			60	6.232	.007				60	3.144	.021
			80	6.216	.007				80	3.145	.021
.001	.816	.01	20	3.170	.030			.03	20	3.142	.032
			40	3.198	.030				40	3.143	.032
			60	3.227	.030				60	3.144	.032
			80	3.255	.030				80	3.145	.032
		.02	20	3.170	.060			.04	20	3.142	.043
			40	3.198	.060				40	3.143	.043
			60	3.277	.060				60	3.144	.043
			80	3.255	.060				80	3.145	.043

Table 8.3. Slope deviations of the experimental conduit

Slope	Max. Deviation, ft	Root-Mean-Square Deviation, ft
.0000052	+.0188	.0116
.0000157	+.0182	.0135
.0000303	+.0214	.0099
.0001325	+.0195	.0099
.0005197	+.0347	.0117
.0010101	+.0279	.0119
.0074578	-.0240	.0133
.0200690	+.0375	.0141

in which $\varepsilon(f)$, $\varepsilon(S_f)$, $\varepsilon(RA^2)$, and $\varepsilon(Q)$ represent errors in f, S_f, RA^2, and Q, respectively. The term RA^2 is called here the section factor. The error $\varepsilon(RA^2)$ of this section factor is evaluated from the error in the depth (y), and given as $\varepsilon(y)$. The derivatives $\partial f/\partial S_f$, $\partial f/\partial(RA^2)$, and $\partial f/\partial Q$ are computed from Eq. 8.9, and the above numerical values of parameters are used to numerically determine these derivatives in Eq. 8.10.

Assuming that the errors in y (±0.005 foot), S_f (±0.00001), and Q (±0.3 cfs) are their respective standard deviations of random errors, then the standard error of random errors in the friction factor, $\sigma(f)$, is

$$\sigma(f) = \{(2.681 \times 0.00001)^2 + (0.000286 \times 0.0997)^2 + (0.0001787 \times 0.3)^2\}^{\frac{1}{2}} = 6.61 \times 10^{-5}.$$

For the representative constant friction factor of 0.012 for this conduit and the range of Reynolds numbers used in this study, this estimated standard error of 6.61×10^{-5} represents only a 0.55 percent error. For this particular numerical case, the largest contribution of errors to the friction factor is from the errors in discharge measurement. The standard error in the friction factor of 6.61×10^{-5} may be considered as a lower boundary in practical evaluations of random errors.

The other aspect of errors in the friction factor is the effect of replacement of a changing friction factor with Reynolds number by an average factor on the shape of computed hydrographs along the conduit. These conditions of the Darcy-Weisbach friction factor f are, therefore, that a (1) single constant value of f is used, and that a (2) friction factor f is a function of Reynolds number given by the Prandtl-von Karman equation of hydraulically smooth boundaries.

To find the effects of various values of f on flood evaluation, a hypothetical inflow hydrograph in the form of the Pearson Type III function is used, with its shape and the numerical values of parameters given in Fig. 8.4. This inflow hydrograph is considered as the inlet boundary condition, and waves are integrated by using the specified intervals numerical integration scheme of the method of characteristics, described in Chapter 5 of this paper, with additional details given in Part IV, Hydrology Paper No. 46.

The friction factor in this study varied between 0.010 to 0.14. Three values of f, 0.010, 0.012 and 0.014, were tested for their effects on flood hydrograph evolution. Figure 8.5 shows the computed depth hydrographs at three positions x = 50.0, 410.0, and 771.7 ft along the channel with the above three constant values of f, as lines (1), (2), and (3). These results and their comparison lead to four conclusions;

(1) Differences of depth hydrographs for f = 0.010 and f = 0.014 at x = 50.0 ft from the inlet

are of the order of 5 percent of the channel diameter. These differences decrease with an increase of x. This decrease can be explained by both the initial conditions being a M2 curve and the downstream boundary conditions being in the critical flow at the conduit outlet.

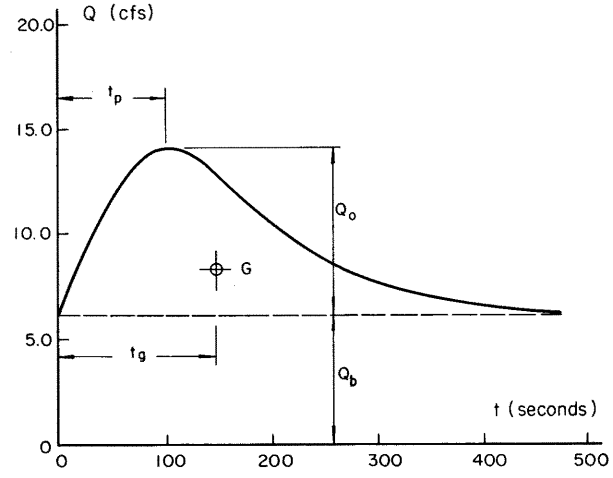

Fig. 8.4. Hypothetical inflow hydrograph of the Pearson Type III function, Eq. 5.32, with the selected parameters: Q_b = 6.21 cfs, Q_o = 8.00 cfs, t_p = 100.00 sec, and t_g = 150.0 sec.

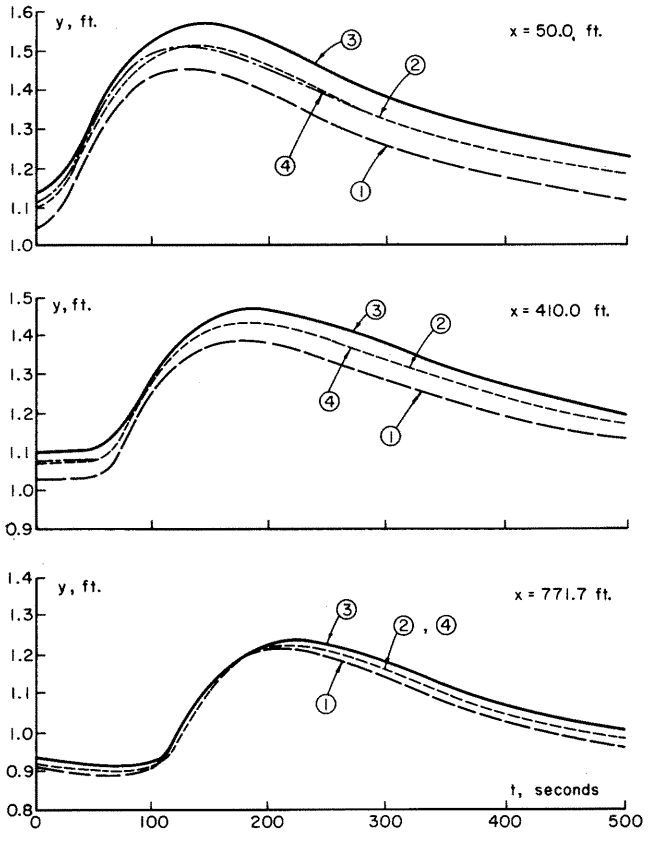

Fig. 8.5. Effect of changes in friction factor, f, at various positions along the channel: (1) f = 0.010, (2) f = 0.012, (3) f = 0.014, and (4) f = f(R_e).

(2) The smaller the friction factor, the smaller are the depths, in general, and the peak depths, in particular, at various positions along the channel. For Fig. 8.5, the differences in peak depths between f = 0.010 and f = 0.014 in relation to the conduit diameter amount to approximately 4 percent at x = 50.0 ft, 3 percent at x = 410.0 ft, and 0.1 percent at x = 771.7 ft. Table 8.4 gives the percentage ratios of peak depth to conduit diameters, at various positions x along the conduit for f = 0.010, 0.012, and 0.014.

(3) The smaller the friction factor the earlier the peak depth occurs. The differences of the time at the peak depth for f = 0.014 and f = 0.010 are approximately 3 percent of the inflow hydrograph rising time (t_p) at x = 50.0 ft, 6 percent at x = 410.0 ft, and about 7 percent at x = 771.7 ft. Table 8.5 gives the times of peak depth percentages to the inflow hydrograph rising time; this shows how significant the effect of the friction factor is on the time occurrence of the peak depth.

(4) Because of downstream boundary conditions of a free fall at the outlet, there are no systematic trends in peak depths, nor are there any at the time of the peak depths along the downstream portion of the conduit within 100 ft of the outlet.

Figure 8.5 and Tables 8.4 and 8.5 give the respective properties of the depth hydrographs when the Darcy-Weisbach friction factor follows the Prandtl-von Karman resistence equation for hydraulically smooth conduits. The comparison of the results of three constant values of friction factor and the friction factor computed by this equation as a function of Reynolds number gives the following conclusions:

(1) Only a very small difference is shown between the depth hydrographs computed by using the average value of f = 0.012 and f as the function of R_e, for the given range of Reynolds numbers. The difference is on the order of 0.3 percent of the conduit diameter.

(2) The differences in peak depths computed by f = 0.012 and by f as the function of R_e are less than 0.4 percent of the conduit diameter at all positions along the conduit, as shown in Table 8.6.

(3) The differences in the time of the occurrence of peak depth computed by f = 0.012 and by f as the function of R_e range along the conduit from 3.9 to 8.5 percent of the rising time (t_p) of the inflow hydrograph. These differences at various positions along the conduit are shown in Table 8.7.

Errors in velocity distribution coefficients. By definition the minimum values of the two velocity distribution coefficients, α and β, are $\alpha = 1$ and $\beta = 1$. As soon as the time mean velocity at points in the cross section is not uniformly distributed, the coefficients are $\alpha > 1$ and $\beta > 1$. It was found in this study that for partly full flowing conduits, and for the depths between 0.3D - 0.8D, with D the conduit diameter, the average coefficient values are $\alpha = 1.03$ and $\beta = 1.01$. In practice, the values $\alpha = 1$ and $\beta = 1$ are nearly always used for the numerical integration of the two partial differential equations of gradually varied free-surface unsteady flow. The investigation of the effects of various values of α and β, particularly of the assumptions $\alpha = 1$ and $\beta = 1$, on the evolution of flood waves along a long storm drain has been accomplished and is presented as follows.

The hypothetical inflow hydrograph (Fig. 8.4) and the numerical integration scheme as it was used to study the friction factor are also used to

Table 8.4. Percentages of peak depth to conduit diameter at various positions, x , along the conduit and various values of f.

	x, position in feet along the conduit																
f	0	50	100	150	200	250	300	350	400	450	500	550	600	650	700	750	800
0.010	49.95	49.62	49.28	48.94	48.59	48.23	47.86	47.48	47.07	46.64	46.16	45.63	45.03	44.36	43.56	42.39	39.76
0.012	52.11	51.72	51.32	50.91	50.50	50.08	49.64	49.19	48.70	48.18	47.61	46.99	46.29	45.50	44.51	42.99	39.81
0.014	54.01	53.56	53.11	52.65	52.18	51.70	51.20	50.68	50.12	49.52	48.88	48.17	47.38	46.47	45.29	43.48	39.86
$f(R_e)$	52.00	51.66	51.30	50.94	50.56	50.17	49.76	49.32	48.86	48.35	47.79	47.16	46.47	45.67	44.70	43.27	40.21

Table 8.5. The percentage ratios of the time of the peak depths to the rising time of inflow hydrograph, at various positions along the conduit, and for several values of friction factor.

	x, position in feet along the conduit							
f	0	50	100	150	200	250	300	350
0.010	124.03	130.47	136.90	142.78	149.29	155.89	162.63	169.05
0.012	126.21	132.55	139.51	145.26	152.38	159.07	166.14	173.19
0.014	128.20	135.06	141.31	148.00	154.87	162.16	169.38	176.23
f(R)	123.03	128.65	134.89	141.24	147.57	153.91	160.24	166.59

Table 8.5. Continued

x, position in feet along the conduit								
400	450	500	550	600	650	700	750	800
175.48	182.74	189.18	196.44	203.70	211.78	222.39	216.93	208.00
180.16	186.51	194.37	202.23	210.09	217.95	221.07	218.11	211.86
183.10	190.74	198.39	206.82	214.45	220.89	222.45	219.40	215.58
172.92	180.07	186.42	193.74	201.50	209.50	215.47	213.21	206.59

Table 8.6. Difference in peak depths computed from f as the function of Reynolds number and three values of f, in percent of conduit diameter.

	x, position in feet along the conduit																
f	0	50	100	150	200	250	300	350	400	450	500	550	600	650	700	750	800
0.010	-2.05	-2.04	-2.02	-2.00	-1.97	-1.94	-1.90	-1.84	-1.79	-1.71	-1.63	-1.53	-1.44	-1.31	-1.14	-0.88	-0.45
0.012	0.11	0.06	0.02	-0.03	-0.06	-0.09	-0.12	-0.13	-0.16	-0.17	-0.18	-0.17	-0.18	-0.17	-0.19	-0.28	-0.40
0.014	2.01	1.90	1.81	1.71	1.62	1.53	1.44	1.36	1.26	1.17	1.09	1.01	0.91	0.80	0.59	0.21	-0.35

Table 8.7. Differences in the occurrence of peak depths, computed from f as the function of Reynolds number and for each of three constant values of f, in percent of the inflow hydrograph rising time.

	x, position in feet along the conduit																
f	0	50	100	150	200	250	300	350	400	450	500	550	600	650	700	750	800
0.010	1.00	1.82	2.01	1.54	1.72	1.98	2.39	2.46	2.56	2.67	2.76	2.70	2.20	2.28	6.92	3.72	1.41
0.012	3.18	3.90	4.62	4.02	4.81	5.16	5.90	6.60	7.24	6.44	7.95	8.49	8.59	8.45	5.60	4.90	5.27
0.014	5.17	6.41	6.42	6.76	7.30	8.25	9.14	9.64	10.18	10.67	11.97	13.08	12.95	11.39	6.98	6.19	8.99

study the effects of the velocity distribution coefficients.

The effects of the velocity distribution coefficient α were studied for three values, 1.01, 1.02, and 1.03, while the coefficient β was kept constant at $\beta = 1.00$. The effects of the velocity distribution coefficient β were then studied for the values of $\beta = 1.005$, and 1.010, and $\alpha = 1.00$. The results can be summarized as follows:

(1) The higher a value of α the higher the depths produced. The differences in depths for various values of α and β, and for $\alpha = 1.00$ and $\beta = 1.00$, with $\alpha = 1.01$, 1.02, 1.03, and $\beta = 1.00$, increase with an increase of time. They are of the order of 0.40 percent of the conduit diameter.

(2) The differences in depths are higher at the upstream than at the downstream part of the conduit, and are on the order of less than 0.10 percent of the conduit diameter.

(3) The higher the α value, the higher are the peak depths at various positions along the channel. The differences in peak depths are less than 0.25 percent of the conduit diameter, as shown by the numbers in the first three rows of Table 8.8.

(4) The higher the α value, the later the peak depth, t_p, occurs. The differences in t_p between $\alpha = 1.01$, 1.02, 1.03 and $\beta = 1.00$, and $\alpha = 1.00$ and $\beta = 1.00$, range from 0.5 to 2.0 percent of the inflow hydrograph time parameter, t_p, as shown by the first three rows of Table 8.9.

Table 8.8. Differences in peak depths, in percent of conduit diameter computed for various values of α and β, and for $\alpha = 1.00$ and $\beta = 1.00$.

α	β	x, position along the conduit, in feet																
		0	50	100	150	200	250	300	350	400	450	500	550	600	650	700	750	800
1.01	1.000	0.08	0.08	0.08	0.09	0.08	0.08	0.08	0.07	0.08	0.08	0.07	0.07	0.07	0.07	0.06	0.05	0.03
1.02	1.000	0.17	0.17	0.17	0.17	0.16	0.16	0.16	0.15	0.15	0.15	0.15	0.14	0.14	0.13	0.13	0.11	0.05
1.03	1.000	0.25	0.25	0.24	0.24	0.23	0.23	0.22	0.21	0.22	0.22	0.21	0.20	0.20	0.19	0.18	0.15	0.07
1.00	1.005	0.01	0.02	0.02	0.03	0.02	0.02	0.02	0.02	0.03	0.03	0.03	0.02	0.02	0.02	0.02	0.02	0.03
1.00	1.010	0.01	0.02	0.02	0.03	0.03	0.02	0.03	0.02	0.03	0.03	0.03	0.02	0.03	0.02	0.02	0.02	0.03
1.03	1.010	0.25	0.19	0.23	0.27	0.30	0.32	0.36	0.37	0.39	0.40	0.41	0.39	0.39	0.37	0.39	0.44	0.49

Table 8.9. Differences in times of peak depths in percent of conduit diameter for various values of α and β and for $\alpha = 1.00$ and $\beta = 1.00$.

α	β	x, position along the conduit, in feet																
		0	50	100	150	200	250	300	350	400	450	500	550	600	650	700	750	800
1.01	1.000	0.72	0.63	0.09	0.70	0.35	0.71	0.69	0.51	-0.03	0.67	-0.05	0.14	0.66	0.21	0.66	0.12	0.66
1.02	1.000	0.63	1.34	0.62	0.87	1.04	1.40	1.11	0.57	0.65	1.35	0.54	0.52	1.05	0.85	1.30	0.78	0.51
1.03	1.000	1.33	1.32	1.31	1.23	1.73	1.71	1.24	1.24	1.31	2.01	1.18	1.17	1.15	1.14	1.12	1.14	1.15
1.00	1.005	0.31	0.24	-0.45	-0.17	0.02	0.05	-0.39	-0.38	-0.27	0.46	-0.33	-0.30	-0.29	-0.27	-0.26	0.02	-0.27
1.00	1.010	-0.18	-0.15	-0.73	-0.08	-0.06	-0.01	-0.26	-0.75	-0.63	0.12	-0.66	-0.62	-0.57	-0.54	0.28	-0.25	0.25
1.03	1.010	2.56	2.73	3.52	3.62	4.06	3.88	4.78	4.96	5.77	5.24	6.23	7.22	6.81	6.70	4.36	4.06	4.38

(5) The higher a value of β the higher the depths produced. The differences in depth between $\beta = 1.005$ and 1.010 and $\beta = 1.000$ decrease with an increase of both the time and distance, and are on the order of 0.08 percent of the conduit diameter.

(6) The differences in depths at the upstream part of the conduit are of the same order as the differences at the downstream part of the conduit.

(7) The higher a value of β, the higher are the peak depths produced at various positions along the conduit. The differences in peak depths are less than 0.03 percent of the conduit diameter as shown by the fourth and fifth row of Table 8.8.

(8) The higher a value of β the earlier the occurrence of the peak depth. The differences in t_p between $\beta = 1.005$, 1.010, and $\beta = 1.000$ for $\alpha = 1.00$ range from 0.01 to 0.75 percent of the inflow hydrograph parameter t_p, as shown by the fourth and fifth row of Table 8.9.

When both $\alpha > 1.00$ and $\beta > 1.00$ are used, particularly $\alpha = 1.03$ and $\beta = 1.01$, the differences in Tables 8.8 and 8.9, the sixth row, show the largest values. The differences in peak depths between $\alpha = 1.03$ and $\beta = 1.01$ and $\alpha = 1.00$ and $\beta = 1.00$ reach 0.50 percent of the conduit diameter at $x = 800$ ft. This value is relatively negligible.

In summary, replacing the average values of $\alpha = 1.03$ and $\beta = 1.01$ of free-surface conduit flow, for the flow depths $y = 0.3\,D - 0.8\,D$, by minimum values of $\alpha = 1.00$ and $\beta = 1.00$, only slightly affects the evolution of flood waves along the circular storm drainage conduits.

8.3 Errors in Computations

Computational errors resulting from procedures used in this study are the product of the following:

(1) The approximation of infinitesimal variations by finite values. This is a result of assuming, in general, linear relations rather than true curvilinear relations. This is a systematic error, which is not readily determined since it may be positive or negative during different stages of the computations.

(2) Truncation of numerical values. This is due to the limited precision of any discrete-element calculator. The computer used for these studies was programmed for single precision computations using 15 decimal digits.

(3) Round-off in the printed output. The computer used for the calculations rounded off all numbers in a manner similar to a manual calculator.

The following discussion evaluates the effects of control variables in the solution of the unsteady flow equations. These equations are considered under the computational schemes with the incremental length and incremental time interval during which the integration process proceeds.

Determination of computational parameter Δt. The grid sizes of Δx and Δt in the computational schemes is limited by the characteristic directions ξ_+, ξ_-, encountered during the integration. In order to assure that this condition exists, it is necessary that

$$\Delta t < \frac{\Delta x}{V + \sqrt{gA/B}} \quad . \tag{8.11}$$

Computations require that Δt be computed before the integration process. The incremental distance Δx was arbitrarily established. The computed velocity (V) was based on conditions that would produce the maximum critical velocity. The geometric term gA/B, which goes to infinity for full size flow, was computed for a depth of 0.82 of the diameter.

Effect of computational parameter Δx. The method of characteristics using a specified intervals scheme gives the complete numerical solution of the free-surface unsteady flow. The accuracy of the results depends on the size of the rectangular grids Δx and Δt.

If n is the number of intervals along the conduit and x_L is the length of the conduit, then

$$\Delta x = \frac{x_L}{n} \quad , \tag{8.12}$$

with n an arbitrarily selected number. The smaller the Δx presumable the more accurate are the results. But also, the smaller the Δx, the greater the required computing time. In compromising these two conditions to satisfy the objectives of this study, several values of n for the fixed x_L were tried for the inflow hydrograph of Fig. 8.4 and the circular experimental conduit of this study.

Figure 8.6 shows the effect of the size of Δx on the depth hydrographs at three positions along the conduit. The upper graph is the depth hydrograph at a position 50.0 ft downstream from the inlet and for a Δx of 40.91, 20.45, 10.23, and 5.12 ft corresponding to n values of 20, 40, 80, and 160, respectively. The center and lower graphs are the depth hydrographs at 410.0 ft and at 771.7 ft from the inlet, respectively. The initial condition for each computation is the steady-state water surface for a free outfall.

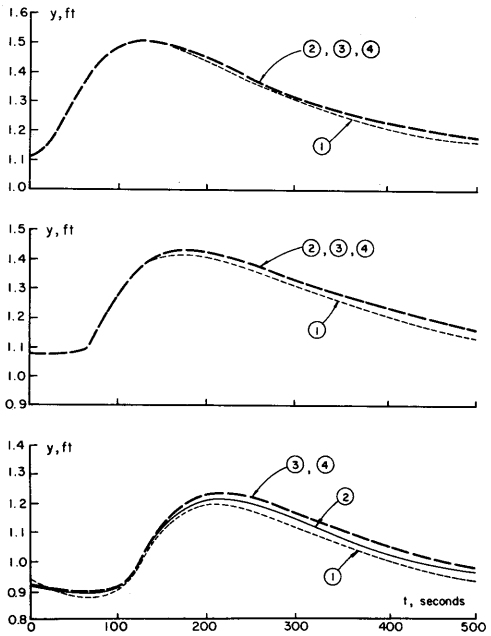

Fig. 8.6. Effect of Δx on hydrographs at various positions along the conduit; (1) $\Delta x = 40.91$ ft, (2) $\Delta x = 20.45$ ft, (3) $\Delta x = 10.23$ ft, and (4) $\Delta x = 5.12$ ft, at three locations of conduit $x = 50.0$ ft (upper graph) $x = 410.0$ ft (center graph), and $x = 771.7$ ft (lower graph).

Comparing the depth hydrographs of Fig. 8.6 with the inflow discharge hydrograph of Fig. 8.4 it was found that:

(1) The critical portion of the conduit for computing depth hydrographs is near the outlet where there is the greatest curvature of the base-flow water-surface profile. The maximum differences between the computed depths, with Δx being 40.91 and 5.12 ft, are approximately 0.3, 0.6, and 1.0 percent of the conduit diameter at 50.0, 410.0, and 771.7 ft from the inlet, respectively.

(2) There is no significant increase in accuracy over 0.005 ft or 0.15 percent of the conduit diameter when Δx is less than 10.23 ft. Therefore, a Δx equal to 10.23 ft, or n equal to 80, was selected for computations.

The peak depth y_p and the time to peak depth t_p are two important parameters describing a depth hydrograph. The required accuracy of a computed hydrograph at various positions along the conduit can be measured by the peak depth, y_p, relative to the diameter, D, of the conduit, for various lengths Δx. Also, the accuracy can be measured by the time to peak depth, t_p, relative to the peak discharge, time t_p, of the inflow discharge hydrograph of Fig. 8.4, for various lengths Δx and the same positions x.

From the selected criteria for defining the accuracy of a computed hydrograph for a given Δx, it was found that the percentage differences of y_p,

$$\frac{(y_p)_i - (y_p)_{min}}{D} \times 100 \quad ,$$

in which the index "min" refers to the depth y_p of the smallest difference used, Δx = 5.12 ft, and the index "i" refers to depths of any other Δx > 5.12 ft, ranged from 0.0 percent to 2.1 percent for Δx ranging from 5.12 to 40.91 ft, and at various positions x, as shown in Table 8.10. At the upstream part of the conduit there was no significant difference between y_p/D for different values of Δx as expected. At the approximate middle of the conduit there was a 0.2 percent difference. At the downstream end, the difference was 2.1 percent. No significant change in the percentage difference of y_p/D was found when Δx was reduced below 10.23 ft.

In using the other parameter, T_p to define the accuracy of computed depth hydrographs with different values of Δx and various positions x, the measure of accuracy was

$$\frac{(T_p)_i - (T_p)_{min}}{t_p} \times 100 \quad ,$$

in which the indices "min" and "i" refer to Δx = 5.12 ft and all other values of Δx, respectively. It was found that there were no significant differences for values Δx > 5.12 ft, and for various positions x. The percentages were about 1.2 percent at the upstream, 2.0 percent at the middle, and 8.5 percent at the downstream part of the conduit. It was also found that there was no significant change of the percentages of T_p to t_p (which was about 1.9 percent) when Δx was reduced below 10.23 ft, as shown in Table 8.11.

Tables 8.10 and 8.11 show the percentage differences of y_p to the diameter D of the conduit, and T_p to t_p, respectively, with different values of Δx and at various positions of x. These values at even distances (0, 50, 100,...,ft) were computed by linear interpolation from the values in the grid system; therefore, some error may have been introduced. However, the change in shape of the depth hydrograph due to varying Δx was considered to be small. Larger Δx produced a lower and later peak depth.

8.4 Errors in Experimental Observations

Errors in geometric variables. A summary of this type of error has been already presented in Section 8.1. The two sources of geometric errors, the irregularities of conduit cross section and invert slope, were discussed in Chapter 6, Hydrology Paper No. 44 for the observed results, and were analyzed in detail in Chapter 2, Hydrology Paper No. 45.

Time difference errors. A systematic error was introduced into all tests because the flow-measuring orifice was located 82.2 feet upstream of what was considered the beginning of the test conduit. For much of this distance the conduit was flowing full and providing instantaneous transmission of changes in flow. This systematic error effected primarily

Table 8.10. Difference in y_p computed from various sizes of Δx (in percent of conduit diameter D).

Δx	Distance, ft																
(ft)	0	50	100	150	200	250	300	350	400	450	500	550	600	650	700	750	800
40.91	0	-0.02	-0.16	-0.04	-0.06	-0.08	-0.11	-0.16	-0.24	-0.31	-0.41	-0.50	-0.59	-0.70	-0.94	-1.43	-2.07
20.45	0	-0.01	-0.02	-0.02	-0.03	-0.04	-0.04	-0.06	-0.10	-0.13	0.18	-0.22	-0.27	-0.39	-0.42	-0.66	-0.99
10.23	0	0	-0.01	0	-0.01	-0.01	-0.01	-0.02	-0.03	-0.04	-0.06	-0.08	-0.09	-0.11	-0.14	-0.23	-0.39

Table 8.11. Difference in T_p computed from various sizes of Δx (in percent of t_p).

Δx	Distance, ft																
(ft)	0	50	100	150	200	250	300	350	400	450	500	550	600	650	700	750	800
40.91	1.23	-0.09	0.18	0.14	-1.21	-0.36	-1.62	-2.04	-2.02	-1.81	-1.09	1.21	-0.96	-1.43	-8.47	-7.32	-3.48
20.45	-0.40	-0.09	0	0.14	0.05	-0.06	0	-0.40	-0.40	-1.81	-2.73	-0.42	-0.40	0	-3.58	-4.07	-2.04
10.23	0.41	0	0	0.14	0.05	0	0	-0.22	-0.40	0	-1.90	-0.24	-0.42	0	-1.49	-1.62	-0.41

the time correlations of observed and computed depths. A secondary effect is due to a minor modification of the inflow hydrograph between the hydrograph observed at the orifice and the actual hydrograph observed at the beginning of the conduit. The distance between the point where a free surface formed and the beginning point of the test conduit, however, provided a varying time lag between observed and computed data of from 8 to 14 seconds. That is, the time recorded by the orifice transducer for a given flow discharge was ahead of the time when that discharge actually reached the conduit test section by the amount of time it took the wave to travel the 82.2 feet. To eliminate this difference, time shifts can be estimated visually from comparison plots (depth versus time) and experimental times can be adjusted by this amount. This shift in time is discussed more fully in Chapter 6.

Instrumentation errors. Instrumentation errors were analyzed on the basis of calibration results. Since the true values of physical quantities are never exactly measured, the calibration process of each instrument was considered to be an accurate estimate of the errors in the measured quantities.

A common method of placing boundaries on the errors used the unbiased standard deviation, s, defined by

$$s = \left[\sum^{N} \frac{(q_i - q_o)^2}{N - 1} \right]^{\frac{1}{2}} , \qquad (8.15)$$

in which q_i is the individual reading observed in a given range, q_o is the corresponding reading from a reference curve in the same given range as q_i, and N is the total number of observations.

For a Gaussian distribution of errors at an approximately 95 percent significance level, the physical quantities measured by each instrument can be expressed as

$$q_o = q_i \pm 2\,s \quad . \qquad (8.16)$$

Equation 8.16 means that 95 percent of the measured quantities q_i lie within the range of $\pm 2\,s$ of q_o.

Table 8.12 gives a summary of the calibration results of the orifice meters, current meters, and pressure transducers using Equation 8.16.

Reproducibility errors. An attempt was made to perform some experiments with conditions exactly the same as conditions of some selected previous runs. This was done to have some measure of the errors that were inherently reproduced in the experimental system. By running two runs under exactly the same conditions, the differences between the observed wave depths would be a measure of this type of error. If no errors were generated by the system, the observed values for both runs would be the same. This manner of comparison would not, however, be a measure of the random errors.

During the experiments, seven attempts were made to duplicate the conditions of previous runs. Only one of these runs, however, was successful. The other six could not be used in this evaluation because either the base or peak flows did not correspond to the earlier conditions or the time of one wave was longer than that of the previous run, resulting in different total water volumes. The runs with matching conditions were 010013 and 019913. The error was small.

Table 8.12. Estimate of instrumentation errors.

		s Standard Deviation	Error Bounds with 2.5% Level	Range
Orifice Meters	Small Opening	0.00413	$\alpha = \alpha \pm 0.00826$	Reynolds No. $3\times10^5 \sim 2\times10^6$
	Medium Opening	0.00220	$\alpha = \alpha \pm 0.00440$	Reynolds No. $2\times10^5 \sim 2\times10^6$
	Large Opening	0.00320	$\alpha = \alpha \pm 0.00640$	Reynolds No. $5\times10^5 \sim 2\times10^6$
	Large Opening	0.01619 ft^3	$\forall = \forall \pm 0.03238$ ft^3	Volume 8 ∿ 15 ft^3
Current Meters		0.0141 ft/sec	$v = v \pm 0.0282$ ft/sec	Velocity 1 ∿ 8 ft/sec
		0.0451 ft/sec	$v = v \pm 0.0902$ ft/sec	Velocity 8 ∿ 16 ft/sec
Pressure Transducers		0.0002 ft of water	$H = H \pm 0.0004$ ft of water	Pressure ± 1 psi Voltage ± 3 volts
		0.0003 ft of water	$H = H \pm 0.0006$ ft of water	Pressure ± 5 psi Voltage ± 3 volts

8.5 Total Errors

The discrepancy between a computed value of analytical waves and the corresponding observed value from a physical wave experiment is attributable to numerous sources. These discrepancies are the result of systematic and random errors in the observational system and possible systematic errors in computational procedures. Random errors are a result of unavoidable accidental variations in the physical system.

The comparison of computed and observed waves, as discussed in Chapter 6, include both the systematic and the random errors. The systematic errors are mainly in the form of base depth shifts due to zero-reading shifts, and in the form of time shifts because of the difficulty of coordinating the zero time of computed and observed waves. Additional systematic errors result in using average or lower bounds of friction factor and velocity distribution coefficients. All other differences between the computed and observed waves are attributable to random errors in observations and systematic errors in computations.

In previous analysis of individual sources of errors, and effects of various simplifications in hydraulic parameters, can not be simply integrated into the expression of a total error because: (1) errors are of different types, and (2) they may be dependent, with the dependence unknown. Therefore, it was not considered feasible to attempt to develop an overall formula for total errors.

It is reasonable to state that the gradually varied free-surface unsteady flow is in such a stage of development that the theory can be less effective for further contribution than a systematic analysis of all sources of errors.

Chapter 9

CONCLUSIONS, LIMITATIONS AND RECOMMENDATIONS.

9.1 Conclusions.

General conclusions, regarding this Part I, Hydrology Paper No. 43, as well as general results presented in detail in Parts II, III, and IV, Hydrology Papers 44, 45, and 46, are summarized as follows.

(1) The comparison of the solution of the theoretical equations of unsteady flow by numerical integration with accurately observed waves or the comparison of analytical and physical gradually varied free-surface waves, with the same boundary and initial conditions shows good practical agreement, provided systematic shifts in depth or in the time in some of the observed waves are considered.

(2) Observed waves in this study were subjected to a variety of sources of systematic and random errors. The systematic errors in recording the base flow depth, the recorded discharge as a function of time at the entrance into the conduit, and the energy head losses at the junction boxes are sometimes much larger than the cumulative random errors of various other sources of errors (measurements of discharge, depths, hydraulic parameters, etc.).

(3) Though the experimental conduit was 3 ft in diameter and 822 ft long, the observational errors on waves produced in this conduit, and the computational errors in the numerical finite-difference integration methods of the unsteady flow differential equations, did not permit an assessment of the differences between the physical and analytical waves, with these differences resulting from the basic hypotheses underlying the development of the continuity and momentum partial differential equations of gradually varied free-surface unsteady flow.

(4) The unique experimental facilities in this study of flow in conduits made it possible, through experimental investigations and observations, to understand various aspects of gradually varied free-surface unsteady flow.

(5) The geometric and hydraulic parameters such as area, depth, surface width, hydraulic radius, friction factor, velocity distribution coefficients, junction box losses, etc., which define the coefficients in the continuity and momentum partial differential equations, have been evaluated with sufficient validation from the experimental conduit so that a reliable numerical integration of these equations can be obtained.

(6) The recommended numerical integration procedure, which is based on experimental evidence, is the specified intervals scheme of the method of characteristics, in which case the four ordinary characteristic equations equivalently replace the two partial differential equations of unsteady flow.

(7) To simplify the coefficients of the characteristic equations, the velocity distribution coefficients, α and β, are taken as unities. This research shows that substituting constant α and β for functions of α and β on Reynolds numbers or on the depth of water in partly full conduits does not significantly affect the floods routed along the circular conduits. Similarly, the use of a Darcy-Weisbach friction factor, $f = 0.012$, for the range of Reynolds numbers in this study, instead of using the function $f(R_e)$, did not significantly affect the routed flood waves.

(8) It is doubtful that simplified flood routing methods have any significant advantage over numerical solutions of the theoretical equations for the design of storm drains. Simplified flood routing methods may be useful in those cases when the diameter of the conduit may be obtained explicitly from the equations or graphs, as the initial assumed dimension for the more accurate computations by the method of characteristics, or when these methods substantially save computer time with only a small loss in the accuracy of the solution.

(9) Research results in this study are considered as the basic information necessary for the expected development of practical flood routing methods for storm drain design, based on the unsteady flow approach to flood routing through a storm drain by using the most complete differential equations.

(10) The only flood routing method that can meet various field conditions is a method that uses the most complete differential equations of unsteady flow. A versatile new flood routing method should be applicable under various conditions such as branching of storm drains, upstream flow under particular conditions, different boundary and initial conditions, subcritical and supercritical flows and their transitions, etc.

(11) It is expected that in the future more accurate estimations of inlet flood hydrographs will be produced and the hydraulic conditions of storm drains will become better known so that extremely accurate flood routing methods will be both required and justified in practice. For that purpose, the use of digital computers and numerical integration schemes of the complete differential equations of unsteady flow will be used for both the design of storm drains, and the eventual prediction of flood hydrographs at particular points of existing storm drainage systems.

Conclusions in more detail are given in the last chapters of Papers 44, 45, and 46.

9.2 Limitations in the Developed Results.

The proposed method of using the most complete differential equations of unsteady flow for flood routing through storm drains, particularly in applying the numerical integration by the finite-differences specified intervals scheme of the method of characteristics, has some limitations and conditions of application; they are as follows.

(1) The method is applicable only to gradually varied free-surface unsteady flow, which implies a neglible vertical acceleration, or, in general, the method is applicable to flood waves which attenuate as they progress along the conduit.

(2) Waves must be one-dimensional or the velocity components in the horizontal direction normal to the conduit axis are negligible.

(3) The hydraulic resistance and velocity distribution coefficients in unsteady flow do not deviate significantly from the resistance and coefficients in steady flow, for the same Reynolds numbers.

(4) The method can not accommodate accurately the case when the flood wave moves on a dry bed, particularly for the frontal part of the wave.

(5) The method as developed can not take into account the instability and air entrainment effects in a conduit flowing nearly full.

(6) The second boundary condition at the upper end of the conduit (the first being the inflow hydrograph) in the supercritical flow, as a discharge-versus-depth relation, is assumed usually to be the normal depth relation. This approach may depart from actual physical conditions, which makes it difficult for computed waves to correspond with physical waves, at least at the upper sections of the conduit.

(7) Unavoidable inaccuracies in estimating junction box energy losses, particularly with the lower inlet position of laterals, result in significant differences between observed and computed flood hydrographs in storm drains.

(8) Though the method of characteristics with its specified intervals scheme may be improved by nonlinear interpolations of velocities and depths along the initial time t_j, when their values at time t_{j+1} must be computed, there is still a lack of information for determing whether the interpolation should be made through three or four points for the supercritical regime; there is also insufficient information for determing what advantage four-point interpolation can produce. This is a limitation in assessing the accuracy of results under the various conditions of nonlinear interpolations.

(9) The basic limitations in applying the proposed finite-difference scheme is related to the accuracy available in describing boundary and initial conditions. The better they are defined and the closer they are to the physical boundary and initial conditions, the more reliable are the numerical solutions.

9.3 Recommendations for Future Research.

Recommendations for further experimental research are given in more detail in subchapter 8.2 of Part III, Hydrology Paper No. 45; the potential of the developed facilities for further experimental investigations is given in subchapter 7.2 of Part II, Hydrology Paper No. 44. Recommendations for further studies of numerical integration schemes of complete differential equations of unsteady flow are given in subchapter 5.2 of Part IV, Hydrology Paper No. 46. Although recommendations in detail can be found as cited, general recommendations for future research are summarized as follows.

(1) The energy head losses of certain types of singularities, which occur in storm drains, should be investigated systematically. Such energy losses occur at various junction-box structures, boxes with various angles and diameters of joining drains, or boxes at which the direction and/or the slope of the main drain change, drop-structures for which there is a backwater effect of downstream reach on the upstream section during the peak flows, and similar types of structures along the storm drains. Of particular interest is the dissipation of additional turbulence created by the structures of concentrated energy losses along the immediate downstream section of storm drains.

(2) Investigation is necessary for the air-water interaction when the conduit flows nearly full; all instability phenomena in the passage from the free-surface flow to flow under pressure, or the opposite, should also be investigated. Because the drain dimensions are determined by the design flood hydrograph, and because the peak depth for that hydrograph should approximately coincide with the depth of the largest drain capacity in free-surface flow, which occurs in the depth range of relatively unstable flow, this air-water interaction has particular relevance to storm drain design.

(3) The peak depth of a well designed storm drain is largest immediately downstream of the junction box, or the peak depth is at the upper end of the conduit between the two junction boxes, if the flood hydrograph is in the attenuation regime. This is the case if the flow is with the Froude number approximately less than F=2. The second largest peak depth may be produced immediately upstream of the junction box because of the backwater produced by the energy loss at the junction box. The section downstream of the junction box is also subject to dissipation of surplus turbulence generated in the junction box; this is equivalent to additional roughness. Therefore, the critical design conditions are either in the conduit sections where both the instability of nearly full conduit flow of air-water interaction and the additional turbulence occur, or in the section where significant backwater effect occurs. These phenomena which greatly affect design conditions, need to be researched.

(4) Observations in the 3 ft diameter and 822 ft long conduit, containing both systematic and random observational and computational errors, were unable to throw light on the differences between analytical and physical free-surface conduit waves, with these differences resulting from the five hypotheses underlying the derivation of the continuity and momentum partial differential equations of gradually varied free-surface unsteady flow. This objective of studying effects of basic hypotheses should be pursued in future research with appropriate improvements in the accuracy of all observations and computations. Future research in gradually varied unsteady flow might be more relevant if the accuracy of solutions are determined rather than reworking in the new light fundamentals of the basic equations.

(5) New finite-difference schemes for integrating the quasi-linear hyperbolic partial differential equations are proposed from time to time. Thus, literature should be surveyed systematically for these various schemes; they should be then subjected to investigations, particularly if they concern stability, accuracy, versatility and flexibility of application, and economy of computer time.

REFERENCES

External References

1. Yevjevich, V. M., 1964, Bibliography and discussion of flood-routing methods and unsteady flow in channels, U.S. Geological Survey Water-Supply Paper 1690.

2. Courant, R. and Friedricks, W. R., 1948, Supersonic flow and shock waves, Interscience Publishers, New York.

3. Lister, M., 1960, The numerical solutions of hyperbolic partial differential equations by the method of characteristics in mathematical methods for digital computers, edited by A. Ralston and H. S. Wilf, John Wiley and Sons, pp. 165-179.

4. Ackers, P. and Harrison, A. J. M., 1963, The attenuation of flood waves in part-full pipes, Hydrualic Research Station, Wallingford, Berkshire, England, Report No. INT 31, December.

5. Ackers, P. and Harrison, A. J. M., 1964, The attenuation of flood waves in part-full pipes, Proceedings, Institute of Civil Engineers (London), Vol. 28, Paper No. 6777.

6. Henderson, F. M., 1964, Steady flow in sinusoidally varying channels, Hydraulics and Fluid Mechanics, R. Silvester (Editor), McMillan Company, New York, pp. 51-67.

7. Henderson, F. M., 1966, Open channel flow, McMillan Company, New York.

8. Harris, G. S., 1970, Real time routing of flood hydrographs in storm sewers, American Society of Civil Engineers, Journal of Hydraulics Division, paper 7327, HY6.

9. Chow, Ven Te, 1959, Open channel hydraulics, McGraw-Hill Book Company, New York.

Internal References

From the Project Reports and Theses

1. Yevjevich, V. M., June 1961, "Unsteady Free Surface Flow in a Storm Drain" - General and Analytical Study. Report for the U.S. Bureau of Public Roads, Eng. Research Center, Colorado State University. CER61-VMY38

2. Barnes, A. H., August 1965, "Predictability of Free-Surface Profiles for Steady Non-uniform Flow in a Circular Cross-section," Ph.D. dissertation, Dept. of Civil Eng., Colorado State University.

3. Frye, W. B., June 1966, "A Development of a Numerical Solution to a System of Partial Differential Equations," M.S. Thesis - Dept. of Mathematics, Colorado State University.

4. Lorah, W. L., June 1966, "Free-Surface Flow Energy Losses in a 90° Junction Box," M.S. Thesis, Dept. of Civil Eng., Colorado State University.

5. Yevjevich, V. M. and Barnes, A. H., August 1966, "Hydraulic Roughness of Free-Surface Flow in a Smooth Steel Pipe," Report for U.S. Bureau of Public Roads, Eng. Research Center, Colorado State University.

6. Pinkayan, S., Sept., 1966, "Solution of the Unsteady Free Surface Flow in a Storm Drain by the Method of Characteristics," Report for U.S. Bureau of Public Roads, Eng. Research Center, Colorado State University. CER66-SP29

7. Barnes, A. H., October 1966, "Velocity Distribution Factors in a Circular Cross-section," Report of U.S. Bureau of Public Roads, Eng. Research Center, Colorado State University.

8. Pinkayan, S. and Barnes, A. H., Feb. 1967, "Unsteady Free-Surface Flow in a Storm Drain with Lateral Inflows," Report for U.S. Bureau of Public Roads, Eng. Research Center, Colorado State University.

9. Mitchell, J. S., March 1967, "Comparison of Mathematical versus Experimental Flood Wave Attenuation in Part-Full Pipes II," Report for U.S. Bureau of Public Roads, Eng. Research Center, Colorado State University.

10. Mitchell, J. S., April 1967, "Comparison of Mathematical versus Experimental Flood Wave Attenuation in Part-Full Pipes," M.S. Thesis, Dept. of Civil Eng., Colorado State University, also Report for U.S. Bureau of Public Roads.

11. Futrakul, S., June 1967, "Flood Routing in a Circular Section," M.S. Thesis, Dept. of Civil Eng., Colorado State University.

12. Safai, J., May 1968, "Non-dimensional Analysis of Attenuation of Flood Waves in Partly Full Circular Conduits," Report for U.S. Bureau of Public Roads, Eng. Research Center, Colorado State University. CER67-68JS8

13. Barnes, A. H., June 1969, "Unsteady Flow in a Storm Drainage System, Part A - Theory and Error Considerations," Report for U.S. Bureau of Public Roads, Eng. Research Center, Colorado State University. CER69-70AB1

14. Barnes, A. H., January 1970, "Unsteady Flow in a Storm Drainage System, Part B - Hydraulic Parameters, Boundary and Initial Conditions," Report for U.S. Bureau of Public Roads, Eng. Research Center, Colorado State University. CER69-70AB1

APPENDIX 1

Description of Research Project

UNSTEADY FLOW IN A STORM DRAIN

Part One

THE BROAD PROBLEM

Construction of highways in urban areas (and sometimes elsewhere) requires disposal of storm water by means of underground storm drains because property values and other considerations prohibit carrying storm water in open channels. These systems frequently include picking up storm water contributed by areas outside the right-of-way. The usual design procedure is to compute sizes of pipe by the so-called "rational method." When the highway is depressed the highway department usually attempts to exclude all water falling outside of the depressed section so that the size of the system collecting water for the highway itself (and usually requiring pumping) will be a minimum.

Storm drains for depressed highways sometimes are miles in length (West Route in Chicago for example is about six miles) this producing a watershed that is very long in relation to its width. There is good reason to doubt that the rational method is reliable in such a case, (nor for that matter has the rational method been scientifically proved in any case). A flood-routing procedure beginning with routing of overland flow to inlets is generally conceded to be the logical approach especially since digital computers would permit investigation of various storm patterns both as to time and areal distribution in testing the probable functioning of a given system and indicated modifications. Such a procedure would make it possible to know where every cubic foot of water was at any time so that opportunities for temporary storage reducing the peak load could be investigated. Major economies in initial cost might result and are worthwhile exploring since the usual storm-drain system for a depressed highway will cost around $500,000 per mile.

To my knowledge no one has developed a procedure for routing storm water through a storm drain by any except grossly approximate methods.

The problem then is to study the hydrodynamics of unsteady flow in storm drains with the objective of developing a sound procedure adopted to a digital computer, verifying the procedure by hydraulic model tests and field measurements as may seem necessary. The ultimate purpose is to provide a working design method applicable to any situation where storm drains are used for removal of storm water. However, there are many variations possible in the physical set-up as will be shown in the following paragraphs.

Part Two

AN OUTLINE OF THE FACTORS INVOLVED IN THE HYDRODYNAMICS ANALYSIS

The inflow hydrographs to the storm-drain system will not be considered as part of the hydrodynamics of the storm drain as that is a separate problem. It can be assumed that methods of computing inflow hydrographs will be provided. The system will also be assumed to consist of a single continuous line of pipe with inflow from inlets, or from laterals collecting flow from a series of inlets all located on the highway right-of-way. The right-of-way may include large interchange areas in which case lateral inflow may be substantial in relation to flow in the main drain and conceivably may be large enough to require analysis as a system by itself. For purpose of analysis it may be assumed that flow entering system at any point will have no momentum in the direction of the outflow pipe.

Conduit may be circular or of any shape commonly used, either precast or monolithic concrete, generally will increase in size in downstream direction, changes in size being made at manholes open to atmospheric pressure, and crown-lines will match up except in case where a drop manhole occurs. The latter would be equi-equivalent to a free outlet for system upstream. In large drains especially those of monolithic construction, conduit may be continuous with manhole rising at one side in which case transitions will be used for changes in size.

The slope of the main drain will change usually with breaks at manholes but could be constructed on a vertical curve. Slopes may be subcritical or supercritical and can be very steep, slopes of 3-5% sometimes occurring in main drains. The latter may produce augmented rates of discharge. A single line may involve a wide range of slopes, the usual situation involving steep slopes on upstream reaches becoming mild on downstream end. A break to a steeper slope, however, is also possible.

Alignment commonly will be straight or with relatively small deflections at manholes. Curved alignment is possible but rare. As a rule the main drain will not involve abrupt changes in direction such as 90^0 except at a connection to existing interceptor which case should be given special treatment which is beyond the scope of this problem.

Design criteria ordinarily provide that conduit will not flow under pressure for the design storm. But it should be possible to compute what will happen in the main drain when any part does flow full. Outflow may be either free, or subject to back pressure from stream or conduit into which drain discharges, or from water in wet well of a pumping station. In the latter case flow may be subject to surges created by sudden stoppage of pumps due to power failure.

Manholes are commonly constructed either round or square with or without a stream-lined invert conforming to invert of conduit; section through manhole normal to direction of flow will be as large or larger than cross section of conduit. Common practice is to bring all laterals in at manholes and may be at any elevation at or above flow line of main drain. The laterals for individual inlets are brought increasingly in a a T or Y connection (inflow from one inlet is usually so small relative to flow in main drain that momentum in downstream direction may be neglected).

Inflow hydrographs may have a single peak, or more than one peak. A situation will also occur where a second storm follows so closely after the first that only a part of the volume from the first storm will have been discharged from the system, when the inflow from the second storm begins.

Part Three

LIMITATIONS OF ANALYTICAL STUDY FOR THE FIRST YEAR

The numerous possible variations in boundary conditions, inflow hydrographs, and outlet conditions require that the analytical study contemplated for the first year be limited so that initial solution for the more simple cases will be possible.

During the first year the study will be limited to hydrodynamic analysis of a single storm drain on straight alignment with single-peak hydrographs (not necessarily identical) introduced at discrete points along the line, and a free outlet.

The conduit shall be considered to be circular in cross section (other cross sections may be introduced if feasible), changing in size at manholes, with crown lines matched up and changes in slope at manholes but not necessarily at every manhole.

The conduit shall be considered to be smooth concrete with resistance factor Darch-Weisbach "f" varying as a function of the Reynolds Number of the flow in accordance with latest results from full-scale tests made for the Florida State Road Department and Public Roads at the St. Anthony Falls Hydraulic Laboratory. In the event this requirement complicates the solution unduly, then an average value of "f" for each size may be used.

Only the case of free-water surface at atmospheric pressure is to be studied initially. Flows as introduced to line shall be considered to have no momentum in direction of outflow line. Both subcritical and supercritical slopes shall be studied but not as steep as to augment the rate of discharge. Disturbances created by discontinuity of boundary at manholes shall be given consideration based on assumption that manhole is an abrupt enlargement over entire periphery of conduit except at flow line and distance across manhole in direction of flow is not more than three pipe diameters.

The hydrodynamic analysis shall be made having in mind conversion of the results to solution by a digital computer. The contract will provide for employment of a consultant on machine computation to assist in that development. It is hoped that the end result will be a program whereby the outflow hydrograph for the simple case herein described may be printed out for any set of inflow hydrographs which do not cause the line to flow under pressure at any point (i.e. to flow full).

The analysis is quite likely to require experimental verification and establishment of certain constants by empirical tests. The study should outline the tests and how they should be made, but no experimental work is to be included under the intital contract.

Carl F. Izzard, Chief
Div. of Hydraulic Research
U.S. Bureau of Public Roads

August 1960
Washington 25, D.C.

APPENDIX 2

GENERAL REFERENCES ON FREE-SURFACE UNSTEADY FLOW

This general list of references follows closely the method of annotation given in the "Bibliography and Discussion of Flood-Routing and Unsteady Flow in Channels," U. S. Geological Survey Water-Supply Paper 1690, U. S. Government Printing Office, Washington, D. C., 1964 (prepared by V. Yevjevich).

References on subjects devoted to the general theory of wave motion in channels as well as references describing practical methods and procedures for flood routing are included. Only references which are not included in the above mentioned bibliography are given in the following list, mainly containing the works produced or published during the decade 1960-1969.

The list comprises references to papers that are original reprints of studies made, and also references to papers that are restatements, summarizing the results of previous studies. No abstract of 145 references is given in this list. The list gives references in the chronological sequence by years, and within a particular year the sequence of references is by author's name, in alphabetical order. Thus arranged, references have been numbered consecutively. Each reference can therefore be identified by its number, author or authors, and year of publication. No index by authors or by subjects is provided. The coverage of years 1968-1970 is not as complete as is for the previous years.

BIBLIOGRAPHY

1. Hayashi, T., Nougaro, J., 1959, (in French), Sur la similitude des régimes non-permanents dans les canaux découverts (On the similutude of unsteady flow regimes in open channels): Comptes rendus de l'Academie des Sciences (Paris), Sept.

2. Mongiardini, V., 1959, (in Italian), La popagazione delle onde di traslazione nelle deviazioni curvilinee e rettilinee dei canali (Propagation of translation waves in the straight and curvilinear deviations of channels): L'Acqua, nos. 4-5, year XXXVII, July-August, September-October.

3. Pezzoli, G., 1959, (in Italian), L'attenuazione delle onde negli alvei a fondo orizontale (Waves attenuation in channels with the horizontal bed): VI Convegno di idraulica e construzioni idrauliche, Padova, (VIth Congress of Hydraulics and Hydraulic Structures, Padua), 25-27 May 1959, pp. 1-5.

4. Bata, G., 1960, (in Serbo-Croatian), Prolazak poplavnih talasa u prirodnim koritima (Propagation of flood waves in natural channels): Saopstenja, Hidrotehnicki Institut, Beograd (Yugoslavia), no. 20-21.

5. Kartvelishvili, N. A., 1960, (in Russian), Kolebaniya urovnya nizhnego byefa v stvore GES pri sutochnom regulirovanii (The fluctuations of tailrace level at a hydroelectric power station due to daily regulations): Gidrotekhnicheskoe Stroitel'stvo, no. 11, p. 45-47.

6. Keller, H. B., Levine, D. A., Whitham, G. B., 1960, Motion of a bore on a sloping beach: Journal of Fluid Mechanics, no. 7, pp. 302-316.

7. Moklyak, V. I., 1960, (in Ukrainian), Do osnov razrakhunku neustalenogo rukhu vodi u vidkritikh ruslakh (On the fundamentals of computation of unsteady water flow in open channels): Izvestiya Instituta Akad. Nauk Ukrainskoy S.S.R., tom 16, p. 68-78.

8. Montuori, C., 1960, (in Italian), Immissione di una portata constante in un canale vuoto (Inflow of a constant discharge in an empty canal): Atti Fondazione Politecnica del Mezzogiorno, vol. V.

9. Obrezkov, V.I., 1960, (in Russian), Opyt primeneniya sredstv vychislitel'noy tekhniki dlya raschota neustanovivshegosya dvizheniya v nizhnem byefe GES (Experiment with the application of means of computational technique for the computation of unsteady motion in the tailrace canal of a hydroelectric power station): Gidrotekhnicheskoe Stroitel'stvo, no. 3, p. 32-36.

10. Phillips, O.M., 1960, On the dynamics of unsteady gravity waves of finite amplitude, Part I, The elementary interaction: Journal of Fluid Mechanics, vol. 9, part 2, October.

11. U.S. Army Corps of Engineers, 1960, Routing of floods through river channels: U.S. Army Corps of Eng., Manual Em1110-2-1408, March.

12. U.S. Army Corps of Engrs., 1960, Flood resulting from suddenly breached dams, Miscellaneous papers no. 2-374, report 1, Feb., Smooth Channel.

13. Bird, G.A., 1961, The motion of a shock-wave through a region of non-uniform density: Journal of Fluid Mechanics, vol. 11, part 2, September, pp. 180-208.

14. Bock, H., 1961, Problems arising from surge and suction waves caused by a sudden shut-down of a turbine: Permanent International Assoc., 20th International Congress on Navigation, Baltimore, U.S.A., (Interior navigation, Section I, subject 2, 1961).

15. Chen, T.C., 1961, Experimental study on the solitary wave reflection along a straight sloped wall at oblique angle of incidence: Department of the Army, Beach Erosion Board (U.S.A.), Technical memorandum No. R4, March.

16. Glukhovskij, B. Kh., 1961, (in Russian), Study of wave attenuation with depth by correlation analysis: Meteorologiya i Gidrologiya (U.S.S.R), no. 11, pp. 22-30.

17. Hughes, B.A., Stewart, R.W., 1961, Interaction between gravity waves and a shear flow: Journal of Fluid Mechanics, vol. 10, part 3, May.

18. Hunt, J.N., 1961, (in French), Les ondes interfaciales d'amplitude finie (Interfacial waves of finite amplitude): La Houille Blanch (France), no. 4, pp. 515-531, August-September.

19. Johnson, J.W., 1961, Deficiencies in research on gravity surface waves: Council on Wave Research, U.S.A.

20. Kartvelishvili, N.A., 1961, (in Russian), The present state of the hydraulic theory of unsteady flow resulting from research in U.S.S.R.: Isvestiya Akademii Nauk, Mekhanika i Mashinostroyeniye, U.S.S.R.

21. Longuet-Higgins, M.S., Stewart, R.W., 1961, The changes in amplitude of short gravity waves on steady non-uniform currents: Journal of Fluid Mechanics, vol. 10, part 4, June.

22. Mongiardini, V., 1961, (in Italian), Considerazioni sulle soluzioni analitiche del movimento ondoso stazionario (Considerations on the analytical solutions of the stationary wave movement): L'Energia Elettrica, fasc. 5.

23. Starosolszky, O., 1961, (in Hungarian), A hullamzas hidraulikaja (Hydraulics of waves): Visügyi Közlemenyek (Hungary), No. 3, pp. 293-312.

24. Ursell, F., 1961, The transmission of surface waves under surface obstacles: Proceedings of the Cambridge Philosophical Society (England) vol. 57, part 3, pp. 638-668, July.

25. U.S. Army Corps of Engineers, 1961, Flood resulting from suddenly breached dams: Miscellaneous Paper No. 2-374, report No. 2, Rough Channel.

26. Escoffier, F.F., Boyd, M.B., 1962, Stability aspects of flow in open channels: Proceedings A.S.C.E., vol 88, no. HY6, November.

27. Fox, L., 1962, Numerical solutions of ordinary partial differential equations: Addison-Wesley Publishing Co., Inc., Reading, Mass.

28. Gary, J., 1962, On certain finite difference schemes for the equations of hydrodynamics: AEC Computing and Applied Mathematics Center, Paper NYO-9188, March.

29. Grushevsky, M.S., 1962, (In Russian), The use of an electronic digital computer for computing unsteady flow in a prismatic channel: Transactions the U.S.S.R. State Hydrologic Institute, No. 94, pp. 136-183.

30. Kovalenko, E.P., 1962, (In Russian) Computation of unsteady flow in channels: Gidrotekhnicheskoye Stroitel'stvo, U.S.S.R., No. 3, pp. 31-32.

31. Lillevang, O.J., 1962, Mean direction of waves and wave energy: Trans. A.S.C.E., vol. 127, part IV, pp. 193-220.

32. Miles, J.W., 1962, On the generation of surface waves by shear flows: Journal of Fluid Mechanics (England), vol. 13, part 3, pp. 433-448, July.

33. Rybka, V.G., 1962, (Original in Russian), Investigation of the forms of flood waves of rain caused floods in the Prut and Stryy Rivers: Soviet Hydrology Selected Papers, American Geophysical Union, No. 4.

34. Sandover, J.A., 1962, Cnoidal waves and bores: La Houille Blanche, vol. 17, no. 3, pp. 443-455, July-Aug.

35. Shinbrot, M., 1962, Waves in shallow water: Archive for Rational Mechanics and Analysis (Germany), vol. 9, no. 3, pp. 234-244, January.

36. Tammekivi, W., 1962, Evaluation of methods of flood routing in open channels: Northwestern University, M.S. Thesis, Evanston, Illinois.

37. Wackernagel, A., 1962, Computation of flood waves from dam breaches: Schweiz. Bauzeitung, v. 80, no. 22, pp. 370-373, May.

38. Abbott, M.B., 1963, The solution of wave propagation problems using an iterative operator: La Houille Blanche, No. 5, pp. 513-524, Aug-Sept.

39. Bledermann, R., 1963, (In German), Numerical approximate procedures for the computation of reservoir emptying (Two-dimensional flow patterns): Mitteilungen der Versuchsanstalt Fuer Wasserbau and Erdbau and der Eidgenoessischen Technischen Hochschule in Zunich, no. 61, 89 p.

40. Cunge, J.A., Wegner, M., 1963, (In French), Intégration numérique des équations d'écoulement de Barré de St. Venant par un schéma implicite de différences finies (Numerical integration of Barré de St. Venant equations by an implicit finite-difference scheme): Sogreah, Grenoble, France, NT. 1073, Sept.

41. Faure, J., Nahas, N., 1963, (in French), Deux problèmes de mouvements non-permanents à surface libre resolus sur ordinateur électronique: Centre de Recherches et d'Essais de Châtou, Department Mécanique des Fluides, HF/3/E307, p. 37, Châtou, France.

42. Gary, J., 1963, Some implicit finite difference schemes for hyperbolic systems: New York University, Courant Institute of Mathematical Sciences, paper NYO-10426, March.

43. Henderson, F.M., 1963, Flood waves in prismatic channels: Proceedings ASCE, vol. 89, Hydraulic Division, no. HY4, part 1, paper 3568, p. 39, July.

44. Kalinin, G.P., Kuchment, L.S., 1963, (in Russian) O chislennykh metodakh resheniya uravneniy Sen-Venana dlya rashota neustanovivshegosya dvizheniya vody v rekakh (On the numerical solution methods of De Saint-Venant equations for the computation of unsteady water flow in rivers): Meteorologiya i Gidrologiya, U.S.S.R. (Meterology and Hydrology Journal), no. 6, p. 3-9.

45. Rantz, S.E., 1963, An empirical method of determining momentary discharge of tide-affected streams: U.S. Geological Survey Water-Supply Paper 1586-D.

46. Richtmyer, D., 1963, A survey of difference methods for non-steady fluid dynamics: National Center for Atmospheric Research, NCAR, Technical Notes 63-2.

47. Schnoor, E., 1963, (In German), Berechnung der Tidewelle in beliebig verzweigten Stromsystemen vermittels des differenzenverfahrens (Computation of tide wave in any branching stream system by the finite-difference schemes): Der Bauingenieur, no. 11, pp. 426-430, November.

48. Shipley, A.M., 1963, On measuring long waves with a tide gauge: Deutsche Hydrographische Zeitschrift, no. 3, pp. 136-140.

49. Simon, A.L., 1963, Travel time of waves in backwaters: A.S.C.E. Proceedings, Journal of the Hydraulics Division, vol. 89, no. HY6, pp. 1-13, November.

50. Supino, Giulio, 1963, (In Italian), Propagazione ondoze nei canali a marea, (Wave propagation in tidal channels): Accademia Nazionale dei Lincei, Class Physical, Mathematical and Natural Sciences; Nota I (Note I), ser. VIII, vol. XXXIV, fasc. 3 and 4, pp. 230-231; Nota II (Note II), p. 345-351.

51. Sveishi, T., 1963, Runoff estimation in storm sewer system using equivalent roughness: Japan Society of Civil Engineers, Trans. no. 91, pp. 41-54, March.

52. Vasyliev, O.F., Godunov, S.K., Pritvits, N.A., Temnoeva, T.A., Fryazinova, I.L. and Shugrin, S.M., 1963, (In Russian), Chislennyy metod raschota rasprostranyeniya dlinnykh voln v otkrytykh ruslakh i prilozhenie evo k zadache o povodke (Numerical method of computation of long wave movement in open channels and its contribution to problems of floods): Doklady Akademii Nauk USSR, (Transactions of USSR. Academy of Sciences), v. 151, no.3 pp. 525-527.

53. Zheleznyak, I.A., 1963, (In Russian), Uproshchenyy raschot dvizheniya volny popuska v nizhnem byefe GES po krivym obyom (A simplified computation of wave release movement in the tail-race canals of hydroelectric power plant by the volume curves): Meteorologiya i Gidrologiya, U.S.S.R., no. 3, p. 36-42.

54. Ackers, P. and Harrison, J.A.M., 1964, Attenuation of flood waves in part-full pipes: proceedings Institution of Civil Engineers, London, vol. 28, pp. 361-382, July. Also the same title: Dept. of Scientific and Industrial Research Hydraulics Research Station, Wallingford, Berkshire, England, report no. INT31, December 1963.

55. Amein, M., 1964, Bore inception and propagation by nonlinear wave theory: Proceedings of 9th Conference on Coastal Engineering, Lisbonne, June 1964, pp. 70-81.

56. Balek, J., 1964, (in Slovakian), Vypocty charakteristik povodnovych vin (Computation of wave characteristics): Vodohospodarsky Časopis, no. 2, pp. 137-160, with English summary, p. 159.

57. Bretherton, F.P., 1964, Resonant interactions between waves. The case of discrete oscillations: Journal of Fluid Mechanics, vol. 20, part 3, pp. 457-479, November.

58. Cunge, J.A., Wegner, M., 1964, (In French). Intégration numériques des équations d'écoulement de Barré de Saint-Venant par un schéma implicite de différences finies. Application au cas d'une galérie tantôt en charge tantôt à surface libre (Numerical integration of Barré de Saint-Venant's flow equations by means of an implicite scheme of finite differences. Application to the case of alternately free and pressurized flow in a tunnel): La Houille Blanche, pp. 33-39, Jan.-Feb.

59. Daubert, A., 1964, (In French), Quelques aspects de la propagation des crues (Some aspects of flood routing): La Houille Blanche, no. 3, pp. 341-346, May-June.

60. Dronkers, J.J., 1964, Tidal computations: John Wiley and Sons, Inc., New York.

61. Freeman, J.C., LeMéhauté, B., 1964, Wave breakers on a beach and surges on a dry bed: Proceedings A.S.C.E., vol. 90, no. HY2, part 1, pp. 187-216, March, (Discussion Nov. 1964).

62. Grushevskiy, M.S., 1964, (Original in Russian), The effect of flood plains on the flattening of waves of discharge releases, (according to observational data of GGI for Tvertsa River): Soviet Hydrology Selected Papers, no. 6, 1964, American Geophysical Union, pp. 579-586.

63. Higgins, R.V., Boley, D.W., Leighton, A.J., 1964, Aids to forecasting the performance of water floods: Journal of Petrol Technol., U.S.A., vol. 16, no. 9, pp. 1076-1082, September.

64. Koshcheyev, A.N., 1964, (In Russian), Calculation of long waves on continental bodies of water: Transaction of the U.S.S.R. State Hydrologic Institute, Trudy GGI, no. 113, pp. 36-81.

65. Masch, F.D., 1964, Cnoidal waves in shallow water: Proceedings of the 9th Conference on Coastal Engineering, Lisbonne, pp. 1-22, June.

66. Nougaro, J., Castex, L., Bacquie, S., 1964, (In French), Influence d'une vallée lateral sur la propagation de l'onde de rupture d'un barrage (Effect of a lateral valley on the propagation of wave due to a dam breach): Comtes rendus de l'Academie des Sciences (France), tome 259, no. 16, pp. 2596-2598, 19 Octobre.

67. Ribeny, F.M.J., 1964, Flood routing with a unit hydrograph approach: The Journal of the Instituion of Engineer (Australia), vol. 36, no. 1-2, pp. 9-22, January and February.

68. Thirriot, C., Bednarczyk, S., 1964, (In French), Ondulations secondaires en front d'intumescences et ondes solitaires (Secondary oscillations in front of waves and solitary waves): La Houille Blanche, no. 8, pp. 879-888, December.

69. Williams, J.A., 1964, A non-linear problem in surface water waves: University of California Hydraulic Engineering Laboratory, techn. rep. no. HEL 1-5, p. 245, October.

70. Arnborg, L., 1965, Unsteady flows in open channels: IAHR 11th International Congress, Leningrad, September.

71. Brakensiek, D.L., Comer, G.H., 1965, Re-examination of flood routing method comparison: Journal of Hydrology, Amsterdam, Netherlands, no. 3-4, pp. 225-230, Nov.

72. Bramble, J.H., 1965, Numerical solutions of partial differential equations (Flood waves in rivers): Academic Press, pp. 42-49.

73. Cioc, D., Amaftiesci, R., Finkelstein, A., 1965, (In French), Sur le mouvement non-permanent avec discontinuité dans une galéries de fuite (On the unsteady flow with a discontinuity in the tail-race galery): IAHR 11th International Congress, Leningrad, September.

74. Escoffier, F.F., 1965, Routing flood waves apalachicola River: IAHR 11th International Congress, Leningrad, September.

75. Escande, L., Nougaro, J., Castex, L., Bacquie, S., 1965, Propagation d'une onde de crue subite a la suite de l'effacement d'un barrage (Propagation of flood wave created by dam breach): IAHR 11th International Congress, Leningrad, September.

76. Ghambarian, H.H., 1965, On waves in inclined open channels: IAHR 11th International Congress, Leningrad, vol. 1(11), pp. 1-10, September. .

77. Harlow, F.H., Shannon, J.P., Welch, J.E., 1965, Liquid waves by computer: AAAS, Science, vol. 149, no. 3688, September.

78. Hayashi, T., 1965, Propagation and deformation of flood waves in natural channels: IAHR 11th International Congress, Leningrad, vol. 1 (1-12), pp. 1-7, September.

79. Ito, T., 1965, Study on flood waves by analog computer: IAHR 11th International Congress, Leningrad, vol. 3 (3-39), pp. 1-6, September.

80. Krivoshey, M.I., 1965, (Original in Russian), Review of laboratory investigations of unsteady movement of water in open channels: Soviet Hydrology Selected Papers, American Geophysical Union, no. 1, pp. 12-20.

81. Lai, C., 1965, Flows of homogeneous density in tidal reaches - Solution by the implicit method: U.S. Geological Survey, Open-File Report, Washington, D.C.

82. Lean, G. H., 1965, A particular case of steady wave propagation along a parallel-sided open channel: IAHR Journal of Hydraulic Research (Netherland), vol. 3, no. 1, pp. 2829-2838.

83. Levin, L., 1965, (In French), Calcul approché de mouvement non-permanent avec oscillations secondaires dòns les canaux trapézoidaux (Approximate computation of unsteady flow with the secondary oscillations in the trapezoidal channels): IAHR 11th International Congress, Leningrad, September.

84. Levy, I.R., 1965, (In French), Mouvement non-permanent dans les lits instables (Unsteady flow in instable channels): IAHR 11th International Congress, Leningrad, vol. 3 (3-41), pp. 1-8, September.

85. Meijer, J.G.P., Vreugdenhil, C.B., DeVries, M., 1965, A method of computation for non-stationary flow in open-channel networks: Hydraulics Laboratory, Delft, Netherlands, pub. no. 34, September.

86. Moklyak, V.I., 1965, (Original in Russian), On the calculation of movement of release wave: Transaction of the State Hydrologic Institute (U.S.S.R.), Trudy GGI, no. 125.

87. Montuori, C., 1965, (In French), Introduction d'un débit constant dans un canal vide (Inflow of a constant flow in an empty canal): IAHR 11th Congress, Leningrad, September.

88. Morgali, J.R., Linsley, R.K., 1965, Computer analysis of overland flow: Proceedings ASCE, vol. 91, HY3, pp. 81-100, May.

89. Newman, J.N., 1965, Propagation of water waves past long two-dimensional obstacles: Journal of Fluid Mechanics, (England), vol. 23, part 1, pp. 23-29.

90. Novak, P., 1965, Model research on flood waves passing through a series of reservoirs and a river channel: IAHR 11th International Congress, Leningrad, vol. 3 (3-27), pp. 1-5, September.

91. Puzanov, A., 1965, Velocity and pressure distribution in plane positive surges: IAHR 11th International Congress, Leningrad, September.

92. Quick, M.C., 1965, River flood flows, Forecasts and probabilities: Proceedings ASCE, vol. 91, no. HY3, pp. 1-8, May.

93. Riquois, R., and Ract-Madoux, X., 1965, (In French), Intumescences observées sur le canal d'amenée de la chute d'Oraison lors des variations rapides de charge (Waves observed in a head-race canal of the cascade d'Oraison, during a rapid variation of flow): IAHR 11th International Congress, Leningrad, September.

94. Rozovsky, I.L., Yeremenko, E.V., Shabrin, A.N., and Vlasenko, Y.D., 1965, Experimental investigations of unsteady motion in open channels of rectangular cross-section rectilinear and curvilinear in the plan: IAHR 11th International Congress, Leningrad, September.

95. Rzhanitzin, N.A., Rabkova, E.K., 1965, Kinematics of a stream and channel deformations in the lower reaches of hydro-projects at the daily regulation: IAHR 11th International Congress, Leningrad, September.

96. Starosolczky, O., 1965, (In French), Surge waves in the vicinity of hydroelectric power plants: IAHR 11th International Congress, Leningrad, September.

97. Strelkoff, T., Amorocho, J., 1965, Gradually varied unsteady flow in a controlled canal system: IAHR 11th International Congress, Leningrad, September.

98. Szigyarto, Z., 1965, A new method for calculating discharge wave profiles: IAHR 11th International Congress, Leningrad, September.

99. Thirriot C., Bednarczyk, S., 1965 (In French), Considération sur les ondulations secondaires en front d'intumescences dans les canaux découvertes (Note on the secondary undulations in front of open channel waves): IAHR 11th International Congress, Leningrad, September.

100. Varley, E., Cumberbatch, E., 1965, Non-linear theory of wave-front propagation: Journal of Institute of Mathematics and its Applications (England), vol. 1, no. 2, pp. 101-112, June.

101. Vasyliev, O.F., Gladyshev, M.T., Pritvits, N.A. and Sudobicher, V.G., 1965, Numerical methods for the calculation of shock wave propagation in open channels: IAHR 11th International Congress, Leningrad, September.

102. Vasyliev, O.F., Temnoeva, T.A., and Shugrin, S.M. 1965, (In Russian), Chislennyy metod raschota neustanovivshikhsya techeniy v otkrytykh ruslakh (Numerical computational method of unsteady flow in open channels): Izvestiya Akademii nauk SSSR, Mekhanika (Proceedings of the U.S.S.R. Academy of Sciences, Section Mechanics), no. 2, pp. 17-25.

103. Yamada, H., Okabe, J., 1965, On the resonance effect in a storm surge (Parts I and II): Bulletin of the Disaster Prevention Research Institute, Kyoto University, Japan, vol. 15.

104. Yevjevich, V.M., 1965, Rate of change of the peak for floods progressing along a channel: IAHR 11th International Congress, Leningrad, September.

105. Zierep, J., Heynatz, J.Th., 1965, (In German), Ein analitisches Verfahren zur Berechnung der nichtlinearen Wellenausbreitung (An analytic method for computation of non-linear wave propagation): Zeitschrift fuer angewandte Mathematik and Mechanik, (Germany), vol. 45, no. 1, pp. 37-46.

106. Amein, M., 1966, Streamflow routing on computer by characteristics: Journal of Water Resources Research (U.S.A.), vol. 2, no. 1, pp. 123-130.

107. Cunge, J.A., 1966, (In French), Comparaison des résultats des essais d'intumescences effectués sur le modèle reduit et sur le modèle mathématique sur canal Oraison- Manosque (Comparison of results of wave experiments on a reduced model and the mathematical model of the canal Oraison-Manosque): La Houille Blanche, no. 1.

108. Evangelisti, G., 1966, On the numerical solution of the equations of propagation by the method of characteristics: Meccanica, Journal of the Italian Association of Theoretical and Applied Mechanics, no. 1-2, Tamburini Editor, Milano.

109. Liggett, J.A., Graf, W. H., 1966, Steady and unsteady effects on discharge in a river connecting two reservoirs: Great Lakes Research Division, pub. no. 15, University of Michigan.

110. Lister, M., 1966, Numerical solution of hyperbolic partial differential equations by the method of characteristics: Mathematical Methods for Digital Computers by Anthony Ralston and Herber S. Wilf, pp. 165-179, John Wiley and Sons, Inc. Publishers, ninth printing, July.

111. Pezzoli, G., 1966, Non-linear mechanics of translatory waves in channels: Meccanica, Journal of Italian Association of Theoretical and Applied Mechanics, No. 1-2, Tamburini Editor, Milano.

112. Welch, E.J., 1966, Computer simulation of water waves: Datamation, vol. 12, no. 1, pp. 41-47, November.

113. Wood, D.J., Dorsch, R.G., Lightner, C., 1966, Wave-plan analysis of unsteady flow in closed conduits: ASCE Journal of Hydraulics Division, vol. 92, no. HY2, pp. 83-110, March.

114. Abbott, M.B., 1967, An Introduction to the Method of Characteristics: American Elsevier Publishing Co., Inc., New York.

115. Abbott, M.B., Ionescu, F., 1967, On the numerical computation of nearly horizontal flows; IAHR, Journal of Hydraulic Research, vol. 5, no. 2.

116. Anonymous, 1967, Mathematical model of Mekong River Delta-Descriptive and Operating Manual: United Nations Educational Scientific and Cultural Organization.

117. Barnes, A.H., 1967, Comparison of computed and observed flood routing in a circular section: Proceedings, International Hydrology Sumposium, Fort Collins, Colorado, September.

118. Dooge, J.C., Harley, B.M, 1967, Linear routing in uniform open channels: Proceedings International Hydrology Sumposium, Fort Collins, Colorado, Sept. 6-8, pp. 1-8.

119. Dracos, T.A., Glenne, B., 1967, Stability criteria for open-channel flow: Proc. ASCE, vol. 93, No. HY6, November.

120. Fletcher, A. G., Wallis, S., Hamilton, W. S., 1967, Flood routing in an irregular channel: Proc. ASCE, vol. 93, no. EM3, pp. 45-62, June.

121. Lai, C., 1967, Computation of transient flows in rivers and estuaries by the multiple-reach method of characteristics: Geological Survey Research 1967, U.S. Geological Survey Prof. Paper 575-D, PD273-D280.

122. Laitone, E.V., 1967, Shallow water waves in canals of variable section: ASCE, Journal of Waterways and Harbors Division, May, WW2, paper No. 5246, p. 237.

123. Liggett, J.A., Woolhiser, D.A., 1967, Difference solutions of the shallow-water equation: Proc. ASCE, vol. 93, no. EM2, Paper 5189, April.

124. Liggett, J.A., Woolhiser, D.A., 1967, The use of the shallow water equations in runoff computation: Proc. 3rd Annual American Water Resources Conference, San Francisco, November 8-10.

125. Streeter, V. L., Wylie, E.B., 1967, Hydraulic Transients: McGraw-Hill Book Co., New York.

126. Woolhiser, D.A., Liggett, J.A., 1967, Unsteady one-dimensional flow over a plane-The rising hydrograph: Journal of Water Resources Research, vol. 3, no. 3.

127. Baltzer, R.A., Chintu, Lai, 1968, Computer simulation of unsteady flows in waterways; Proc. ASCE, vol. 94, HY4, paper 6048, July.

128. Liggett, J.A., 1968, Mathematical flow determination in open channels: Proc. ASCE, vol. 94, EM4, paper 6078, August.

129. Miller, R.L., 1968, Experimental determination of run-up of undular and fully developed bores: Jour. of Geo. Research, vol. 73, no. 14, July 15, p. 4497-4510.

130. Peregrine, D.H., 1968, Long waves in a uniform channel of arbitrary cross-section: Journal of Fluid Mechanics (England), vol. 32, part 2, pp. 353-365, May.

131. Balloffet, A., 1969, One-dimensional analysis of floods and tides in open channels: Proc. ASCE, vol. 95, HY4, paper 6695, pp. 1429-1451, July.

132. Chervet, A., Dallèves, P., 1969, (In French), Calcul sur ordinateur d'écoulements instationaires dans des canaux découverts (Computer calculations of the nonstationary flow in open channels): IAHR 13th International Congress, Kyoto, Japan, 1969, vol. 1, pp. 259-266.

133. DiSilvio, G., 1969, Flood wave modification along prismatic channels: Proc. ASCE, vol. 95, HY5, paper 6777, pp. 1589-1614, Sept.

134. DiToro, D.M., 1969, Stream equations and method of characteristics: Proc. ASCE, vol. 95, SA4, paper 6723, pp. 699-703, August.

135. Dronkers, J.J., 1969, Tidal computations for rivers, coastal areas, and seas: Proc. ASCE, vol. 95, HY1, paper 6341, pp. 29-77, January.

136. Garrison, J.M., Granju, J.P., Price, J.T., 1969, Unsteady flow simulation in rivers and reservoirs: Proc. ASCE, vol. 95, HY5, paper 6771, pp. 1559-1576, September.

137. Martin, C.S., DeFagio, F.G., 1969, Open-channel surge simulation by digital computer: Proc. ASCE, vol. 95, HY6, paper 6911, p. 2049, November.

138. Mozayeny, B., Song, C.S., 1969, Propagation of flood waves in open channels: ASCE, vol. 95, HY3, paper 6561, pp. 877-892, May.

139. Nakagawa, H., Nakamura, S., Ichihashi, K., 1969, Generation and development of a hydraulic bore due to the breaking of a dam: Bulletin of the Disaster Prevention Research Institute Kyoto University (Japan), vol. 19, part 2, no. 154, November.

140. Strelkoff, T., 1969, One-dimensional equations of open-channel flow: Proc. ASCE, vol. 95, HY3, paper 6557, pp. 861-876. May.

141. Terstriep, M.L., Stall, J.B., 1969, Urban runoff by Road Research Laboratory method: Proc. ASCE, vol. 95, HY6, paper 6878, p. 1809, Nov.

142. Wylie, E.B., 1969, Control of transient free-surface flow: Proc. ASCE, vol. 95, HY1, paper 6360, pp. 347-361, January.

143. Cunge, J.A., 1970, (In French), Calcul de propagation des ondes de rupture de barrage (Computation of dam breach waves): La Houille Blanche, no. 1, pp. 25-33.

144. Harris, G.S., 1970, Real time routing of flood hydrographs in storm sewers: Proc. ASCE, vol. 96, no. HY6, June.

145. Zorne, J.J., 1970, The numerical solution of transient superical flow by the method of characteristics with a technique for simulating bore propagation: School of Civil Engineering, ERC-0370, Georgia Institute of Technology, Atlanta, Georgia (U.S.A.).

APPENDIX 3

COMPARISONS OF OBSERVED AND COMPUTED WAVES FOR DEPTH VERSUS TIME RELATIONS, AND DEPTH VERSUS DISTANCE RELATIONS

A total of 50 runs is included in Appendix 3. They are grouped into two different conduit slopes (S_o); the first 14 runs are for $S_o = 0.00048$ and the last 36 runs are for $S_o = 0.00099$. Under each slope, graphs of this appendix are arranged as follows: first, inflow into the main conduit without inflows through laterals; second, inflow into the main conduit plus inflow through one lateral, and finally inflow into the main conduit plus inflows through all three laterals. Inflow hydrographs of laterals are given in the graphs whenever there is an inflow through laterals. In each group of the same type of inflows, the graphs are arranged in the order of increasing base flow discharge in the conduit (QB). For each run presented in this appendix, the inflow hydrographs, the plots of depth versus time at six different positions, and the plots of depth versus distance at six instants in time are presented. Identification of the six positions, the six instants in time, variables and units of coordinates, and the peak flow discharges (QP), all appear in graphs and are self-explanatory.

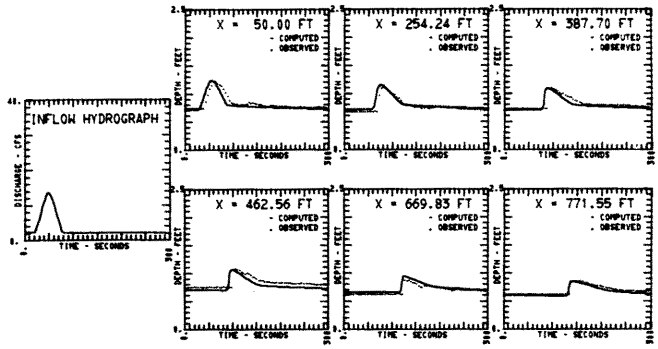

RUN NUMBER 9 1 SO = .000480 QB = 2.47 CFS QP = 13.58 CFS

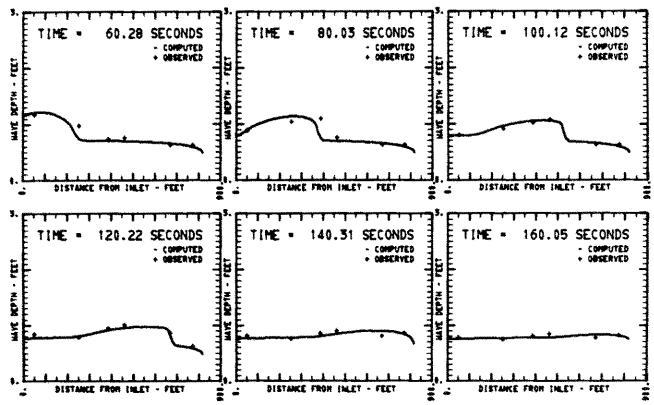

WAVE COMPARISONS AT INSTANTS IN TIME RUN NUMBER 9 1

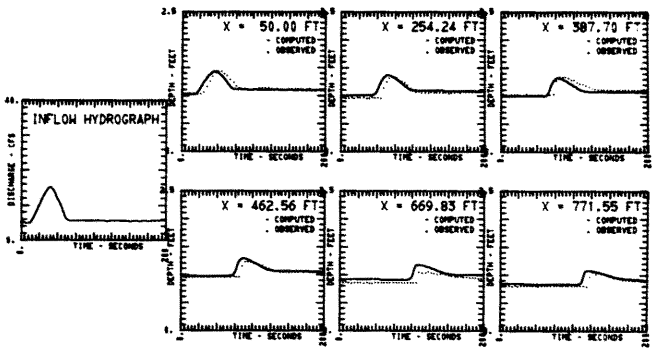

RUN NUMBER 9 3 SO = .000480 QB = 5.03 CFS QP = 15.21 CFS

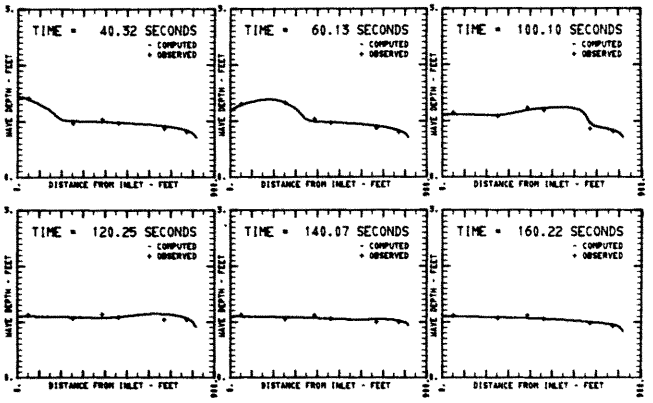

WAVE COMPARISONS AT INSTANTS IN TIME RUN NUMBER 9 3

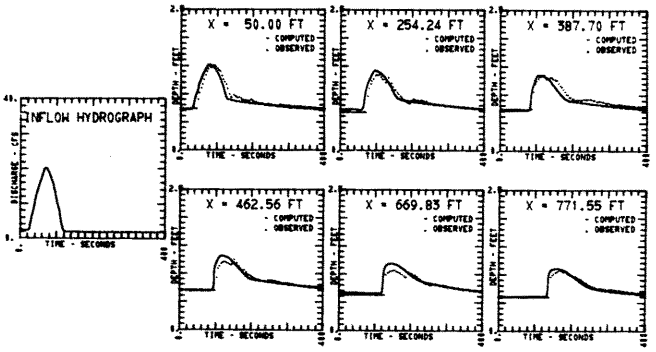

RUN NUMBER 9 2 SO = .000480 QB = 2.54 CFS QP = 20.34 CFS

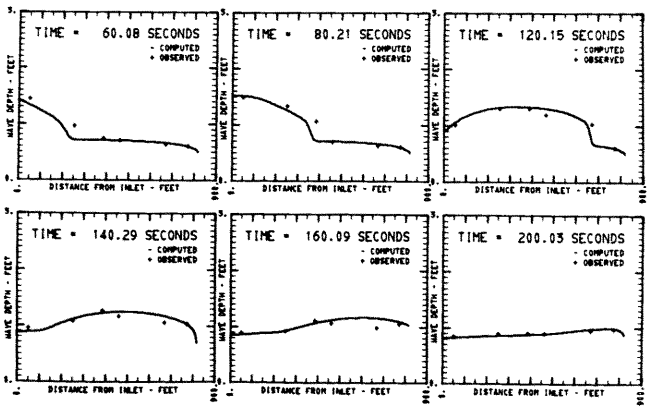

WAVE COMPARISONS AT INSTANTS IN TIME RUN NUMBER 9 2

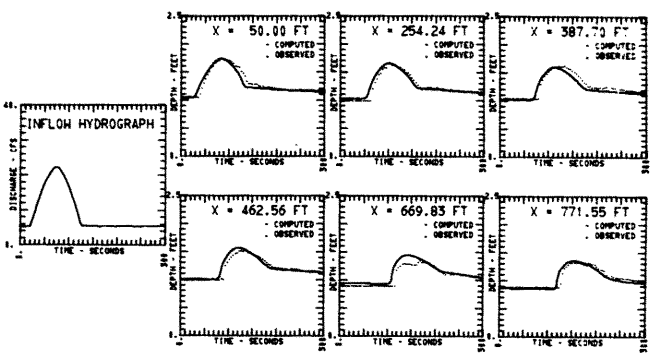

RUN NUMBER 9 4 SO = .000480 QB = 5.29 CFS QP = 22.35 CFS

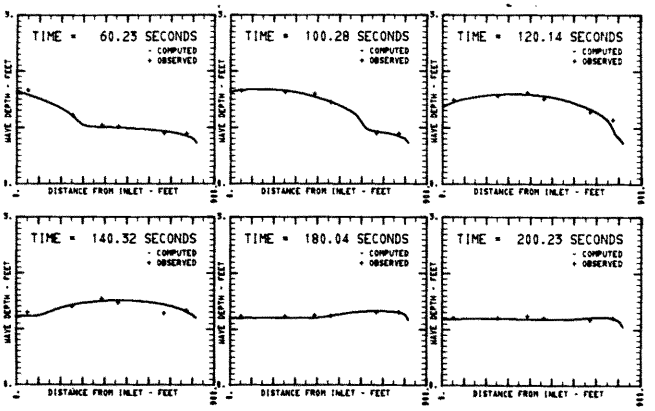

WAVE COMPARISONS AT INSTANTS IN TIME RUN NUMBER 9 4

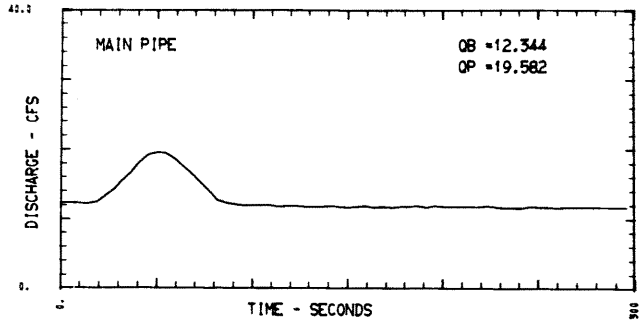

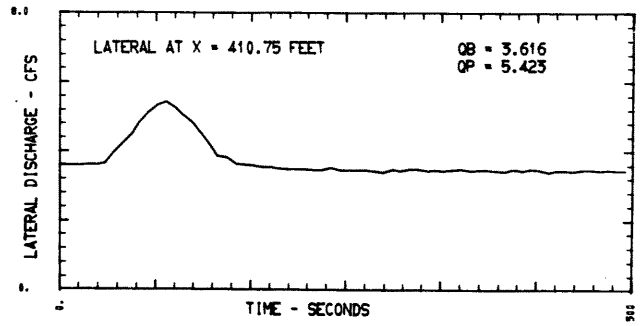

RUN NUMBER 100002 INFLOW HYDROGRAPHS

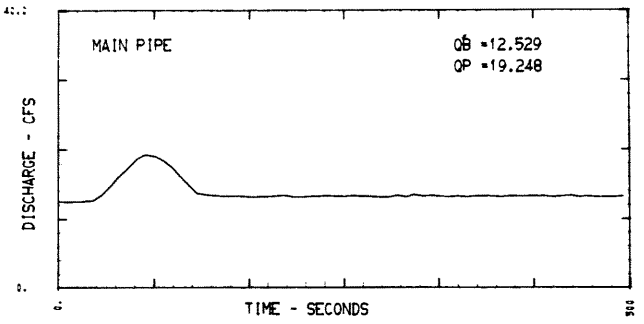

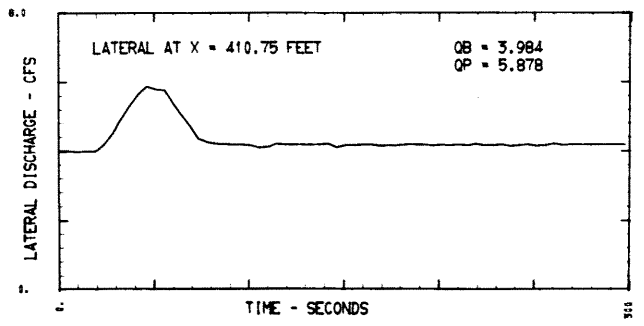

RUN NUMBER 120002 INFLOW HYDROGRAPHS

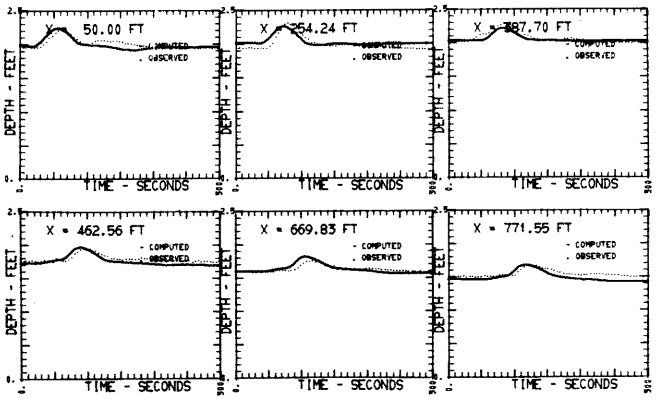

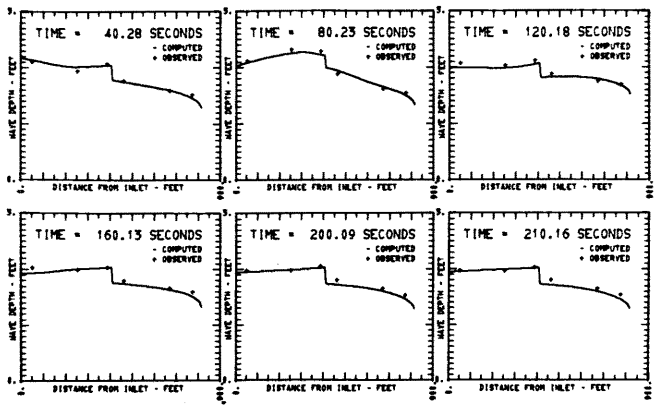

RUN NUMBER 100002 SO = .000480 QB = 12.34 CFS QP = 19.58 CFS

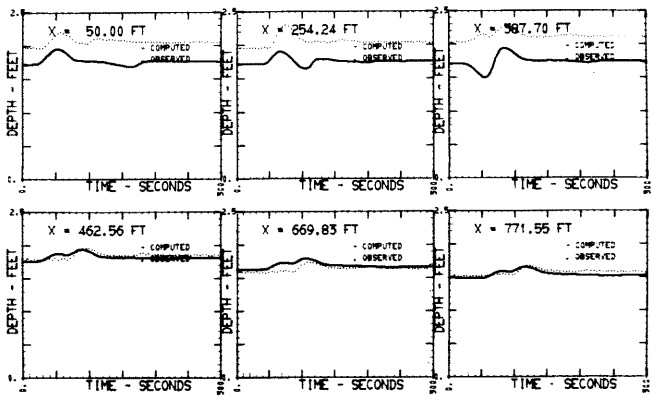

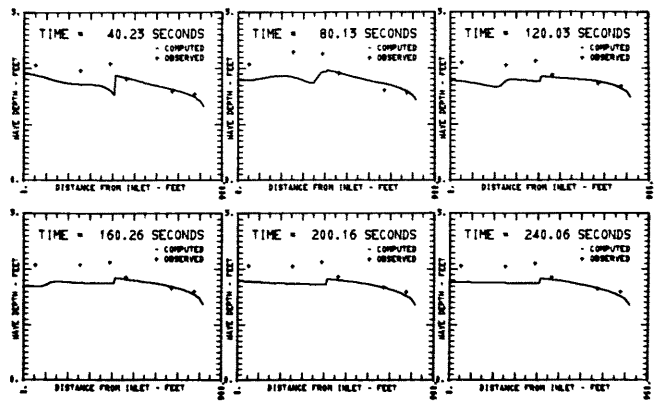

RUN NUMBER 120002 SO = .000480 QB = 12.53 CFS QP = 19.25 CFS

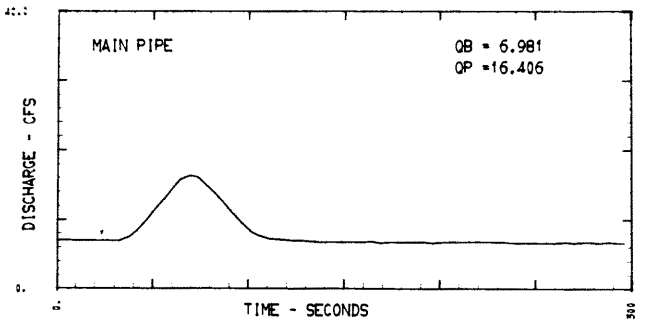

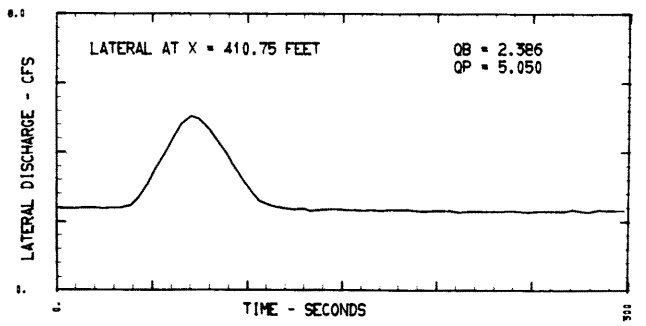

RUN NUMBER 120001 INFLOW HYDROGRAPHS

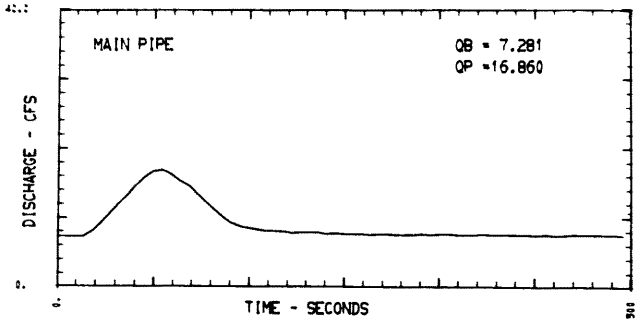

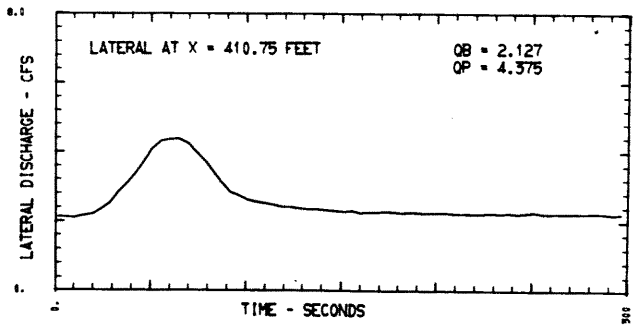

RUN NUMBER 100001 INFLOW HYDROGRAPHS

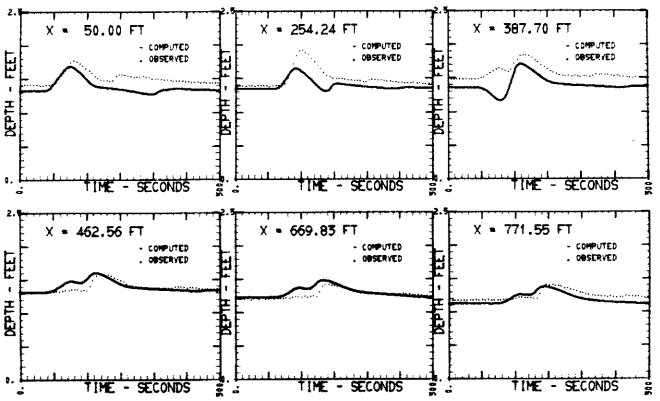

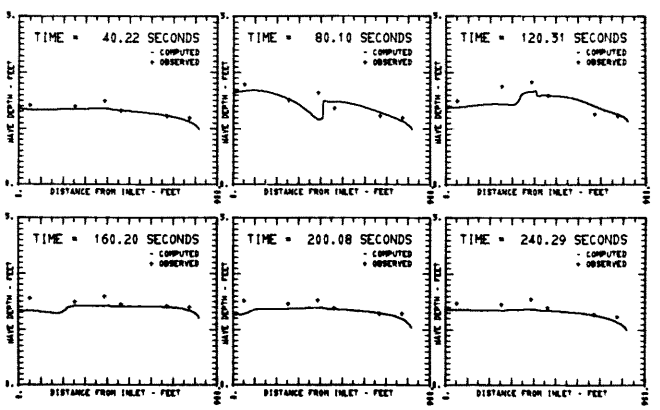

RUN NUMBER 120001 SO = .000480 QB = 6.98 CFS QP = 16.41 CFS

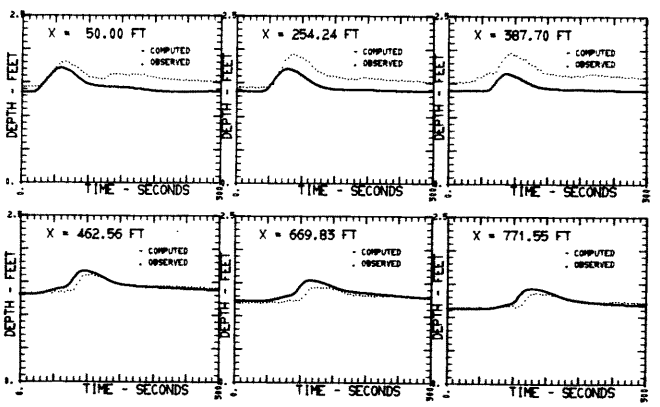

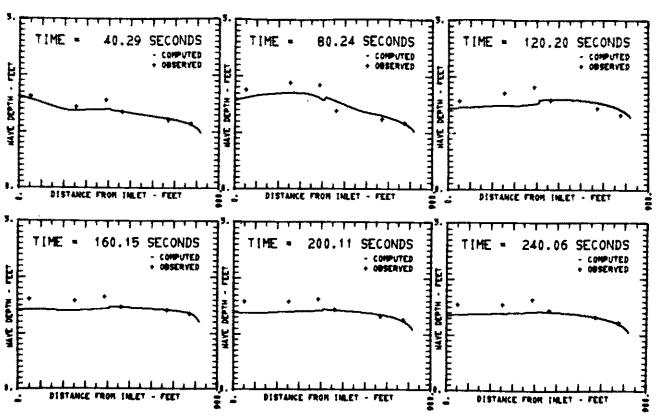

RUN NUMBER 100001 SO = .000480 QB = 7.28 CFS QP = 16.86 CFS

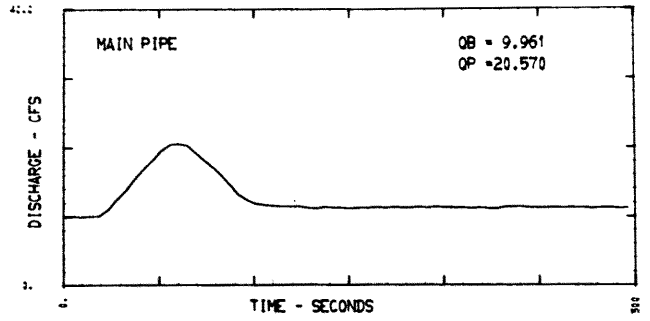

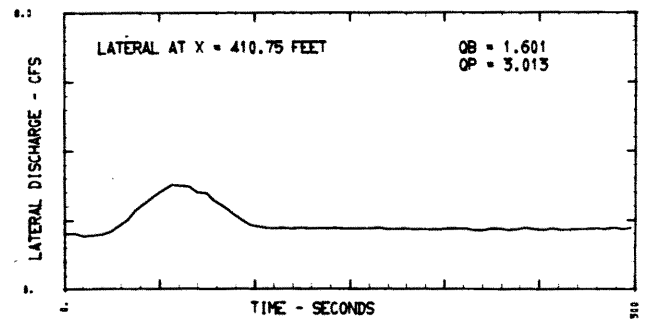

RUN NUMBER 120005 INFLOW HYDROGRAPHS

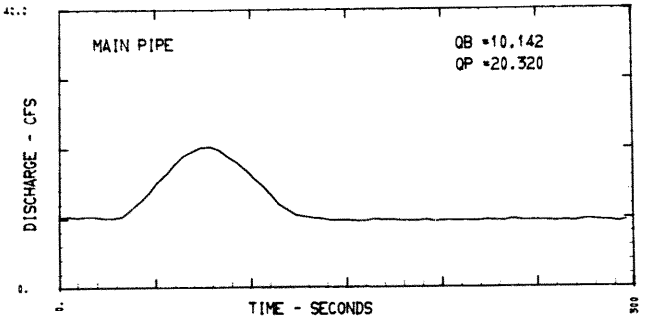

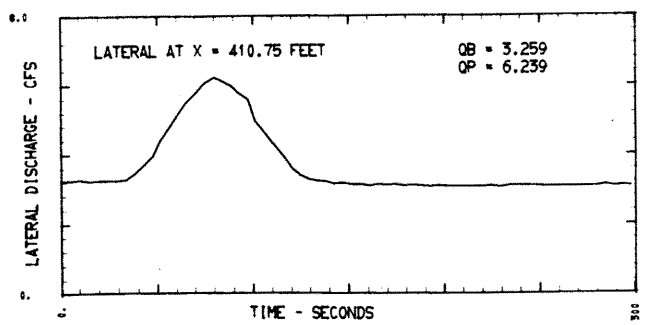

RUN NUMBER 120004 INFLOW HYDROGRAPHS

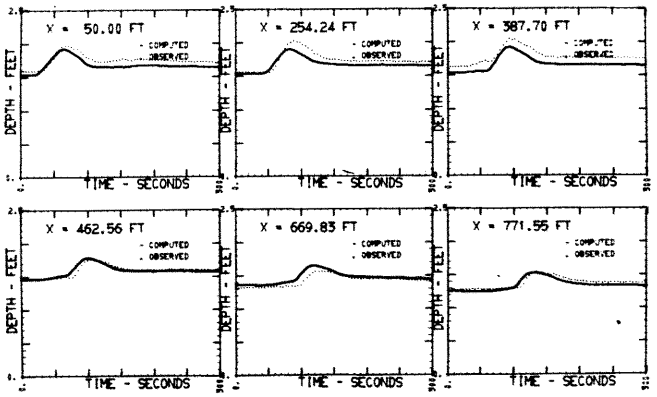

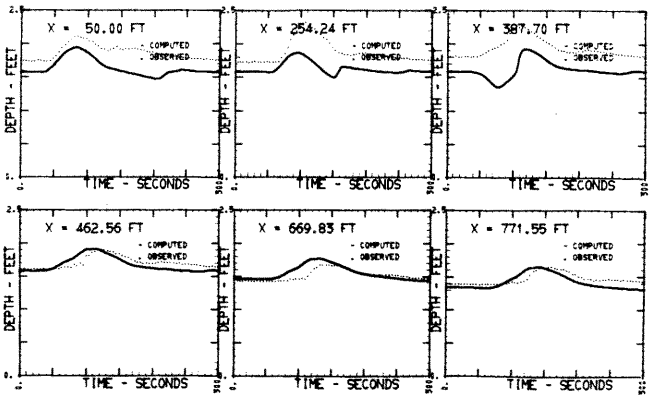

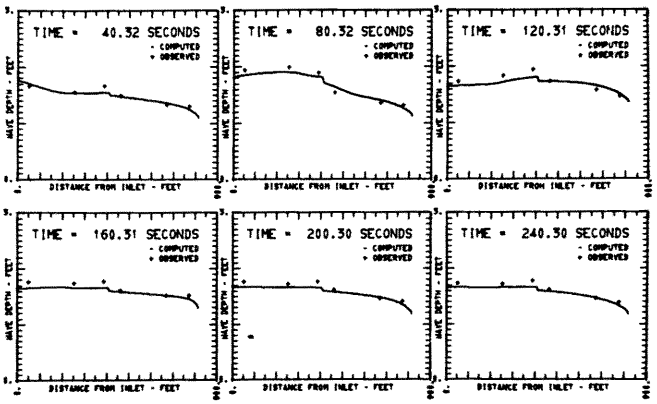

RUN NUMBER 120005 SO = .000480 QB = 9.96 CFS QP = 20.57 CFS

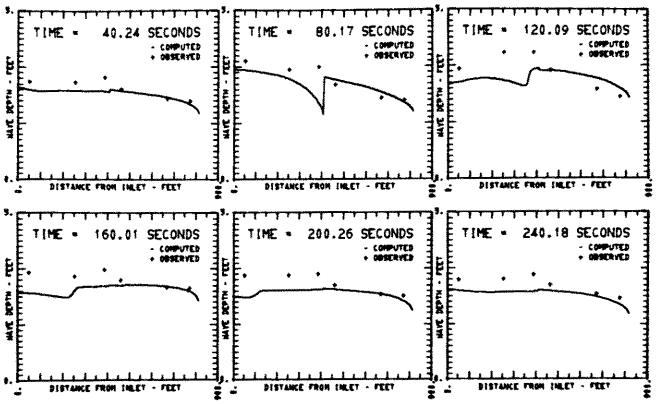

RUN NUMBER 120004 SO = .000480 QB = 10.14 CFS QP = 20.32 CFS

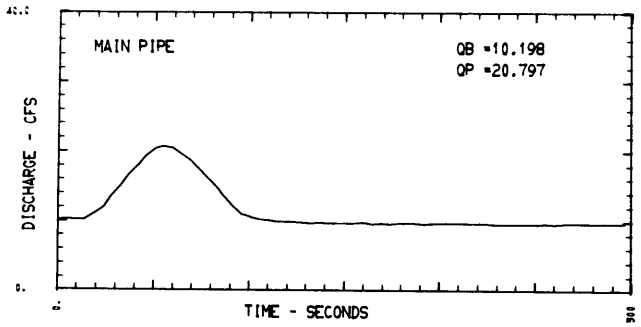

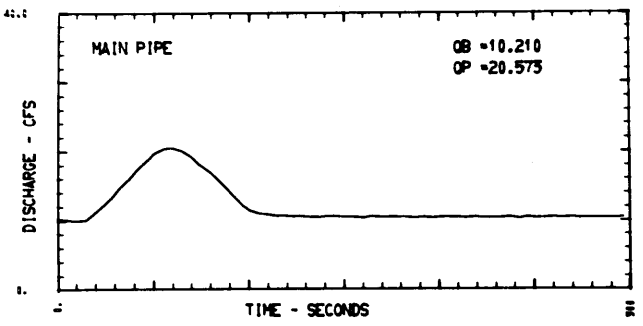

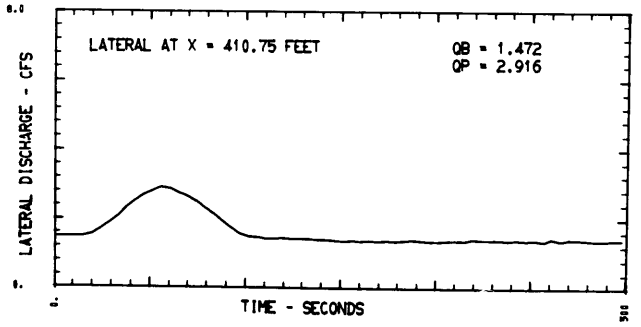

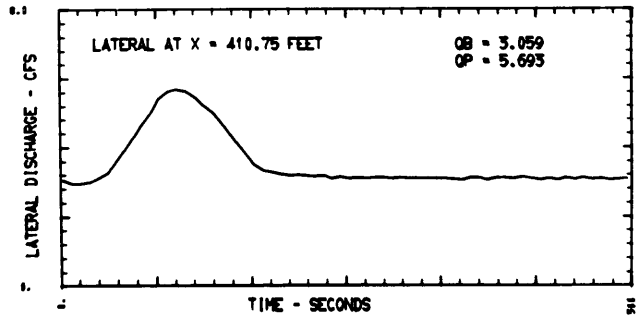

RUN NUMBER 100005 INFLOW HYDROGRAPHS

RUN NUMBER 100004 INFLOW HYDROGRAPHS

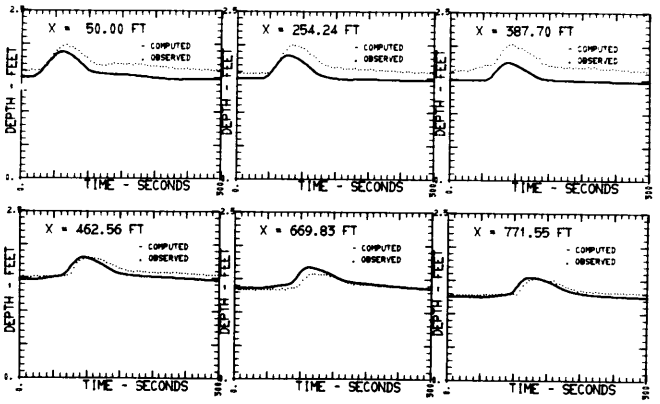

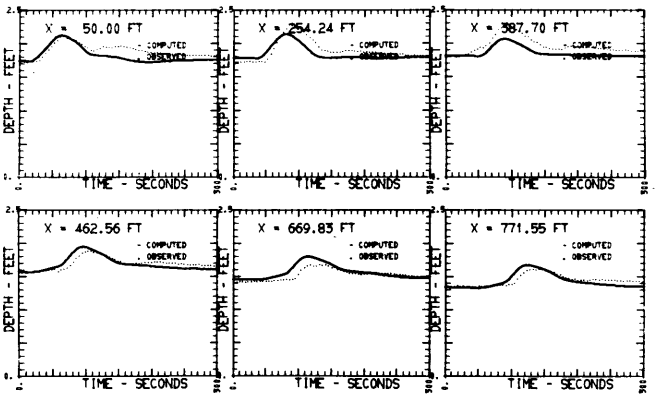

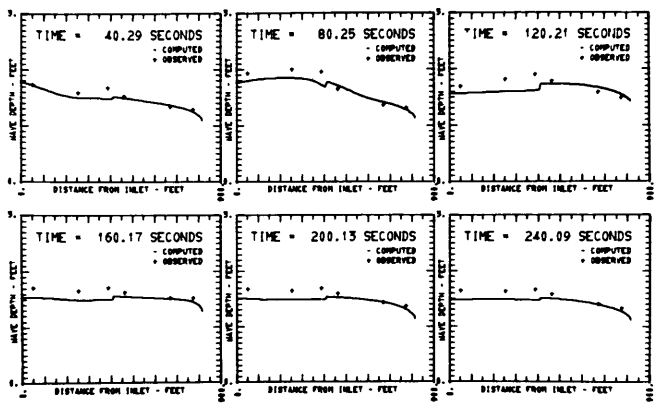

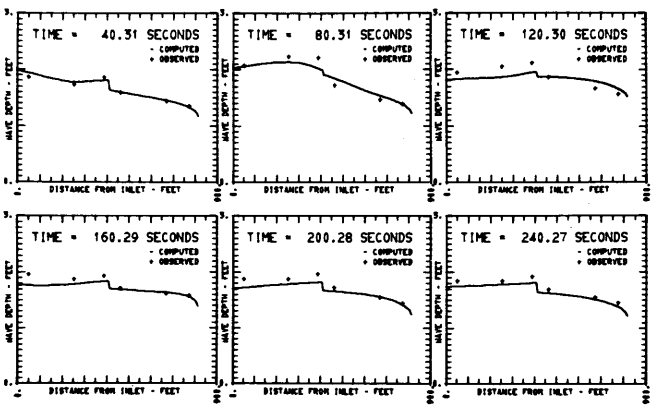

RUN NUMBER 100005 SO = .000480 QB = 10.20 CFS QP = 20.80 CFS

RUN NUMBER 100004 SO = .000480 QB = 10.21 CFS QP = 20.57 CFS

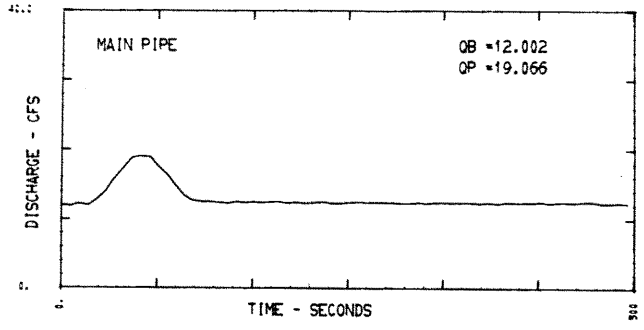

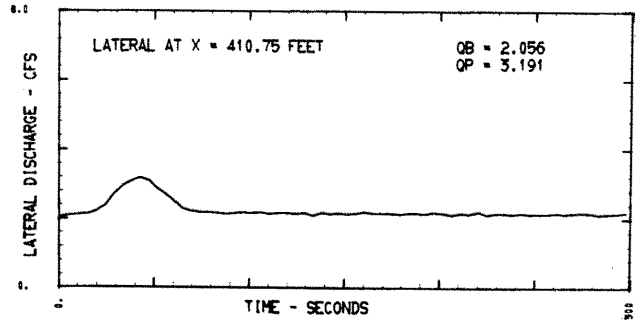

RUN NUMBER 120003 INFLOW HYDROGRAPHS

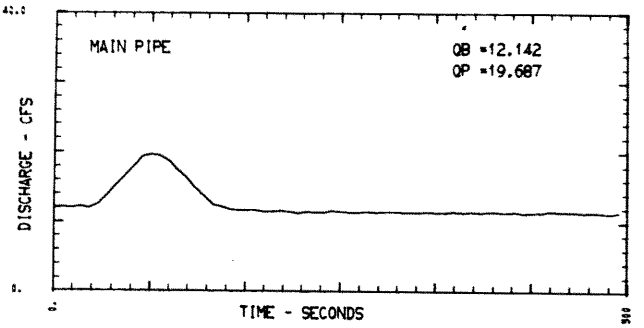

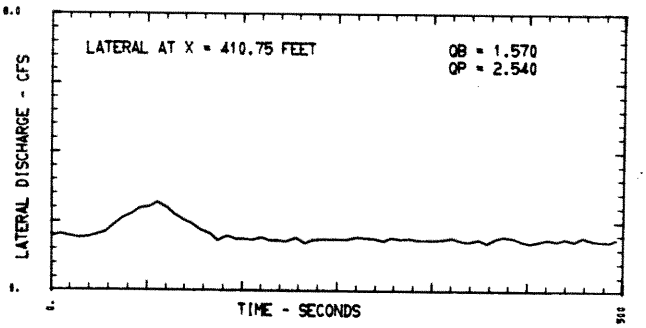

RUN NUMBER 100003 INFLOW HYDROGRAPHS

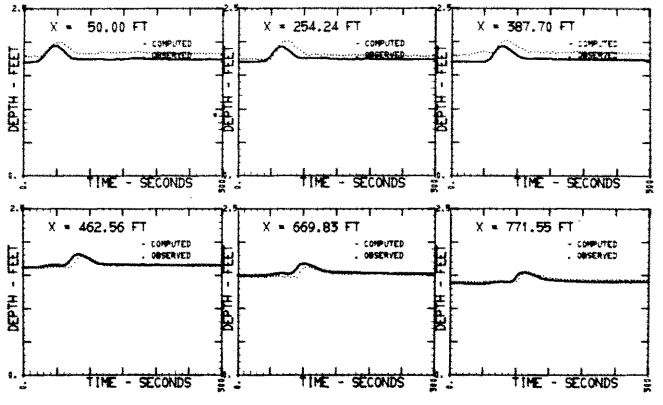

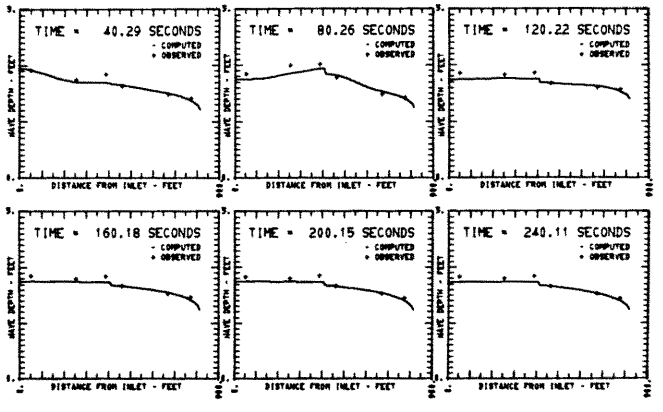

RUN NUMBER 120003 SO = .000480 QB = 12.00 CFS QP = 19.07 CFS

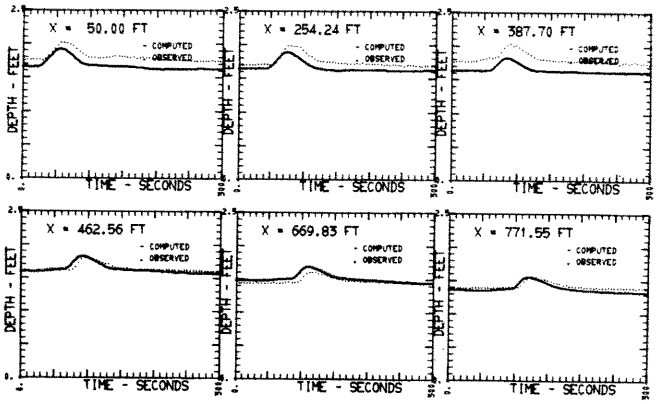

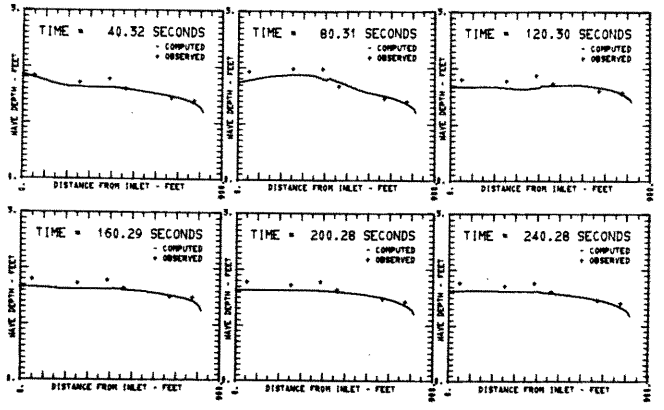

RUN NUMBER 100003 SO = .000480 QB = 12.14 CFS QP = 19.69 CFS

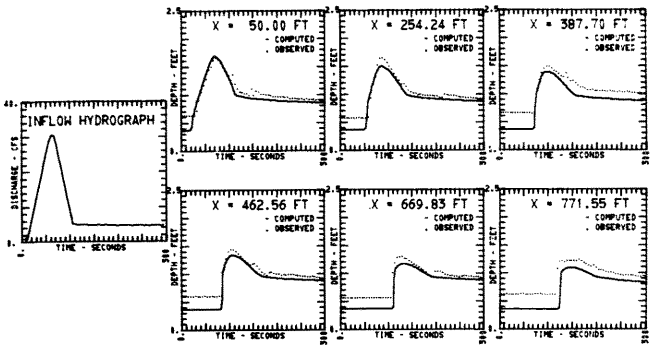

RUN NUMBER 19909 SO = .000990 QB = .90 CFS QP = 30.48 CFS

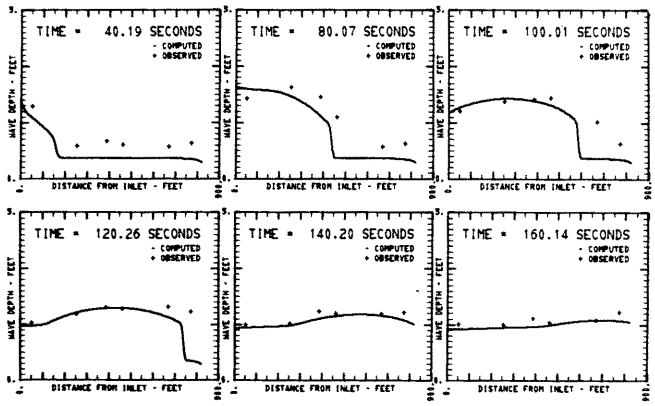

WAVE COMPARISONS AT INSTANTS IN TIME RUN NUMBER 19909

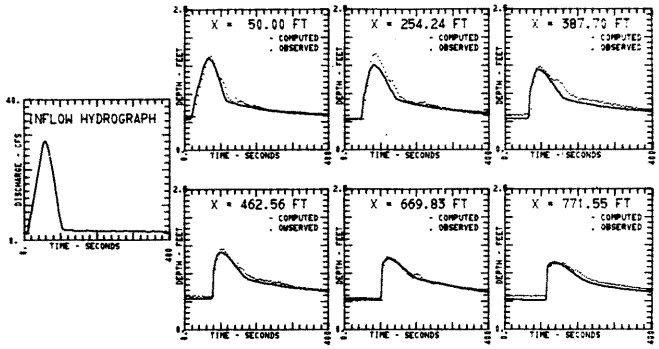

RUN NUMBER 1 10 SO = .000990 QB = 2.08 CFS QP = 28.33 CFS

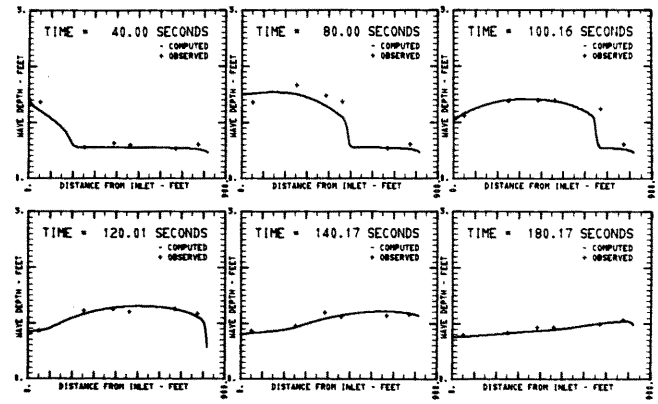

WAVE COMPARISONS AT INSTANTS IN TIME RUN NUMBER 1 10

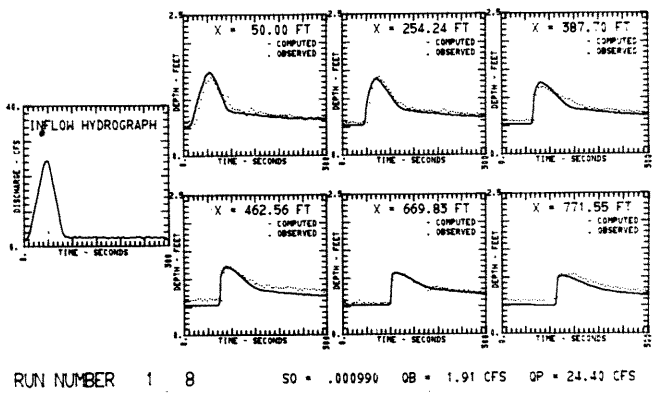

RUN NUMBER 1 8 SO = .000990 QB = 1.91 CFS QP = 24.40 CFS

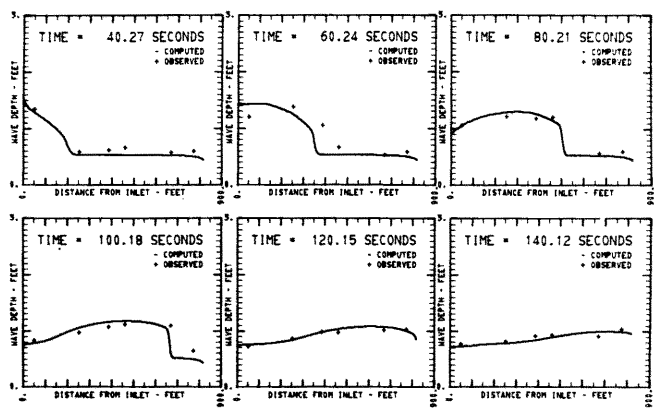

WAVE COMPARISONS AT INSTANTS IN TIME RUN NUMBER 1 8

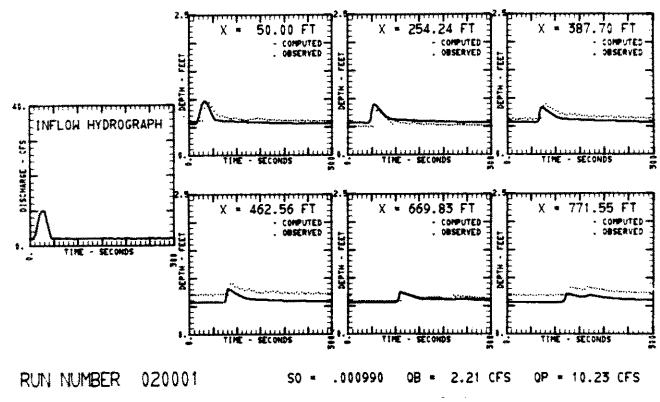

RUN NUMBER 020001 SO = .000990 QB = 2.21 CFS QP = 10.23 CFS

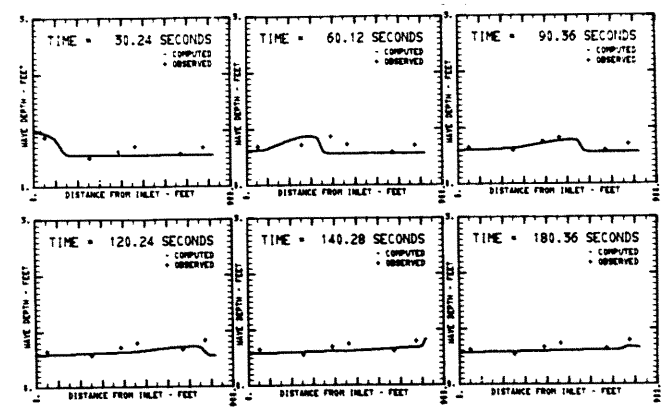

WAVE COMPARISONS AT INSTANTS IN TIME RUN NUMBER 020001

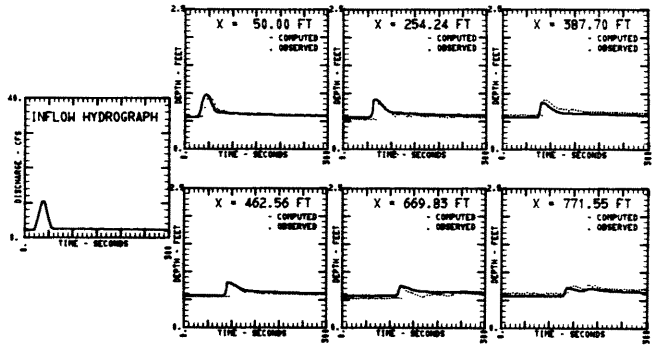

RUN NUMBER 029901 SO = .000990 QB = 2.27 CFS QP = 10.36 CFS

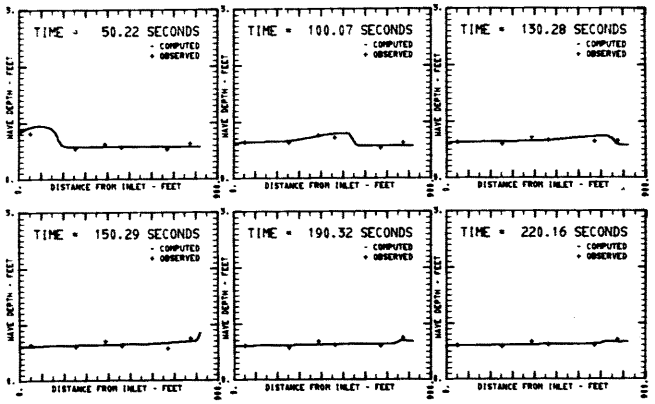

WAVE COMPARISONS AT INSTANTS IN TIME RUN NUMBER 029901

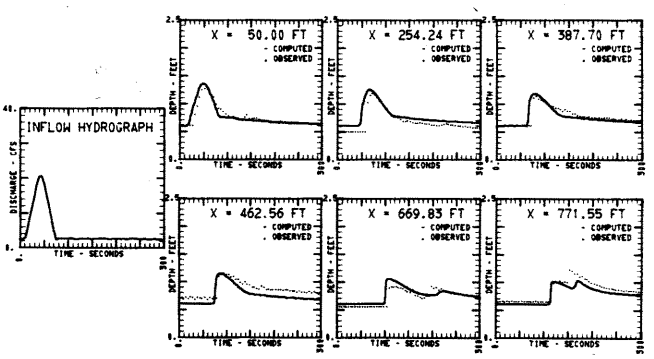

RUN NUMBER 020002 SO = .000990 QB = 2.48 CFS QP = 20.57 CFS

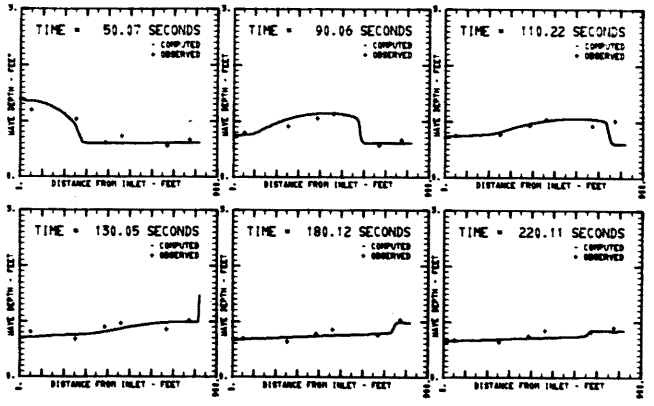

WAVE COMPARISONS AT INSTANTS IN TIME RUN NUMBER 020002

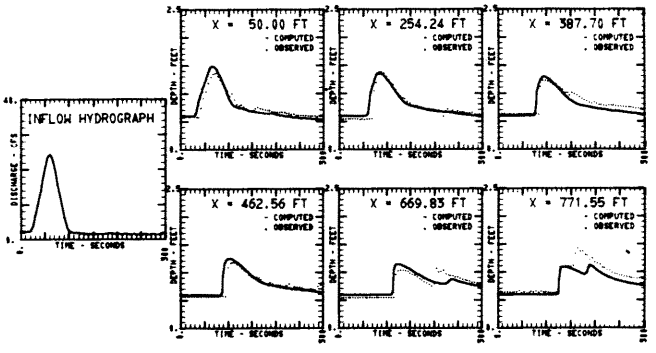

RUN NUMBER 029902 SO = .000990 QB = 2.41 CFS QP = 24.40 CFS

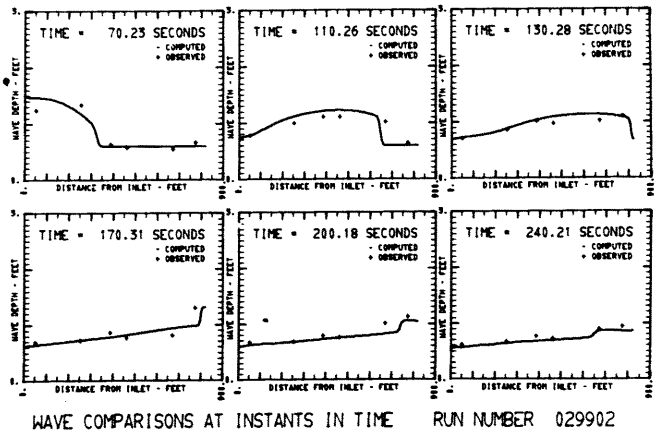

WAVE COMPARISONS AT INSTANTS IN TIME RUN NUMBER 029902

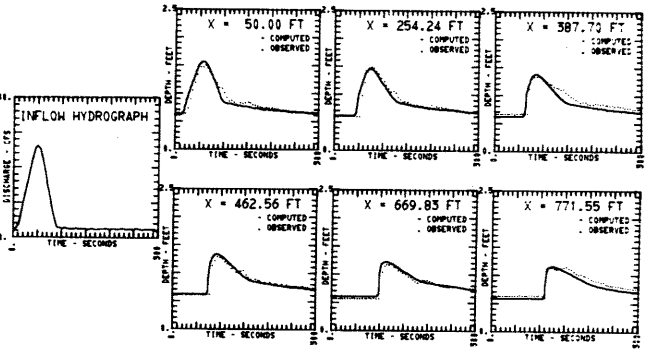

RUN NUMBER 1 9 SO = .000990 QB = 2.60 CFS QP = 26.17 CFS

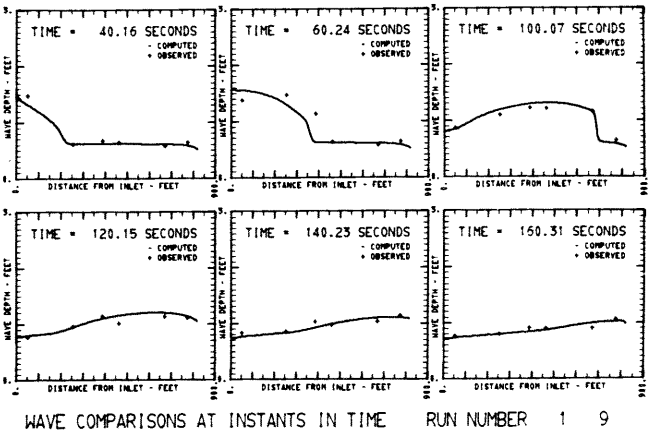

WAVE COMPARISONS AT INSTANTS IN TIME RUN NUMBER 1 9

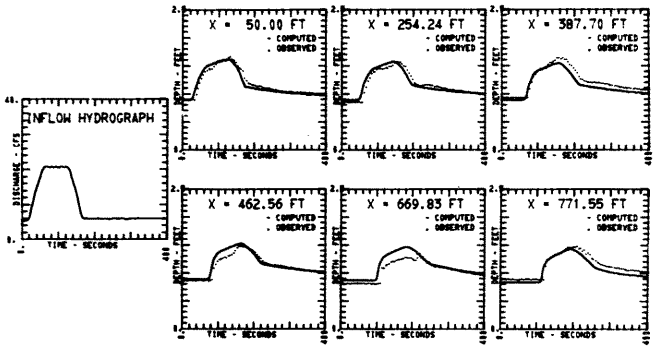

RUN NUMBER 8 1 SO = .000990 QB = 5.44 CFS QP = 20.78 CFS

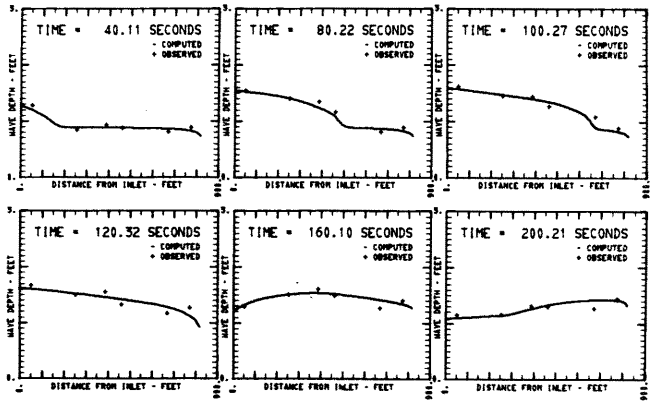

WAVE COMPARISONS AT INSTANTS IN TIME RUN NUMBER 8 1

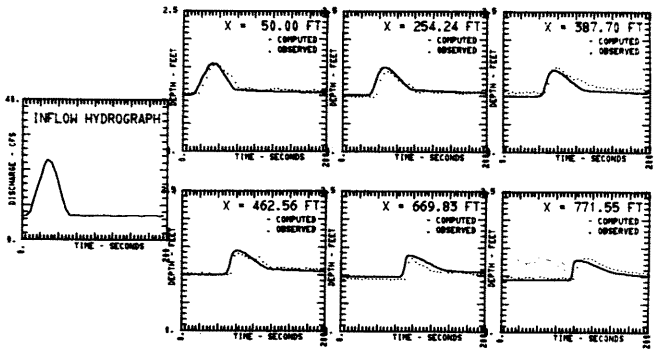

RUN NUMBER 1 11 SO = .000990 QB = 6.85 CFS QP = 22.91 CFS

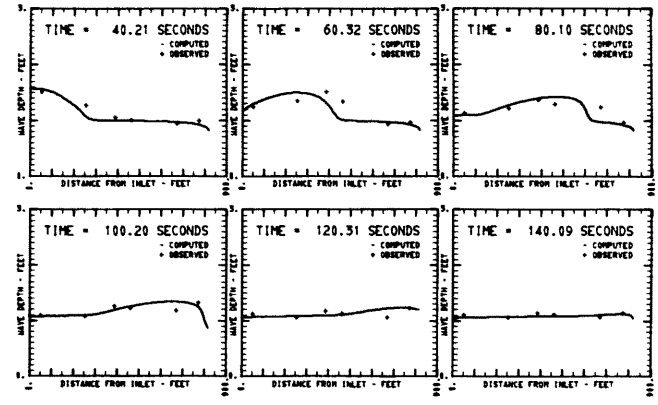

WAVE COMPARISONS AT INSTANTS IN TIME RUN NUMBER 1 11

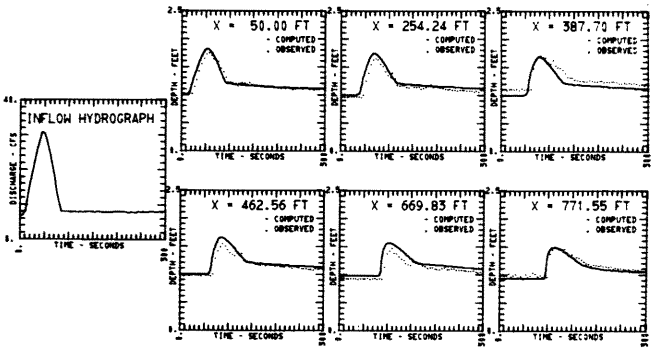

RUN NUMBER 1 12 SO = .000990 QB = 6.83 CFS QP = 30.66 CFS

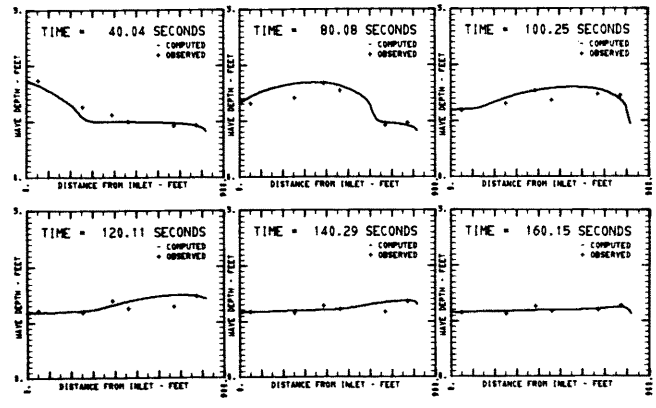

WAVE COMPARISONS AT INSTANTS IN TIME RUN NUMBER 1 12

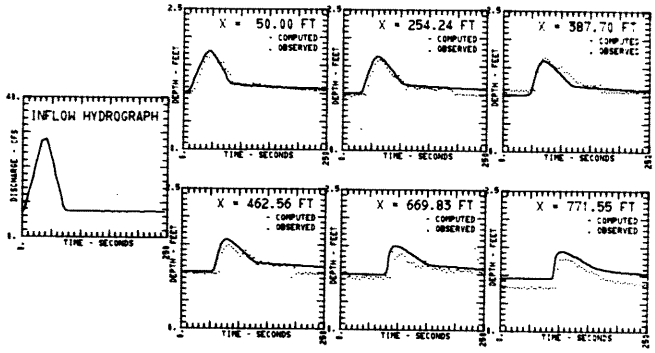

RUN NUMBER 1 3 SO = .000990 QB = 6.99 CFS QP = 28.07 CFS

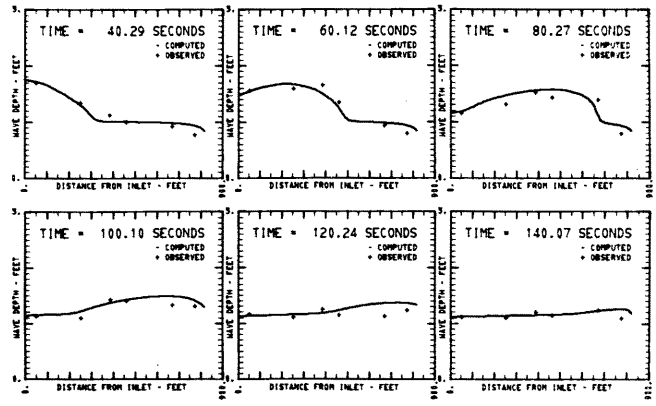

WAVE COMPARISONS AT INSTANTS IN TIME RUN NUMBER 1 3

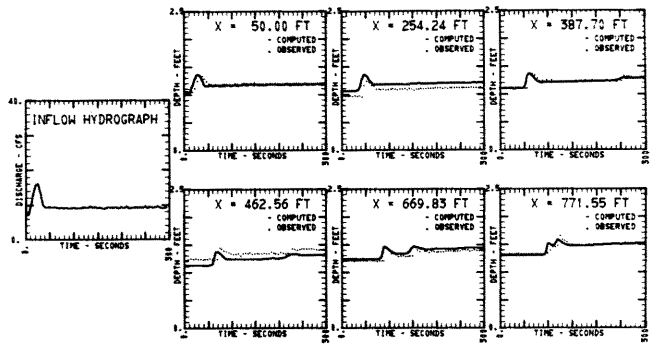

RUN NUMBER 020003 S0 = .000990 QB = 7.17 CFS QP = 16.07 CFS

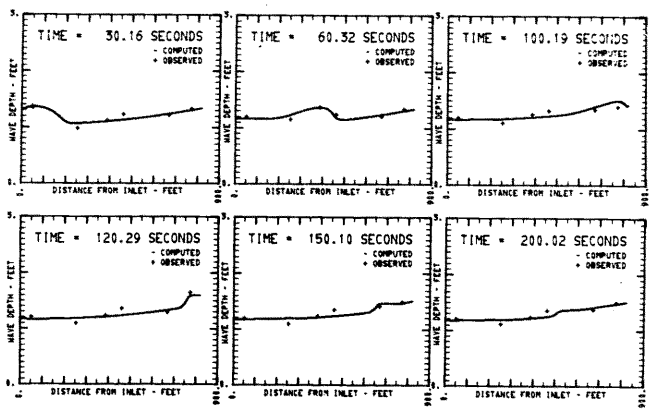

WAVE COMPARISONS AT INSTANTS IN TIME RUN NUMBER 020003

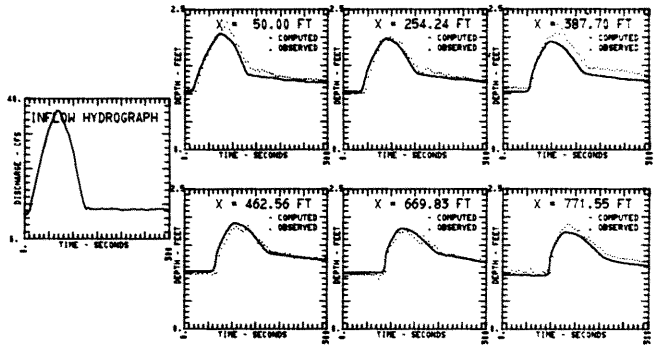

RUN NUMBER 1 13 S0 = .000990 QB = 7.29 CFS QP = 36.53 CFS

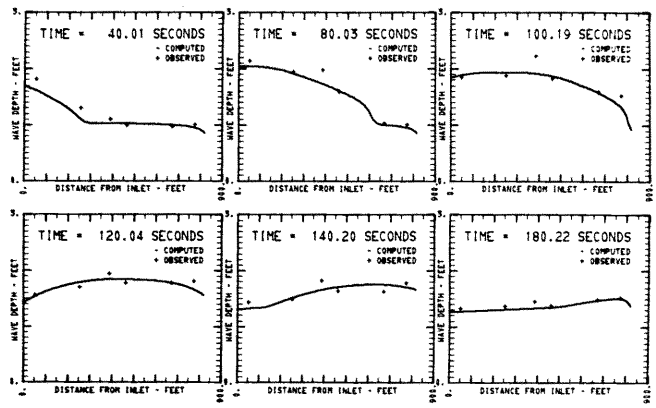

WAVE COMPARISONS AT INSTANTS IN TIME RUN NUMBER 1 13

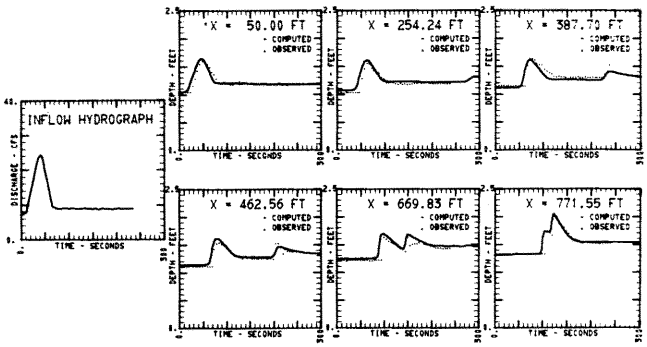

RUN NUMBER 029904 S0 = .000990 QB = 7.26 CFS QP = 24.46 CFS

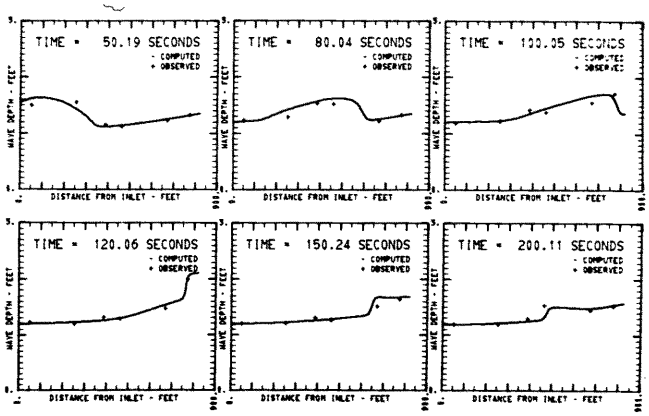

WAVE COMPARISONS AT INSTANTS IN TIME RUN NUMBER 029904

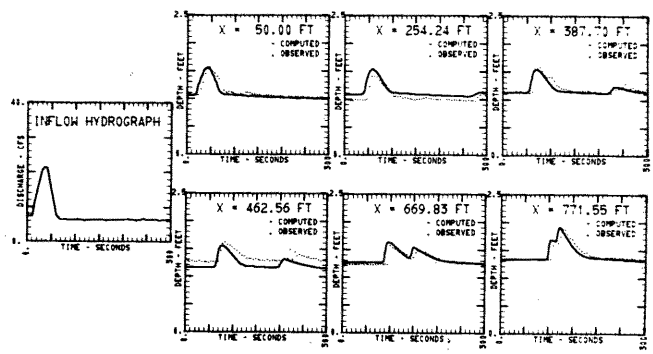

RUN NUMBER 020004 S0 = .000990 QB = 7.36 CFS QP = 21.52 CFS

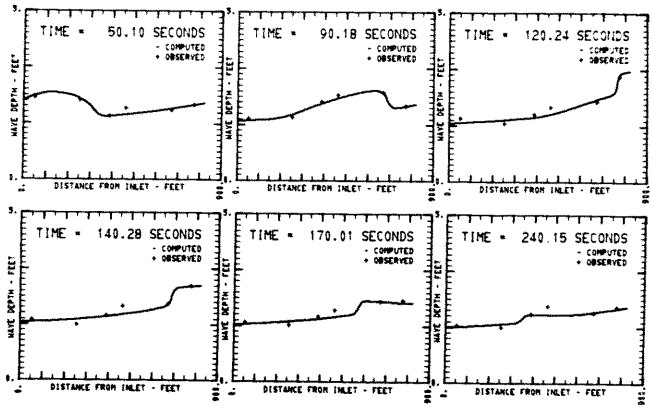

WAVE COMPARISONS AT INSTANTS IN TIME RUN NUMBER 020004

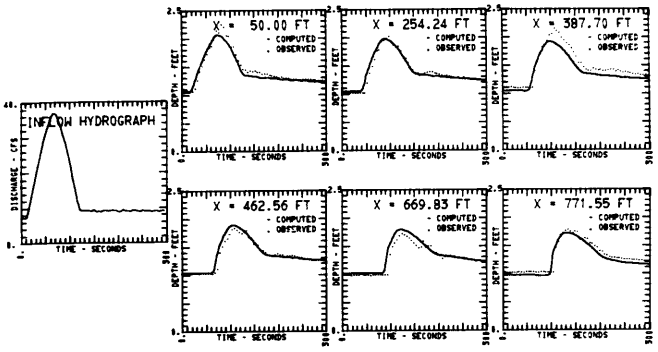

RUN NUMBER 19913 SO = .000990 QB = 7.47 CFS QP = 36.94 CFS

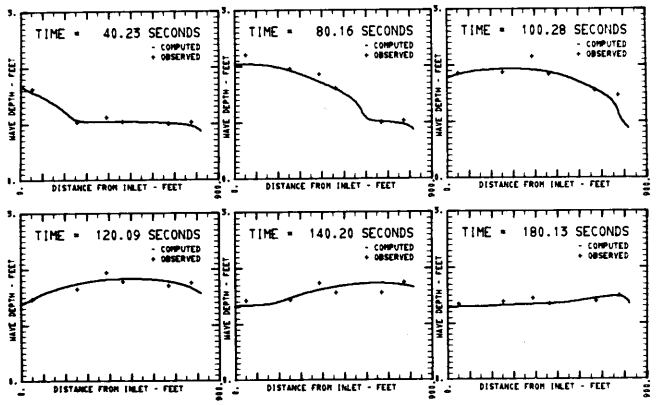

WAVE COMPARISONS AT INSTANTS IN TIME RUN NUMBER 19913

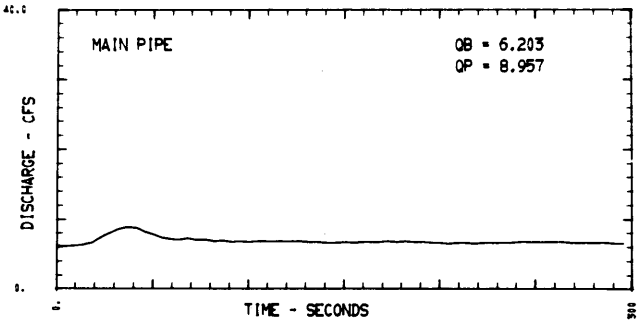

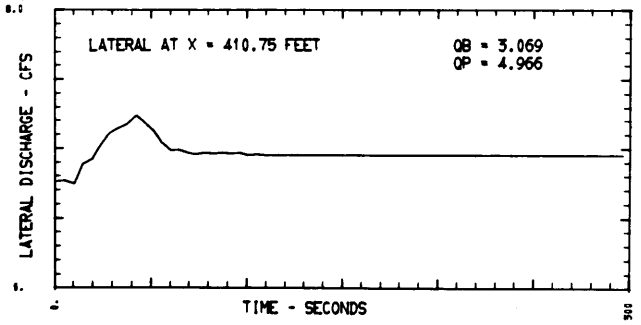

RUN NUMBER 040004 INFLOW HYDROGRAPHS

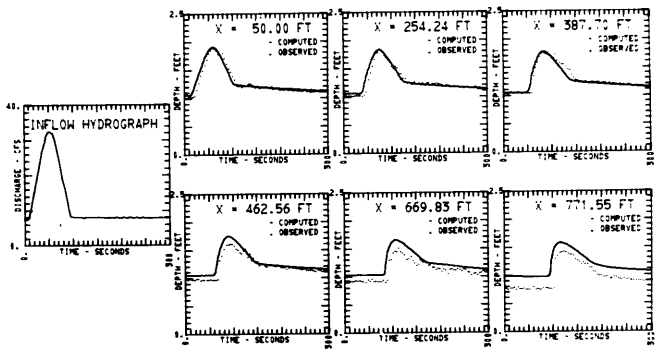

RUN NUMBER 1 4 SO = .000990 QB = 7.59 CFS QP = 32.58 CFS

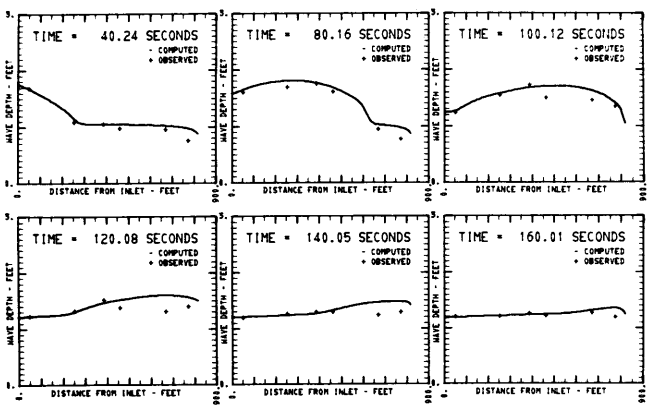

WAVE COMPARISONS AT INSTANTS IN TIME RUN NUMBER 1 4

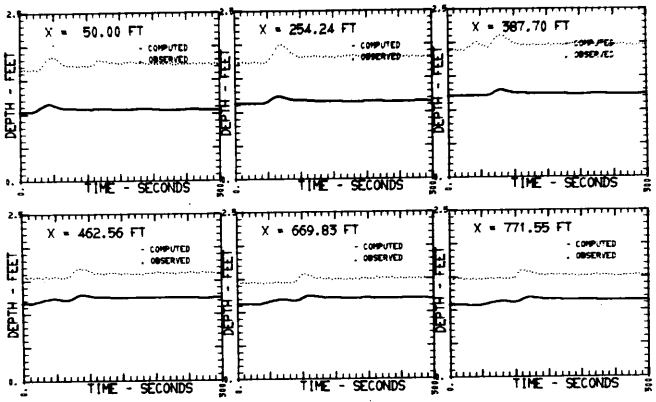

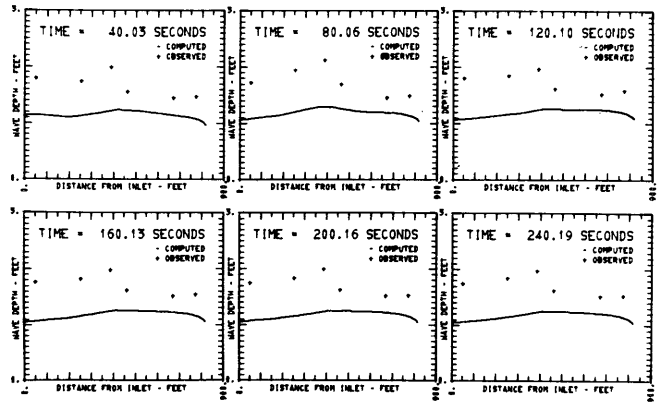

RUN NUMBER 040004 SO = .000990 QB = 6.20 CFS QP = 8.96 CFS

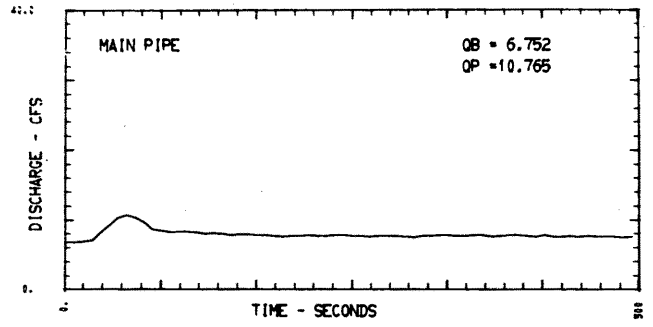

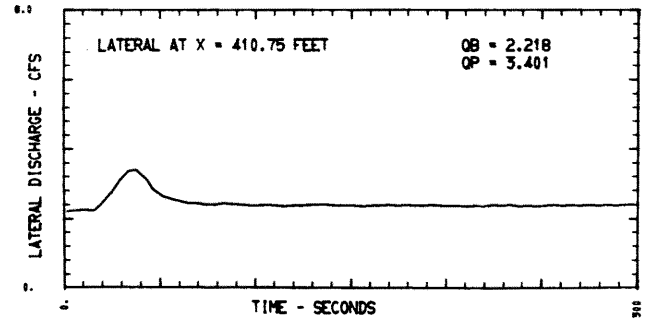

RUN NUMBER 040003 INFLOW HYDROGRAPHS

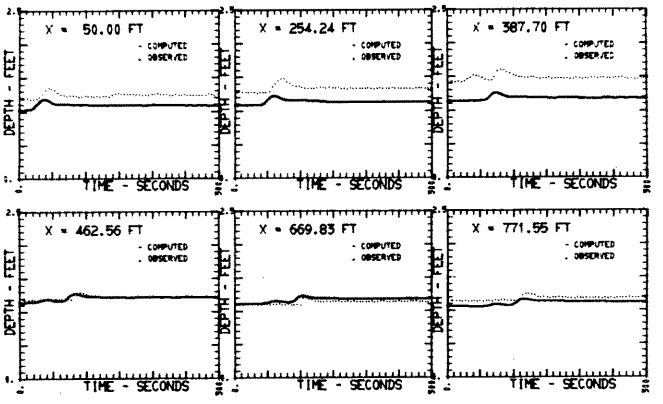

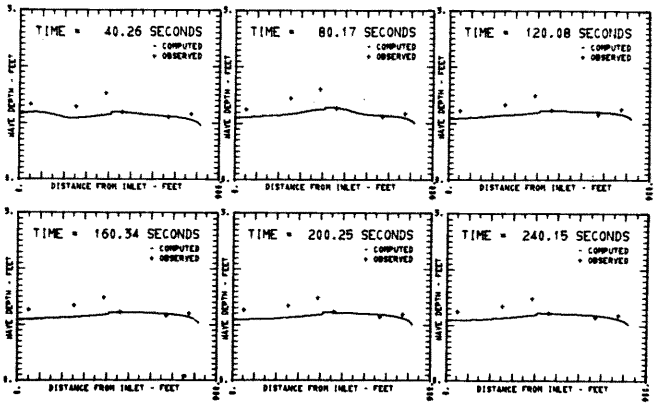

RUN NUMBER 040003 SO = .000990 QB = 6.75 CFS QP = 10.76 CFS

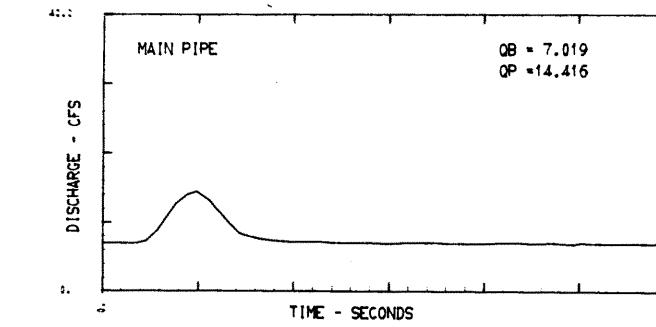

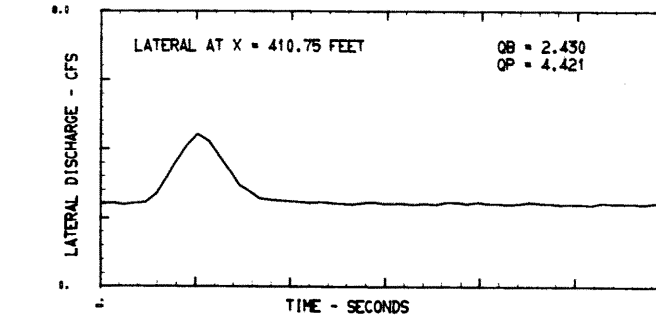

RUN NUMBER 059901 INFLOW HYDROGRAPHS

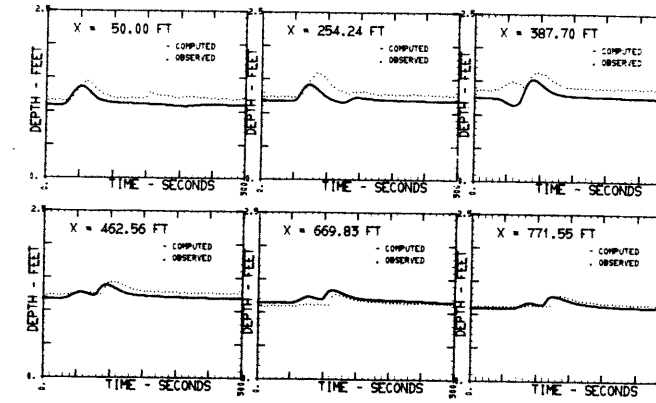

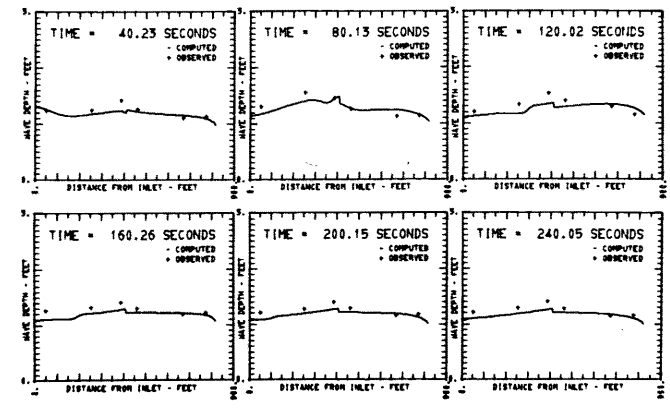

RUN NUMBER 059901 SO = .000990 QB = 7.02 CFS QP = 14.42 CFS

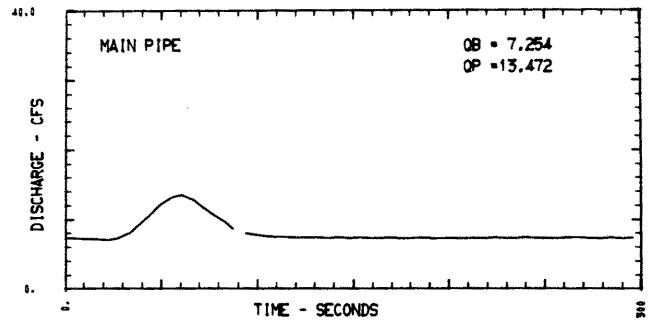

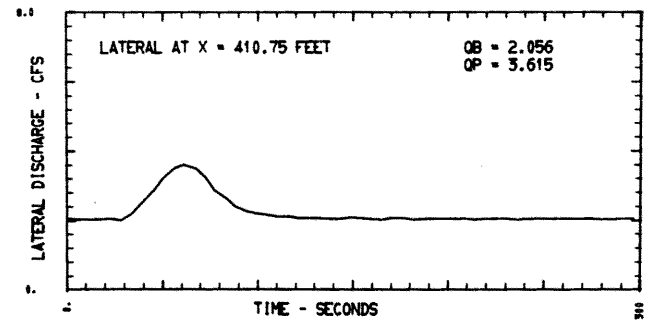

RUN NUMBER 049902 INFLOW HYDROGRAPHS

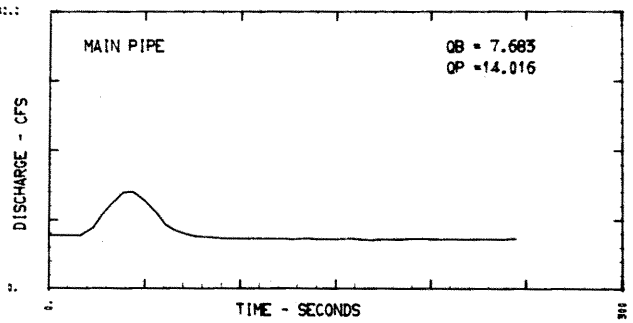

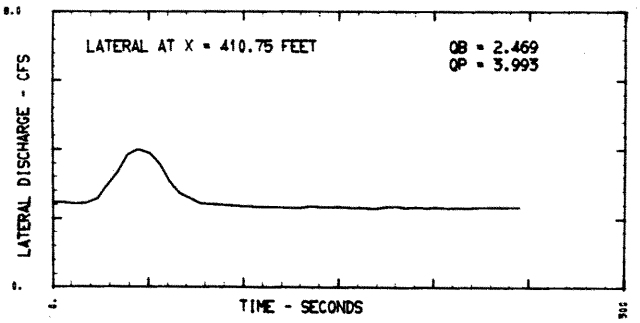

RUN NUMBER 050001 INFLOW HYDROGRAPHS

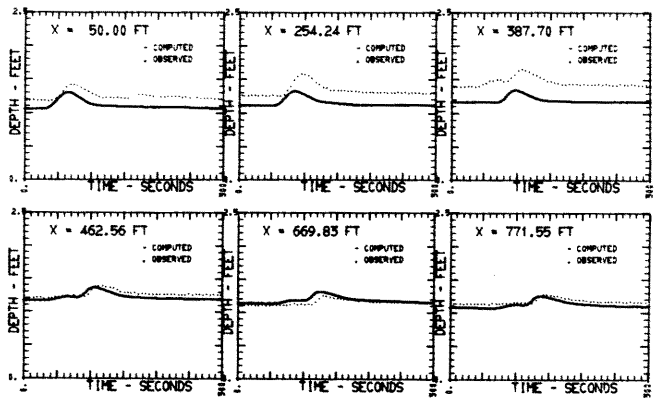

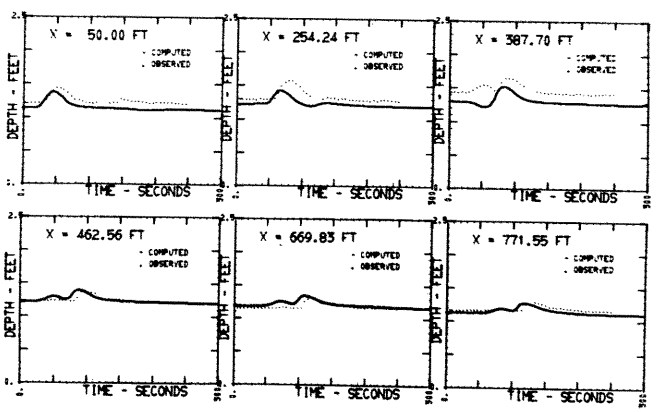

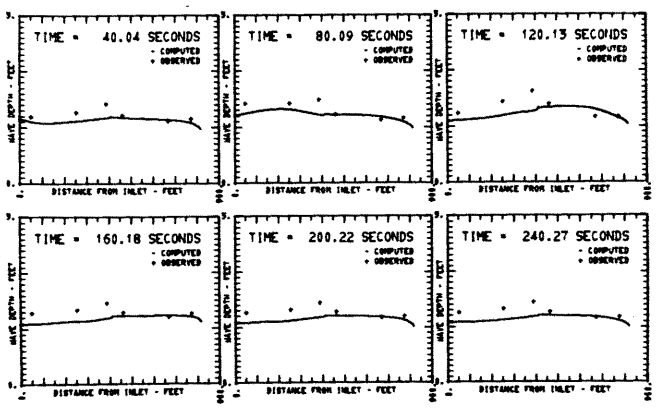

RUN NUMBER 049902 SO = .000990 QB = 7.25 CFS QP = 13.47 CFS

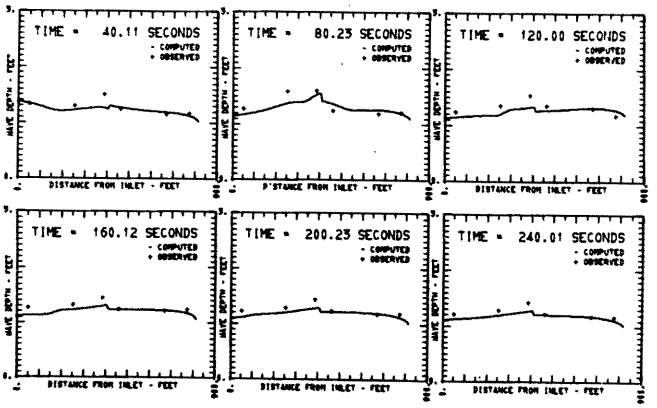

RUN NUMBER 050001 SO = .000990 QB = 7.68 CFS QP = 14.02 CFS

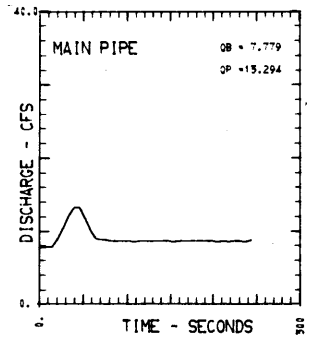

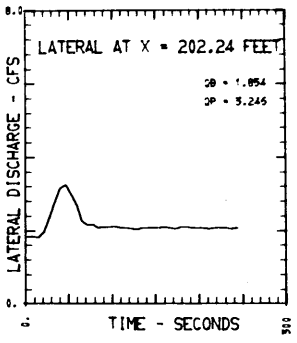

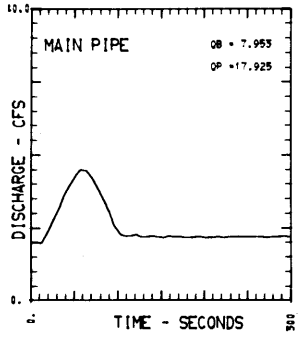

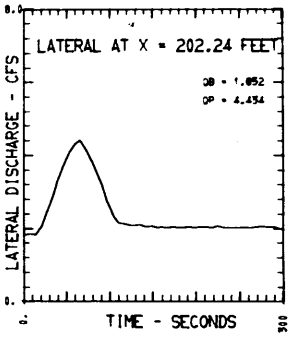

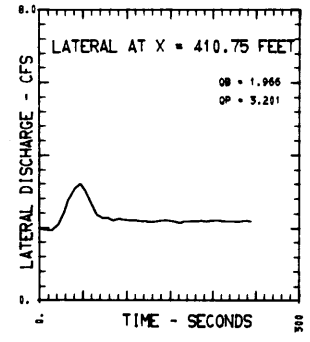

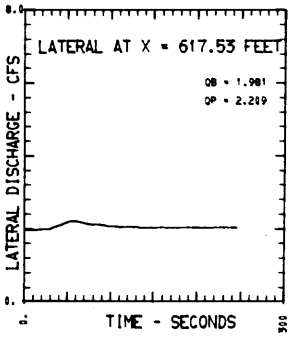

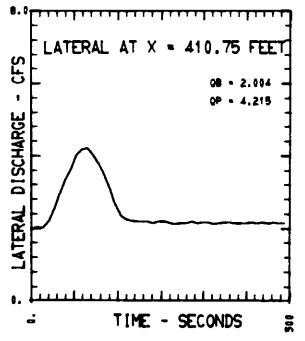

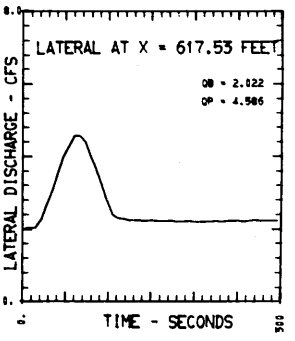

RUN NUMBER 079901 INFLOW HYDROGRAPHS

RUN NUMBER 079992 INFLOW HYDROGRAPHS

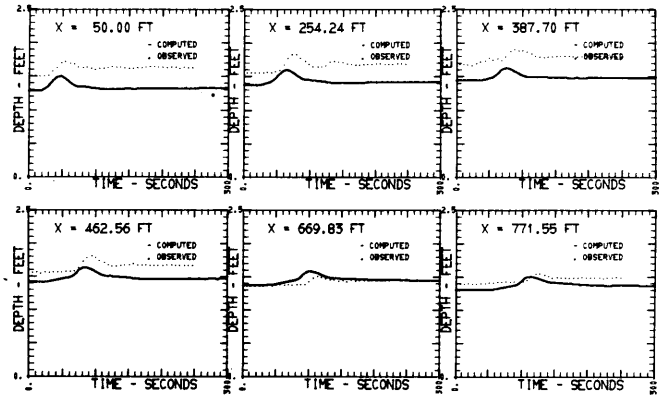

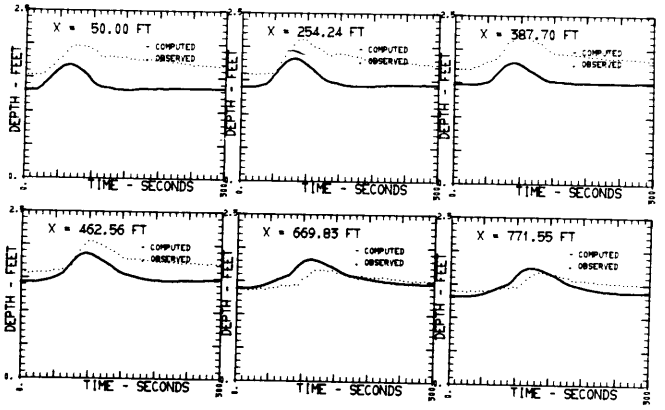

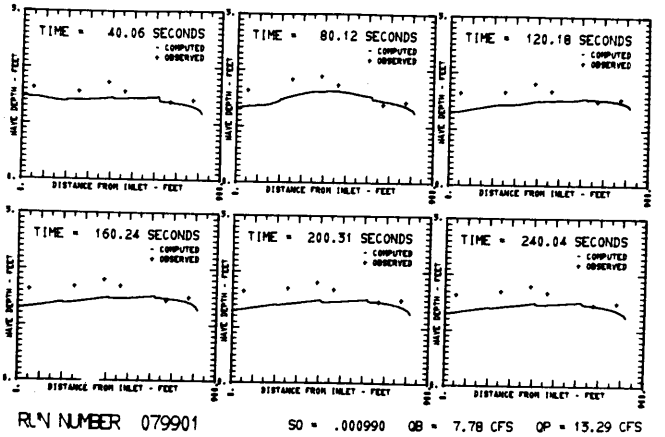

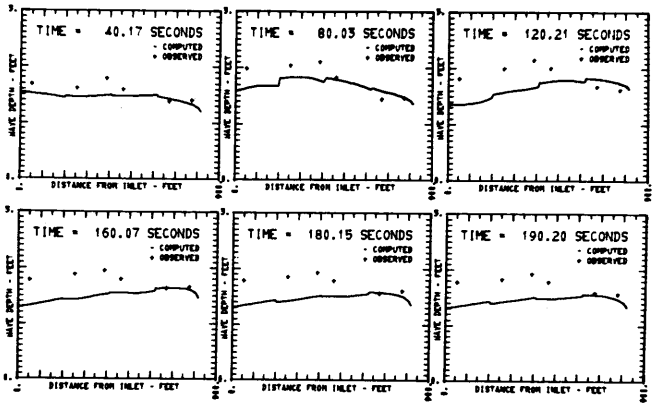

RUN NUMBER 079901 SO = .000990 QB = 7.78 CFS QP = 13.29 CFS

RUN NUMBER 079992 SO = .000990 QB = 7.95 CFS QP = 17.92 CFS

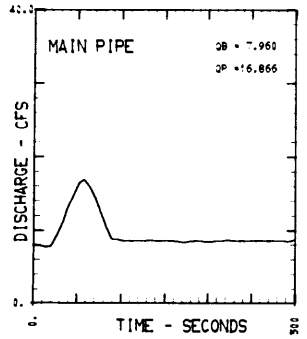

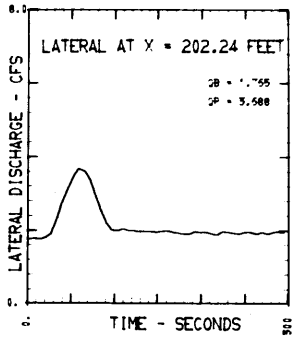

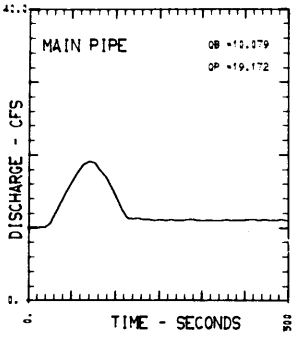

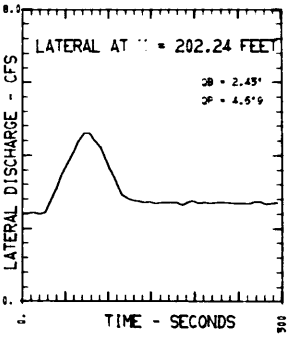

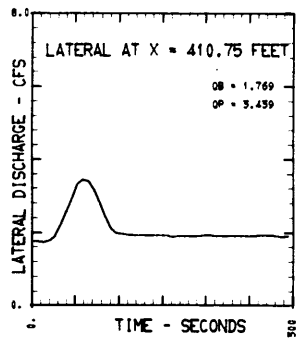

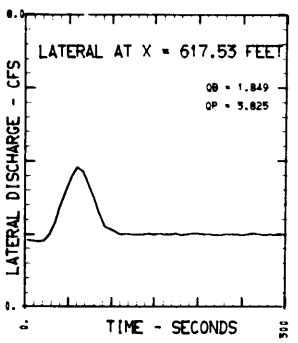

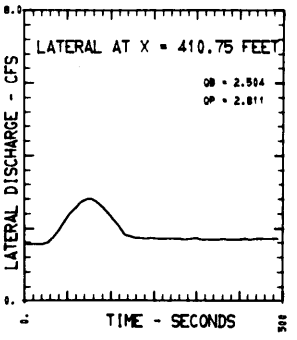

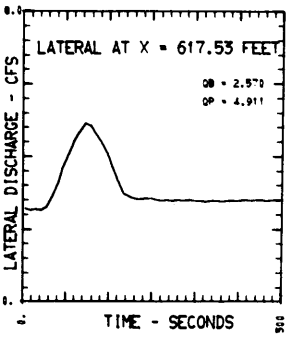

RUN NUMBER 060002 INFLOW HYDROGRAPHS

RUN NUMBER 079905 INFLOW HYDROGRAPHS

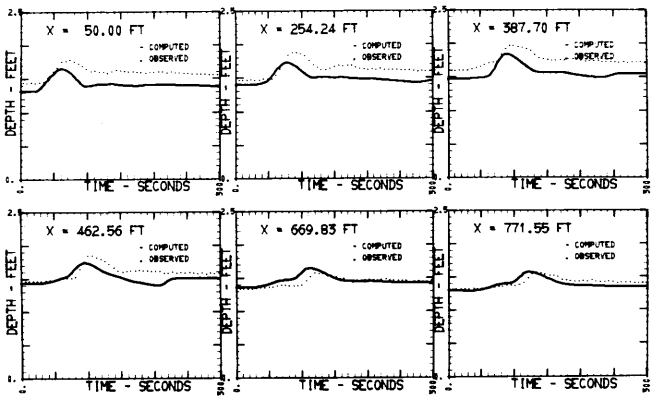

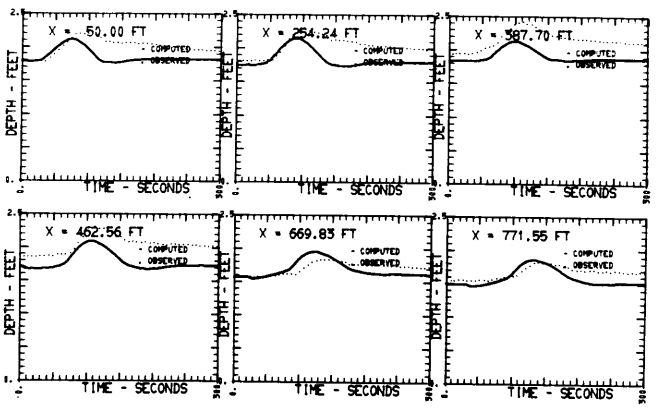

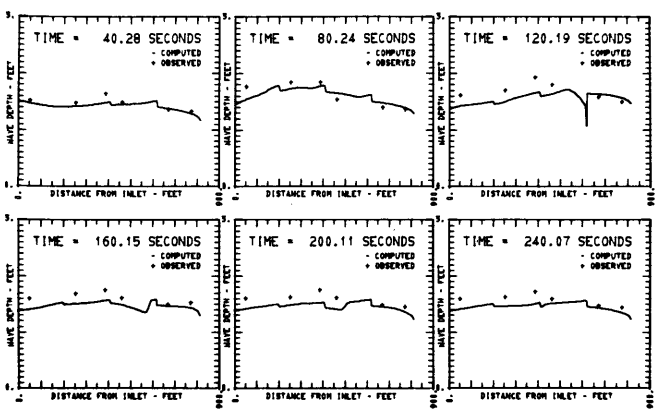

RUN NUMBER 060002 SO = .000990 QB = 7.96 CFS QP = 16.87 CFS

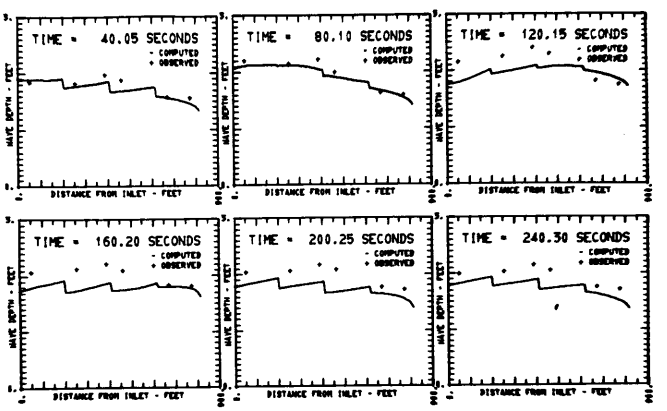

RUN NUMBER 079905 SO = .000990 QB = 10.08 CFS QP = 19.17 CFS

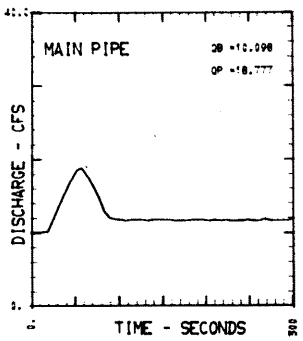

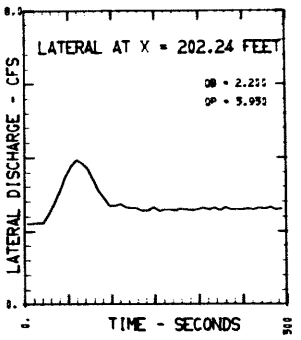

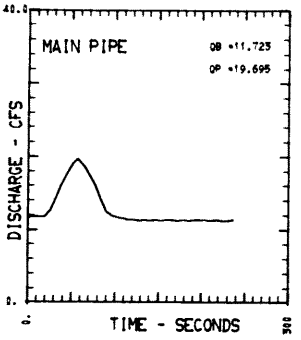

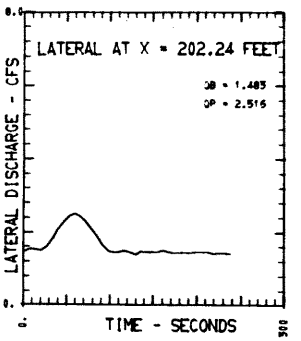

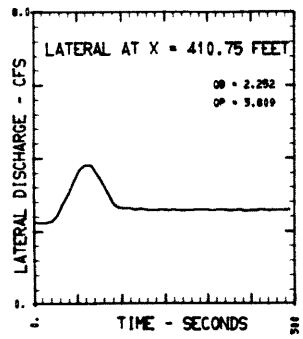

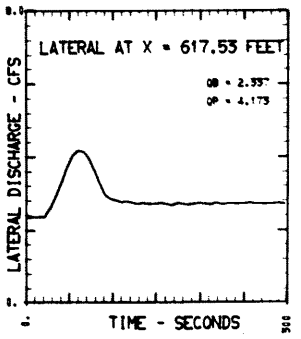

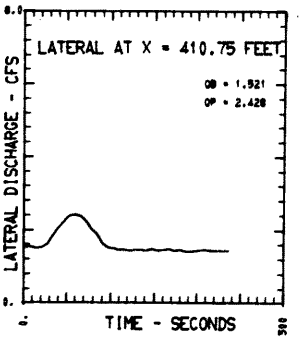

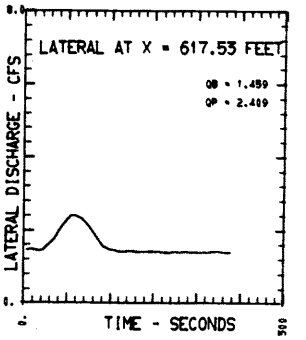

RUN NUMBER 060005 INFLOW HYDROGRAPHS

RUN NUMBER 079904 INFLOW HYDROGRAPHS

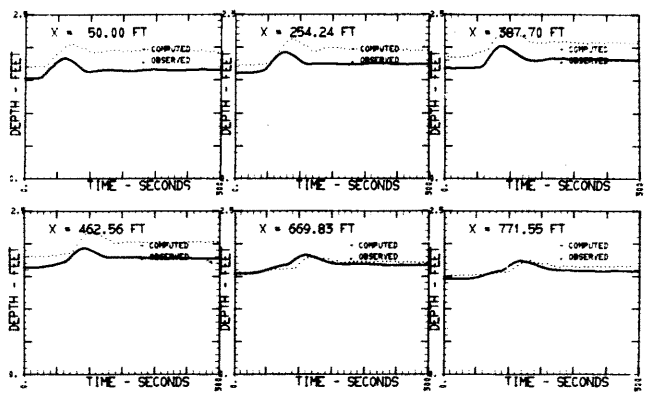

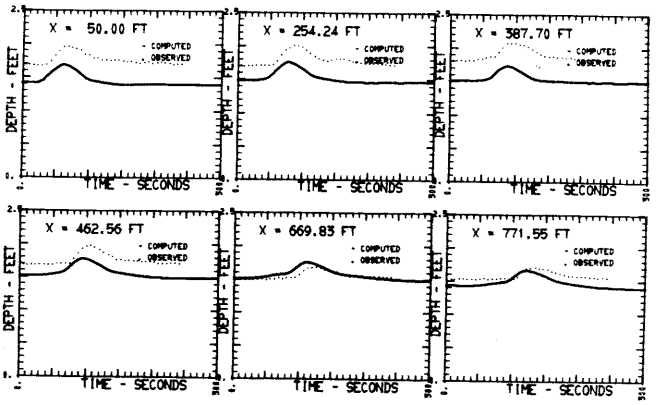

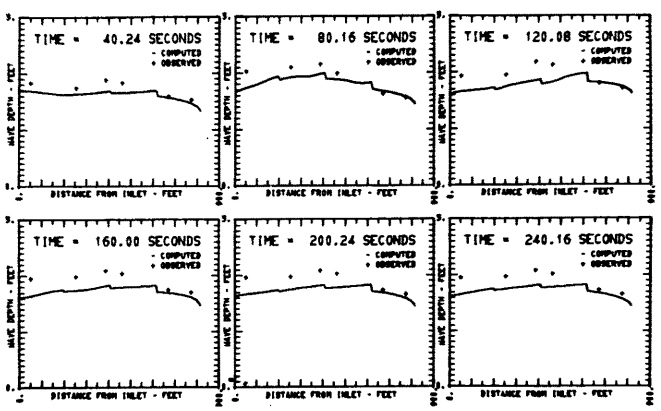

RUN NUMBER 060005 SO = .000990 QB = 10.10 CFS QP = 18.78 CFS

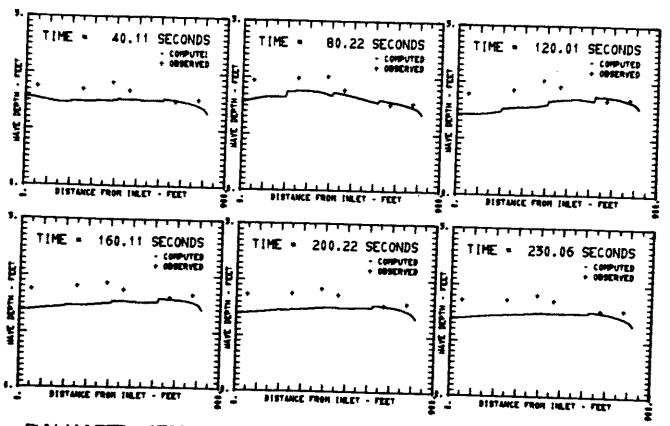

RUN NUMBER 079904 SO = .000990 QB = 11.72 CFS QP = 19.69 CFS

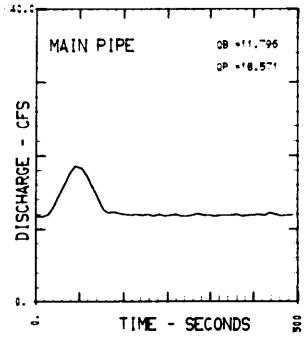

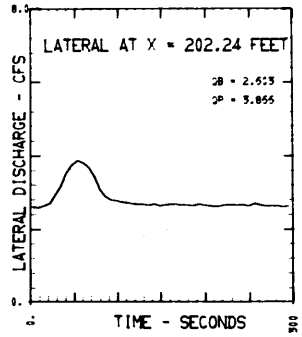

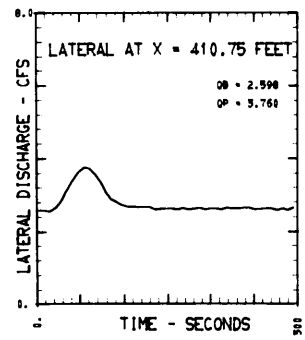

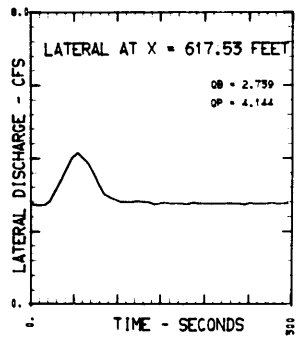

RUN NUMBER 060003 INFLOW HYDROGRAPHS

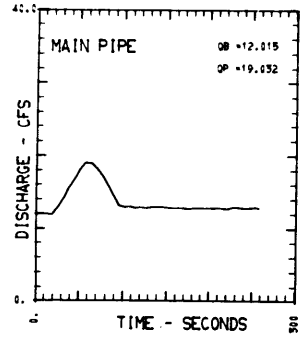

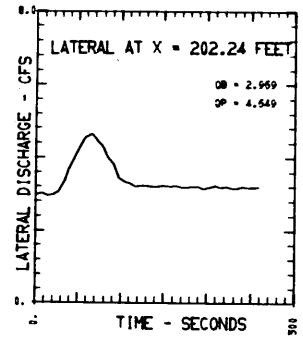

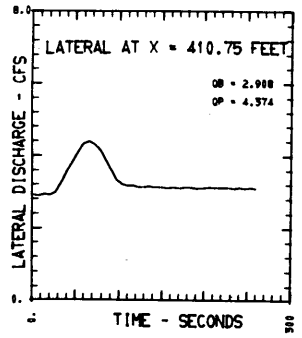

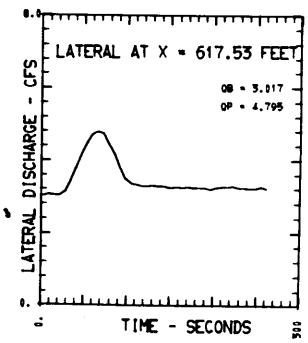

RUN NUMBER 079903 INFLOW HYDROGRAPHS

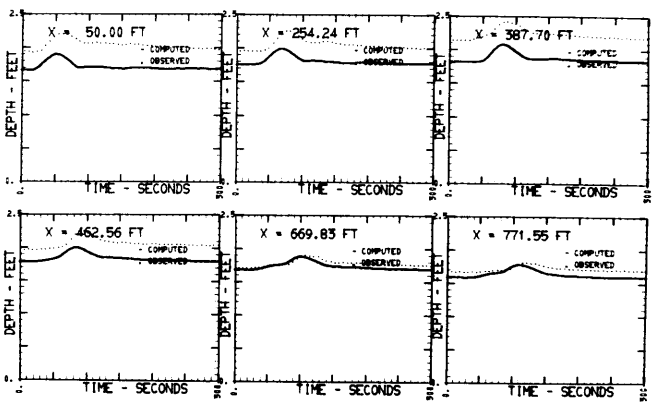

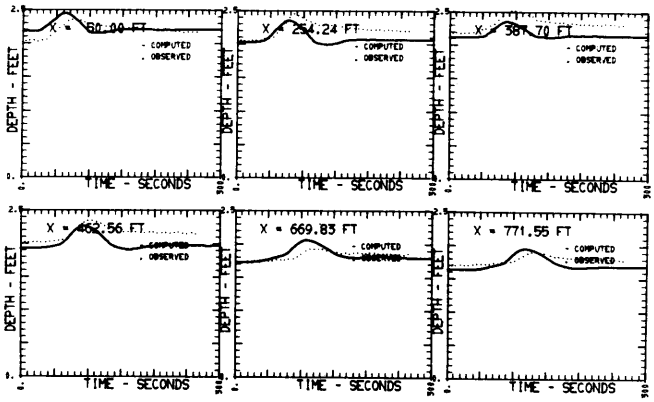

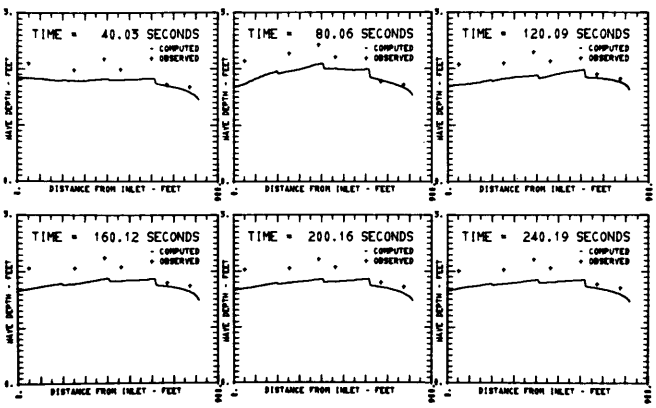

RUN NUMBER 060003 SO = .000990 QB = 11.80 CFS QP = 18.57 CFS

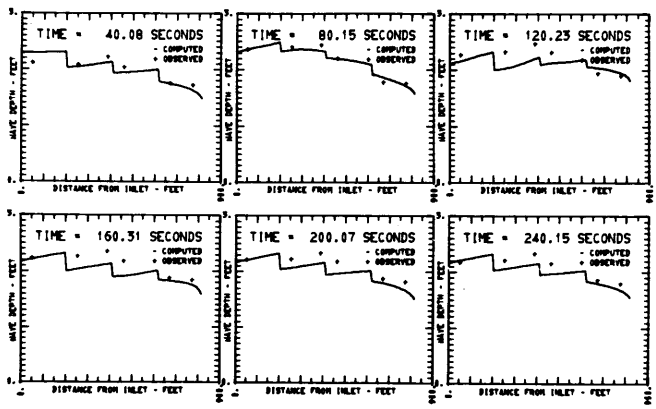

RUN NUMBER 079903 SO = .000990 QB = 12.02 CFS QP = 19.03 CFS

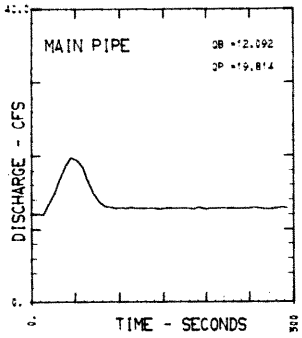

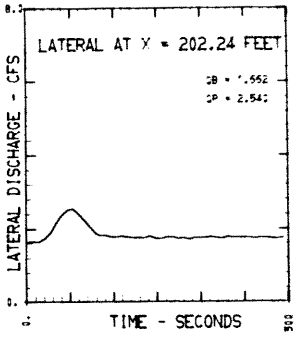

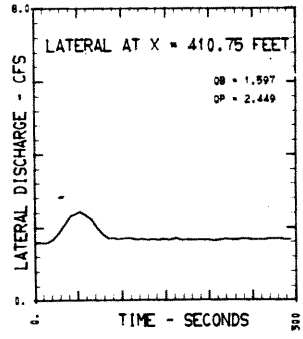

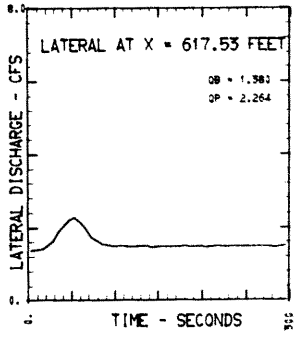

RUN NUMBER 060004 INFLOW HYDROGRAPHS

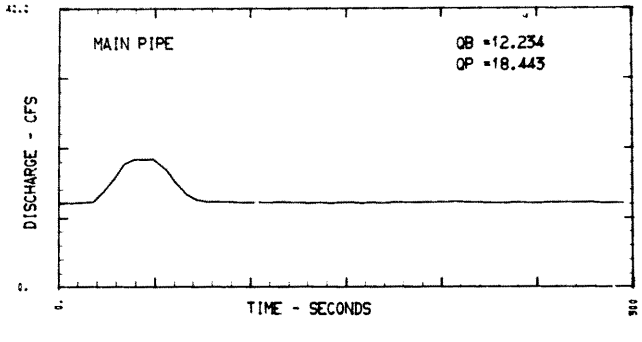

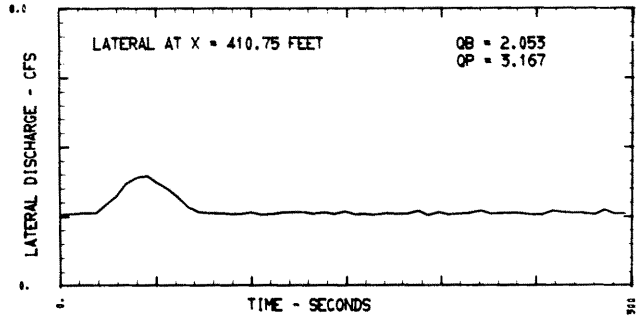

RUN NUMBER 050003 INFLOW HYDROGRAPHS

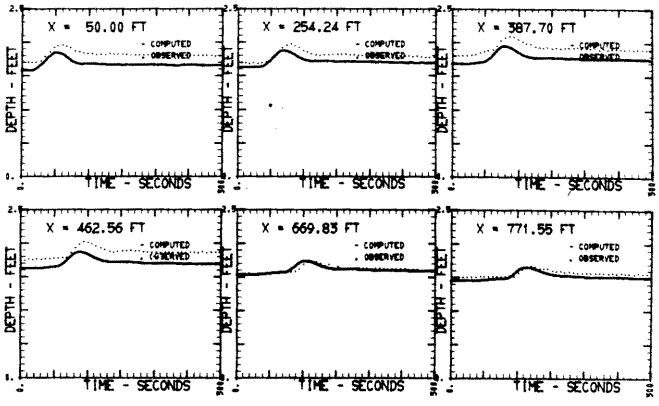

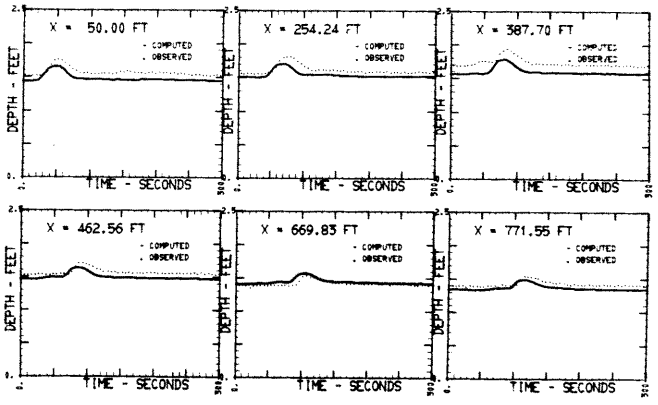

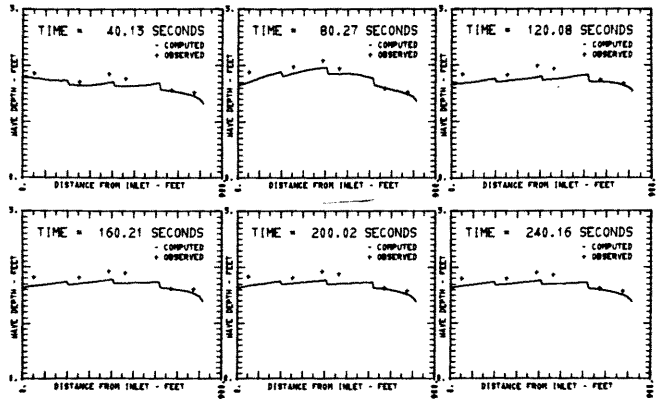

RUN NUMBER 060004 SO = .000990 QB = 12.09 CFS QP = 19.81 CFS

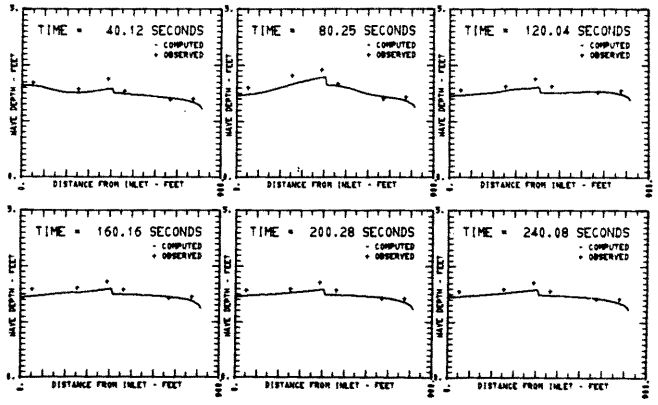

RUN NUMBER 050003 SO = .000990 QB = 12.23 CFS QP = 18.44 CFS

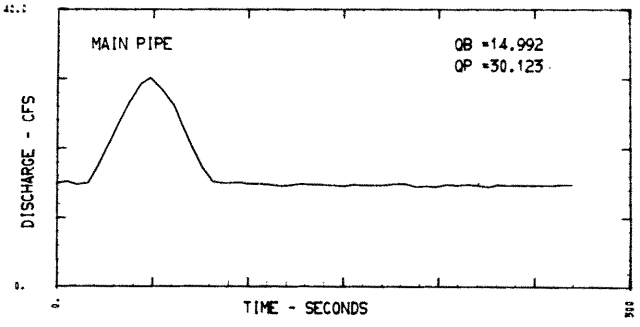

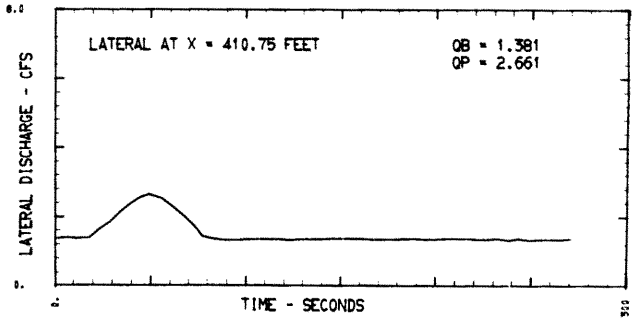

RUN NUMBER 030003 INFLOW HYDROGRAPHS

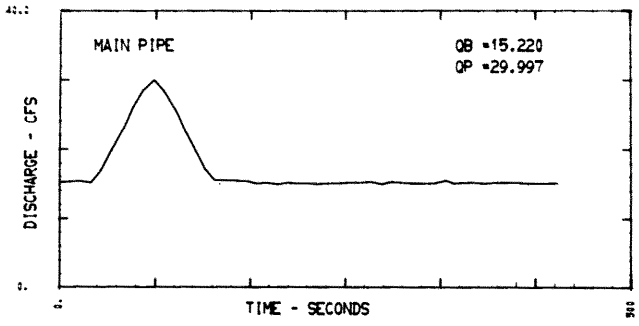

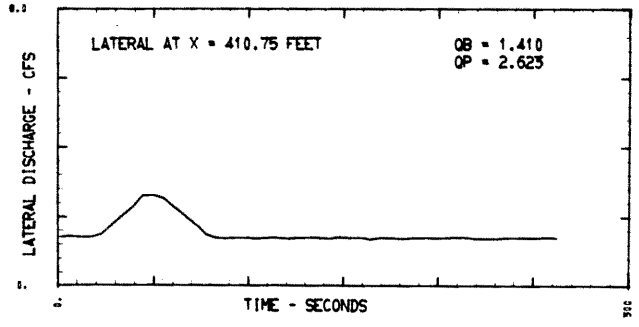

RUN NUMBER 030002 INFLOW HYDROGRAPHS

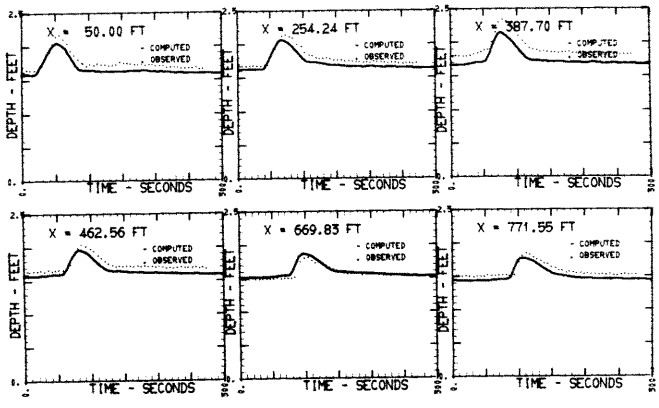

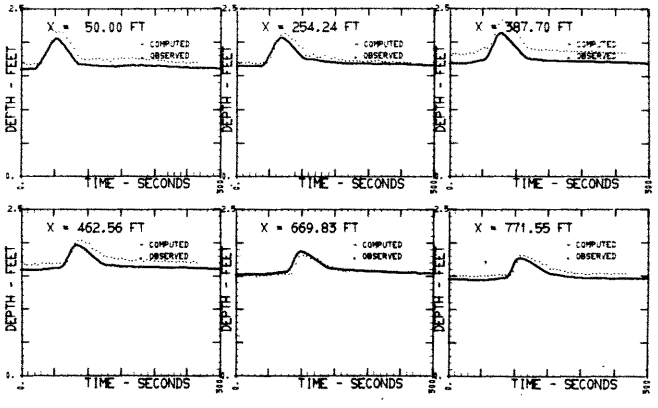

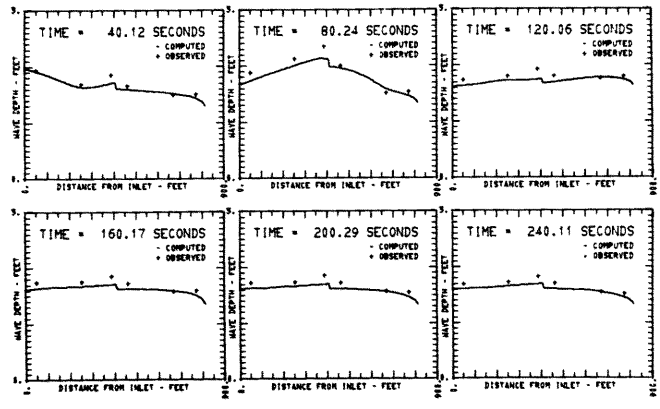

RUN NUMBER 030003 SO = .000990 QB = 14.99 CFS QP = 30.12 CFS

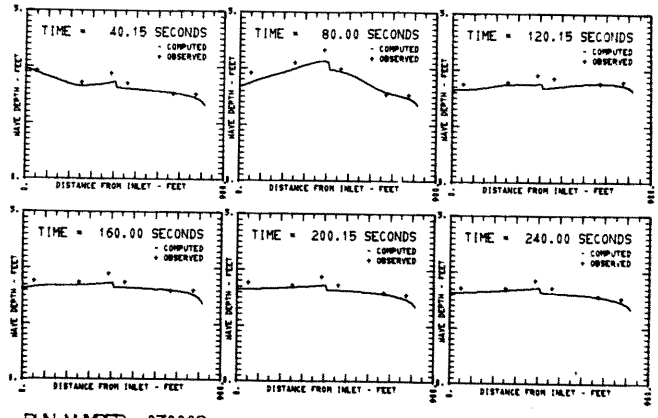

RUN NUMBER 030002 SO = .000990 QB = 15.22 CFS QP = 30.00 CFS

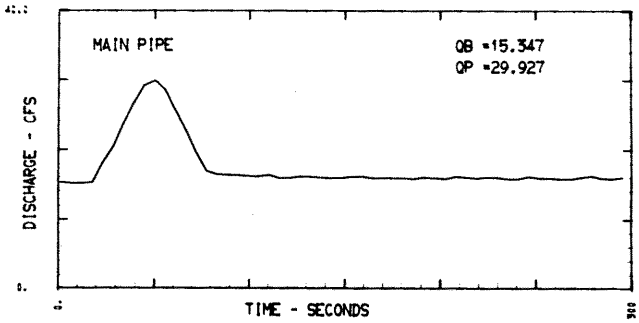

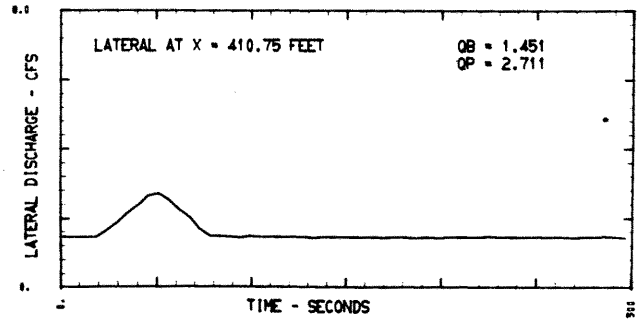

RUN NUMBER 030001 INFLOW HYDROGRAPHS

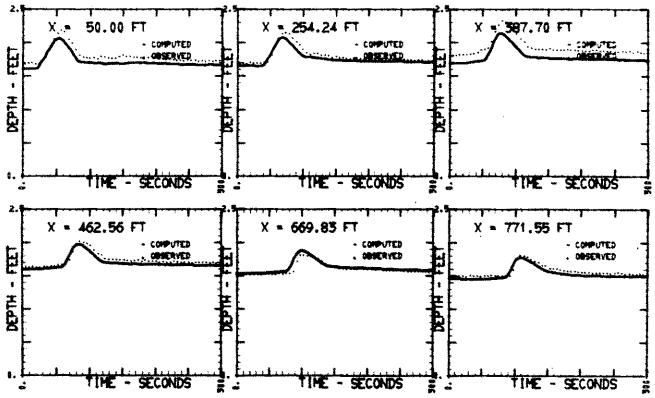

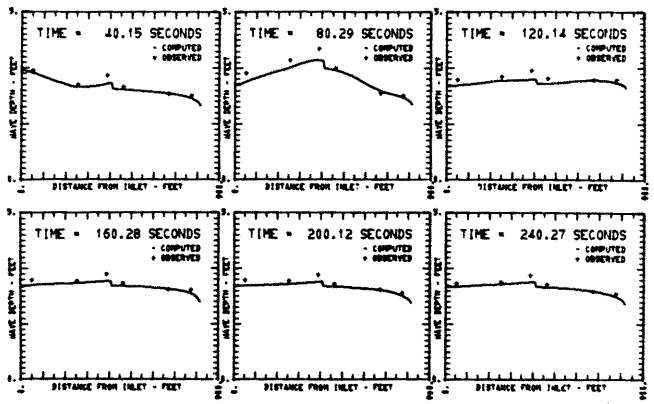

RUN NUMBER 030001 SO = .000990 QB = 15.35 CFS QP = 29.93 CFS

APPENDIX 4

COMPARISONS OF OBSERVED AND COMPUTED WAVES FOR PEAK DEPTH
VERSUS DISTANCE AND TIME WITH CSU DATA

Graphs representing a total of 32 runs are included in this appendix. Test conditions of these 32 runs are listed in Table 6.9, entitled "Summary of Data on CSU Experimental Waves", in Chapter 6 of this paper. For each run the results are plotted as peak depth versus distance (upper graphs), and peak depth versus time (lower graphs). The order of arrangement of the graphs in Appendix 4 follows the same order used in Table 6.9.

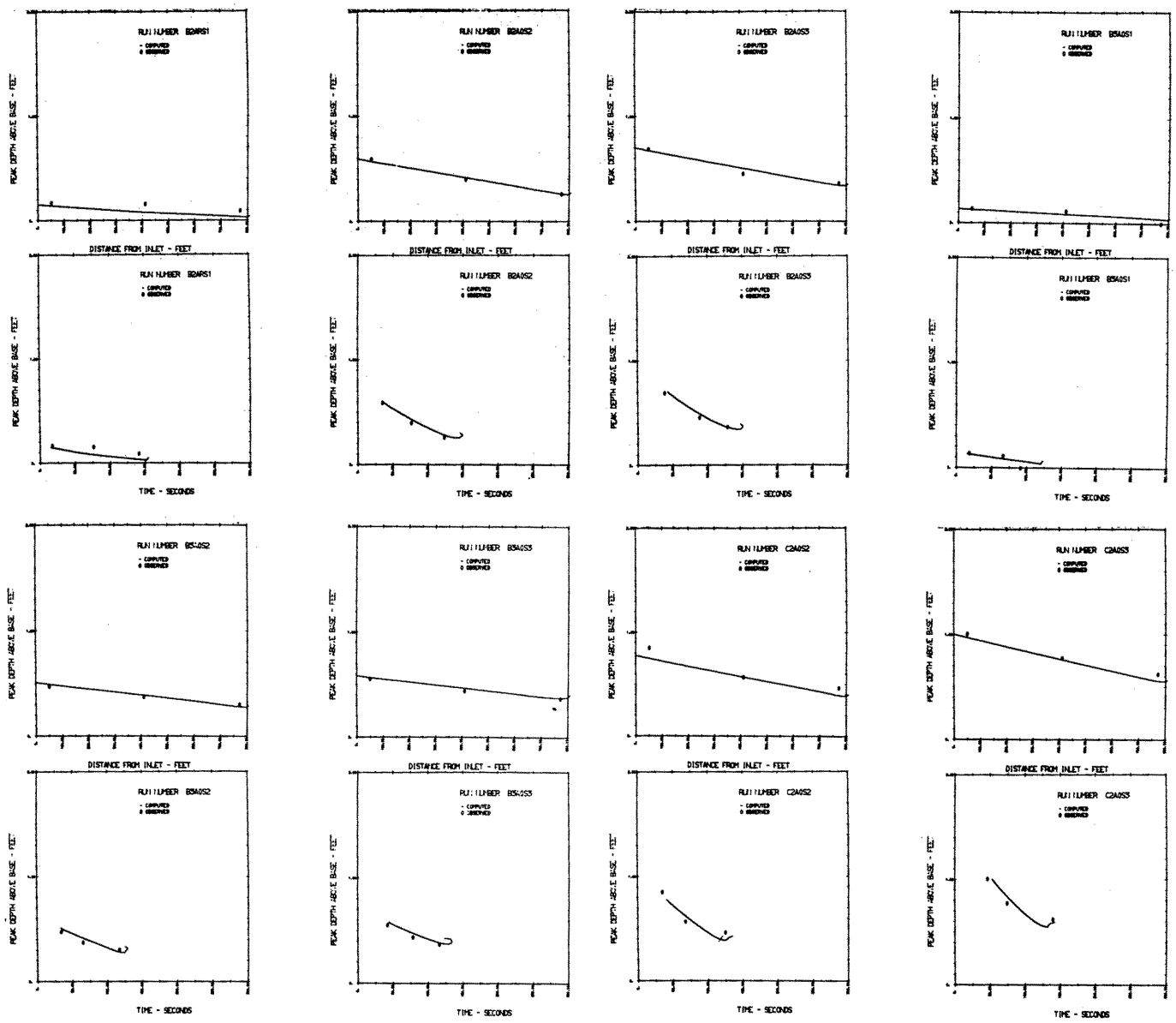

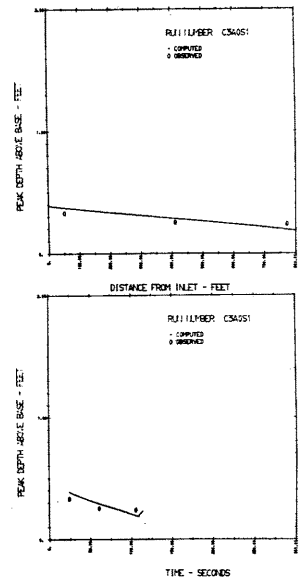
RUN NUMBER C5A0S1
+ COMPUTED
0 OBSERVED
PEAK DEPTH ABOVE BASE - FEET
DISTANCE FROM INLET - FEET
RUN NUMBER C5A0S1
+ COMPUTED
0 OBSERVED
PEAK DEPTH ABOVE BASE - FEET
TIME - SECONDS

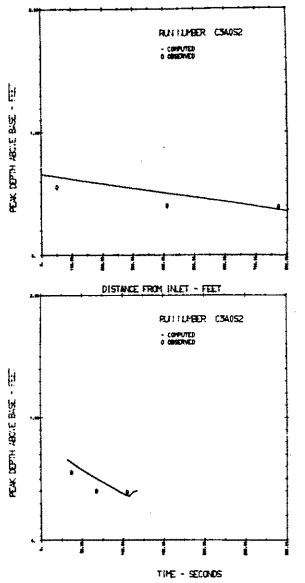
RUN NUMBER C5A0S2
+ COMPUTED
0 OBSERVED
PEAK DEPTH ABOVE BASE - FEET
DISTANCE FROM INLET - FEET
RUN NUMBER C5A0S2
+ COMPUTED
0 OBSERVED
PEAK DEPTH ABOVE BASE - FEET
TIME - SECONDS

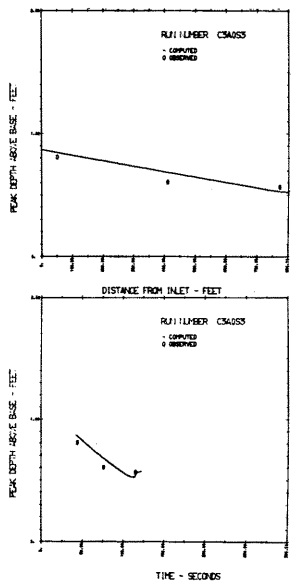
RUN NUMBER C5A0S3
+ COMPUTED
0 OBSERVED
PEAK DEPTH ABOVE BASE - FEET
DISTANCE FROM INLET - FEET
RUN NUMBER C5A0S3
+ COMPUTED
0 OBSERVED
PEAK DEPTH ABOVE BASE - FEET
TIME - SECONDS

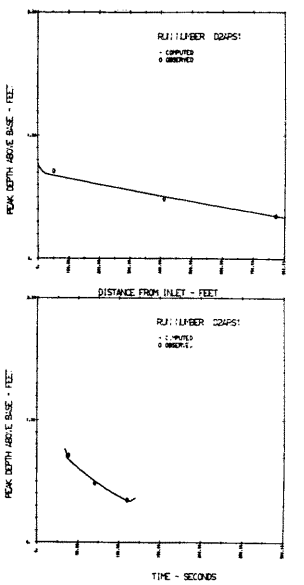
RUN NUMBER D2APS1
+ COMPUTED
0 OBSERVED
PEAK DEPTH ABOVE BASE - FEET
DISTANCE FROM INLET - FEET
RUN NUMBER D2APS1
+ COMPUTED
0 OBSERVED
PEAK DEPTH ABOVE BASE - FEET
TIME - SECONDS

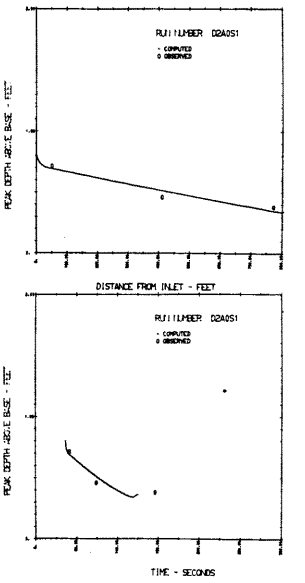
RUN NUMBER D2A0S1
+ COMPUTED
0 OBSERVED
PEAK DEPTH ABOVE BASE - FEET
DISTANCE FROM INLET - FEET
RUN NUMBER D2A0S1
+ COMPUTED
0 OBSERVED
PEAK DEPTH ABOVE BASE - FEET
TIME - SECONDS

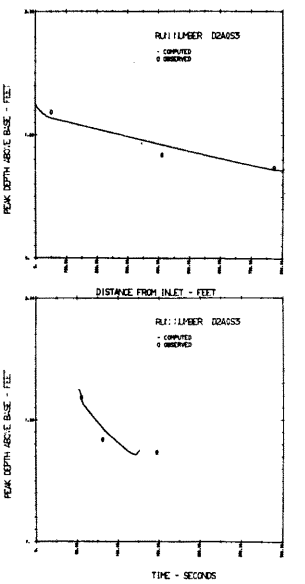
RUN NUMBER D2A0S3
+ COMPUTED
0 OBSERVED
PEAK DEPTH ABOVE BASE - FEET
DISTANCE FROM INLET - FEET
RUN NUMBER D2A0S3
+ COMPUTED
0 OBSERVED
PEAK DEPTH ABOVE BASE - FEET
TIME - SECONDS

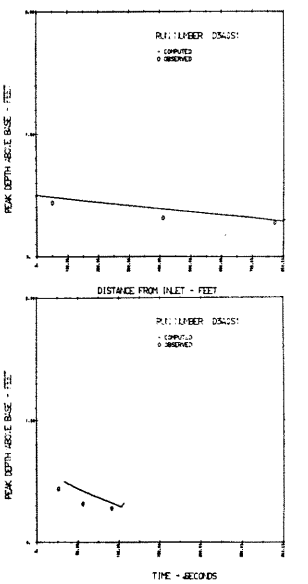
RUN NUMBER D5A0S1
+ COMPUTED
0 OBSERVED
PEAK DEPTH ABOVE BASE - FEET
DISTANCE FROM INLET - FEET
RUN NUMBER D5A0S1
+ COMPUTED
0 OBSERVED
PEAK DEPTH ABOVE BASE - FEET
TIME - SECONDS

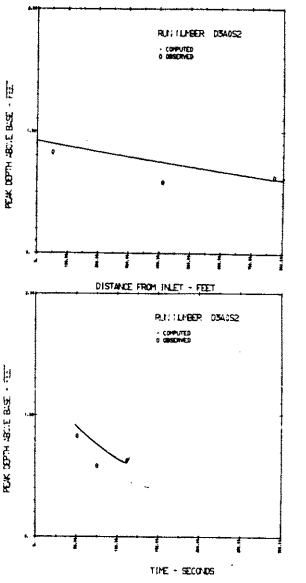
RUN NUMBER D5A0S2
+ COMPUTED
0 OBSERVED
PEAK DEPTH ABOVE BASE - FEET
DISTANCE FROM INLET - FEET
RUN NUMBER D5A0S2
+ COMPUTED
0 OBSERVED
PEAK DEPTH ABOVE BASE - FEET
TIME - SECONDS

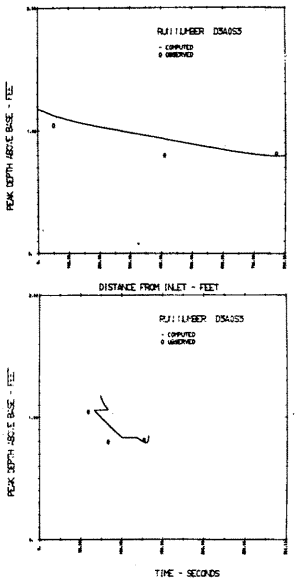
RUN NUMBER D5A0S3
+ COMPUTED
0 OBSERVED
PEAK DEPTH ABOVE BASE - FEET
DISTANCE FROM INLET - FEET
RUN NUMBER D5A0S3
+ COMPUTED
0 OBSERVED
PEAK DEPTH ABOVE BASE - FEET
TIME - SECONDS

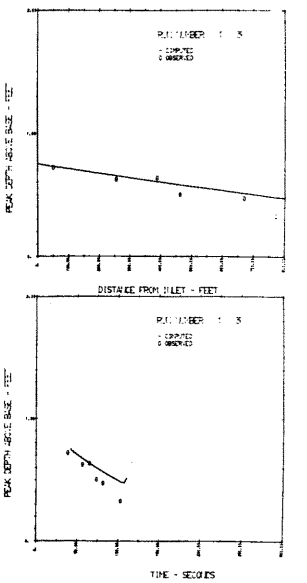
RUN NUMBER 1 5
+ COMPUTED
0 OBSERVED
PEAK DEPTH ABOVE BASE - FEET
DISTANCE FROM INLET - FEET
RUN NUMBER 1 5
+ COMPUTED
0 OBSERVED
PEAK DEPTH ABOVE BASE - FEET
TIME - SECONDS

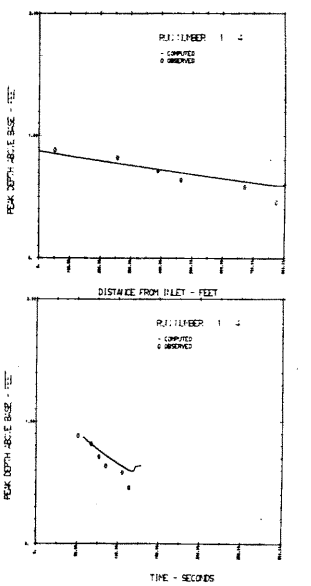
RUN NUMBER 1 4
+ COMPUTED
0 OBSERVED
PEAK DEPTH ABOVE BASE - FEET
DISTANCE FROM INLET - FEET
RUN NUMBER 1 4
+ COMPUTED
0 OBSERVED
PEAK DEPTH ABOVE BASE - FEET
TIME - SECONDS

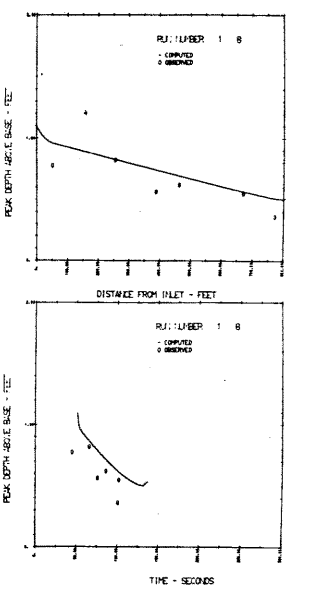
RUN NUMBER 1 8
+ COMPUTED
0 OBSERVED
PEAK DEPTH ABOVE BASE - FEET
DISTANCE FROM INLET - FEET
RUN NUMBER 1 8
+ COMPUTED
0 OBSERVED
PEAK DEPTH ABOVE BASE - FEET
TIME - SECONDS

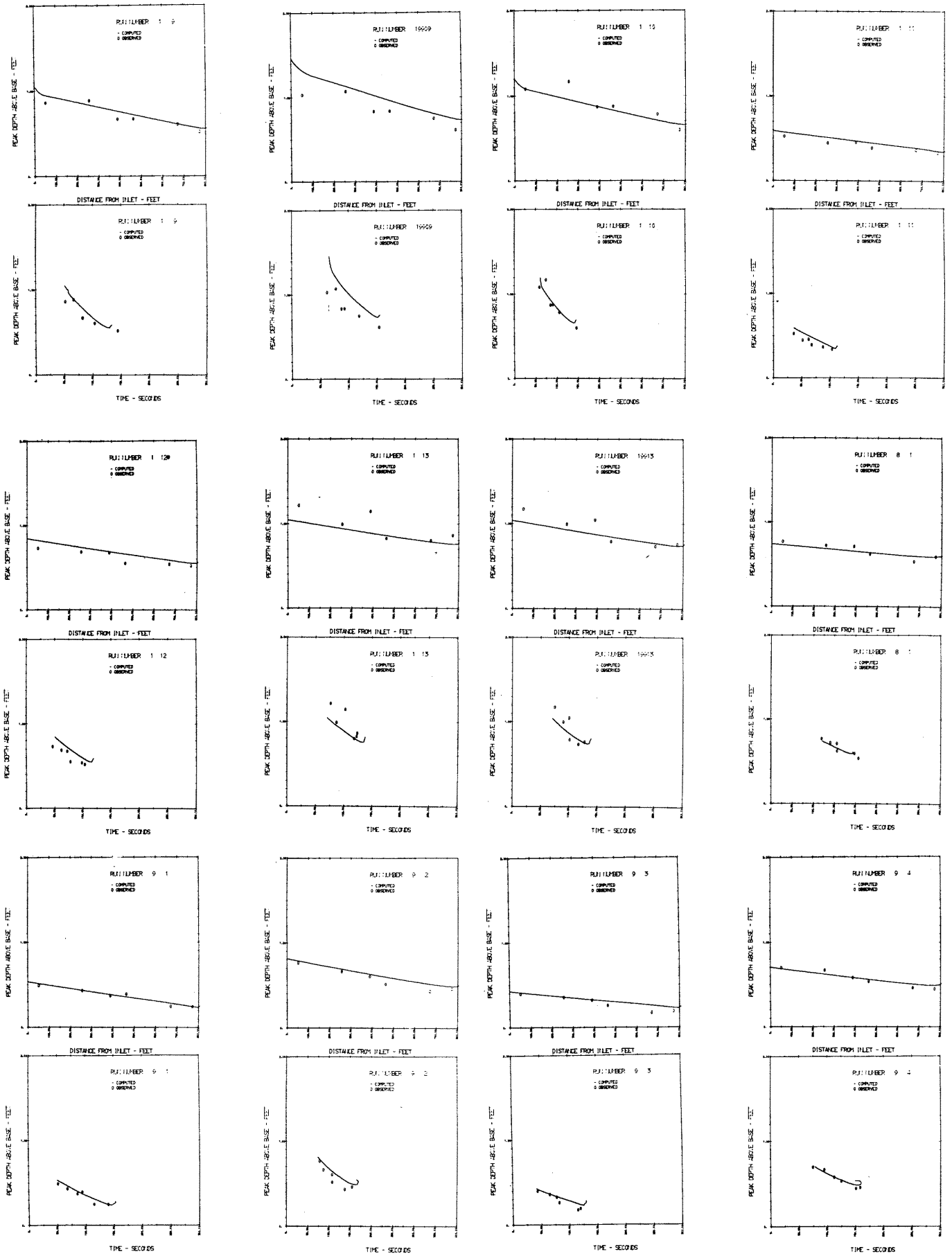
PEAK DEPTH ABOVE BASE - FEET
DISTANCE FROM INLET - FEET
TIME - SECONDS
RUN NUMBER 1 9
RUN NUMBER 19909
RUN NUMBER 1 10
RUN NUMBER 1 11
RUN NUMBER 1 12@
RUN NUMBER 1 13
RUN NUMBER 19913
RUN NUMBER 8 1
RUN NUMBER 1 12
RUN NUMBER 1 13
RUN NUMBER 19913
RUN NUMBER 8 1
RUN NUMBER 9 1
RUN NUMBER 9 2
RUN NUMBER 9 3
RUN NUMBER 9 4
COMPUTED
OBSERVED

APPENDIX 5

COMPARISONS OF OBSERVED AND COMPUTED WAVES FOR PEAK DEPTH
VERSUS DISTANCE AND TIME WITH WALLINGFORD DATA

Graphs representing a total of 41 runs are included in Appendix 5. Test conditions of these 41 runs are listed in Table 6.10, "Summary of Data on Wallingford Experimental Waves", in Chapter 6 of this paper. For each run the results are plotted as peak depth versus distance (upper graphs), and peak depth versus time (lower graphs). The order of arrangement of the graphs in Appendix 5 follows the same order used in Table 6.10.

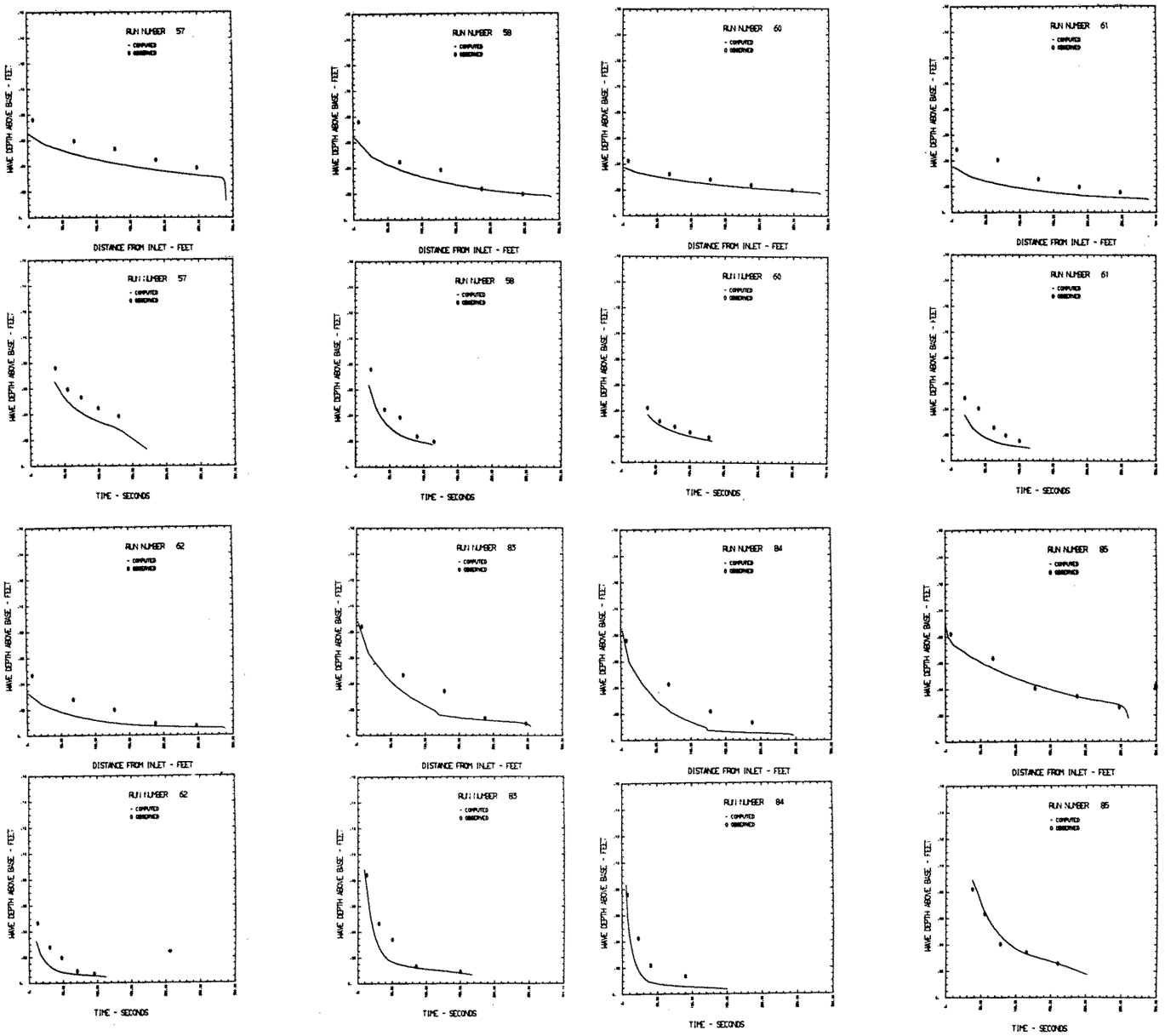

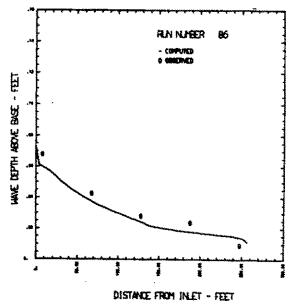
RUN NUMBER 86
- COMPUTED
0 OBSERVED
WAVE DEPTH ABOVE BASE - FEET
DISTANCE FROM INLET - FEET

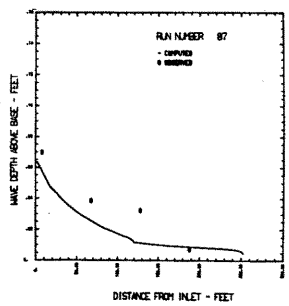
RUN NUMBER 87
- COMPUTED
0 OBSERVED
WAVE DEPTH ABOVE BASE - FEET
DISTANCE FROM INLET - FEET

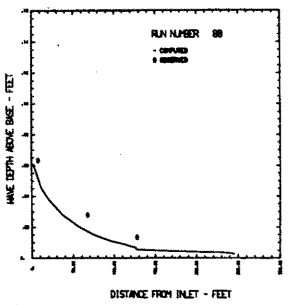
RUN NUMBER 88
- COMPUTED
0 OBSERVED
WAVE DEPTH ABOVE BASE - FEET
DISTANCE FROM INLET - FEET

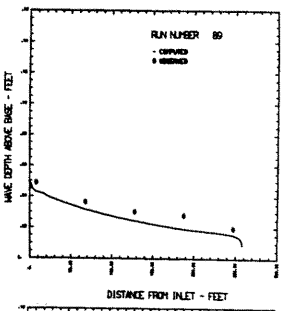
RUN NUMBER 89
- COMPUTED
0 OBSERVED
WAVE DEPTH ABOVE BASE - FEET
DISTANCE FROM INLET - FEET

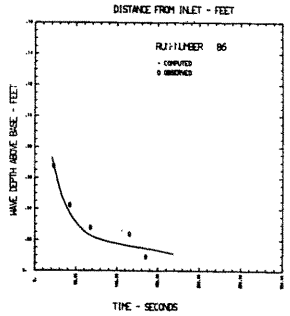
RUN NUMBER 86
- COMPUTED
0 OBSERVED
WAVE DEPTH ABOVE BASE - FEET
TIME - SECONDS

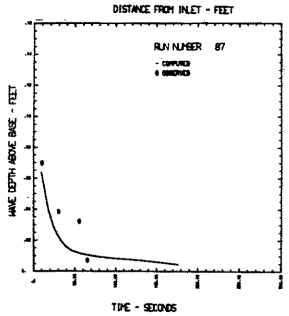
RUN NUMBER 87
- COMPUTED
0 OBSERVED
WAVE DEPTH ABOVE BASE - FEET
TIME - SECONDS

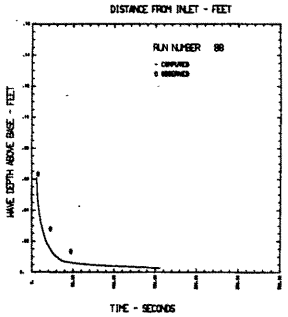
RUN NUMBER 88
- COMPUTED
0 OBSERVED
WAVE DEPTH ABOVE BASE - FEET
TIME - SECONDS

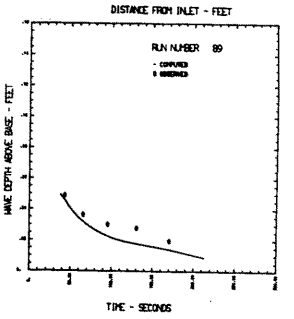
RUN NUMBER 89
- COMPUTED
0 OBSERVED
WAVE DEPTH ABOVE BASE - FEET
TIME - SECONDS

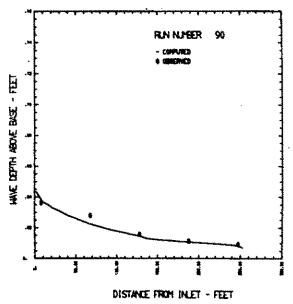
RUN NUMBER 90
- COMPUTED
0 OBSERVED
WAVE DEPTH ABOVE BASE - FEET
DISTANCE FROM INLET - FEET

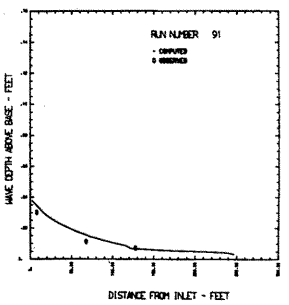
RUN NUMBER 91
- COMPUTED
0 OBSERVED
WAVE DEPTH ABOVE BASE - FEET
DISTANCE FROM INLET - FEET

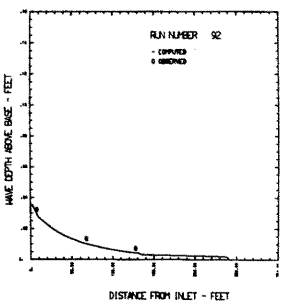
RUN NUMBER 92
- COMPUTED
0 OBSERVED
WAVE DEPTH ABOVE BASE - FEET
DISTANCE FROM INLET - FEET

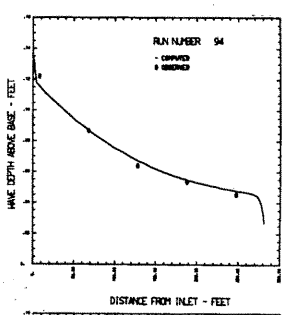
RUN NUMBER 94
- COMPUTED
0 OBSERVED
WAVE DEPTH ABOVE BASE - FEET
DISTANCE FROM INLET - FEET

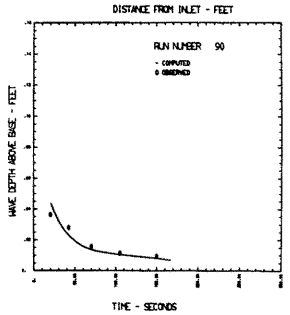
RUN NUMBER 90
- COMPUTED
0 OBSERVED
WAVE DEPTH ABOVE BASE - FEET
TIME - SECONDS

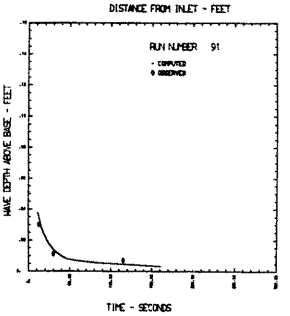
RUN NUMBER 91
- COMPUTED
0 OBSERVED
WAVE DEPTH ABOVE BASE - FEET
TIME - SECONDS

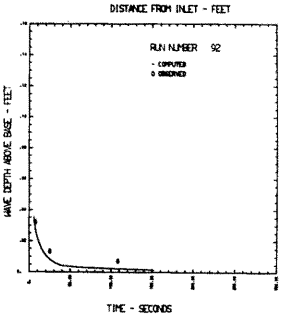
RUN NUMBER 92
- COMPUTED
0 OBSERVED
WAVE DEPTH ABOVE BASE - FEET
TIME - SECONDS

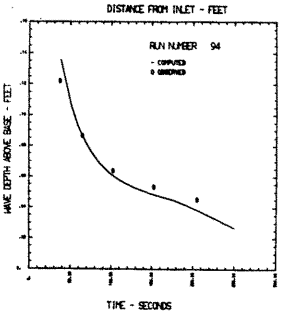
RUN NUMBER 94
- COMPUTED
0 OBSERVED
WAVE DEPTH ABOVE BASE - FEET
TIME - SECONDS

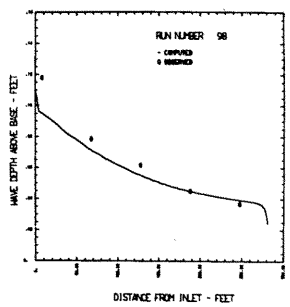
RUN NUMBER 98
- COMPUTED
0 OBSERVED
WAVE DEPTH ABOVE BASE - FEET
DISTANCE FROM INLET - FEET

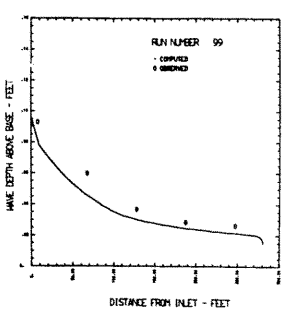
RUN NUMBER 99
- COMPUTED
0 OBSERVED
WAVE DEPTH ABOVE BASE - FEET
DISTANCE FROM INLET - FEET

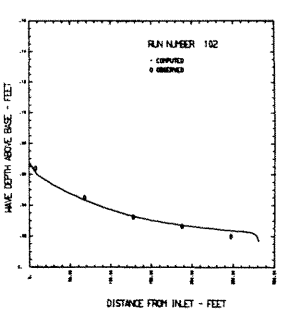
RUN NUMBER 102
- COMPUTED
0 OBSERVED
WAVE DEPTH ABOVE BASE - FEET
DISTANCE FROM INLET - FEET

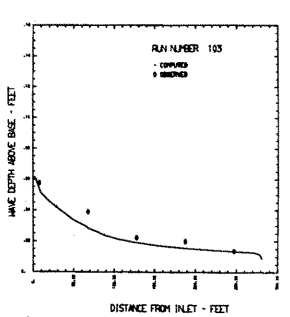
RUN NUMBER 103
- COMPUTED
0 OBSERVED
WAVE DEPTH ABOVE BASE - FEET
DISTANCE FROM INLET - FEET

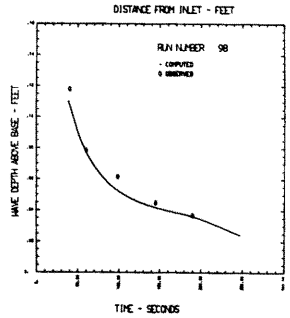
RUN NUMBER 98
- COMPUTED
0 OBSERVED
WAVE DEPTH ABOVE BASE - FEET
TIME - SECONDS

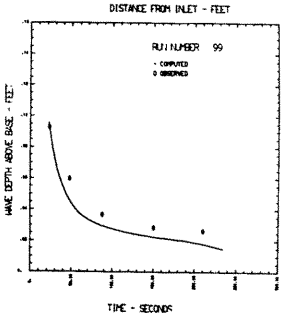
RUN NUMBER 99
- COMPUTED
0 OBSERVED
WAVE DEPTH ABOVE BASE - FEET
TIME - SECONDS

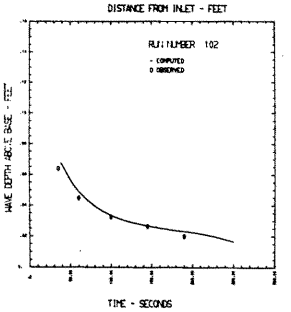
RUN NUMBER 102
- COMPUTED
0 OBSERVED
WAVE DEPTH ABOVE BASE - FEET
TIME - SECONDS

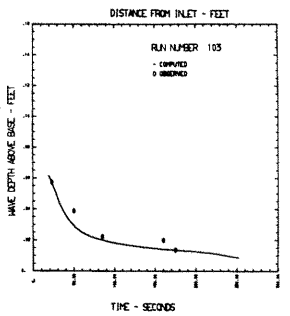
RUN NUMBER 103
- COMPUTED
0 OBSERVED
WAVE DEPTH ABOVE BASE - FEET
TIME - SECONDS

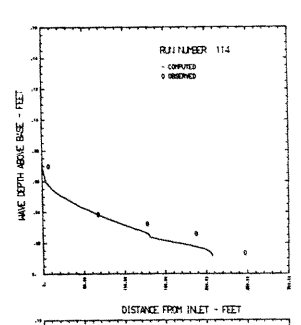
RUN NUMBER 114
- COMPUTED
0 OBSERVED
WAVE DEPTH ABOVE BASE - FEET
DISTANCE FROM INLET - FEET

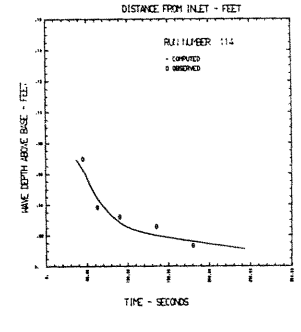
RUN NUMBER 114
- COMPUTED
0 OBSERVED
WAVE DEPTH ABOVE BASE - FEET
TIME - SECONDS

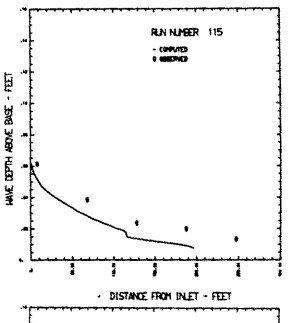
RUN NUMBER 115
- COMPUTED
0 OBSERVED
WAVE DEPTH ABOVE BASE - FEET
DISTANCE FROM INLET - FEET

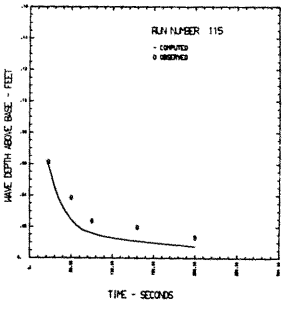
RUN NUMBER 115
- COMPUTED
0 OBSERVED
WAVE DEPTH ABOVE BASE - FEET
TIME - SECONDS

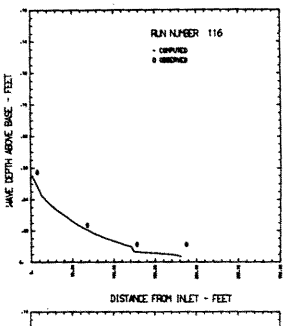
RUN NUMBER 116
- COMPUTED
0 OBSERVED
WAVE DEPTH ABOVE BASE - FEET
DISTANCE FROM INLET - FEET

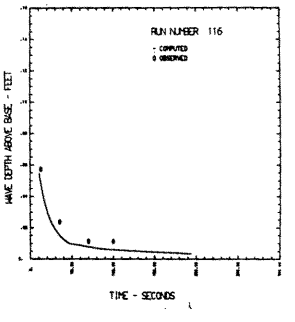
RUN NUMBER 116
- COMPUTED
0 OBSERVED
WAVE DEPTH ABOVE BASE - FEET
TIME - SECONDS

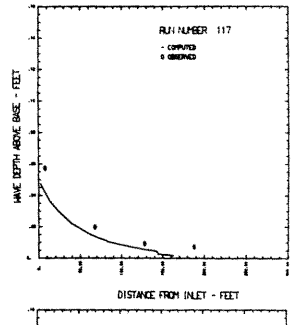
RUN NUMBER 117
- COMPUTED
0 OBSERVED
WAVE DEPTH ABOVE BASE - FEET
DISTANCE FROM INLET - FEET

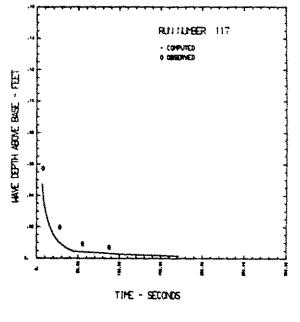
RUN NUMBER 117
- COMPUTED
0 OBSERVED
WAVE DEPTH ABOVE BASE - FEET
TIME - SECONDS

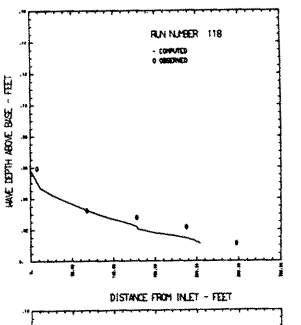
RUN NUMBER 118
- COMPUTED
0 OBSERVED
WAVE DEPTH ABOVE BASE - FEET
DISTANCE FROM INLET - FEET

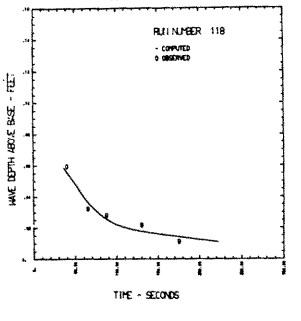
RUN NUMBER 118
- COMPUTED
0 OBSERVED
WAVE DEPTH ABOVE BASE - FEET
TIME - SECONDS

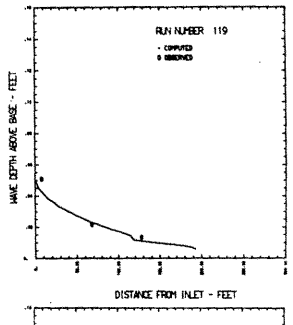
RUN NUMBER 119
- COMPUTED
0 OBSERVED
WAVE DEPTH ABOVE BASE - FEET
DISTANCE FROM INLET - FEET

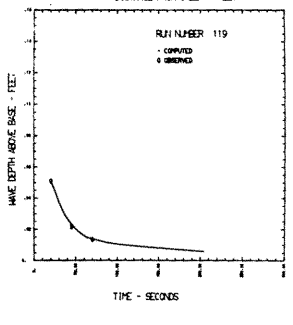
RUN NUMBER 119
- COMPUTED
0 OBSERVED
WAVE DEPTH ABOVE BASE - FEET
TIME - SECONDS

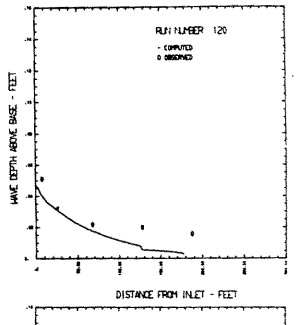
RUN NUMBER 120
- COMPUTED
0 OBSERVED
WAVE DEPTH ABOVE BASE - FEET
DISTANCE FROM INLET - FEET

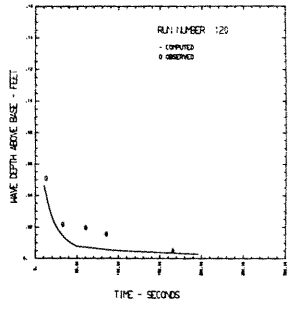
RUN NUMBER 120
- COMPUTED
0 OBSERVED
WAVE DEPTH ABOVE BASE - FEET
TIME - SECONDS

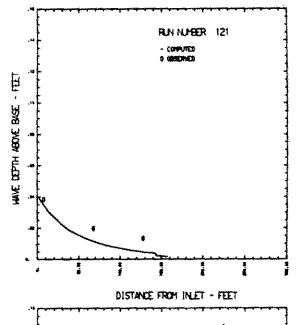
RUN NUMBER 121
- COMPUTED
0 OBSERVED
WAVE DEPTH ABOVE BASE - FEET
DISTANCE FROM INLET - FEET

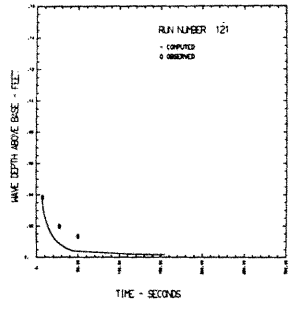
RUN NUMBER 121
- COMPUTED
0 OBSERVED
WAVE DEPTH ABOVE BASE - FEET
TIME - SECONDS

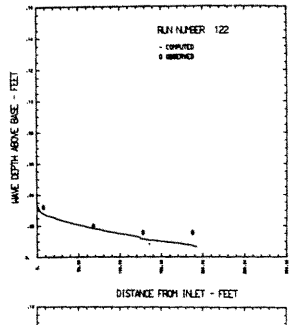
RUN NUMBER 122
- COMPUTED
0 OBSERVED
WAVE DEPTH ABOVE BASE - FEET
DISTANCE FROM INLET - FEET

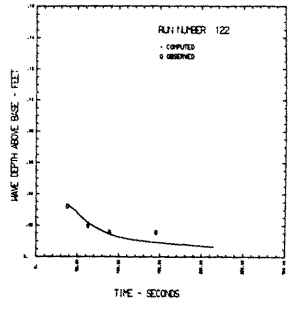
RUN NUMBER 122
- COMPUTED
0 OBSERVED
WAVE DEPTH ABOVE BASE - FEET
TIME - SECONDS

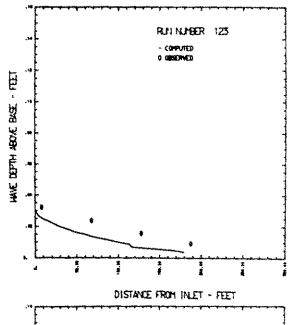
RUN NUMBER 123
- COMPUTED
0 OBSERVED
WAVE DEPTH ABOVE BASE - FEET
DISTANCE FROM INLET - FEET

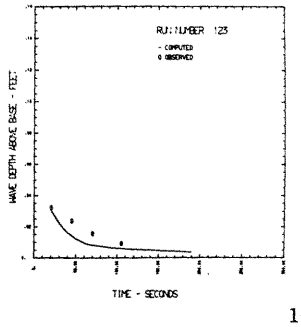
RUN NUMBER 123
- COMPUTED
0 OBSERVED
WAVE DEPTH ABOVE BASE - FEET
TIME - SECONDS

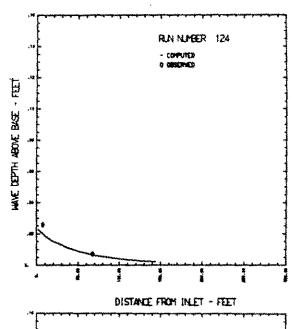
RUN NUMBER 124
- COMPUTED
0 OBSERVED
WAVE DEPTH ABOVE BASE - FEET
DISTANCE FROM INLET - FEET

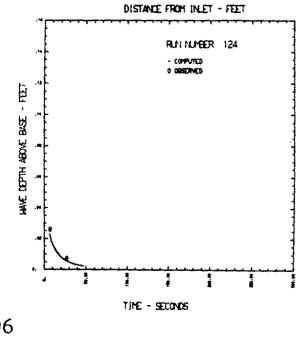
RUN NUMBER 124
- COMPUTED
0 OBSERVED
WAVE DEPTH ABOVE BASE - FEET
TIME - SECONDS

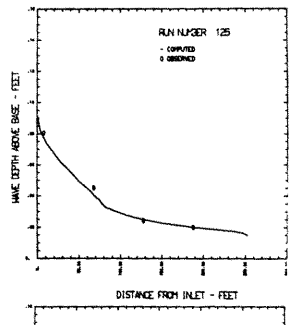
RUN NUMBER 125
- COMPUTED
0 OBSERVED
WAVE DEPTH ABOVE BASE - FEET
DISTANCE FROM INLET - FEET

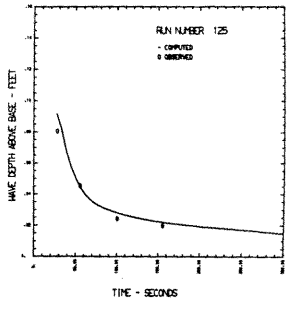
RUN NUMBER 125
- COMPUTED
0 OBSERVED
WAVE DEPTH ABOVE BASE - FEET
TIME - SECONDS

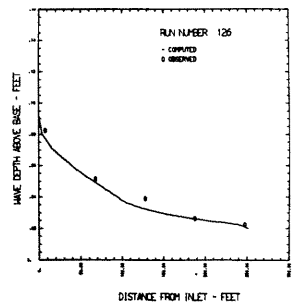
RUN NUMBER 126
- COMPUTED
0 OBSERVED
WAVE DEPTH ABOVE BASE - FEET
DISTANCE FROM INLET - FEET

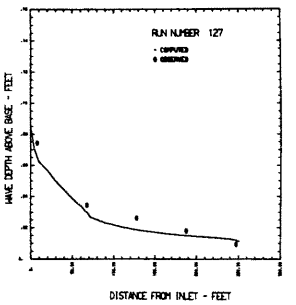
RUN NUMBER 127
- COMPUTED
0 OBSERVED
WAVE DEPTH ABOVE BASE - FEET
DISTANCE FROM INLET - FEET

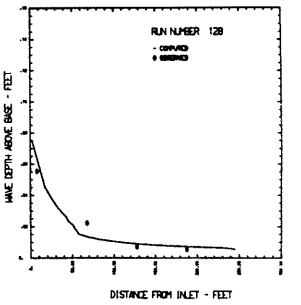
RUN NUMBER 128
- COMPUTED
0 OBSERVED
WAVE DEPTH ABOVE BASE - FEET
DISTANCE FROM INLET - FEET

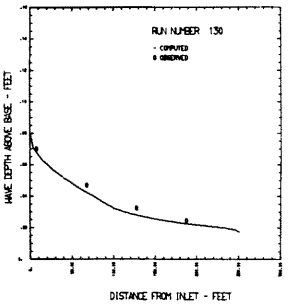
RUN NUMBER 130
- COMPUTED
0 OBSERVED
WAVE DEPTH ABOVE BASE - FEET
DISTANCE FROM INLET - FEET

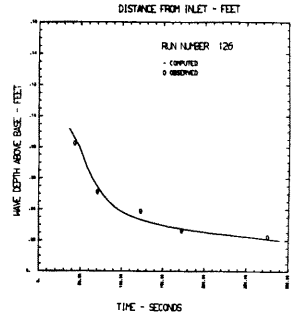
RUN NUMBER 126
- COMPUTED
0 OBSERVED
WAVE DEPTH ABOVE BASE - FEET
TIME - SECONDS

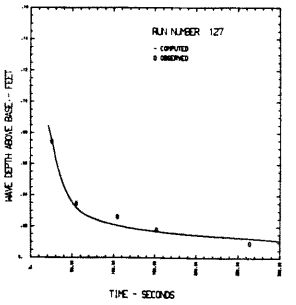
RUN NUMBER 127
- COMPUTED
0 OBSERVED
WAVE DEPTH ABOVE BASE - FEET
TIME - SECONDS

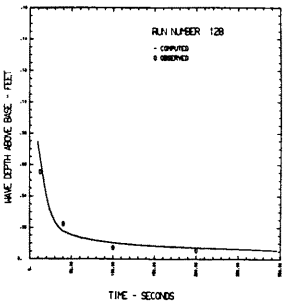
RUN NUMBER 128
- COMPUTED
0 OBSERVED
WAVE DEPTH ABOVE BASE - FEET
TIME - SECONDS

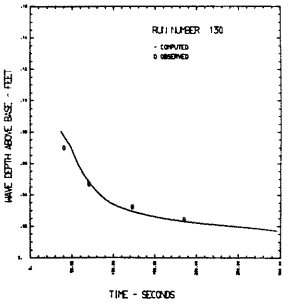
RUN NUMBER 130
- COMPUTED
0 OBSERVED
WAVE DEPTH ABOVE BASE - FEET
TIME - SECONDS

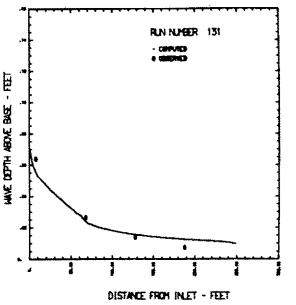
RUN NUMBER 131
- COMPUTED
0 OBSERVED
WAVE DEPTH ABOVE BASE - FEET
DISTANCE FROM INLET - FEET

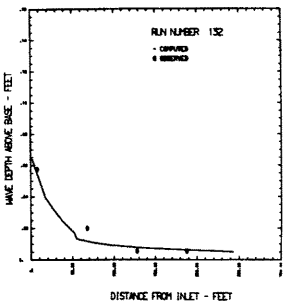
RUN NUMBER 132
- COMPUTED
0 OBSERVED
WAVE DEPTH ABOVE BASE - FEET
DISTANCE FROM INLET - FEET

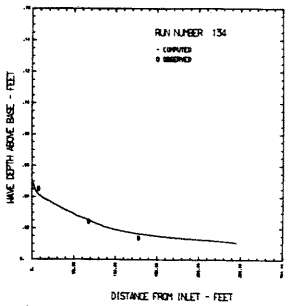
RUN NUMBER 134
- COMPUTED
0 OBSERVED
WAVE DEPTH ABOVE BASE - FEET
DISTANCE FROM INLET - FEET

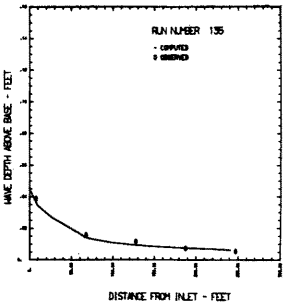
RUN NUMBER 135
- COMPUTED
0 OBSERVED
WAVE DEPTH ABOVE BASE - FEET
DISTANCE FROM INLET - FEET

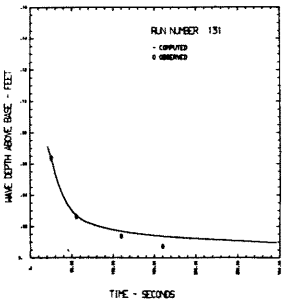
RUN NUMBER 131
- COMPUTED
0 OBSERVED
WAVE DEPTH ABOVE BASE - FEET
TIME - SECONDS

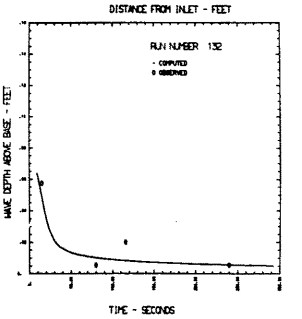
RUN NUMBER 132
- COMPUTED
0 OBSERVED
WAVE DEPTH ABOVE BASE - FEET
TIME - SECONDS

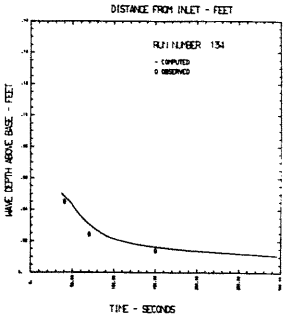
RUN NUMBER 134
- COMPUTED
0 OBSERVED
WAVE DEPTH ABOVE BASE - FEET
TIME - SECONDS

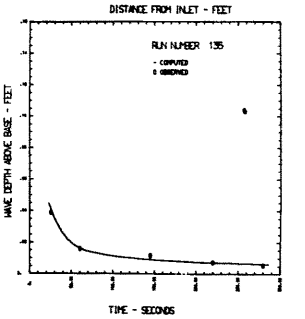
RUN NUMBER 135
- COMPUTED
0 OBSERVED
WAVE DEPTH ABOVE BASE - FEET
TIME - SECONDS

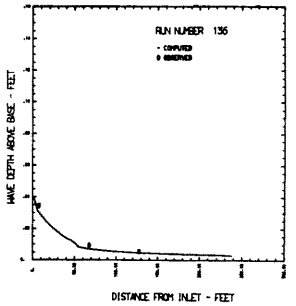
RUN NUMBER 136
- COMPUTED
0 OBSERVED
WAVE DEPTH ABOVE BASE - FEET
DISTANCE FROM INLET - FEET

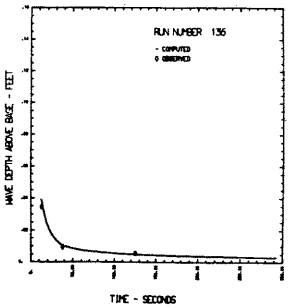
RUN NUMBER 136
- COMPUTED
0 OBSERVED
WAVE DEPTH ABOVE BASE - FEET
TIME - SECONDS

Key Words: Storm Drain, Flood Routing, Unsteady Flow, Numerical Solutions, Wave Experiments, Method of Characteristics.

Abstract: This first part of a four-part series of hydrology papers on flood routing through storm drains presents results of experimental studies in a 3-ft diameter, 822-ft long storm conduit and theoretical studies of the unsteady free-surface flow. The numerical integrations of differential equations by the specified interval scheme of the method of characteristics, the diffusing scheme, and the Lax-Wendroff scheme are discussed; the method of characteristics is selected for the practical integration procedure whenever the complete differential equations are used. Experimental and analytical investigations of the geometric and hydraulic parameters that define the coefficients of the two differential equations are summarized. The initial and boundary conditions are experimentally studied and are expressed mathematically for the numerical solutions. The analytically computed waves are then compared with the experimentally observed waves by using the same initial and boundary conditions. Qualitative and quantitative comparisons are given for depth hydrographs at different positions, for depth wave profiles at different instants in time, and for the peak-depth versus both position and time. From a practical point of view, good agreement is indicated by these comparisons. The errors in conduit geometric parameters, in hydraulic parameters, in numerical computations, and in experimental observations are analyzed and discussed.

Reference: Yevjevich, Vujica and Albert H. Barnes, Colorado State University, Hydrology Paper No. 43 (November 1970) "Flood Routing Through Storm Drains, Part I, Solution of Problems of Unsteady Free Surface Flow in Storm Drains."

Key Words: Storm Drain, Flood Routing, Unsteady Flow, Numerical Solutions, Wave Experiments, Method of Characteristics.

Abstract: This first part of a four-part series of hydrology papers on flood routing through storm drains presents results of experimental studies in a 3-ft diameter, 822-ft long storm conduit and theoretical studies of the unsteady free-surface flow. The numerical integrations of differential equations by the specified interval scheme of the method of characteristics, the diffusing scheme, and the Lax-Wendroff scheme are discussed; the method of characteristics is selected for the practical integration procedure whenever the complete differential equations are used. Experimental and analytical investigations of the geometric and hydraulic parameters that define the coefficients of the two differential equations are summarized. The initial and boundary conditions are experimentally studied and are expressed mathematically for the numerical solutions. The analytically computed waves are then compared with the experimentally observed waves by using the same initial and boundary conditions. Qualitative and quantitative comparisons are given for depth hydrographs at different positions, for depth wave profiles at different instants in time, and for the peak-depth versus both position and time. From a practical point of view, good agreement is indicated by these comparisons. The errors in conduit geometric parameters, in hydraulic parameters, in numerical computations, and in experimental observations are analyzed and discussed.

Reference: Yevjevich, Vujica and Albert H. Barnes, Colorado State University, Hydrology Paper No. 43 (November 1970) "Flood Routing Through Storm Drains, Part I, Solution of Problems of Unsteady Free Surface Flow in Storm Drains."

Key Words: Storm Drain, Flood Routing, Unsteady Flow, Numerical Solutions, Wave Experiments, Method of Characteristics.

Abstract: This first part of a four-part series of hydrology papers on flood routing through storm drains presents results of experimental studies in a 3-ft diameter, 822-ft long storm conduit and theoretical studies of the unsteady free-surface flow. The numerical integrations of differential equations by the specified interval scheme of the method of characteristics, the diffusing scheme, and the Lax-Wendroff scheme are discussed; the method of characteristics is selected for the practical integration procedure whenever the complete differential equations are used. Experimental and analytical investigations of the geometric and hydraulic parameters that define the coefficients of the two differential equations are summarized. The initial and boundary conditions are experimentally studied and are expressed mathematically for the numerical solutions. The analytically computed waves are then compared with the experimentally observed waves by using the same initial and boundary conditions. Qualitative and quantitative comparisons are given for depth hydrographs at different positions, for depth wave profiles at different instants in time, and for the peak-depth versus both position and time. From a practical point of view, good agreement is indicated by these comparisons. The errors in conduit geometric parameters, in hydraulic parameters, in numerical computations, and in experimental observations are analyzed and discussed.

Reference: Yevjevich, Vujica and Albert H. Barnes, Colorado State University, Hydrology Paper No. 43 (November 1970) "Flood Routing Through Storm Drains, Part I, Solution of Problems of Unsteady Free Surface Flow in Storm Drains."

Key Words: Storm Drain, Flood Routing, Unsteady Flow, Numerical Solutions, Wave Experiments, Method of Characteristics.

Abstract: This first part of a four-part series of hydrology papers on flood routing through storm drains presents results of experimental studies in a 3-ft diameter, 822-ft long storm conduit and theoretical studies of the unsteady free-surface flow. The numerical integrations of differential equations by the specified interval scheme of the method of characteristics, the diffusing scheme, and the Lax-Wendroff scheme are discussed; the method of characteristics is selected for the practical integration procedure whenever the complete differential equations are used. Experimental and analytical investigations of the geometric and hydraulic parameters that define the coefficients of the two differential equations are summarized. The initial and boundary conditions are experimentally studied and are expressed mathematically for the numerical solutions. The analytically computed waves are then compared with the experimentally observed waves by using the same initial and boundary conditions. Qualitative and quantitative comparisons are given for depth hydrographs at different positions, for depth wave profiles at different instants in time, and for the peak-depth versus both position and time. From a practical point of view, good agreement is indicated by these comparisons. The errors in conduit geometric parameters, in hydraulic parameters, in numerical computations, and in experimental observations are analyzed and discussed.

Reference: Yevjevich, Vujica and Albert H. Barnes, Colorado State University, Hydrology Paper No. 43 (November 1970) "Flood Routing Through Storm Drains, Part I, Solution of Problems of Unsteady Free Surface Flow in Storm Drains."

PREVIOUSLY PUBLISHED PAPERS OF VOLUME 2

Colorado State University Hydrology Papers

No. 26 "The Investigation of Relationship Between Hydrologic Time Series and Sun Spot Numbers," by Ignacio Rodriguez-Iturbe and Vujica Yevjevich, April 1968.

No. 27 "Diffusion of Entrapped Gas From Porous Media," by Kenneth M. Adam and Arthur T. Corey, April 1968.

No. 28 "Sampling Bacteria in a Mountain Stream," by Samuel H. Kunkle and James R. Meimann, March 1968.

No. 29 "Estimating Design Floods from Extreme Rainfall," by Frederick C. Bell, July 1968.

No. 30 "Conservation of Ground Water by Gravel Mulches," by A.T. Corey and W.D. Kemper, May 1968.

No. 31 "Effects of Truncation on Dependence in Hydrologic Time Series," by Rezaul Karim Bhuiya and Vujica Yevjevich, November 1968.

No. 32 "Properties of Non-Homogeneous Hydrologic Series," by V. Yevjevich and R.I. Jeng, April 1969.

No. 33 "Runs of Precipitation Series," by Jose Llamas and M.M. Siddiqui, May 1969.

No. 34 "Statistical Discrimination of Change in Daily Runoff," by Andre J. Dumas and Hubert J. Morel-Seytoux, August 1969.

No. 35 "Stochastic Process of Precipitation," by P. Todorovic and V. Yevjevich, September 1969.

No. 36 "Suitability of the Upper Colorado River Basin for Precipitation Management", by Hiroshi Nakamichi and Hubert J. Morel-Seytoux, Ocotber 1969.

No. 37 "Regional Discrimination of Change in Runoff," by Viboon Nimmannit and Hubert J. Morel-Seytoux, November 1969.

No. 38 "Evaluation of the Effect of Impoundment on Water Quality in Cheney Reservoir," by J.C. Ward and S. Karaki, March 1970.

No. 39 "The Kinematic Cascade as a Hydrologic Model," by David F. Kibler and David A. Woolhiser, February 1970.

No. 40 "Application of Run-Lengths to Hydrologic Series," by Jaime Saldarriaga and Vujica Yevjevich, April 1970.

No. 41 "Numerical Simulation of Dispersion in Groundwater Aquifers," by Donald Lee Reddell and Daniel K. Sunada.

No. 42 "Theoretical Probability Distributions for Flood Peaks," by Emir Zelenhasic, November 1970.